Stability analysis of coupled ordinary differential systems with a string equation : application to a drilling mechanism

Matthieu Barreau

THÈSE

En vue de l'obtention du

DOCTORAT DE L'UNIVERSITÉ DE TOULOUSE

Délivré par : *l'Université Toulouse 3 Paul Sabatier (UT3 Paul Sabatier)*

Présentée et soutenue le *08/07/2019* **par :**

Matthieu BARREAU

Stability analysis of coupled ordinary differential systems with a string equation - Application to a Drilling Mechanism

---

JURY

Florent DI MEGLIO	MdC Mines ParisTech	Membre du Jury
Antoine GIRARD	DR L2S	Rapporteur
Fréderic GOUAISBAUT	MdC UT3 Paul Sabatier	Directeur de Thèse
Thomas MEURER	Pr. Kiel University	Membre du Jury
Christophe PRIEUR	DR Gipsa-Lab	Rapporteur
Carsten SCHERER	Pr. University of Stuttgart	Membre du Jury
Alexandre SEURET	DR LAAS CNRS	Directeur de Thèse
Sophie TARBOURIECH	DR LAAS CNRS	Membre du Jury

École doctorale et spécialité :
EDSYS : Automatique 4200046
Unité de Recherche :
LAAS-CNRS (UPR 8001)
Directeur(s) de Thèse :
Fréderic GOUAISBAUT et *Alexandre SEURET*
Rapporteurs :
Antoine GIRARD et *Christophe PRIEUR*

Université de Toulouse

Université Paul Sabatier

Stability analysis of coupled ordinary differential systems with a string equation - Application to a Drilling Mechanism

A Dissertation submitted in partial satisfaction of the requirements for the degree of

Doctor of Philosophy

in

Control Engineering

by

Matthieu Barreau

July 2019

Acknowledgments

J'aimerais tout d'abord remercier Alex et Fred, mes superviseurs mais aussi mes amis, avec qui j'ai beaucoup appris et ri. Je garderai un bon souvenir de ces nombreuses réunions de cinq minutes qui se transforment en plusieurs heures. Il n'est pas si courant de laisser autant de liberté, tout en guidant quand même, pendant une thèse, et cela m'a beaucoup aidé à venir au travail avec le sourire.

I also have a special thank to the MST team in Stuttgart who accompanied me during three months. I would like to be even more grateful to Carsten Scherer who immediately accepted to be a member of my jury and to write a recommendation letter.

Je suis également reconnaissant envers les autres membres de mon jury et en particulier les rapporteurs Christophe Prieur et Antoine Girard. Ils ont été bienveillants dans leurs rapports et leurs commentaires. Quant à Thomas Meurer, Florent Di Meglio et Sophie Tarbouriech, merci de m'avoir fait l'honneur d'assister à ma présentation et de me poser des questions précises et intéressantes.

Maintenant, il est plus compliqué de remercier tout le monde. Commençons par mes profs de lycée : Mmes Provost et Vauzelle qui m'ont encouragé à poursuivre mes études. Mes profs de prépa, Laurent Sartre et Guillaume Brevet qui m'ont fait découvrir les sciences et qui sont devenus des amis aujourd'hui. De nombreuses anecdotes que je raconte encore viennent de cette année là.

Plus précisément maintenant, je remercie l'équipe MAC qui m'a hébergé pendant presque trois ans, me fournissant bureau (et ce n'est pas facile au LAAS) et ordinateur. Merci à Mohammed et sa science du baby, à Saïd et nos interminables débats, à Flavien et nos conversations Hi-Tech, à Sabrina et aux sabrinettes, à Mattéo et ses explosions de colère, à Swann et nos prévisions de soirées, à Tillman et Roxana mes allemands préférés... et tant d'autres personnes qui sont passées par mon bureau.

J'ai changé par deux fois de colocs dans notre bel appart et j'ai pu beaucoup partager avec Bruno, mon ami de longue date et Paul, suédois dans l'âme et chercheur sans frontière.

Je remercie bien sûr ma famille pour m'avoir supporté (dans les deux sens du terme !), c'est une mine d'or dans laquelle j'ai souvent puisé. Donc merci à ma mére qui m'a appris la rigueur et m'a encouragé, à mon père pour sa curiosité et à mon frère pour m'avoir suivi en vacances et avoir partagé de nombreux fous rires.

Je termine enfin par ma nouvelle famille, celle que j'ai fondé pendant ces trois années de thèse. À ma compagne Harmony qui est passée par là avant et qui m'a sans cesse encouragé et aidé autant qu'elle pouvait. Puis à mon très cher fils de 5 mois, Léo, qui éclaire chaque moment de notre vie par son sourire. Il m'a laissé rédiger ma thèse alors qu'il n'avait encore même pas un mois !

Abstract

This thesis is about the stability analysis of a coupled finite dimensional system and an infinite dimensional one. This kind of systems emerges in the physics since it is related to the modeling of structures for instance. The generic analysis of such systems is complex, mainly because of their different nature.

Here, the analysis is conducted using different methodologies. First, the recent Quadratic Separation framework is used to deal with the frequency aspect of such systems. Then, a second result is derived using a Lyapunov-based argument. All the results are obtained considering the projections of the infinite dimensional state on a basis of polynomials. It is then possible to take into account the coupling between the two systems. That results in tractable and reliable numerical tests with a moderate conservatism.

Moreover, a hierarchy on the stability conditions is shown in the Lyapunov case. The real application to a drilling mechanism is proposed to illustrate the efficiency of the method and it opens new perspectives. For instance, using the notion of practical stability, we show that a PI-controlled drillstring is subject to a limit cycle and that it is possible to estimate its amplitude.

Keywords: Coupled ODE/PDE, heterogeneous system, wave equation, projection methodology, drilling mechanism, Lyapunov stability, Linear Matrix Inequality.

Résumé

Cette thèse porte sur l'analyse de stabilité de couplage entre deux systèmes, l'un de dimension finie et l'autre infinie. Ce type de système apparait en physique car il est intimement lié aux modèles de structures. L'analyse générique de tels systèmes est complexe à cause des natures très différentes de chacun des sous-systèmes.

Ici, l'analyse est conduite en utilisant deux méthodologies. Tout d'abord, la séparation quadratique est utilisée pour traiter le côté fréquentiel de tels systèmes. L'autre méthode est basée sur la théorie de Lyapunov pour prouver la stabilité asymptotique de l'interconnexion. Tous ces résultats sont obtenus en utilisant la méthode de projection de l'état de dimension infinie sur une base polynomiale. Il est alors possible de prendre en compte le couplage entre les deux systèmes et ainsi d'obtenir des tests numériques fiables, rapides et peu conservatifs.

De plus, une hiérarchie de conditions est établie dans le cas de Lyapunov. L'applica -tion au cas concret du forage pétrolier est proposée pour illustrer l'efficacité de la méthode et les nouvelles perspectives qu'elle offre. Par exemple, en utilisant la notion de stabilité pratique, nous avons montré qu'une tige de forage controlée à l'aide d'un PI est sujette à un cycle limite et qu'il est possible d'estimer son amplitude.

Mots clés: Couplage EDO/EDP, système hétérogène, équation, méthodologie de projection, mécanisme de forage, stabilité de Lyapunov, inégalités matricielles linéaires.

Contents

List of Figures

List of Tables

Notation

This section provides the notations used all along the thesis.

- $\mathbb{N}$: set of positive integers,
- $\mathbb{R}$: set of real numbers,
- $\mathbb{C}$: set of complex numbers,
- $\mathfrak{Re}(z)$: real part of $z \in \mathbb{C}$,
- $\mathfrak{Im}(z)$: imaginary part of $z \in \mathbb{C}$,
- $\mathbb{C}^+ = \{z \in \mathbb{C} \mid \mathfrak{Re}(z) > 0\}$,
- $\bar{\mathbb{C}}^+ \backslash \{0\} = \{z \in \mathbb{C} \mid \mathfrak{Re}(z) \geq 0, z \neq 0\}$,
- $\mathbb{R}^+ = \{x \in \mathbb{R} \mid x \geq 0\}$.

Matrix set, vectors and operations on matrices

- $\mathbb{R}^{n \times m}$: set of real matrices with n rows and m columns,
- $\mathbb{S}^n$: set of real symmetric matrices with n rows,
- $\mathbb{S}^n_+$: set of symmetric semi-definite positive matrices, $M \in \mathbb{S}^n_+ \Leftrightarrow M \succeq 0$,
- $\mathbb{S}^n_{++}$: set of symmetric definite positive matrices, $M \in \mathbb{S}^n_{++} \Leftrightarrow M \succ 0$,
- $M \preceq 0 \Leftrightarrow -M \succeq 0$ and $M \prec 0 \Leftrightarrow -M \succ 0$,
- $M_{k,l}$: for $M \in \mathbb{R}^{n \times m}$, it refers to the number on the k^{th} row and l^{th} column,
- $N = M(n_i : n_j, m_i : m_j)$: $N \in \mathbb{R}^{n_j - n_i \times m_j - m_i}$ where $N_{k,l} = M_{k+n_i, l+m_i}$ for $(k,l) \in [0, n_j - n_i - 1] \times [0, m_j - m_i - 1]$,
- $I_n \in \mathbb{R}^{n \times n}$: identity matrix,
- $0_{n,m}$: null matrix of $\mathbb{R}^{n \times m}$ and $0_n = 0_{n,n}$,
- $M^\top$: transposition of a matrix M,
- M^*: the transpose conjugate,
- $\mathrm{He}(M) = M + M^\top$,
- $v \in \mathbb{R}^n$: a real vector with n rows,
- $\mathrm{col}(v_1, v_2) = \begin{bmatrix} v_1^\top & v_2^\top \end{bmatrix}^\top$ for two vectors v_1 and v_2.

Functional spaces, operators and scalar products

Let X be an Hilbert space.

- $\partial_x^{(k)}$: k^{th} partial differentiation operator with respect to the variable x,
- $f_x = \partial_x$, $\dot{f} = \partial_t f$,
- $L^2([a,b],\mathbb{R}^n)$: the set of square integrable functions from $[a,b] \subset \mathbb{R}$ to $\mathbb{R}^n$,
- $H^m([a,b],\mathbb{R}^n) = \left\{ f \in L^2([a,b],\mathbb{R}^n) \mid \forall k \leq m, \partial_x^{(k)} f \in L^2([a,b],\mathbb{R}^n) \right\}$: Sobolev space,
- $L^2 = L^2([0,1],\mathbb{R})$, $H^m = H^m([0,1],\mathbb{R})$,
- $L^2(a,b) = L^2([a,b],\mathbb{R})$, $H^m(a,b) = H^m([a,b],\mathbb{R})$,
- $\mathbb{X} = H^1 \times L^2$,
- $\mathbb{X}_1 = H^2 \times H^1$,
- $C([a,b],X) = \{ f : [a,b] \to X \mid f \text{ is continuous } \}$,
- $C^m([a,b],X) = \left\{ f \in C([a,b],X) \mid \forall k \leq m, \partial_x^{(k)} f \in C([a,b],X) \right\}$,
- $C_0^m([a,b],X) = \{ f \in C^m([a,b],X) \mid f(a) = f(b) = 0 \}$,
- I_X: identity operator on X,
- 0_X: zero vector of space X,
- $f \in \text{Span}(e_0,\ldots,e_N) \Leftrightarrow \exists a_0,\ldots,a_N \in \mathbb{R}, f = \sum_{k=0}^N a_k e_k$ for $e_0,\ldots,e_N \in L^2$,
- $\langle \cdot,\cdot \rangle_X$: canonical inner product on X,
- $\|f\|_X^2 = \langle f,f \rangle_X$ for $f \in X$,
- $\langle u,v \rangle_{\mathbb{R}^n} = u^\top v$ for $u,v \in \mathbb{R}^n$,
- $\langle f,g \rangle_{L^2([a,b],\mathbb{R}^n)} = \displaystyle\int_a^b f^\top(x) g(x) dx$ for $f,g \in L^2([a,b],\mathbb{R}^n)$,
- $\langle f,g \rangle_{H^m([a,b],\mathbb{R}^n)} = \displaystyle\sum_{k=0}^m \left\langle \partial_x^{(k)} f, \partial_x^{(k)} g \right\rangle_{L^2([a,b],\mathbb{R}^n)}$ for $f,g \in H^m([a,b],\mathbb{R}^n)$,

Miscellaneous

Transfer functions are usually denoted by calligraphic letters, and for $\mathcal{H}$ a transfer function, we definite its infinite norm by:

$$\|\mathcal{H}\|_\infty = \sup_{\omega \in \mathbb{R}^+} |\mathcal{H}(i\omega)|.$$

1 Introduction

If we open a search engine and type in the research bar "why do we use partial differential equations?", many other questions arise such as: "What are the real life applications of partial differential equations?", "Is it possible to approximate a partial differential equation?" or even "How do we solve a partial differential equation?". These questions are mostly written by graduate students who have started for the first time studying the complex world of infinite-dimensional dynamic systems. When we look at the proposed answers, they are often very long and sometimes unclear!

There are many real life applications of Partial Differential Equations (PDEs). The books [55, 169] draw a list of more than thirty PDEs used in physics to describe a transport problem, a diffusion reaction, a fluid movement or even the transformations of a beam subject to external forces. In fact, there are many different domains where a PDE can be derived using the laws of continuum mechanics. As noted by Stéphen Timoshenko in [165], if we try to mathematically describe a phenomenon at a macroscopic scale, then we naturally get PDEs. Consequently, if we zoom enough and consider a microscopic scale or even smaller, the mechanical laws suggest that we may use a sequence of Ordinary Differential Equations (ODEs) to approximate our original problem. It is sometimes interesting to consider a truncation of our problem and examine the system of ODEs for which the current classical theory might bring insights. This is a very common approach because it presents less theoretical barriers. Nevertheless, some characteristics introduced by the infinite-dimensional context might be erased when doing this approximation [156]. Following [41, 55, 161, 162], a complementary approach would be to use modern theories and numerical tools to finely study the original problem.

In this manuscript, after a theoretical part, we get interested in the study of the PDE arising when observing the axial and radial dynamics of a drilling pipe without any finite-dimensional truncation. Considering that the rod is very long leads to a propagation of the twisting moment and axial compression along the pipe. These phenomenons are modeled using flow equations and the resulting problem is then a PDE. More specially, it is a string equation. However, the interaction between the rock and the drilling bit is well-approximated using Newton's laws of motion, leading to a nonlinear ODE. The overall model describing the torsion along the pipe is then a coupled nonlinear ODE/string equation. Analyzing and controlling this system is a real challenge today and it is the subject of some recent thesis [9, 126, 156].

There are many other examples coupling a PDE and an ODE such as gas transport [37], communication network [54] or an overhead crane [43]. Nevertheless, even if the literature about ODE or PDE independently is very rich, there isn't much work focusing

on the coupling between these two systems of different natures. In the following section, we highlight the contribution of this thesis in this field.

1.1 Context and contributions of this thesis

One of the simplest infinite-dimensional linear time-invariant system is a Time-Delay System (TDS) [59, 65]. A delay occurs when there is a time lapse between, for instance, the measurement and the control, but also physically with a chattering mechanism for example [65]. The simplest version of a TDS is given as follows:

$$\begin{cases} \dot{X}(t) = AX(t) + A_d X(t-\tau), & t \geq 0 \\ X(t) = \phi(t), & t \in [-\tau, 0], \end{cases} \tag{1.1}$$

where $\tau > 0$ is the delay, ϕ is the initial condition and $A, A_d \in \mathbb{R}^{n\times n}$. The infinite dimensional behavior can be seen in the initial condition where ϕ belongs to a functional space. Existence and uniqueness theorems can be derived in this case and the regularity on the initial condition implies a different regularity on the solution X as discussed in [22, 67, 68] for instance.

Many studies have been done since the late fifties by Mishkis [110] who was the first to really propose a theory dealing with time-delay systems. There is today a large literature on this subject going from frequency analysis [65, 114] to Lyapunov stability analysis using the so-called Lyapunov-Krasovskii stability theorem [65] or the Razumikhin theorem [123] for instance.

The interesting point comes because a TDS can be seen as a special kind of coupled ODE/PDE. Indeed, let consider the following system:

$$\begin{cases} \dot{X}(t) = AX(t) + A_d z(1,t), & t \geq 0, \\ z_t(x,t) + \rho z_x(x,t) = 0, & x \in (0,1), t \geq 0, \\ z(0,t) = X(t), & t \geq 0, \\ z(x,0) = \phi(-\rho^{-1}x), & x \in (0,1), \end{cases} \tag{1.2}$$

where $\rho > 0$. The second line of this system is a PDE called the transport equation. This system can be interpreted as the interconnection between an ODE and a tube which transports the signal $X(t)$ at a speed ρ. The characteristic method [55] gives an explicit solution to the transport problem for $t \geq \rho^{-1}$ which is: $z(x,t) = X\left(t - x\rho^{-1}\right)$ and in particular, we get $z(1,t) = X(t-\rho^{-1})$. Taking then $\rho = \tau^{-1}$, systems (1.1) and (1.2) are equivalent and have the same initial condition.

This new formulation helps designing new controllers using backstepping for instance. This methodology, inspired from *Smith Predictor* [147], has been developed to convert a system into a target system with the desired properties. Finding the control law issued from backstepping requires tedious calculations but the system performances can be therefore easily designed. This method has been firstly applied to nonlinear ODE systems in [89, 90] and then adapted to parabolic PDEs in [148]. From this point, it gave birth to the control design of many infinite-dimensional systems such as hyperbolic

equations or more exotic ones like Korteweg-de Vries or Kuramoto-Sivashinsky equations [87, 91, 104, 105] and more particularly, to coupled ODE/PDE systems. Notice that this technique leads to an infinite-dimensional dynamical controller which might be hard to implement [87, Chapter 1]. That is why observers are designed if the state is not fully measurable, enabling theoretically the application of such a methodology [87, Chapter 3].

Formulating a TDS as a coupled ODE/PDE system is then fruitful. But it also makes us think that it might be possible to bring some tools developed originally in the context of TDS into the more complex world of coupled ODE/PDE. More precisely, we want to introduce the projection methodology, firstly used for TDS in [143]. This thesis comes within this scope and follows the work done in [128] on the transport equation. We consider in this manuscript a different coupling between an ODE and a string equation [55]. Moreover, we focus on the concrete example of stability analysis of a drillstring. The aim is to show that we can obtain tractable results, useful in the analysis of practical problems.

1.1.1 Structure of the manuscript

The manuscript is organized as follows.

Chapter 2 aims at introducing the problem of vibration control in a drilling pipe. It is presented in a chronological order and starts with the finite-dimensional models to end with the more complex *nonlinear ODE/string equation system*. The core of this chapter is to get a physical understanding of the mechanisms in stage when drilling. It ends with a comparison between the different models to justify the use of the most complex one. A statement of the problem dealt in the thesis is also proposed.

Chapter 3 introduces a simpler *coupled linear ODE/string equation* referred to as the toy-example system. This system can be seen as the linearization of the previous nonlinear system around an operating point. Nevertheless, this system is interesting because several interpretations can be drawn depending on the chosen parameters. This chapter focuses on the wellposedness of such a system using the *strongly continuous semigroup theory*. It also provides the definitions of stability dealt with along the manuscript. As a conclusion, the problem established in Chapter 1 is rephrased using notions from *control theory*.

Chapter 4 is about the input/output stability analysis of the toy-example system. It uses mainly frequency arguments in the *Laplace domain*. Such a work enables to get an exact stability test. Since this test requires exact calculations, it is not well suited to any uncertainties in the parameters. Then, we move to two others stability tests using the *Small Gain theorem* and the *Quadratic Separation approach*. These robust tools are then applied to our problem and lead to *Linear Matrix Inequalities* (LMIs). The results are compared with the exact stability test. This chapter presents the *projection methodology* as a possibility to improve Jensen's inequality.

Chapter 5 is dedicated to the *exponential stability analysis* of the toy-example system. The Lyapunov theory is reminded and used on the toy-example system. A result on robust stability with respect to polytopic uncertainties is also proposed. This chapter considers the *projection methodology* as a state extension or a projection of the complete Lyapunov functional. The stability test is then expressed using LMIs. The results obtained are discussed and compared with the one of the previous chapter.

Chapter 6 comes back to the original problem of *stability analysis of a drilling pipe* controlled by a *Proportional/Integral (PI) controller*. It proposes first an exponential stability test on a linearized drillstring system with a Lyapunov-based analysis. Then, using the notion of practical stability, the original problem is answered. A benchmark for different PI controllers is conducted and the effect on simulations is shown.

Conclusion and Perspectives This last chapter draws a summary of the thesis. It first recaps the main advances done in the field of coupled ODE/string equation. More specifically, it enlightens the main results obtained on the drilling pipe. To conclude the manuscript, some perspectives are stated. We propose an extension of the work in the direction of a more general class of coupled ODE/PDE. We also present some conjectures about the PI control of drillstring vibrations.

The appendices are important results that are not directly incorporated into the chapters because of their technicalities. They nevertheless help having a clearer view of the work done in each chapter.

1.1.2 Contributions

The contributions in this manuscript falls into several categories.

1. We gave an interpretation of the ODE/PDE coupling within the Quadratic Separation framework. The projection methodology was introduced in this framework and lead to a stability test with a low number of decision variables. Adapting the projection methodology in this context was at the core of many theoretical contributions in this field.

2. We provided an extension of the projection methodology using Lyapunov functionals. It leads to a better interpretation of the different terms of the functional and a very sharp stability test.

3. We detailed a frequency analysis of the system, providing an exact stability test. This test is at the core of all our numerical simulations since it helps comparing the conservatism introduced by our methods.

4. We then show the adaptability of our method by looking at a physical system: the mechanics of a drillstring. This study brought many challenges since we had to deal with a nonlinearity. The numerical examples depict that this improved functional helps having a more precise estimate of the oscillations with a moderate increase of numerical complexity.

5. Finally, working with different tools for assessing stability helped us getting a clearer picture of the mechanisms behind our methodology. Thus, we could give an interpretation with a state extension, and, even if it is not written in the manuscript, in terms of filter, proposed in an IQC framework, briefly described in the perspectives.

These contributions are at the core of the ANR project SCIDIS which funded this thesis. The list above concerns only the manuscript but other theoretical contributions were made in the domain of controller synthesis for time-delay systems and wave equations.

1.2 List of publications

The work done during this thesis has led to the publication of two accepted journal papers and one with decision pending. A book chapter and four articles for international conferences were also published. Three of the conference papers are not explored in this thesis and were dedicated to synthesis of controllers. Two of them focus on controller synthesis for time-delay systems while the last one propose an infinite-dimensional control law for a wave equation which is not issued from backstepping. This last paper is closely related to this manuscript and it is therefore proposed in Appendix F. A list of the publications is given below.

International journals

1. M. Barreau, A. Seuret, F. Gouaisbaut, and L. Baudouin. Lyapunov stability analysis of a string equation coupled with an ordinary differential system. *IEEE Transactions on Automatic Control*, 63(11):3850–3857, 2018

2. M. Barreau, F. Gouaisbaut, A. Seuret, and R. Sipahi. Input/output stability of a damped string equation coupled with ordinary differential system. *International Journal of Robust and Nonlinear Control*, 28(18):6053–6069, 2018

3. M. Barreau, F. Gouaisbaut, and A. Seuret. Pratical stability of a drilling pipe under friction with a pi-controller. *IEEE Transaction on Control Systems Technologies*, 2019. Decision pending

International conferences

1. M. Barreau, A. Seuret, and F. Gouaisbaut. Wirtinger-based exponential stability for time-delay systems. In *IFAC World Congress, Toulouse*, volume 50, pages 11984–11989. Elsevier, 2017

2. M. Barreau, F. Gouaisbaut, and A. Seuret. Static state and output feedback synthesis for time-delay systems. In *2018 European Control Conference (ECC)*, pages 1195–1200, 2018

3. M. Barreau, A. Seuret, and F. Gouaisbaut. Exponential Lyapunov stability analysis of a drilling mechanism. In *57th Annual Conference on Decision and Control (CDC), Miami*, pages 2952–2957, 2018

4. M. Barreau, A. Seuret, and F. Gouaisbaut. Stabilization of an unstable wave equation using an infinite dimensional dynamic controller. In *57th Annual Conference on Decision and Control (CDC), Miami*, pages 2952–2957, 2018

Book chapter

1. M. Barreau, A. Seuret, and F. Gouaisbaut. Lyapunov stability of a coupled ordinary differential system and a string equation with polytopic uncertainties. In *Advances on Delays and Dynamics*. Springer, 2019

National journals

1. M. Barreau. Stabilité et stabilisation de systèmes linéaires à l'aide d'inégalités matricielles linéaires. *Quadrature*, July 2019

2

A motivation example : A drilling pipe - models and challenges

The control of a drilling pipe is a rather difficult challenge from the engineering and mathematical points of view. Indeed, even if it is possible to use classical mechanics to derive a third order model for the mechanism [32, 97], this model is not adapted to long pipes where torsional and axial deformations occur all along the well [133]. Furthermore, using the laws of continuum mechanics to derive a PDE leads to a difficult interpretation of the boundary conditions. Then, adding the nonlinear effects due to friction between the bit and the rocks makes the model even more complex.

This introducing chapter is developed as follows. The first section is devoted to a short overview of existing models in the literature, to better motivate the model used and its main features. The second section of this chapter is devoted to the problem statement. In this part, we talk about the mathematical models for drilling and the control objective.

2.1 Drilling pipes' models

A drilling pipe is a mechanism used to pump oil deep under the surface thanks to a drilling pipe as illustrated in Figure 2.1. Throughout the thesis, $\Phi(\cdot, t)$ is the twisting angle along the pipe and then $\Phi(0, t)$ and $\Phi(L, t)$ are the angles at the top and at the bottom of the well respectively. The well is a long metal string of around one kilometer and consequently, the rotational velocity applied at the top using the torque $u_1(t)$ is different from the one at the bottom. Moreover, there is an extra torque at the bottom coming from the interaction of the bit with the rock inducing a fluctuation of the bottom velocity.

As the bit drills the rock, an axial compression of the rod occurs and is denoted Ψ. This compression arises because of the propagation along the string of the vertical force $u_2(t)$ applied at the top to push up and down the well.

This description leads naturally to two control objectives to prevent the mechanism from breaking. The first one is to maintain the rotational speed at the end of the pipe $\Phi(L, t)$ at a constant value denoted here Ω_0, preventing any twisting of the pipe. The other one is to keep the penetration rate constant such that there is no compression along the string.

Several models have been proposed in the literature to achieve these control objectives. They are of very different natures and lead to a large variety of analysis and

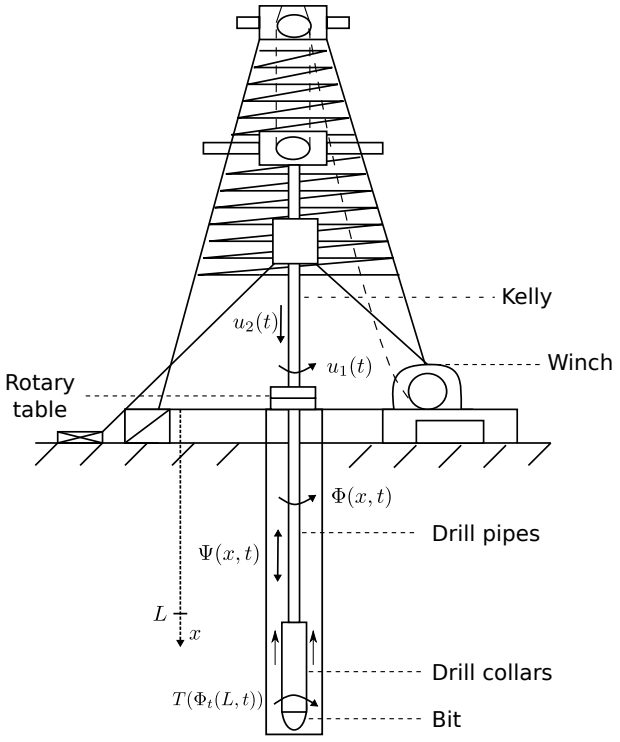

Figure 2.1: Schematic of a drilling mechanism originally taken from [134]. Data corresponding to physical vaues are given in Table 2.2.

control techniques. The book [133, Chap. 2] and the survey [135] provide an overview of these techniques, which are, basically, of four kinds. To better motivate the model used in the sequel, a brief overview of the existing modeling tools is proposed but the reader can refer to [135] and the original papers to get a better understanding of how the models are constructed.

2.1.1 Lumped Parameter Models (LPM)

These models are the first obtained in the literature [32, 97, 140] and the full mechanism is described by a sequence of harmonic oscillators. They can be classified into two main categories:

1. The first kind assumes that the dynamics of the twisting angles $\Phi(0,t) = \Phi_r(t)$ (at the top) and $\Phi(L,t) = \Phi_b(t)$ (at the bottom) are described by two coupled harmonic oscillators. The torque u_1 driving the system is applied on the dynamic of Φ_r and the controlled angle is Φ_b. The axial dynamic is not taken into account in this model. Such a description can be found in [32, 113, 140] for instance.

2. The other two degrees of freedom model is described in [97, 125] for example. There are also two coupled harmonic oscillators for $\Psi(L,t)$ and $\Phi(L,t)$ representing the axial and torsional dynamics. This model only considers the motions at the end of the pipe and forgets about the physics occurring along the string.

Using the fundamental principle of mechanics, the first class of models can be then

Parameter/Physical interpretation		Value
I_r	Rotary table and drive inertia	2122 kg.m^2
I_b	Bit and drillstring inertia	374 kg.m^2
k	Drillstring stiffness	1111 N.m.rad^{-1}
λ_r	Coupled damping at top	425 N.m.s.rad^{-1}
λ_b	Coupled damping at bottom	23.2 N.m.s.rad^{-1}
d_r	Rotary table damping	425 N.m.s.rad^{-1}
d_b	Bit damping	50 N.m.s.rad^{-1}
γ_b	Velocity decrease rate	0.9 s.rad^{-1}
μ_{cb}	Coulomb friction coefficient	0.5
μ_{sb}	Static friction coefficient	0.8
c_b	Bottom damping constant	0.03 N.m.s.rad^{-1}
T_{sb}	Static/Friction torque	15 145 N.m
η_1	Torque decay	5.5
η_2	Velocity decrease rate	2.2 s.rad^{-1}
η_3	Switching time	3500 s

Table 2.1: Description of the parameters for a LPM model, their physical interpretation and their approximate numerical values taken from [32, 113, 140].

described by the following set of equations:

$$\begin{cases} I_r\ddot{\Phi}_r + \lambda_r(\dot{\Phi}_r - \dot{\Phi}_b) + k(\Phi_r - \Phi_b) + d_r\dot{\Phi}_r = u_1, \\ I_b\ddot{\Phi}_b + \lambda_b(\dot{\Phi}_b - \dot{\Phi}_r) + k(\Phi_b - \Phi_r) + d_b\dot{\Phi}_b = -T(\dot{\Phi}_b), \end{cases} \tag{2.1}$$

where the parameters are given in Table 2.1. T is a torque modeled by a nonlinear function of $\dot{\Phi}_b$, it describes the bit-rock interaction[1]. A second-order LPM can be derived by only taking into account the two dominant poles of the previous model.

An example of on-field measurements [140], depicted in Figure 2.2, shows the effect of torque T on the angular speed. The periodic scheme which arises is called *stick-slip*. It emerges because of the difference between the static and Coulomb friction coefficients making an antidamping on the torque function T. Even though the surface angular velocity does not seem to vary much, there is a cycle for the downhole one and the angular speed is periodically close to zero, meaning that the bit is stuck to the rock.

The stick-slip effect appears mostly when dealing with a low desired angular velocity Ω_0 on a controlled drilling mechanism. Indeed, if the angular speed $\dot{\Phi}_b(t)$ is small, the torque provided by the rotary table at $x = 0$ increases the torsion along the pipe. This increase leads to a higher $\dot{\Phi}_b(t)$ but the negative damping on the torque function implies a smaller T. Consequently $\dot{\Phi}_b(t)$ increases, this phenomenon is called the *slipping* phase. Then, the control law reduces the torque in order to match $\dot{\Phi}_r(t)$ to Ω_0. Since the torque increases as well, that leads to a *sticking* phase where $\dot{\Phi}_b(t)$ remains close to 0. A stick-slip cycle then emerges. Notice that this is not the case for high values of Ω_0 since the friction torque T does not vary much with respect to $\dot{\Phi}_b(t)$, making the system easier to control.

[1]See [133, Chap. 3] for a detailed description about various models for T.

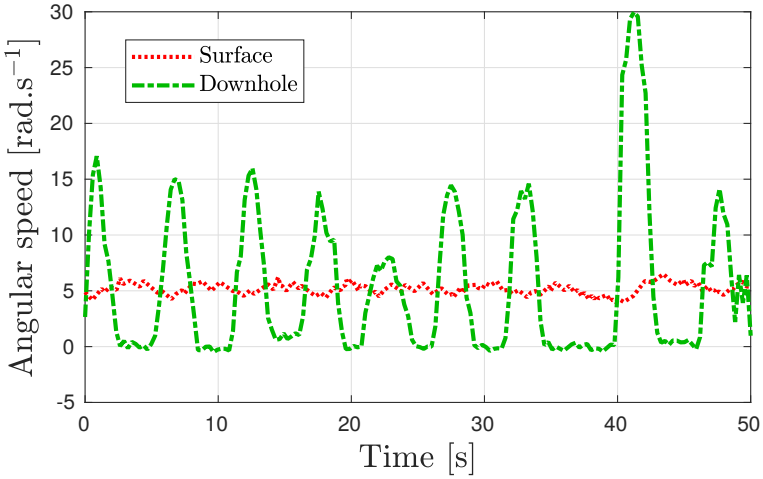

Figure 2.2: Nonlinear effect on the drilling mechanism due to the friction torque at the bottom of the pipe. These measurements are done on the field [140].

Modeling this phenomenon is of great importance as friction effects are quite common when studying mechanical machinery. Some models of T are compared in [135], and the conclusion is that they produce very similar results. The main characteristic is a decrease of T as $\dot{\Phi}_b(t)$ increases. One standard model refers to the preliminary work of Karnopp [81] and Armstrong-Helouvry [6, 7] with an exponential decaying friction term as described in [112] for instance. This law is written thereafter where $\theta = \Phi_t(L, \cdot)$ is expressed in rad.s^{-1}:

$$\begin{cases} T(\theta) = T_l(\theta) + T_{nl}(\theta), \\ T_l(\theta) = c_b\theta, \\ T_{nl}(\theta) = T_{sb}\left(\mu_{cb} + (\mu_{sb} - \mu_{cb})\, e^{-\gamma_b|\theta|}\right)\mathrm{sign}(\theta). \end{cases} \tag{2.2}$$

This model has been used in [113, 133] for instance. A smooth approximation of T_{nl} has been later proposed in [21, 132, 168] and consists in:

$$T_{smooth}(\theta) = \frac{2T_{sb}\mu_{cb}}{\pi}\left(\eta_1\theta e^{-\eta_2|\theta|} + \arctan(\eta_3\theta)\right). \tag{2.3}$$

Parameters η_1, η_2 and η_3 are then obtained from curve fitting with (2.2). This second model catches the observed behavior around $\theta = 0$ in a better way since it should be linear with respect to the angular velocity θ but produces an overshoot for a slightly higher θ. Both torques T_{nl} and T_{smooth} are depicted in Figure 2.3 where $T_{max} = T_{sb}\mu_{sb}$ and $T_{min} = T_{sb}\mu_{cb}$. The nonlinear part induces the so-called stick-slip phenomenon.

Notice that an on-field description of this mechanism applied to the particular context of drilling systems was provided in [2] and concludes that these models are fair approximations of the nonlinear phenomena visible in similar structures. The effectiveness of the two proposed laws to model the torque will be nevertheless shown in the simulation section.

In Appendix D, the describing function methodology is applied on this model and it appears that the stick-slip mechanism is well described.

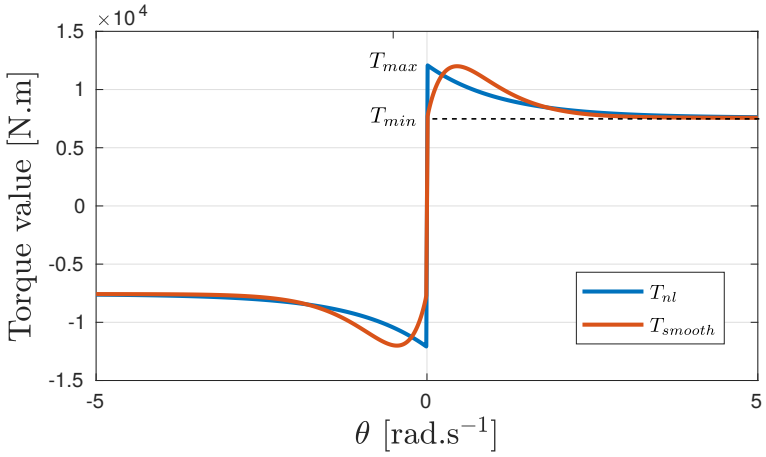

Figure 2.3: Nonlinear part of the torque. T_{nl} and T_{smooth} are both approximations of Karnopp's work [81] on friction.

A LPM gives, in general, a fair approximation for small wells. When the length of the drilling pipe increases, torsional and axial deformations of the pipe need to be considered and it cannot be approximated by an ODE anymore. To go further, we need to consider distributed parameter systems.

2.1.2 Distributed parameter models (DPM)

A deeper modeling can be done with the laws of continuum mechanics. That leads to a set of PDEs as described in the works [35, 165]. This model has been enriched in [1, 2, 51] where the system is presented from a control viewpoint and compared to on-field measurements. In the first papers (see [60] for one of the first control theory analysis of such a system), the model focuses on the propagation of the torsion only along the pipe. The axial propagation was introduced in the model by [1, 135]. The new model is made up of two one-dimensional wave equations representing each deformation for $x \in (0, L)$ and $t > 0$:

$$\Phi_{tt}(x,t) = c_t^2 \Phi_{xx}(x,t) - \gamma_t \Phi_t(x,t), \tag{2.4a}$$
$$\Psi_{tt}(x,t) = c_a^2 \Psi_{xx}(x,t) - \gamma_a \Psi_t(x,t), \tag{2.4b}$$

where again Φ is the twist angle, Ψ is the axial movement, $c_t = \sqrt{G/\rho}$ is the propagation speed of the angle, γ_t is the internal damping, $c_a = \sqrt{E/\rho}$ is the axial velocity and γ_a is the axial distributed damping. A list of physical parameters and their values is given in Table 2.2 and Figure 2.1 helps giving a better understanding of the physical system. In other words, if $\Psi(\cdot, t) = 0$, then there is no compression in the pipe, meaning that the bit does not bounce; if $\Phi_{tt}(\cdot, t) = 0$, then the angular speed along the pipe is the same, meaning that there is no increase or decrease of the torsion.

For the previous model to be well-posed, top and bottom boundary conditions (at $x = 0$ and $x = L$) must be incorporated in (2.4). There is a viscous damping at $x = 0$, and consequently a mismatch between the applied torque at the top and the angular speed. The topside boundary condition for the axial part is built on the same scheme

Parameter/Physical interpretation		Value
L	Pipe length	2000m
G	Shear modulus	79.3×10^9 N.m^{-2}
E	Young modulus	200×10^9 N.m^{-2}
Γ	Drillstring's cross-section	35×10^{-4} m^4
J	Second moment of inertia	1.19×10^{-5} m^4
I_B	Bottom hole assembly lumped inertia	89 kg.m^2
M_B	Bottom hole assembly mass	40 000 kg
ρ	Density	8000 kg.m^3
g	Angular momentum	2000 N.m.s.rad^{-1}
h	Viscous friction coefficient	200 kg.s^{-1}
γ_a	Distributed axial damping	0.69 s^{-1}
γ_t	Distributed angle damping	0.27 s^{-1}
δ	Weight on bit coefficient	1 m^{-1}

Table 2.2: Physical parameters, meanings and their values [1, 135].

and the following conditions are obtained for $t > 0$:

$$GJ\Phi_x(0,t) = g\Phi_t(0,t) - u_1(t), \tag{2.5a}$$
$$E\Gamma\Psi_x(0,t) = h\Psi_t(0,t) - u_2(t). \tag{2.5b}$$

The downside boundary condition ($x = L$) is more difficult to grasp and is consequently derived later when dealing with a more complex model.

2.1.3 Neutral-type time-delay model

The equations obtained previously are damped wave equations, but, for the special case where $\gamma_a = \gamma_t = 0$, the system can be converted into a neutral time-delay system as done in [133]. This new formulation enables to use other tools to analyze its stability as the Lyapunov-Krasovskii theorem [65] or a frequency domain approach [65, 114] making its stability analysis slightly easier. Nevertheless, the main drawback of this formulation is the assumption that the damping occurs at the boundary and not all along the pipe [134]. This useful simplification, even though it is encountered in many articles [27, 133, 134], is known to change in a significant manner the behavior of the system [1]. Indeed, (2.4) becomes a system of transport equations and consequently acts as a delay in the system such that $\Phi_t(0,t)$ is proportional to $\Phi_t(L, t-\tau)$ where $\tau = Lc_t^{-1}$. The velocity at the surface is then directly related to the velocity at the end of the pipe, enabling a delayed observation of the downhole angular speed. The internal damping breaks this proportional rules since it brings an internal dissipation, making the system more difficult to observe.

2.1.4 Coupled ODE/PDE model

To keep the model simple without neglecting the internal damping, a simpler model than the one derived in (2.4) is proposed in [134], where an harmonic oscillator is used

to describe axial vibrations and the model results in a coupled ODE/PDE.
A second possibility, reported in [35, 133] for instance, is to propose a second order ODE as the bottom boundary condition ($x = L$) for $t > 0$:

$$GJ\Phi_x(L,t) = -I_B\Phi_{tt}(L,t) - T\left(\Phi_t(L,t)\right), \tag{2.6a}$$
$$E\Gamma\Psi_x(L,t) = -M_B\Psi_{tt}(L,t) - \delta T\left(\Phi_t(L,t)\right), \tag{2.6b}$$

where T represents the torque applied on the drilling bit by the rocks, described in equation (2.2). Notice that equation (2.6a) is coming from the conservation of angular momentum where $GJ\Phi_x(L,t)$ is the torque coming from the top of the pipe. Equation (2.6b) is the direct application of Newton's second law of motion where $E\Gamma\Psi_x(L,t)$ is the force transmitted from the top to the bit and $\delta T\left(\Phi_t(L,t)\right)$ is the weight on bit due to the rock interaction. Since (2.6) is a second order in time differential equation, note that (2.4) together with (2.6) indeed is coupled ODE/PDE system.

There exist other bottom boundary conditions leading to a more complex coupling between axial and torsional dynamics. They nevertheless introduce delays, which requires to have a better knowledge of the drilling bit. To keep the content general, the boundary conditions (2.6) used throughout this thesis are proposed accordingly with [35, 134, 158].
As a final remark, using some transformations based on (2.7), (2.5a) and (2.6a), it is possible to derive a system for which backstepping controllers can be used [27, 132]. This is the main reason why this model has been widely used up to now.

2.1.5 Models comparison

We propose in this subsection to compare the coupled ODE/PDE model and the lumped parameter models for the torsion only. We consider here a linearization of the system for large Ω_0 and consequently we neglect the stick-slip effect by setting $T = 0$.

First, denote by $\mathcal{H}_{DPM}$ the transfer function from u_1 to $\Phi(1,\cdot)$ for the DPM and $\mathcal{H}_{LPM}$ from u_1 to Φ_b for the LPM. We also define by $\mathcal{H}_{LPM2}$ a truncation of $\mathcal{H}_{LPM}$ considering only the two dominant poles. The Bode diagrams of $\mathcal{H}_{DPM}$, $\mathcal{H}_{LPM}$ and $\mathcal{H}_{LPM2}$ are drawn in Figure 2.4.

Clearly, the LPMs catch the behavior of the DPM at steady states and low frequencies until the resonance, occurring around $\sqrt{k/I_b}$ rad.s^{-1}. From a control viewpoint, the DPM has infinitely many harmonics as it can be seen on the plots but of lower magnitudes and damped as the frequency increases (around -10 dB at each decade). The magnitude plots are not sufficient to make a huge difference between the three models. Nevertheless, considering the phase, we see a clear difference. It appears that the DPM crosses the frequency -180 many times making the control margins quite difficult to assess. Moreover, that shows that the DPM is harder to control because of the huge difference of behavior after the resonance. They may consequently have a very different behavior when controlled. That is why we focus in this study on the DPM, even if it is far more challenging to control than the LPMs.

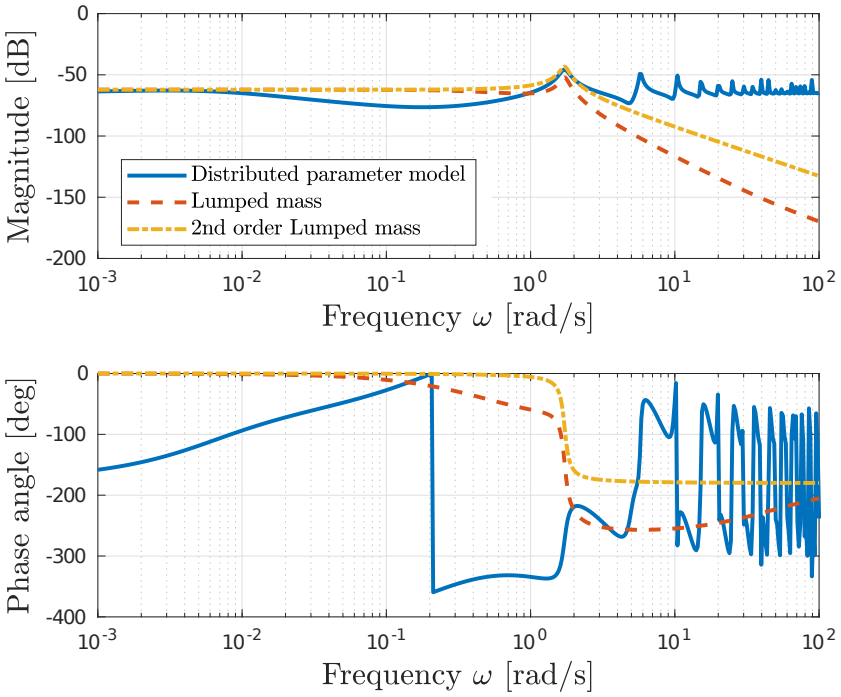

Figure 2.4: Bode diagram of $\mathcal{H}_{DPM}$, $\mathcal{H}_{LPM}$ and $\mathcal{H}_{LPM2}$.

2.2 Problem statement

The coupled nonlinear ODE/PDE model derived in the previous section can be written using normalized parameters. For the twisting dynamics, we get for $t > 0$ and $x \in [0, 1]$:

$$\begin{cases} \phi_{tt}(x,t) = \tilde{c}_t^2 \phi_{xx}(x,t) - \gamma_t \phi_t(x,t), \\ \phi_x(0,t) = \tilde{g}\phi_t(0,t) - \tilde{u}_1(t), \\ \phi_t(1,t) = z_1(t), \\ \dot{z}_1(t) = -\alpha_1 \phi_x(1,t) - \alpha_2 T(z_1(t)). \end{cases} \tag{2.7}$$

The axial dynamics are then:

$$\begin{cases} \psi_{tt}(x,t) = \tilde{c}_a^2 \psi_{xx}(x,t) - \gamma_a \psi_t(x,t), \\ \psi_x(0,t) = \tilde{h}\psi_t(0,t) - \tilde{u}_2(t), \\ \psi_t(1,t) = y_1(t), \\ \dot{y}_1(t) = -\beta_1 \psi_x(1,t) - \beta_2 T(z_1(t)), \end{cases} \tag{2.8}$$

The normalized parameters are given in Table 2.3 and the initial conditions are as follows:

$$\begin{cases} \phi(x,0) = \phi^0(x), & \phi_t(x,0) = \phi^1(x), \\ \psi(x,0) = \psi^0(x), & \psi_t(x,0) = \psi^1(x), \\ z_1(0) = \phi^1(1), & y_1(0) = \psi^1(1). \end{cases}$$

Parameter/Signal	Expression	Value	Parameter/Signal	Expression	Value
$\phi(x,t)$	$\Phi(xL,t)$	-	$\psi(x,t)$	$\Psi(xL,t)$	-
$\tilde{c}_t$	$c_t L^{-1}$	1.57	$\tilde{c}_a$	$c_a L^{-1}$	2.5
α_1	$\frac{GJ}{LI_B}$	5.3	β_1	$\frac{E\Gamma}{LM_B}$	8.75
α_2	I_B^{-1}	$1.12 \cdot 10^{-2}$	β_2	$\frac{\delta}{M_B}$	$2.5 \cdot 10^{-5}$
$\tilde{g}$	$\frac{g}{GJ}$	$2.1 \cdot 10^{-3}$	$\tilde{h}$	$\frac{h}{E\Gamma}$	$2.86 \cdot 10^{-7}$
$\tilde{u}_1(t)$	$\frac{1}{GJ}u_1(t)$	-	$\tilde{u}_2(t)$	$\frac{1}{E\Gamma}u_2(t)$	-

Table 2.3: Normalized parameters for a drilling pipe.

A proof of existence and uniqueness of a solution to (2.7)-(2.8) could be done using the tools of the following section in the linearized case. Nevertheless, this problem has been widely studied (see [21, 27, 132, 134, 158] among many others) and since it is not the main contribution of this thesis, *the existence and uniqueness of a solution to the previous problem is assumed* in the sequel. If the initial conditions satisfy the boundary conditions with the following regularity

$$(\phi^0, \phi^1, \psi^0, \psi^1) \in (\mathbb{X}_1)^2 = \left(H^2 \times H^1\right)^2$$

then, (see [20] and the following section for more details), there exists a unique solution to our problem and:

$$(\phi, \phi_t, \psi, \psi_t, z_1, y_1) \in C^0(\mathbb{X}_1^2 \times \mathbb{R}^2).$$

System (2.7)-(2.8) can be divided into two cascaded subsystems:

1. System (2.7) with a coupled nonlinear ODE/string equation describing the torsion angle ϕ.

2. System (2.8) with a coupled linear ODE/string equation subject to an external perturbation (here $T(z_1)$) for the axial displacement.

It appears quite clearly that the perturbation on the second subsystem depends on the first subsystem in ϕ. Then, a first step consists in studying system (2.7), which describes the dynamic of ϕ only. The response of the system for $\tilde{u}_1 = \Omega_0 = 10$ is shown in Figure 2.5. We can clearly see that without closing the loop we get an unstable system. Consequently, we would like to solve the following problem.

Problem 1: Control of the torsion system (2.7)

Let $\Omega_0 > 0$ be the desired angular speed.
The control objective is to maintain the rotational speed at the end of the pipe $\phi(1,t)$ close to the constant value Ω_0.

This problem is related to the practical stability[2] since it is, most of the time, acceptable from an engineering point of view while the classical definitions of exponential or asymptotic stability are more dedicated to "theoretical problems". These two notions are nevertheless highly related as we will see in the following chapter.

[2]This is also called ultimate boundedness in [82] or dissipativity in [95].

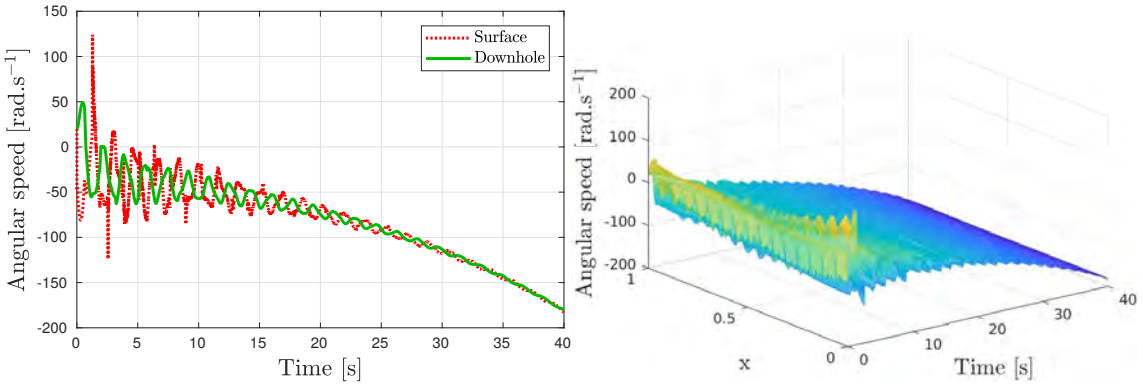

(a) $\phi_t(0,\cdot)$ and $\phi_t(1,\cdot)$ (b) $\phi(1,\cdot)$

Figure 2.5: Open loop response of systems (2.7) to a step for $\tilde{u}_1 = \Omega_0 = 10$ rad.s^{-1}.

2.3 Conclusion

This chapter presented a short overview of existing models for a drilling pipe. There are numerous ways to describe the phenomena arising in this mechanism. This chapter shows that the obtained models are consistent one with the other but the one that seems the closest to the real behavior of the system is the coupled ODE/string equation. At the end, we stated the problem dealt in the final chapter of this manuscript. Since studying this nonlinear and infinite-dimensional system is rather challenging, we propose to develop our methods on a simpler system, made up of an ODE and a PDE, described in the following chapter. Then, after understanding the methodology, we can come back to the drilling problems.

3

Coupled linear ODE/string equation: Notions of existence and stability

From a more mathematical point of view, the most complex resulting model of the previous chapter is a coupled nonlinear ODE/PDE. Since stating the existence and uniqueness of a solution to this problem is really demanding, a simpler system is proposed in this chapter. This thesis focuses on how to manage the infinite-dimensional characteristic of the previous problem, that is why we consider here a coupled linear ODE/string equation system. This system is very close to the drilling mechanism but it forgets about the nonlinearity.

The first section aims at introducing this new system and why it is interesting. We formally prove the existence of a solution using the strongly continuous semi-group theory [41, 100, 162]. The second section is an introducing part about the basic concepts in stability analysis. The stability notions are defined depending on the context and they are finally related to the control objective of the previous chapter.

3.1 Existence of a solution to a coupled ODE/string equation

The model derived in equations (2.7)-(2.8) is a coupled nonlinear ODE/string equation. Since it is rather difficult to study this system directly, we propose to simplify the problem by removing the nonlinearity. That leads to a coupled ODE/string equation. This part focuses on proving the existence and uniqueness of a solution to this simpler system.

3.1.1 A toy-example of a linear coupled system

Let consider the slightly different and simpler toy-example, depicted in Figure 3.1:

$$\dot{X}(t) = AX(t) + Bu(1,t), \qquad t \geq 0, \tag{3.1a}$$
$$u_{tt}(x,t) = c^2 u_{xx}(x,t), \qquad x \in [0,1], t \geq 0, \tag{3.1b}$$
$$u(0,t) = KX(t), \qquad t \geq 0, \tag{3.1c}$$
$$u_x(1,t) = -c_0 u_t(1,t), \qquad t \geq 0, \tag{3.1d}$$

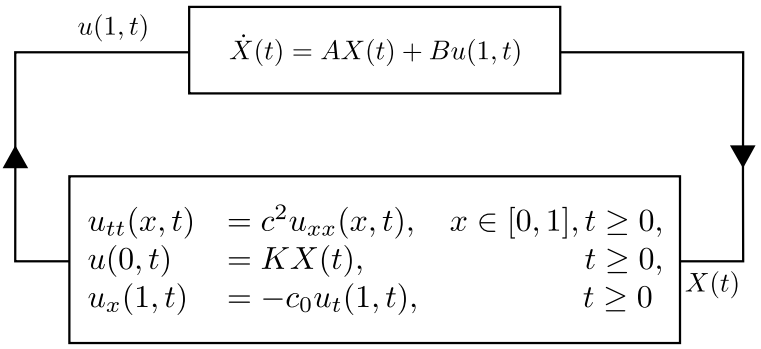

Figure 3.1: Block diagram for the system described by equation (3.1).

with the following initial conditions:

$$u(x,0) = u^0(x), \qquad x \in [0,1], \tag{3.2a}$$
$$u_t(x,0) = v^0(x), \qquad x \in [0,1], \tag{3.2b}$$
$$X(0) = X^0, \tag{3.2c}$$

We assume that $X^0 \in \mathbb{R}^n$ and $(u^0, v^0) \in \mathbb{X}_1 = H^2 \times H^1$ such that equations (3.1c) and (3.1d) are respected. In this case, the initial conditions (X^0, u^0, v^0) are compatibles with the boundary conditions.

System (3.1) represents the interconnection of a linear time invariant system with a string equation. Here, the state u denotes the amplitude of the wave, which belongs to a functional space and consequently is of infinite dimension. We assume that the state $u(x,t)$ belongs to $\mathbb{R}$ but the analysis described in the following chapters can be extended without difficulty to $\mathbb{R}^m$, $m > 1$.

The overall system is composed by two subsystems: The ODE described by equation (3.1a) and the PDE related to equations (3.1b)-(3.1c) and (3.1d). The input of the PDE is defined as $u(0,\cdot)$ and its output is $u(1,\cdot)$. They are both of Dirichlet kind, that is, the output and the input depend on the state u at different positions but not on its derivative.

For the system to be well-posed, another boundary condition is needed. The so-called boundary damping equation (3.1d) is commonly used. It has been shown in [64, 92], for instance, that this boundary condition ensures the stability of the wave equation itself; i.e. $K = 0$, if and only if $c_0 > 0$. The case $c_0 = 0$ removes the damping, leading to a "pure" wave equation. Finally, $c_0 < 0$ makes the subsystem unstable. Notice that these two subsystems can be coupled (or interconnected) if $K = 0$ or $B = 0$. Otherwise, they are cascaded. This is explained by the block diagrams in Figure 3.2, where one can easily understand the different natures of the interconnection.

(a) Coupled system (3.1) with $B \neq 0$ and $K \neq 0$ (b) Cascaded system (3.1) with $B = 0$ (top) and $K = 0$ (bottom)

Figure 3.2: Block diagrams of coupled and cascaded systems represented by (3.1).

Remark 3.1

The wave equation operator associated to the boundary conditions described above is known to be diagonalizable[a]. Once diagonalized, it can be expressed as the composition of two transport equations, one going forward and another backward. Boundary condition (3.1d) implies a reflection of the forward wave with a coefficient $\alpha = \frac{1-cc_0}{1+cc_0}$ as explained in [99]. Enforcing $c_0 > 0$ implies $|\alpha| < 1$ and, consequently, the energy of the wave is decreasing.

[a]To see the detailed proof of this statement, the reader can refer to [100], [162] and the references therein.

There are several practical interpretations of this system. Hence, the string equation can be seen for instance as a communication channel and we study the robustness of the ODE subject to this communication constraint. On the other hand, we can study the string equation and see the ODE as a controller to enhance the performance of the PDE. These two cases lead to three different scenarii:

1. The ODE and the PDE are asymptotically stable. Then we study the robustness of the interconnection. The ODE can be seen as a filter which aims at enhancing the performance of the coupled system.

2. The ODE is unstable and the PDE is stable. The focus is then made on the stabilizing properties of the string equation.

3. The PDE is unstable. The ODE can be seen then as a controller for the PDE.

It appears that most of the works today [33, 54, 107, 109, 152, 154, 166] deal with the first case and present a robustness result. The second case is less classical and uses the stabilizing effect of the PDE to compensate the unstable behavior of the ODE. There does not exist many examples in the literature of such systems since proving the stability of this interconnection is rather tedious. Note that in the case of a stable closed-loop ODE, i.e. $A+BK$ is Hurwitz, and with a fast wave equation, i.e. c is large, [34] shows that we can use the singular perturbation methodology and get the stability of the closed-loop system.

The third case is dealt for instance in [41] where it is shown that the proposed interconnection cannot be stable if the PDE is unstable. This case illustrates the notion of ill-posed problem from a control viewpoint, studied in [73, 107, 108, 109] for

instance. There are many other names for a similar definition as small-τ stabilizability (coming from [22, 67, 116] and derived in the following chapter). This phenomenon can be understood as follows. If the PDE is unstable, i.e. $c_0 < 0$, there are infinitively many poles in the right-half plane [14]. Consequently, there does not exist a proper finite-dimensional controller moving infinitively many poles in the left-half plane. On the contrary, if $c_0 = 0$, there might exist a controller ensuring the asymptotic stabilization of the coupled system but it cannot be robust to any delay in the loop, which is not acceptable from a practical viewpoint [73, 107]. That is the reason why we decided not to address this last scenario and focus on the two first ones.

The existence of a solution and its regularity is not the main concern of this manuscript. The focus is made on stability analysis and, consequently, its dissipativity. Nevertheless, studying the wellposedness of the interconnection is one key point before studying its stability. Indeed, in some cases, knowing the regularity of the solution helps proving stability (see [102] among many others for instance). For proving the wellposedness of the interconnection, we propose to derive the operator formulation of system (3.1). To this extend, we introduce the following notations for $(X, u, v) \in \mathbb{R}^n \times \mathbb{X} = \mathbb{R}^n \times H^1 \times L^2$:

$$\begin{aligned}
\mathscr{A} : \ \mathbb{R}^n \times \mathbb{X} &\to \mathbb{R}^n \times \mathbb{X} \\
\begin{bmatrix} X \\ u \\ v \end{bmatrix} &\mapsto \begin{bmatrix} A & 0 & 0 \\ 0 & 0 & 1 \\ 0 & c^2\partial_{xx} & 0 \end{bmatrix} \begin{bmatrix} X \\ u \\ v \end{bmatrix} + \begin{bmatrix} Bu(1) \\ 0 \\ 0 \end{bmatrix}, \\
\mathscr{D}(\mathscr{A}) = \{(X, u, v) \in \mathbb{R}^n \times \mathbb{X}_1 \mid\ & u(0) = KX,\ v(0) = K(AX + Bu(1)), \\
& u_x(1) = -c_0 v(1)\},
\end{aligned} \tag{3.3}$$

where $\mathbb{X}_1 = H^2 \times H^1$. The space $\mathbb{R}^n \times \mathbb{X}$ is the smallest set giving a meaning to operator $\mathscr{A}$ if the derivative is understood in the weak sense. The following subsection aims at showing that there exists a unique solution to system (3.1), modeled as follows for $t \geq 0$:

$$\begin{aligned}
&\frac{d}{dt} \begin{bmatrix} X(t) \\ u(t) \\ v(t) \end{bmatrix} = \mathscr{A} \begin{bmatrix} X(t) \\ u(t) \\ v(t) \end{bmatrix}, \\
&u(0,t) = KX(t), \quad u_x(1,t) = -c_0 v(1,t), \quad v(0) = K(AX + Bu(1)), \\
&(X(0), u(\cdot,0), v(\cdot,0)) = (X^0, u^0, v^0) \in \mathscr{D}(\mathscr{A}).
\end{aligned} \tag{3.4}$$

3.1.2 The strongly continuous semi-group theory in this context

The existence of a solution to an infinite-dimensional system leads to much more difficulties compared to finite-dimensional problems since there does not exist any on-the-shelf Cauchy theorem. But, there are many other ways to prove the existence and uniqueness of a solution. One can, for example, use a Galerkin-like methodology [55]. A more formal and traditional way is to use the famous Lax-Milgram theorem [28, Corollary 5.8] which relies on Banach fixed-point theorem. This is nevertheless quite tedious and is left for some nonlinear systems. We can also express the problem using an operator

formulation and then use Hile-Yosida theorem (Theorem 7.4 from [28] for instance), especially if the operator is linear.

From a system theory perspective, the most intuitive concept is the so-called strongly continuous semi-group theory [41, 100, 106, 162]. This subsection is devoted to some key-results and definitions in this field. The concept of strongly continuous semigroup [41, Definition 2.1.2] is at the core of this theory and is defined in the context of (3.1) in the following definition.

Definition 3.1: Strongly continuous semigroup

Let $\mathbb{X} = H^1 \times L^2$ and $\mathbb{X}_1 = H^2 \times H^1$.
A **strongly continuous semigroup** is an operator-valued function $\mathbb{T}_t$ from $\mathbb{R}^+$ to the set of bounded linear operators from $\mathbb{R}^n \times \mathbb{X}$ into itself that satisfies the following properties:

$$\mathbb{T}_{t+s} = \mathbb{T}_t \mathbb{T}_s, \qquad \text{for } t, s \geq 0, \tag{3.5a}$$

$$\mathbb{T}_0 = I, \tag{3.5b}$$

$$\left\| \mathbb{T}_t \begin{bmatrix} X \\ u \\ v \end{bmatrix} - \begin{bmatrix} X \\ u \\ v \end{bmatrix} \right\| \xrightarrow[t \to 0^+]{} 0, \qquad \forall \begin{bmatrix} X \\ u \\ v \end{bmatrix} \in \mathbb{R}^n \times \mathbb{X}. \tag{3.5c}$$

$\mathbb{T}_t$ is also called a C_0-semigroup for brevity.

To better motivate this definition, consider the following ODE:

$$\dot{X} = AX, \quad X(0) = X^0 \in \mathbb{R}^n,$$

where $A \in \mathbb{R}^{n \times n}$. It is well-known that a solution to the previous problem is

$$t \in [0, \infty] \mapsto e^{At} X^0.$$

Definition 3.1 enlarges the concept of exponential of a matrix to the highly more abstract concept of the "exponential of an operator". Example 2.1.3 from [41] shows that the function $t \mapsto \exp(At)$ indeed satisfies the three properties (3.5). Property (3.5c) is also known as "strong continuity" and implies that the solution continuously depends on its initial condition.

Note that $\frac{1}{t}\left(e^{At} - I_n\right) \xrightarrow[t \to 0]{} A$, and pursuing the same idea, it appears that a C_0-semigroup is generated by an operator defined as follows [41, Definition 2.1.8].

Definition 3.2: Infinitesimal generator of a C_0-semigroup

The **infinitesimal generator** $\mathscr{A}$ of a C_0-semigroup on $\mathbb{R}^n \times \mathbb{X}$ is defined by

$$\mathscr{A} \begin{bmatrix} X \\ u \\ v \end{bmatrix} = \lim_{t \to 0^+} \frac{1}{t} \left(\mathbb{T}_t - I \right) \begin{bmatrix} X \\ u \\ v \end{bmatrix},$$

whenever the limit exists; the domain of $\mathscr{A}$, $\mathscr{D}(\mathscr{A})$ being the set of elements in $\mathbb{R}^n \times \mathbb{X}_1$ for which the limit exists.

Thanks to the previous definition, it appears that if the semi-group generated by $\mathscr{A}$ exists, then there is a unique solution to (3.4). Such a conclusion nevertheless requires more calculations, summarized by the following proposition [162, Theorem 2.3.5].

Proposition 3.1: Existence and uniqueness of a solution

Let $\mathbb{T}_t$ be a C_0-semigroup on $\mathbb{R}^n \times \mathbb{X}$ with infinitesimal generator $\mathscr{A}$. Let $(X^0, u^0, v^0) \in \mathscr{D}(\mathscr{A})$ and define the following function:

$$\begin{array}{rccc} (X,u,v): & [0,\infty) & \to & \mathscr{D}(\mathscr{A}) \\ & t & \mapsto & \mathbb{T}_t \left[\begin{smallmatrix} X^0 \\ u^0 \\ v^0 \end{smallmatrix}\right]. \end{array}$$

Then (X,u,v) is continuous[a] and $(X,u,v) \in C^1([0,\infty), \mathbb{R}^n \times \mathbb{X}_1)$. Moreover, it is the unique function with these properties satisfying the initial value problem (3.4).

[a] The space $\mathscr{D}(\mathscr{A})$ is equipped with the graph norm $\|(X,u,v)\|_{\mathbb{R}^n\times\mathbb{X}_1} + \|\mathscr{A}(X,u,v)\|_{\mathbb{R}^n\times\mathbb{X}_1}$.

Expressed differently, we say that the solution (X,u,v) is complete. The previous proposition is useful but it is quite difficult in practice to explicitly determine $\mathbb{T}_t$ using Definition 3.2. There exists another way to prove that $\mathscr{A}$ is the infinitesimal generator of a C_0-semigroup without explicitly determining $\mathbb{T}_t$.

Proposition 3.2: Existence of a C_0-semigroup

Let $\mathscr{A} : \mathscr{D}(\mathscr{A}) \to \mathbb{R}^n \times \mathbb{X}$ and $\langle \cdot, \cdot \rangle_{\mathscr{D}(\mathscr{A})}$ be a scalar product on $\mathscr{D}(\mathscr{A})$. If there exists $w \in \mathbb{R}$ and $s_0 \in \mathbb{R}^+$ such that

$$\left\langle \mathscr{A} \left[\begin{smallmatrix} X \\ u \\ v \end{smallmatrix}\right], \left[\begin{smallmatrix} X \\ u \\ v \end{smallmatrix}\right] \right\rangle_{\mathscr{D}(\mathscr{A})} \leq \omega \|(X,u,v)\|_{\mathscr{D}(\mathscr{A})}, \quad \text{for } (X,u,v) \in \mathscr{D}(\mathscr{A}), \tag{3.6}$$

$$\forall s > s_0, \quad \left\{ (sI - \mathscr{A}) \left[\begin{smallmatrix} X \\ u \\ v \end{smallmatrix}\right] \mid \left[\begin{smallmatrix} X \\ u \\ v \end{smallmatrix}\right] \in \mathscr{D}(\mathscr{A}) \right\} = \mathbb{R}^n \times \mathbb{X}, \tag{3.7}$$

then $\mathscr{A}$ is the infinitesimal generator of a C_0-semigroup.

Proof : This proposition is an adaption of [41, Corollary 2.2.3], but with a quite different proof. First, rewrite equation (3.6) to the following equivalent expression for $(X,u,v) \in \mathscr{D}(\mathscr{A})$:

$$\left\langle (\mathscr{A} - wI) \left[\begin{smallmatrix} X \\ u \\ v \end{smallmatrix}\right], \left[\begin{smallmatrix} X \\ u \\ v \end{smallmatrix}\right] \right\rangle \leq 0.$$

Consequently, $\mathscr{A}_2 = \mathscr{A} - wI$ is dissipative (see Definition 3.1.1 from [162]). It is obvious from Definition 3.2 that $\mathscr{D}(\mathscr{A}_2) = \mathscr{D}(\mathscr{A} - wI) = \mathscr{D}(\mathscr{A})$ and consequently for $s \in \mathbb{R}^+$:

$$\left\{ (sI - \mathscr{A}_2) \left[\begin{smallmatrix} X \\ u \\ v \end{smallmatrix}\right] \mid \left[\begin{smallmatrix} X \\ u \\ v \end{smallmatrix}\right] \in \mathscr{D}(\mathscr{A}_2) \right\} = \left\{ ((s+w)I - \mathscr{A}) \left[\begin{smallmatrix} X \\ u \\ v \end{smallmatrix}\right] \mid \left[\begin{smallmatrix} X \\ u \\ v \end{smallmatrix}\right] \in \mathscr{D}(\mathscr{A}) \right\}.$$

Then, for all $s > \max(s_0 + w, 0)$, thanks to (3.7), we get:

$$\left\{ (sI - \mathscr{A}_2) \left[\begin{smallmatrix} X \\ u \\ v \end{smallmatrix}\right] \mid \left[\begin{smallmatrix} X \\ u \\ v \end{smallmatrix}\right] \in \mathscr{D}(\mathscr{A}_2) \right\} = \mathbb{R}^n \times \mathbb{X}.$$

Using now Lumer-Phillips theorem [162, Theorem 3.8.4], we get that $\mathscr{A}_2$ generates a C_0-semigroup $\mathbb{T}_{2,t}$. Let now $\mathbb{T}_t = \mathbb{T}_{2,t} e^{wt} = e^{wt} \mathbb{T}_{2,t}$, since $\mathbb{T}_{2,t}$ is a C_0-semigroup, we get

the following:

$$\begin{aligned}
&\mathbb{T}_0 = I,\\
&\mathbb{T}_t\mathbb{T}_s = \mathbb{T}_{2,t}e^{wt}\mathbb{T}_{2,s}e^{ws} = \mathbb{T}_{2,t+s}e^{w(t+s)} = \mathbb{T}_{t+s}, && \text{for all } t,s \in \mathbb{R}^+,\\
&\left\|\mathbb{T}_t \begin{bmatrix} X \\ u \\ v \end{bmatrix} - \begin{bmatrix} X \\ u \\ v \end{bmatrix}\right\| = \left\|\mathbb{T}_{2,t}e^{wt} \begin{bmatrix} X \\ u \\ v \end{bmatrix} - \begin{bmatrix} X \\ u \\ v \end{bmatrix}\right\| \xrightarrow[t\to 0^+]{} 0, && \forall \begin{bmatrix} X \\ u \\ v \end{bmatrix} \in \mathbb{R}^n \times \mathbb{X}_1.
\end{aligned}$$

Then, according to Definition 3.1, $\mathbb{T}_t$ is a C_0-semigroup. We get that

$$\lim_{t\to 0^+} \frac{1}{t}\left(\mathbb{T}_t - I\right) = \lim_{t\to 0^+} \frac{1}{t}\left(\mathbb{T}_{2,t}e^{wt} - I\right) = \lim_{t\to 0^+} \frac{1}{t}\left(\mathbb{T}_{2,t}(1+wt) - I\right) = \mathscr{A}$$

and using Definition 3.2, $\mathscr{A}$ is the infinitesimal generator of $\mathbb{T}_t$. ♢

Compared to traditional existence theorems, the previous proposition does not require the solution to be stable. In Lumer-Phillips theorem [162, Theorem 3.8.4], the generated C_0-semigroup $\mathbb{T}_t$ is necessarily a contraction semigroup since $w \leq 0$. Formulated in terms of control theory, that means we can only prove the existence of a solution to a stable system, which is quite conservative. The concept in Proposition 3.2 is less restrictive than dissipativity and is called quasi-dissipativity in [20, Appendix A]. To say it simply, condition (3.6) guarantees that the solution (X, u, v) does not blow up in finite time and that its estimate is an unbounded exponential. Condition (3.7) is related to the density of $\mathscr{D}(\mathscr{A})$ in $\mathbb{R}^n \times \mathbb{X}$. Note that if $\mathscr{D}(\mathscr{A})$ is not well-defined, then conditions (3.6) and (3.7) cannot hold.

Remark 3.2: On the sufficiency of Proposition 3.2

Considering finite-dimensional systems, Cauchy theorem [28, Theorem 7.3] states that there always exists a solution for an infinitesimal generator $A \in \mathbb{R}^{n\times n}$. Proposition 3.2 provides an equivalent formulation in this case. Equations (3.6) and (3.7) hold if A has bounded complex eigenvalues, which is always true.
One can also note that Proposition 3.2 is not a necessary and sufficient condition for the existence of a C_0-semigroup, such a theorem is derived in [118, Chap. 1] but requires different conditions.

3.1.3 Existence of a solution to the interconnected system

The aim of this subsection is to use the semigroup theory developed in the previous subsection for system (3.1). Using Proposition 3.2, we get the following theorem.

Theorem 3.1: Existence and regularity of the solution to (3.1)

Assume $c_0 > 0$. If $(X^0, u^0, v^0) \in \mathscr{D}(\mathscr{A})$, then there exists a unique solution (X, u, u_t) to system (3.1) with the following regularity property:

$$(X, u, u_t) \in C([0,+\infty), \mathscr{D}(\mathscr{A})) \cap C^1([0,+\infty), \mathbb{R}^n \times \mathbb{X}).$$

Moreover, u, u_t, u_x, u_{tt} and u_{xx} are L^2 on each compact set of $\mathbb{R}^+$.

The proof is technical and is not of main importance in the sequel, it is therefore detailed in Appendix A.

Remark 3.3: Weak solutions to system (3.1)

According to Propositions 2.10.1 and 2.10.2 and Remark 4.1.2 from [162] (or equivalently [41, Theorem 3.1.7]), there exists a unique weak solution (defined in [55, p. 7]) to system (3.1) in $\mathbb{R}^n \times \mathbb{X}$. This can be proven using a density argument and [162, Theorem 3.1.7] and we get that for $(X^0, u^0, v^0) \in \mathbb{R}^n \times \mathbb{X}_1$, the solution of (3.1) has the following regularity:

$$(X, u, u_t) \in C([0, +\infty), \mathbb{R}^n \times \mathbb{X}).$$

Note that the previous theorem does not state the existence of a solution to nonlinear system (2.7) -(2.8). The techniques are really different for this nonlinear problem and we do not explore them in this manuscript.

3.2 Stability analysis of a coupled ODE/string equation

As said previously, the aim of this thesis is not to prove the existence of solutions to (3.1) but to characterize the behavior of the trajectory. The existence of a solution is then a prerequisite.

We can briefly define stability analysis as the response of a system to a perturbation. This perturbation can be of different kinds, leading to different notions of stability. This section provides some useful definitions used in the sequel. It is divided in two subsections since we are not interested in this thesis by the same objectives whether the system is linear or not.

3.2.1 Notions of stability for the toy-example

The first chapters of this manuscript are dedicated to the stability analysis of a linear system. Two notions of stability are investigated here. The first one, called input/output stability studies the behavior of a trajectory with an exogenous perturbation. The second kind of stability is referred to as exponential stability and focuses on the response of the system to initial conditions.

Input/Output stability

In this case, we study the response of a system to an input and we forget about the transient behavior due to the initial conditions. Then, we naturally need to slightly

change the system to introduce an input r and an output y:

$$\begin{aligned}
\dot{X}(t) &= AX(t) + B\left(u(1,t) + r(t)\right), && t \geq 0, && \text{(3.8a)}\\
y(t) &= KX(t), && t \geq 0, && \text{(3.8b)}\\
u_{tt}(x,t) &= c^2 u_{xx}(x,t), && x \in [0,1], t \geq 0, && \text{(3.8c)}\\
u(0,t) &= y(t), && t \geq 0, && \text{(3.8d)}\\
u_x(1,t) &= -c_0 u_t(1,t), && t \geq 0, && \text{(3.8e)}\\
& && && \text{(3.8f)}
\end{aligned}$$

with the following initial conditions:

$$\begin{aligned}
X(0) &= 0, && && \text{(3.9a)}\\
u(x,0) &= 0, && x \in [0,1], && \text{(3.9b)}\\
u_t(x,0) &= 0, && x \in [0,1]. && \text{(3.9c)}
\end{aligned}$$

Compared to (3.1), the input is the function r and the initial conditions (3.9b), (3.9c) and (3.9a) are set to 0. Note that the input affects directly the ODE (3.8a) and indirectly (3.8d) and (3.8e), meaning that the initial conditions are still compatible with the boundary conditions, no matter the value of $r(0)$. This consideration implies that Proposition 3.2 applies to (3.8)-(3.9) and the solution still exists with the same regularity.

The notions of input/output stability is then easy to define in this context. Using energy considerations, we say that a system is stable if it does not create energy, in other words, if it is dissipative. Since there is an input, we want to show that the energy inside the system remains bounded if the input is of bounded energy. This concept is formalized by the following definition.

Definition 3.3: Input/Output stability

System (3.8)-(3.9) is said to be **input/output stable** if there exists $\gamma > 0$ such that the following holds:

$$\forall T > 0, \quad \forall r \in L^2([0,T],\mathbb{R}), \qquad \int_0^T |y(t)|^2 dt \leq \gamma \int_0^T |r(t)|^2 dt.$$

Chapter 4 studies the input/output stability of system (3.8)-(3.9).

Asymptotic and exponential stability of an equilibrium point

This part is dedicated to the concept of stability of an equilibrium point. We do not consider any input here but we keep the intuitive notion of stability: the system should not generate energy. That means here that we give an energy at $t = 0$ and we want to show that the energy inside the system does not blow infinitely. More formally, we define the energy of the system using a norm on $\mathscr{D}(\mathscr{A})$.

Definition 3.4: Norm on $\mathscr{D}(\mathscr{A})$

For $(X, u, v), (\bar{X}, \bar{u}, \bar{v}) \in \mathscr{D}(\mathscr{A})$, we define the following inner product and norm:

$$\begin{aligned}\langle (X, u, v), (\bar{X}, \bar{u}, \bar{v}) \rangle_{\mathscr{D}(\mathscr{A})} &= X^\top \bar{X} + \langle u, \bar{u} \rangle_{L^2} + c^2 \langle u_x, \bar{u}_x \rangle_{L^2} + \langle v, \bar{v} \rangle_{L^2}, \\ \|(X, u, v)\|^2_{\mathscr{D}(\mathscr{A})} &= \langle (X, u, v), (X, u, v) \rangle_{\mathscr{D}(\mathscr{A})} \\ &= \|X\|_n^2 + \|u\|^2_{L^2} + c^2 \|u_x\|^2_{L^2} + \|v\|^2_{L^2}.\end{aligned}$$

Remark 3.4

Of course, $\|\cdot\|_{\mathscr{D}(\mathscr{A})}$ is equivalent to $\|\cdot\|_{\mathbb{R}^n \times \mathbb{X}}$.

There exist some particular trajectories of system (3.1) for which the energy is not varying and remains constant. The definition of stability depends on these points.

Definition 3.5: Equilibrium point of (3.1)

A point $(X_e, u_e, v_e) \in \mathscr{D}(\mathscr{A})$ is **an equilibrium point** of (3.1) if the trajectory $(X, u, v) \in C^1([0, \infty), \mathbb{R}^n \times \mathbb{X})$ of (3.1) with initial condition (X_e, u_e, v_e) verifies the following:

$$\forall t > 0, \qquad \|(\dot{X}, \dot{u}, \dot{u}_t)\|_{\mathscr{D}(\mathscr{A})} = 0_{\mathbb{R}^n \times \mathbb{X}_1}.$$

The equilibrium points of (3.1) are studied in the following proposition.

Proposition 3.3: Equilibrium points of system (3.1)

An equilibrium $(X_e, u_e, v_e) \in \mathscr{D}(\mathscr{A})$ of system (5.2) verifies

$$(A + BK)X_e = 0, \quad u_e = KX_e, \quad v_e = 0.$$

Moreover, if $A + BK$ is not singular, there is a unique equilibrium $0_{\mathbb{R}^n \times \mathbb{X}}$.

Proof : Since the trajectory u_e and v_e are continuous, an equilibrium point $(X_e, u_e, v_e) \in \mathscr{D}(\mathscr{A})$ of system (5.2) is such that:

$$\begin{aligned} 0 &= AX_e + Bu_e(1), && && \text{(3.10a)} \\ 0 &= c^2 \partial_{xx} u_e(x), && x \in [0, 1], && \text{(3.10b)} \\ v_e(x) &= 0, && x \in [0, 1], && \text{(3.10c)} \\ u_e(0) &= KX_e, && && \text{(3.10d)} \\ \partial_x u_e(1) &= 0. && && \text{(3.10e)} \end{aligned}$$

A solution to equation (3.10b) is $u_e(x) = ax + b$ where $a, b \in \mathbb{R}$. In accordance to equation (3.10e), u_e is a constant function and using equation (3.10d), we get $u_e = KX_e$. Since (3.10a) holds, that leads to: $(A + BK)\, X_e = 0$. ♢

The definitions of stability and asymptotic stability are then a direct interpretation of what we said previously.

Definition 3.6: Stability and asymptotic stability [61, Definition 1.3]

1. An equilibrium point $(X_e, u_e, v_e) \in \mathscr{D}(\mathscr{A})$ is **stable** if for $\varepsilon > 0$, there exists $\delta > 0$ such that the following holds for all $(X^0, u^0, v^0) \in \mathscr{D}(\mathscr{A})$:

$$\|(X^0 - X_e, u^0 - u_e, v^0 - v_e)\|_{\mathscr{D}(\mathscr{A})} < \delta$$
$$\Rightarrow \ \forall t \geq 0, \ \|(X(t) - X_e, u(t) - u_e, u_t(t) - v_e)\|_{\mathscr{D}(\mathscr{A})} < \varepsilon,$$

   for the trajectory (X, u, v) of (3.1) with initial condition (X^0, u^0, v^0).

2. An equilibrium point $(X_e, u_e, v_e) \in \mathscr{D}(\mathscr{A})$ is **asymptotically stable** if it is stable and for any $(X^0, u^0, v^0) \in \mathscr{D}(\mathscr{A})$, the following holds:

$$\lim_{t\to\infty} \|(X(t) - X_e, u(t) - u_e, u_t(t) - v_e)\|_{\mathscr{D}(\mathscr{A})} = 0,$$

   for the trajectory (X, u, v) of (3.1) with initial condition (X^0, u^0, v^0).

We are interested in this thesis only in *global* properties and consequently, the previous definitions have a meaning only if there is a unique equilibrium point $(X_e, u_e, v_e) \in \mathscr{D}(\mathscr{A})$. In other words, we require to have $A + BK$ not singular. To keep the content clear, since (3.1) is linear, we will assume without loss of generality that the unique equilibrium point is $0_{\mathbb{R}^n \times \mathbb{X}}$. The stronger notion of exponential stability is defined thereafter in this context.

Definition 3.7: Exponential stability

The equilibrium point $(X_e, u_e, v_e) = 0_{\mathbb{R}^n \times \mathbb{X}}$ is **exponentially stable** if there exists $\mu > 0, \gamma \geq 1$ such that the following holds:

$$\forall t \geq 0, \qquad \|(X(t), u(t), u_t(t))\|_{\mathscr{D}(\mathscr{A})} \leq \gamma \|(X^0, u^0, v^0)\|_{\mathscr{D}(\mathscr{A})} e^{-\mu t},$$

where (X, u, v) is the trajectory of (3.1) with initial condition $(X^0, u^0, v^0) \in \mathscr{D}(\mathscr{A})$.
It is said to be **exponentially stable with a decay-rate of at least** μ^* with $\mu^* > 0$ if μ in the previous definition is greater than or equal to μ^*.

Of course, if an equilibrium point is exponentially stable, it is also asymptotically stable. Contrary to finite-dimensional systems, for infinite-dimensional systems, exponential stability is not equivalent to asymptotic stability [107]. Proving the exponential stability of system (3.1) is the main concern of Chapter 5.

3.2.2 Stability for a drilling pipe

For nonlinear systems, looking for global exponential stability is rather complicated and sometimes impossible because there are several equilibrium points or because the trajectories do not converge exponentially. There exist many alternatives such as considering local versions of the previous definitions. This is nevertheless not investigated

in this thesis but left in the perspectives. Another interesting point is to relax the definition of asymptotic stability to get the asymptotic stability to a set $\mathcal{P}$ as defined in [95] and in the following definition.

Definition 3.8: Practical stability of a set $\mathcal{P}$ [82, 95]

System (3.1) is said to be practically stable to $\mathcal{P} \subset \mathbb{R}^n \times \mathbb{X}$ if the following two properties are verified:

1. For any initial condition $(X^0, u^0, v^0) \in \mathscr{D}(\mathscr{A})$,

$$\min_{(X_\mathcal{P}, u_\mathcal{P}, v_\mathcal{P})} \|(X(t) - X_\mathcal{P}, u(t) - u_\mathcal{P}, u_t(t) - v_\mathcal{P})\|_{\mathscr{D}(\mathscr{A})} \xrightarrow[t\to\infty]{} 0.$$

2. For any initial condition $(X^0, u^0, v^0) \in \mathcal{P}$,

$$\forall t \geq 0, \qquad (X(t), u(t), u_t(t)) \in \mathcal{P},$$

where $(X(t), u(t), u_t(t))$ is the unique trajectory of (3.1) with initial condition (X^0, u^0, v^0).

In practice, we are looking for a level set of a Lyapunov functional. In this case, the previous definition means that the trajectories of (3.1) are converging towards a ball of radius X_{bound} (attractivity) and that once inside this ball, they cannot escape (invariance). In other words, X, u and u_t are bounded. If $X_{bound} = 0$, we recover the definition of asymptotic stability. This notion provides a new expression for Problem 1.

Problem 2: Practical stability of the torsion system (2.7)

Let $\Omega_0 > 0$ be the desired angular speed.
We want to find a control law u_1 minimizing $z_{bound} > 0$ defined as follows:

$$\forall \eta > 0, \quad \exists T > 0, \quad \forall t \geq T, \qquad |z_1(t) - \Omega_0| \leq z_{bound} + \eta. \tag{3.11}$$

3.3 Conclusion

This chapter was dedicated to the toy-example system. It was enlighten that, as expected, studying the existence of a solution to a linear infinite-dimensional problem is far more difficult than for finite-dimensional systems. We have summarized some well-known results coming C_0-semigroup theory which provides existence of a solution and we used them for our problem.

Finally, the second part of this chapter dealt with different notions of stability. We saw how these definitions are related one to the other and to the problems coming from the control of drill-vibrations. These definitions are guiding us all along the following chapters.

Now that the basic properties of the toy-example system are known, the following chapter is dealing with its input/output stability.

4

Frequency analysis of coupled ODE/boundary-damped string equation

The previous chapter introduces the problem and studied the existence and regularity of a solution. This chapter investigates the frequency analysis of the toy example system stated in (3.1). This approach has been successfully applied to linear time-invariant finite-dimensional systems (see [61] for instance). The main interest of this method was to assess stability of such a system with an algebraic condition on the roots of a polynomial, which is a necessary and sufficient condition for stability. Such an approach has been extended to some classes of infinite-dimensional problems [41, 162].

For a time-delay system, one of the simplest infinite-dimensional systems, the frequency analysis approach assesses stability as a condition on the roots of a quasi-polynomial, which is a polynomial with complex exponentials [114]. In many cases, this is a very tedious problem which can sometimes be solved using algorithms such as the Cluster Treatment of Characteristic Roots (CTCR) [115, 116] or using pseudospectral approach [25].

In a more general setting, finding the roots represents a real challenge. To answer this problem, the robust community proposes tools which do not require to solve algebraic equations. The cleverness was to split the problem into smallest and more manageable subsystems, which can be encapsulated into uncertainty sets. This new formulation helps getting numerical criteria which are, most of the time, not equivalent but sufficient to prove the stability of the initial system. Robust stability can be assessed using the Small-Gain Theorem [50, 167], Integral Quadratic Constraints (IQCs) [103] or Quadratic Separation (QS) [4, 77, 119] for instance.

This chapter is organized as follows. Section 1 proposes an equivalent formulation of ODE/string equation (3.8) in terms of neutral-type time-delay systems. This formulation enables us to derive necessary stability conditions. In particular, we can apply the CTCR algorithm to detect the number of unstable poles and then get an exact stability test. A problem with the previous test lies in its lack of robustness. This will be dealt in Section 2 using the Small-Gain Theorem. This conservative but simple result is then extended in Section 3 using Quadratic Separation which refines the previous stability test.

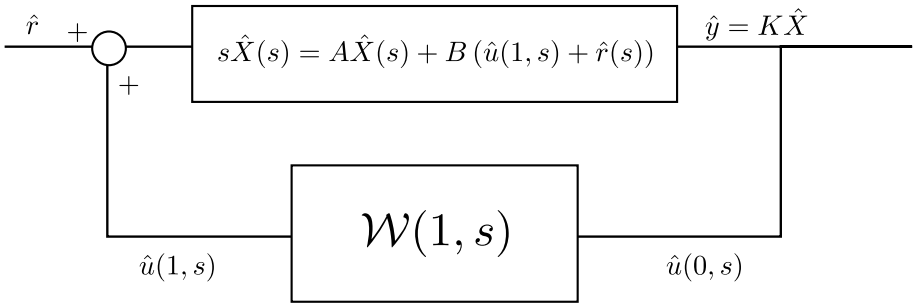

Figure 4.1: Block diagram of system (4.1) where $\hat{r}$ is the input and $\hat{y} = K\hat{X}$, the output.

4.1 Time-delay system description

It is well-known that a wave equation can often be written as a time-delay system [85, 87, 133]. This alternative formulation arises naturally when applying the Laplace transform of the ODE/PDE system. It enables using different tools to assess the input/output stability of (3.8).

4.1.1 Laplace transform of the coupled system

The notion of Laplace transform extends easily to infinite-dimensional systems from its traditional definition for finite-dimensional systems as noted in [52]. This transformation is possible if the variables under concern are L^2 in time on each compact set of $\mathbb{R}^+$, which is the case in (3.8) as discussed in Section 3.1.

Applying the Laplace transform to (3.8), with $s \in \mathbb{C}$ denoting the Laplace variable, system (3.8) translates into the following equations:

$$s\hat{X}(s) = A\hat{X}(s) + B\left(\hat{u}(1,s) + \hat{r}(s)\right), \tag{4.1a}$$
$$s^2\hat{u}(x,s) = c^2\hat{u}_{xx}(x,s), \qquad x \in [0,1], \tag{4.1b}$$
$$\hat{u}(0,s) = K\hat{X}(s) = \hat{y}(s), \tag{4.1c}$$
$$\hat{u}_x(1,s) = -c_0 s\hat{u}(1,s), \tag{4.1d}$$

where $\hat{X}, \hat{u}$ and $\hat{y}$ denote the Laplace transforms of X, u and y respectively. The block diagram of this system is depicted in Figure 4.1 where $\mathcal{W}(x,s)$ is the transfer function from $\hat{u}(0,s)$ to $\hat{u}(x,s)$ for $x \in [0,1]$. In order to simplify this set of equations, let us note that (4.1b) is a differential equation in x that can be easily solved, and the solution is:

$$\hat{u}(x,s) = A_{\mathcal{W}}(s)e^{\frac{s}{c}x} + B_{\mathcal{W}}(s)e^{-\frac{s}{c}x},$$

with A and B two transfer functions to be defined using the boundary conditions (4.1c) and (4.1d). This leads to the following system:

$$\begin{cases} (4.1c) \Leftrightarrow A_{\mathcal{W}}(s) + B_{\mathcal{W}}(s) = \hat{y}(s), \\ (4.1d) \Leftrightarrow \frac{s}{c}\left(A_{\mathcal{W}}(s)e^{\frac{s}{c}} - B_{\mathcal{W}}(s)e^{-\frac{s}{c}}\right) = -sc_0\hat{u}(1,s) = -sc_0\left(A_{\mathcal{W}}(s)e^{\frac{s}{c}} + B_{\mathcal{W}}(s)e^{-\frac{s}{c}}\right). \end{cases}$$

We derive from the previous system of equations the expression of the transfer function of the string equation, which is given by:

$$\mathcal{W}(x,s) = \frac{\hat{u}(x,s)}{\hat{y}(s)} = \frac{e^{-\frac{s}{c}x} + \alpha e^{\frac{s}{c}(x-2)}}{1+\alpha e^{-2\frac{s}{c}}}, \tag{4.2}$$

with $\alpha = \frac{1-cc_0}{1+cc_0}$ and $x \in [0,1]$. In particular, the transfer function from $\hat{y}(s)$ to $\hat{u}(1,s)$ reads:

$$\mathcal{W}(1,s) = \mathcal{W}(s) = \frac{\hat{u}(1,s)}{\hat{y}(s)} = \frac{(1+\alpha)e^{-s/c}}{1+\alpha e^{-2s/c}} = \frac{2e^{-s/c}}{1+cc_0+(1-cc_0)e^{-2s/c}}. \tag{4.3}$$

Notice that $\mathcal{W}(x,s)$ has infinitely many poles. These poles are independent on the spatial variable x and their real part $\frac{c}{2}\log|\alpha|$ is strictly negative if $cc_0 \neq 1$ and $c_0 > 0$.

Remark 4.1: On the stability of $\mathcal{W}$

When $c_0 = 0$, $\mathcal{W}$ has infinitely many poles on the imaginary axis and for $c_0 < 0$, there are infinitely many poles with a strictly positive real part. Applying Corollary 9.1.4 from [41], for any finite-dimensional system, the coupled system (4.1) cannot be input/output stable if the $\mathcal{W}$ is not stable.
In other words, the third scenario in Section 3.1 (p. 17) cannot be dealt using this method here. We will come back to this point later in this chapter.

In order to obtain the transfer function of Figure 4.1, let us first express the transfer function between $\hat{r} + \hat{u}(1,\cdot)$ and $\hat{y}$:

$$\mathcal{H}(s) = \frac{\hat{y}(s)}{\hat{u}(1,s)+\hat{r}(s)} = K(sI_n - A)^{-1}B = \frac{N(s)}{D(s)}, \tag{4.4}$$

where N and D are two polynomials of degree $n-1$ and n, respectively. Using the expression of $\mathcal{W}$ developed previously, we obtain the following transfer function:

$$\mathcal{F}(s) = \frac{\hat{y}(s)}{\hat{r}(s)} = \frac{\mathcal{H}(s)}{1-\mathcal{H}(s)\mathcal{W}(s)} = \frac{N(s)\left(1+\alpha e^{-2s/c}\right)}{(1+cc_0)c_{eq}(s,c)}, \tag{4.5}$$

where

$$c_{eq}(s,c) = \left(1+cc_0+(1-cc_0)e^{-2s/c}\right)D(s) - 2N(s)e^{-s/c}. \tag{4.6}$$

The stability of system (4.1) is determined by the location of the roots of (4.6). These roots are called the poles of $\mathcal{F}$ and their influence on the stability is discussed in details in the following subsection.

4.1.2 A neutral type time-delay system

A time-delay system is of *neutral type* when its highest order derivative is affected by a delay term τ. Given a characteristic equation, this feature appears as the highest power of the Laplace variable s is multiplied by the delay operator $e^{-\tau s}$. Inspecting the corresponding transfer function $\mathcal{F}$ or the characteristic equation (4.6) of system (4.1),

it is easy to see that this system exhibits the neutral characteristic if $cc_0 \neq 1$. The theory on Neutral Functional Differential Equations (NFDE) is detailed in [84, 114] for instance. We can re-write system (4.1) in the standard NFDE form by collecting the derivative of the states on the left-hand side:

$$\dot{X}(t) + \alpha\dot{X}(t - 2c^{-1}) = AX(t) + \frac{2}{1 + cc_0}BKX(t - c^{-1}) + \alpha AX(t - 2c^{-1}) + Br(t) + \alpha Br(t - c^{-1}), \quad (4.7)$$

where from [67, 116] the difference operator is defined for all $t \in \mathbb{R}^+$ as:

$$D_\alpha(X)(t) = X(t) + \alpha X(t - 2c^{-1}). \quad (4.8)$$

Remark 4.2: $\mathcal{F}$ represents a time-delay system if $\alpha = 0$

One can see that for $cc_0 = 1$, we have $\alpha = 0$ and system (4.1) is no longer a neutral type system but a *retarded* one [22]. This distinction is critical for the stability analysis since there is a finite number of unstable poles for a time-delay system, which is not necessarily the case for a neutral time-delay system. It will also help building various examples and enables a comparison with the stability tests already available for time-delay systems.

When it comes to study stability of NFDEs, contrary to functional differential equations of retarded type, inspecting the pole locations of the corresponding characteristic equation is not sufficient to guarantee its input/output stability. A prerequisite for the study of stability is the so-called small τ-stabilizability, this is also known as small-delay phenomenon or strong stability. When an NFDE is small τ-stabilizable, it is guaranteed that the poles of the NFDE behave continuously as the delay value changes from 0 to 0^+. Whenever this property holds, then studying the pole locations of an NFDE allows one to conclude on the stability of an NFDE (see [22, 68] for more information). If this is not the case, even if all the poles are with a strictly negative real parts, there might exist an input which makes the system diverges. The following definition of small τ-stabilizable comes from [67, 116].

Definition 4.1: Small τ-stabilizable

An NFDE system is said to be **small τ-stabilizable** if the difference operator $D_\alpha(X)(t)$ is stable.

This definition leads to the following proposition.

Proposition 4.1

System (4.1) is neutral and small τ-stabilizable if and only if

$$c_0 > 0 \text{ and } cc_0 \neq 1.$$

Proof : According to Theorem 12.5.1 and Corollary 12.5.1 from [67], the difference operator (4.8) is stable if and only if $|\alpha|$ is strictly less than 1. This is the case if and

only if $c_0 > 0$. Moreover, the system is neutral if $\alpha \neq 0$ and then $cc_0 \neq 1$. ♢

Finally, since the system is small τ-stabilizable under the previous condition, its input/output stability can be discussed. The following theorem is a rephrasing of Theorem 9.9.1 from [68].

Corollary 4.1

System (4.1) is input/output stable if the two following conditions are satisfied:

1. $c_0 > 0$,
2. $\forall s \in \mathbb{C}^+, \quad c_{eq}(s, c) \neq 0$.

As one established some key properties regarding the neutral aspect of (4.1), the stability analysis can be pursued.

4.1.3 Pole crossing approach

Once the characteristic equation is derived, different methodologies can be applied to assert input/output stability of system (4.1). Various techniques can be adopted for this purpose, see for example [145]: 2-D stability tests [65, Section 2.2.1] [80], pseudo-delay methods [75, 124], direct/robust analysis [114] or bifurcation analysis [25, 111, 164] among many others. Since the coefficients of c_{eq} in (4.6) are delay-dependent, it is generally difficult to apply the classical techniques used to assess the stability of time-delay systems. This problem has been investigated in some studies [23, 79] and usually requires a tedious analysis.

In this part, we focus on a method allowing to find the exact condition for which the system in closed loop (4.1) is input/output stable. Specifically, we use an analysis based on a pole location argument that is the Cluster Treatment of Characteristic Roots (CTCR) methodology, originally proposed in [115].

Let $\tau = c^{-1}$ for clarity and regrouping the terms by their delay dependence, characteristic equation (4.6) becomes:

$$c_{eq}(s, \tau) = a_0(s, \tau) + a_1(s, \tau)e^{-\tau s} + a_2(s, \tau)e^{-2\tau s}, \tag{4.9}$$

with $a_0(s, \tau) = \left(1 + \frac{c_0}{\tau}\right) D(s)$, $a_1(s, \tau) = -2N(s)$ and $a_2(s, \tau) = \left(1 - \frac{c_0}{\tau}\right) D(s)$. It is clear that the system described by $\mathcal{F}$ can switch from stable to unstable behavior, or vice-versa, only if (4.6) has a pole on the imaginary axis for a given delay [115].

The CTCR algorithm starts by exhaustively detecting all the imaginary poles $s = i\omega$, along with their corresponding delay values (Proposition 1 of [115]). Next, CTCR identifies that each pole $s = i\omega$ has a unique crossing direction over the imaginary axis for all the delays creating this crossing (Proposition 2 of [115]). Knowing the number of unstable poles at $\tau = 0$, which is trivial to assess, it is then possible to use the information regarding crossing directions and at which delay values such crossings occur to find the pole locations across the imaginary axis. With this idea, it becomes possible to count the number of poles on the right-half plane for a given delay value

$\tau > 0$. Whenever there are no unstable poles for certain delays, using Corollary 4.1, we state that the system is input/output stable for those delays.

The CTCR framework has already been used for neutral systems [116] while respecting the small τ-stabilizability property. In the following, we briefly summarize this framework [115, 116] and also point out the main difference introduced while studying the particular system (4.1). Following the process described in [115, 116], the Rekasius substitution [124] is defined as:

$$e^{-\tau s} := \frac{1 - Ts}{1 + Ts}, \quad \tau \in \mathbb{R}^+, \quad T \in \mathbb{R}, \quad s = i\omega, \tag{4.10}$$

which is an *exact* substitution of exponential terms when $s = i\omega$. The mapping transformation is bijective and its inverse is given for $\omega > 0$ by:

$$\tau = \frac{2}{\omega}\left[\tan^{-1}(\omega T) \pm \ell\pi\right], \quad \ell = \ell_0, \ell_0 + 1, \dots \tag{4.11}$$

Here, ℓ_0 is the first integer for which τ is positive.

Next, substituting (4.10) into the characteristic equation (4.6) and expanding by $(1 + Ts)^2$, which does not bring any artificial imaginary poles, we obtain a *transformed* characteristic equation, given by:

$$\bar{c}_{eq}(s, T) = \left(1 + \frac{2c_0}{\tau}Ts + T^2s^2\right) D(s) - N(s)(1 - T^2s^2),$$

which is nothing but a multinomial in s and T. Note that the imaginary poles $s = i\omega$ of the original characteristic equation c_{eq} and this multinomial $\bar{c}_{eq}$ are identical. Hence, one can alternatively compute the imaginary poles $s = i\omega$ from this multinomial, which is a much easier task. To this end, we first build the coefficients $\{b_k(T, \tau)\}_{k\in(0,n+2)}$, such that:

$$\bar{c}_{eq}(s, T) = \sum_{k=0}^{n+2} b_k(T, \tau)s^k. \tag{4.12}$$

It is worth noting that multinomial (4.12) is not exactly of the required form to apply the CTCR methodology. The main problem is that coefficients b_n depend explicitly on the delay τ. This brings an additional difficulty to our problem because it may also rule out certain periodicity properties (Proposition 2 in [115]). However, we will show in the next paragraph that this issue can be solved.

Indeed, consider the following manipulation. As c_0 is always divided by the delay τ in b_k, if one defines a new positive variable $c_1 = c_0\tau^{-1} = c_0c$, then b_k depends only on c_1 and not on τ anymore. Working at a given strictly positive c_1 removes the dependence of b_k in τ. Since they are now independent, the methodology applies. This manipulation also shows that $c_1 = c_0c$ is a variable of interest when it comes to study the stability of boundary damped strings.

Using b_k and a_k as defined in equations (4.9) and (4.12), the CTCR methodology provides the boundaries of the parameter space in which the input-output stability of system (4.1) holds[1]. The algorithm to obtain the stability chart is summarized as follows for a given $c_1 = c_0\tau^{-1}$ and originally comes from [14].

[1]Here, we provide the general framework of CTCR for an exact stability analysis. Handling degenerate cases requires care as was demonstrated in [146]. Such special cases, for a slightly different c_1, will however not arise.

Algorithm 4.1

1. Using $\bar{c}_{eq}$, one can find the roots $s = i\omega$ corresponding to $T \in \mathbb{R}$, e.g., by using Routh's array. There are only a finite number of such solutions (Proposition 1 of [115]);
2. For each $T \in \mathbb{R}$ obtained previously, we already know the angular frequency ω for which a crossing on the imaginary axis occurs. For each ω, there is a root tendency, indicating the unique direction of the crossing independent of the delays creating that crossing (Proposition 2 of [115]).
3. Then, using the inverse transformation of Rekasius transformation in (4.10), it is possible to find all the delays $\{\tau_\ell\}$ corresponding to each pair of (T, ω) and falling in an interval from 0 up to a target delay value τ_{max}. Sorting these delays in ascending order, and starting with the number of unstable poles for $\tau = 0$, the number of unstable poles for a delay $\tau < \tau_{max}$ can be accounted by observing the root tendency property of the crossings.
4. The stability areas of system (4.1) for a given $c_1 = c_0\tau^{-1}$ are obtained if no unstable poles are detected (Corollary 4.1). Since τ is known at this point, c_0 can be recovered as $c_0 = c_1\tau$.

Remark 4.3: Stability chart of (4.1)

Notice that the coefficients b_k depend linearly on c_1 and then the roots of $\bar{c}_{eq}(\cdot, T)$ vary continuously with respect to c_1. In other words, the delays τ for which there is a crossing vary continuously relatively to c_1. The border of each stability area on the map (c_1, τ) is consequently continuous.
This observation indicates that to plot a stability chart, we can use the mapping (c_1, τ) or equivalently $(\alpha = \frac{1-c_1}{1+c_1}, \tau)$.

The tool presented in this chapter enables to get an exact stability test. However, it suffers from a lack of robustness because it depends on a perfect knowledge of c_{eq}. The following sections deal with this issue.

4.2 Small-Gain Theorem

A complementary approach dealing with robustness issues (with respect to uncertainties on A or c for instance) considers the wave $\mathcal{W}$ as an uncertain system. Characterizing these uncertainties by some inequalities allows us to use classica robust control tools such as the Small-Gain Theorem [50, 167].

4.2.1 Adapted Small-Gain Theorem

Since the system under study is an interconnection between two subsystems as shown in Figure 4.1, the stability of the interconnection can be stated under some conditions on

each subsystem. The first tool coming from the robust stability community considered here is the Small Gain Theorem for infinite-dimensional systems [41].

Consider the block diagram of Figure 4.1 where the wave equation is modeled as an uncertain transfer function. The following stability criteria is a direct application of the Small-Gain Theorem.

Theorem 4.1: Small-Gain Theorem [14]

System (4.1) is input-output stable for $(c, c_0) \in (0, \infty)^2$ if the following condition is satisfied:

$$\|\mathcal{H}\|_\infty = \|K(sI_n - A)^{-1}B\|_\infty < \min(cc_0, 1). \tag{4.13}$$

Remark 4.4

If the previous theorem holds, then $cc_0 > 0$ and system (4.1) is small τ-stabilizable.

Proof : Beforehand, let evaluate the H_∞-norm of $\mathcal{W}$. Some calculations lead to:

$$\|\mathcal{W}\|_\infty = \max_{w\in\mathbb{R}^+} |\mathcal{H}(iw)| = \frac{2}{(1+cc_0)\min_{\omega\geq 0}|1+\alpha e^{-2i\omega/c}|},$$

where $\alpha = \frac{1-cc_0}{1+cc_0}$. For $|\alpha| < 1$, the function $\omega \mapsto 1 + \alpha e^{-2i\tau\omega}$ is inside the circle on the complex plane centered at 1 and of radius $|\alpha| < 1$. Consequently, we get:

$$\min_{\omega\geq 0}\left|1+\alpha e^{-2i\omega/c}\right| = \begin{cases} \frac{2cc_0}{1+cc_0} & \text{if } cc_0 < 1, \\ \frac{2}{1+cc_0} & \text{otherwise .} \end{cases}$$

Consequently, we get:

$$\|\mathcal{W}\|_\infty = \max\left(\frac{1}{cc_0}, 1\right).$$

Then, using the Small-Gain Theorem for infinite-dimensional systems as stated in [41, Theorem 9.1.7], the interconnected system is input/output stable if each subsystem is stable and $\|\mathcal{H}\|_\infty\|\mathcal{W}\|_\infty < 1$. The first condition is ensured if $\|\mathcal{H}\|_\infty < 1$ and $c_0 > 0$. The second condition is verified depending on the value of cc_0.

1. Assume $cc_0 \leq 1$. That leads to $\|\mathcal{W}\|_\infty = \frac{1}{cc_0}$, it then follows that robust stability is ensured if $\|\mathcal{H}\|_\infty\|\mathcal{W}\|_\infty = \frac{\|\mathcal{H}\|_\infty}{cc_0} < 1$. This is equivalent to (4.13).

2. If $cc_0 > 1$, then $\|\mathcal{W}\|_\infty = 1$. Stability is ensured if $\|\mathcal{H}\|_\infty < 1$, which is equivalent to (4.13).

♢

Remark 4.5: Delay-robustness of the criterion

The proof of the previous theorem shows that the interconnection (4.1) is robustly stable for all uncertainties $\mathcal{W}$ verifying $\|\mathcal{W}\|_\infty = \max\left(\frac{1}{cc_0}, 1\right)$.
For instance, consider the uncertainty $\mathcal{W}_h(s) = \mathcal{W}(s)e^{-hs}$ for $h > 0$. We get easily that $\mathcal{W}$ and $\mathcal{W}_h$ have the same $\mathcal{H}_\infty$-norm. Consequently, Theorem 4.1 ensures that (4.1) is robust to the addition of a delay h, whatever the value $c > 0$ as long as $c_0 > 0$. This point is discussed in the following proposition.

The main advantage of the previous theorem lies in its simplicity. Indeed, it is an algebraic test and some properties can be easily deduced.

Proposition 4.2: Consequences of the Small-Gain Theorem

Assume (4.13) holds. The following properties are then verified:

1. $A + BK$ is Hurwitz,
2. There exists a function

$$\begin{array}{rccc} c_{min}: & (0,+\infty) & \to & \mathbb{R}^+ \\ & c_0 & \mapsto & c_{min}(c_0) \end{array}$$

   where $c_{min}(c_0) \leq \|\mathcal{H}\|_\infty c_0^{-1}$ such that system (4.1) is input/output stable for all $c \geq c_{min}(c_0)$. Moreover, $\lim\limits_{c_0 \to +\infty} c_{min}(c_0) = 0$.

3. Let $\alpha = \dfrac{1 - cc_0}{1 + cc_0}$, if $c_0 > 0$, condition (4.13) is equivalent to:

$$\alpha < \frac{1 - \|\mathcal{H}\|_\infty}{1 + \|\mathcal{H}\|_\infty}. \tag{4.14}$$

Proof :

1. Since $\|\mathcal{H}\|_\infty < 1$, applying the Small Gain Theorem leads to $A + BK$ Hurwitz.
2. Since $\|\mathcal{H}\|_\infty < cc_0$, we get that $c > \|\mathcal{H}\|_\infty c_0^{-1}$. This point is a very interesting robustness result. It means for all wave speed larger than $\|\mathcal{H}\|_\infty c_0^{-1}$, system (4.1) remains stable. That naturally leads to the existence of the function c_{min} with the above properties.
3. Since $\|\mathcal{H}\|_\infty < cc_0$, we get that $1 - \|\mathcal{H}\|_\infty > 1 - cc_0$ and $(1 + \|\mathcal{H}\|_\infty)^{-1} > (1 + cc_0)^{-1}$. Combining these two equations leads to (4.14).

♢

Note that the last property implies that at a given and fixed $c_1 = cc_0$, the input/output stability of system (4.1) is independent on the delay $\tau = c^{-1}$, as noted in

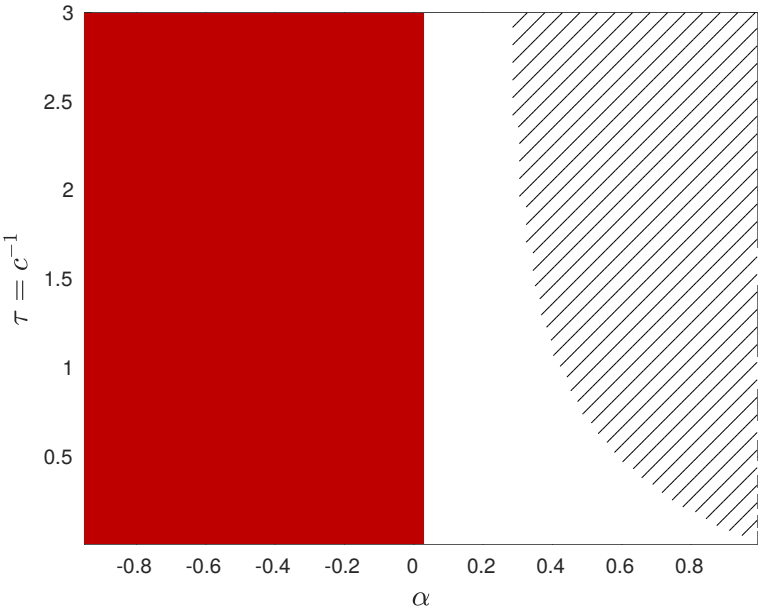

Figure 4.2: Stability chart of (4.1) with (4.15). The hatched area is the exact unstable area according to the CTCR algorithm presented in Section 4.1.3, while Theorem 4.1 gives that the red area is stable.

Remark 4.5. This remark shows that the theorem does not provide a speed dependent stability test and is therefore conservative.

4.2.2 Example and numerical test

Consider the following example coming from [14]:

$$A = \begin{bmatrix} -2 & 1 \\ 0 & -1 \end{bmatrix}, \quad B = \begin{bmatrix} 1 \\ 1 \end{bmatrix}, \quad K = \begin{bmatrix} 0 & -\frac{20}{21} \end{bmatrix}. \tag{4.15}$$

We note that $\|\mathcal{H}\|_\infty = 0.9524 < 1$, then, Theorem 4.1 and Proposition 4.2 apply. One obtain that the closed-loop system (4.1) is stable for all $\alpha < 0.0244$. Figure 4.2 shows the stability chart for $\alpha \in (0, 1)$ and $c \in [0.33, 100]$ with the two methods proposed: The CTCR algorithm and the Small Gain Theorem.

We can clearly see on that example that Theorem 4.1 produces very conservative results. Indeed, the white area is stable but is not detected by the Small-Gain theorem. The following section proposes a different framework to enhance the previous result, at the price of a more complex stability test.

4.3 Quadratic Separation

The Small-Gain Theorem ensures the input/output stability of an interconnected system composed of a disturbance and a plant which are both stable. To decrease the conservatism and consider a broader class of interconnected systems, the Quadratic

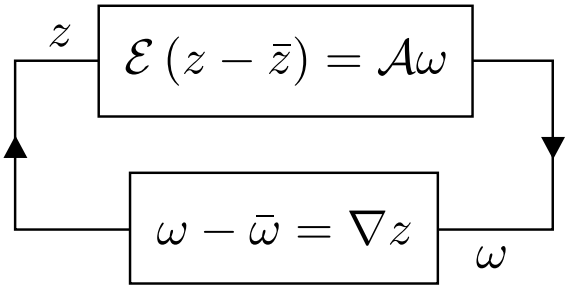

Figure 4.3: Feedback system for quadratic separation. $\mathcal{A}$ and $\mathcal{E}$ are matrices and ∇ is an uncertain operator. $\bar{\omega}$ and $\bar{z}$ are the references.

Separation (QS) framework can be used. This framework has been originally proposed in [77] and extended in [119]. It studies the wellposedness of a closed-loop system made up of an uncertain linear transformation and a known linear transformation as in Figure 4.3. Note that in this framework, $\omega, \bar{\omega}, z$ and $\bar{z}$ are complex vectors.

4.3.1 Framework and methodology

First, we describe the methodology of QS and then we apply this theory to provide a preliminary result on system (4.1) in the following subsection. Then we will extend this stability analysis to provide less conservative results. QS states the wellposedness of a generic system described in Figure 4.3, where $z, \bar{z} \in \mathbb{C}^{n_z}$ and $\omega, \bar{\omega} \in \mathbb{C}^{n_\omega}$, $\mathcal{E} \in \mathbb{C}^{n_\mathcal{E} \times n_z}$ is full-column rank, $\mathcal{A} \in \mathbb{C}^{n_\mathcal{E} \times n_\omega}$ and $\nabla \in \mathbb{C}^{n_\omega \times n_z}$ is a transfer function.

In our case here, we consider that this operator acts on two signals w and z in the Laplace domain. We assume here that ∇ depends on a variable $s \in \bar{\mathbb{C}}^+ \backslash \{0\}$ only and consequently, the system described in Figure 4.3 rewrites as:

$$\forall s \in \bar{\mathbb{C}}^+ \backslash \{0\}, \qquad \begin{cases} \hat{\omega}(s) - \hat{\bar{\omega}}(s) = \nabla(s)\hat{z}(s), \\ \mathcal{E}\left(\hat{z}(s) - \hat{\bar{z}}(s)\right) = \mathcal{A}\hat{\omega}(s). \end{cases} \tag{4.16}$$

To ease the notation in the sequel, we introduce the following definition.

Definition 4.2: System $\Sigma(\mathcal{E}, \mathcal{A}, \nabla)$

The system in Figure 4.3 and equation (4.16) can be written as $\Sigma(\mathcal{E}, \mathcal{A}, \nabla)$ where $\mathcal{E}$ is full-column rank.

The quadratic separation methodology ensures the wellposedness of the interconnection, defined as follows for a system $\Sigma(\mathcal{E}, \mathcal{A}, \nabla)$.

Definition 4.3: Wellposedness of $\Sigma(\mathcal{E}, \mathcal{A}, \nabla)$ [77]

The interconnected system described on Figure 4.3 is wellposed if for each s in $\bar{\mathbb{C}}^+ \backslash \{0\}$, the map $(\bar{\omega}, \bar{z}) \in \mathbb{C}^{n_\omega} \times \mathbb{C}^{n_z} \mapsto (\omega, z) \in \mathbb{C}^{n_\omega} \times \mathbb{C}^{n_z}$ is bijective.

Remark 4.6

Note that the notion of wellposedness considered here is not directly related to the definition of wellposedness in Hadamar sense for PDEs [41, p. 15]. In the general quadratic separation framework as described in [77, 119], ∇ is assume to be uncertain and we study the wellposedness of the interconnection with respect to this operator.

To better understand the wellposedness of (4.16), an equivalent definition for this system is given by the following proposition.

Proposition 4.3: Wellposedness of $\Sigma(\mathcal{E}, \mathcal{A}, \nabla)$

If $\Sigma(\mathcal{E}, \mathcal{A}, \nabla)$ is wellposed then

$$\forall s \in \bar{\mathbb{C}}^+ \backslash \{0\}, \quad \det\left(\begin{bmatrix} I_{n_z} & -\mathcal{E}^+\mathcal{A} \\ -\nabla & I_{n_\omega} \end{bmatrix}\right) \neq 0 \tag{4.17}$$

holds where $\mathcal{E}^+$ is a left pseudo-inverse of $\mathcal{E}$, such that $\mathcal{E}^+\mathcal{E} = I_{n_z}$.

Proof : This proof is inspired from [77] and can be found in [119]. For $s \in \bar{\mathbb{C}}^+ \backslash \{0\}$, system (4.16) rewrites as:

$$\begin{bmatrix} \mathcal{E} & -\mathcal{A} \\ -\nabla(s) & I_{n_\omega} \end{bmatrix} \begin{bmatrix} z \\ \omega \end{bmatrix} = \begin{bmatrix} \mathcal{E} & 0 \\ 0 & I_{n_\omega} \end{bmatrix} \begin{bmatrix} \bar{z} \\ \bar{\omega} \end{bmatrix}. \tag{4.18}$$

Since $\mathcal{E}$ is full-column rank, there exists a pseudo-inverse $\mathcal{E}^+ \in \mathbb{C}^{n_z \times n_\mathcal{E}}$ such that $\mathcal{E}^+\mathcal{E} = I_{n_z}$. System (4.18) implies the following:

$$\begin{bmatrix} \mathcal{E}^+ & 0 \\ 0 & I_{n_\omega} \end{bmatrix} \begin{bmatrix} \mathcal{E} & -\mathcal{A} \\ -\nabla(s) & I_{n_\omega} \end{bmatrix} \begin{bmatrix} z \\ \omega \end{bmatrix} = \begin{bmatrix} I_{n_z} & -\mathcal{E}^+\mathcal{A} \\ -\nabla(s) & I_{n_\omega} \end{bmatrix} \begin{bmatrix} z \\ \omega \end{bmatrix} = \begin{bmatrix} \bar{z} \\ \bar{\omega} \end{bmatrix}. \tag{4.19}$$

If the system is wellposed, then for a given $(\bar{\omega}, \bar{z}) \in \mathbb{C}^{n_\omega} \times \mathbb{C}^{n_z}$ there is a unique $(\omega, z) \in \mathbb{C}^{n_\omega} \times \mathbb{C}^{n_z}$ verifying (4.19) for all $s \in \bar{\mathbb{C}}^+ \backslash \{0\}$. This is equivalent to equation (4.17). ♢

Nevertheless, stating the wellposedness of $\Sigma(\mathcal{E}, \mathcal{A}, \nabla)$ seems difficult. Theorem 1 and Corollary 2 from [119] give a necessary and sufficient condition for the wellposedness of the general system (4.16). These results are summarized and adapted to our case in the following theorem.

Theorem 4.2: Quadratic Separation [119]

The system described by Figure 4.3 and equation (4.16) is wellposed if and only if there exists a real matrix $\Theta = \Theta^\top$ of appropriate dimension such that:

$$\forall s \in \bar{\mathbb{C}}^+ \backslash \{0\}, \quad \Xi = \begin{bmatrix} I \\ \nabla(s) \end{bmatrix}^* \Theta \begin{bmatrix} I \\ \nabla(s) \end{bmatrix} \preceq 0, \tag{4.20}$$

$$\begin{bmatrix} \mathcal{E} & -\mathcal{A} \end{bmatrix}^{\perp^\top} \Theta \begin{bmatrix} \mathcal{E} & -\mathcal{A} \end{bmatrix}^{\perp} \succeq 0, \tag{4.21}$$

where ∇^* is the trans-conjugate of ∇ and $\mathcal{E}$ is full-column rank.

Remark 4.7

The previous theorem highlights a main difference with usual Lyapunov-based theorem. Indeed, multiplying by the kernel on the left and on the right leads to less decision variables than classical theorems and a better interpretation of the slack-variables [62].
Moreover, the quadratic separation approach can be easily extended to some robust cases as done in [119].

The methodology to apply Theorem 4.2 is quite simple. We try to find a separator Θ satisfying (4.20). This can be difficult to assess since it must hold for all $s \in \bar{\mathbb{C}}^+ \backslash \{0\}$ and has to be as flexible as possible. To this extend, we then assume Θ is a linear function in the decision variables to be defined. Then (4.21) should be an LMI in the former decision variables, which is suitable for computational resolution.

Note that if (4.21) cannot be solved for a given separator defined a priori, that does not mean (4.16) is not wellposed. Indeed, one looses the equivalence by imposing a structure to Θ. We therefore obtain a sufficient condition of wellposedness.

The solution explored in this chapter to reduce the conservatism introduced by the choice of the separator is to extend system $\Sigma(\mathcal{E}, \mathcal{A}, \nabla)$ as defined in the following.

Definition 4.4: Extended system

Let $\Sigma_\circ = \Sigma(\mathcal{E}_\circ, \mathcal{A}_\circ, \nabla_\circ)$ and $\Sigma_e = \Sigma(\mathcal{E}_e, \mathcal{A}_e, \nabla_e)$.
Σ_e is said to be **an extension of** $\Sigma_\circ$ if the following holds:

$$\mathcal{E}_e = \begin{bmatrix} \mathcal{E}_\circ & 0 \\ \mathcal{E}_1 & \mathcal{E}_2 \end{bmatrix}, \quad \mathcal{A}_e = \begin{bmatrix} \mathcal{A}_\circ & 0 \\ \mathcal{A}_1 & \mathcal{A}_2 \end{bmatrix}, \quad \nabla_e = \begin{bmatrix} \nabla_\circ & 0 \\ \nabla_1 & \nabla_2 \end{bmatrix},$$

where $\mathcal{E}_1, \mathcal{E}_2, \mathcal{A}_1$ and $\mathcal{A}_2$ are matrices of appropriate dimensions. ∇_1 and ∇_2 are transfer functions.

Extended system has the following interesting property.

Theorem 4.3: Wellposedness of an extended system

If Σ_e is wellposed, then $\Sigma_\circ$ is wellposed.

Proof : The proof of this result is technical and it is therefore left in Appendix B. ♢

In the sequel, we will firstly derive a new model of the form (4.16) for system (4.1). Then, we will provide several conditions ensuring its wellposedness.

4.3.2 First stability result

The aim of this introducing part is to derive a first stability result for (4.1) using quadratic separation. First, note that (4.3) can be written differently as:

$$\mathcal{W}(s) = \frac{2(1+cc_0)e^{-\tau s}}{1+\alpha e^{-2\tau s}} = \frac{1+\alpha}{1+\alpha e^{-2\tau s}} e^{-\tau s} = \delta(s)e^{-\tau s},$$

where $\delta(s) = \frac{1+\alpha}{1+\alpha e^{-2\tau s}}$. System (4.1) is then equivalent to:

$$s\hat{X}(s) = A\hat{X}(s) + B\delta(s)e^{-\tau s}\left(K\hat{X}(s) + \hat{r}(s)\right) = A\hat{X}(s) + B(\hat{u}(1,s) + \hat{r}(s)). \quad (4.22)$$

Consider the following signals:

$$\begin{aligned} z_\oplus(t) &= \mathrm{col}\left(\dot{X}(t),\ KX(t),\ KX(t-\tau)\right), \\ \omega_\oplus(t) &= \mathrm{col}\left(X(t),\ KX(t-\tau),\ u(1,t)\right). \end{aligned} \quad (4.23)$$

Then, $\Sigma(\mathcal{E}_\oplus, \mathcal{A}_\oplus, \nabla_\oplus)$ is a new formulation of system (4.1) with $\mathcal{E}_\oplus, \mathcal{A}_\oplus$ and $\nabla_\oplus$ defined as follows:

$$\begin{aligned} \nabla_\oplus(s) &= \mathrm{diag}\left(s^{-1}I_n, e^{-\tau s}, \delta(s)\right), \\ \mathcal{E}_\oplus = I_{n+2}, \quad \mathcal{A}_\oplus &= \begin{bmatrix} A & 0_{n,1} & B \\ K & 0 & 0 \\ 0_{1,n} & 1 & 0 \end{bmatrix}. \end{aligned} \quad (4.24)$$

The following proposition makes the link between the wellposedness of $\Sigma(\mathcal{E}_\oplus, \mathcal{A}_\oplus, \nabla_\oplus)$ and the input/output stability of (4.1).

Proposition 4.4

If $\Sigma(\mathcal{E}_\oplus, \mathcal{A}_\oplus, \nabla_\oplus)$ is wellposed with $c_0 > 0$ and $\det(A+BK) \neq 0$, then system (4.1) is input/output stable.

Proof : This proof is technical and it is therefore reported in Appendix B. ♢

Remark 4.8

Note that the condition $\det(A+BK) \neq 0$ is not restrictive since it is equivalent to the existence of a unique equilibrium point of (4.1). The other condition $c_0 > 0$ is the classical assumption to be small-τ stabilizable.

In this subsection, we propose a structure for the real-valued separator Θ such that inequality (4.20) applied to $\nabla_\oplus$ always holds for $s \in \bar{\mathbb{C}}^+\backslash\{0\}$.

Proposition 4.5

Let $c, c_0 > 0$ and $\alpha = \frac{1-cc_0}{1+cc_0}$. Assume $\Theta_\oplus = \begin{bmatrix} \Theta_\oplus^{11} & \Theta_\oplus^{12} \\ \Theta_\oplus^{12\top} & \Theta_\oplus^{22} \end{bmatrix}$ such that

$$\begin{aligned} \Theta_\oplus^{11} &= \operatorname{diag}\left(0_n, -Q, R(1+\alpha)\right), \\ \Theta_\oplus^{12} &= \operatorname{diag}\left(-P, 0, -R\tfrac{1}{1-\alpha}\right), \\ \Theta_\oplus^{22} &= \operatorname{diag}\left(0_n, Q, R\right). \end{aligned} \tag{4.25}$$

Then, for any $P \in \mathbb{S}_+^n$ and $Q, R \in \mathbb{R}^+$, the inequality:

$$\Xi_\oplus = \begin{bmatrix} I \\ \nabla_\oplus(s) \end{bmatrix}^* \Theta_\oplus \begin{bmatrix} I \\ \nabla_\oplus(s) \end{bmatrix} \preceq 0, \tag{4.26}$$

holds for all $s \in \bar{\mathbb{C}}^+\backslash\{0\}$ where $\nabla_\oplus$ is given in (4.24).

Proof : For any $s \in \bar{\mathbb{C}}^+\backslash\{0\}$, let us compute $\Xi_\oplus$:

$$\Xi_\oplus = \begin{bmatrix} -2P\mathfrak{Re}(s^{-1}) & 0_{n,1} & 0_{n,1} \\ 0_{1,n} & Q(|e^{-\tau s}|^2 - 1) & 0 \\ 0_{1,n} & 0 & R\delta_{-1}(s) \end{bmatrix}, \tag{4.27}$$

where $\gamma = \frac{1}{1-\alpha}$ and $\delta_{-1}(s) = 1 + \alpha - \frac{2}{1-\alpha}\mathfrak{Re}\left(\delta(s)\right) + |\delta(s)|^2$. We need to prove that this matrix is negative.

First, note that for $s \in \bar{\mathbb{C}}^+\backslash\{0\}$, we get $\mathfrak{Re}(s^{-1}) = \mathfrak{Re}(s)|s|^{-2} \geq 0$, and consequently:

$$\forall s \in \bar{\mathbb{C}}^+\backslash\{0\}, \quad -2P\mathfrak{Re}(s^{-1}) \preceq 0.$$

Secondly, since for all $s \in \bar{\mathbb{C}}^+\backslash\{0\}$, $|e^{-\tau s}|^2 \leq 1$, we obtain:

$$\forall s \in \bar{\mathbb{C}}^+\backslash\{0\}, \quad Q(\left|e^{-\tau s}\right|^2 - 1) \leq 0.$$

Finally, since $w \mapsto \delta(iw)$ is the Moëbius transformation of a circle, calculations show that it is consequently a circle of diameter $\gamma = \frac{1}{1-\alpha}$ and radius $|\alpha|\gamma$. Then, $s \mapsto \delta(s)$ is inside a circle of center γ and radius $|\alpha|\gamma$. Hence, we get that $|\delta(s) - \gamma|^2 \leq |\alpha|^2\gamma^2$ for $s \in \bar{\mathbb{C}}^+\backslash\{0\}$. In other words $|\delta(s)|^2 - 2\gamma\mathfrak{Re}(\delta(s)) + (1-\alpha^2)\gamma^2 \leq 0$. That leads to:

$$\forall s \in \bar{\mathbb{C}}^+\backslash\{0\}, \quad R\delta_{-1}(s) \leq 0.$$

These considerations imply that $\Xi_\oplus \preceq 0$. ♢

Remark 4.9

The structure of the previous separator $\Theta_\oplus$ is not new and has already been used many times in [77, 119] for instance.

Using Theorem 4.2 leads to the following theorem.

Theorem 4.4: First stability result

Assume $c > 0$, $c_0 > 0$ and $\det(A + BK) \neq 0$.
Let $\Theta_\oplus = \begin{bmatrix} \Theta_\oplus^{11} & \Theta_\oplus^{12} \\ {\Theta_\oplus^{12}}^\top & \Theta_\oplus^{22} \end{bmatrix}$ such that

$$\begin{aligned} &\Theta_\oplus^{11} = \operatorname{diag}\left(0_n, -Q, R(1+\alpha)\right), \qquad \Theta_\oplus^{12} = \operatorname{diag}\left(-P, 0, -R\tfrac{1}{1-\alpha}\right), \\ &\Theta_\oplus^{22} = \operatorname{diag}\left(0_n, Q, R\right). \end{aligned} \tag{4.28}$$

If there exist $P \in \mathbb{S}_+^n$ and $Q, R \in \mathbb{R}^+$ such that the following LMI holds:

$$\begin{bmatrix} \mathcal{E}_\oplus & -\mathcal{A}_\oplus \end{bmatrix}^{\perp\top} \Theta \begin{bmatrix} \mathcal{E}_\oplus & -\mathcal{A}_\oplus \end{bmatrix}^{\perp} \succeq 0,$$

then system (4.1) is input/output stable.

Proof : First, thanks to Proposition 4.5, Theorem 4.2 holds. Since $\det(A+BK) \neq 0$ and $c_0 > 0$, then Proposition 4.4 states that system (4.1) is input/output stable. ♢

We can easily see that the previous condition is independent on the value of the delay τ. The obtained results are therefore not depending on the delay and we get a similar condition to the Small-Gain Theorem of the previous part. There is not enough information on the uncertainty $\nabla_\oplus$ to get a sharper stability criterion. We then need to characterize the uncertainty $\nabla_\oplus$ as much as possible. Following some studies on time-delay systems, [119] shows that the following interpretation of Figure 4.1 can be used:

$$\begin{aligned} z_0(t) &= \operatorname{col}\left(\dot{X}(t),\ KX(t),\ KX(t-\tau),\ K\dot{X}(t)\right), \\ \omega_0(t) &= \operatorname{col}\left(X(t),\ KX(t-\tau),\ u(1,t),\ K\left(X(t) - X(t-\tau)\right)\right). \end{aligned} \tag{4.29}$$

with

$$\nabla_0(s) = \begin{bmatrix} \nabla_\oplus(s) & 0 \\ 0 & \delta_0(s) \end{bmatrix}, \qquad \delta_0(s) = \tfrac{1-e^{-\tau s}}{s}$$

$$\mathcal{E}_0 = \left[\begin{array}{ccc|c} & \mathcal{E}_\oplus & & 0_{n+2,1} \\ \hline -K & 0 & 0 & 1 \\ 0_{1,n} & 1 & -1 & 0 \end{array}\right], \qquad \mathcal{A}_0 = \left[\begin{array}{c|c} \mathcal{A}_\oplus & 0_{n+2,1} \\ \hline 0_{2,n+2} & \begin{array}{c} 0 \\ 1 \end{array} \end{array}\right]. \tag{4.30}$$

Note that $\mathcal{E}_0$ is full-column rank. Consequently, in the sense of Definition 4.4, $\Sigma(\mathcal{E}_0, \mathcal{A}_0, \nabla_0)$ is an extension of $\Sigma(\mathcal{E}_\oplus, \mathcal{A}_\oplus, \nabla_\oplus)$. Compared to the previous system, we added two sig-

nals $K\dot{X}$ in z_0 and $K(X(t) - X(t-\tau))$ in ω_0. These new signals help characterizing the uncertainty ∇_0 as shown by the following theorem.

Theorem 4.5: Quadratic Separation stability test [14]

Assume $c_0 > 0$ and $\det(A + BK) \neq 0$.
Let $\Theta_0 = \begin{bmatrix} \Theta_0^{11} & \Theta_0^{12} \\ \Theta_0^{12\top} & \Theta_0^{22} \end{bmatrix}$ is proposed:

$$\begin{aligned} &\Theta_0^{11} = \operatorname{diag}\left(0_n, -Q, R(1-\alpha), -\tau^2 S\right), \qquad \Theta_0^{12} = \operatorname{diag}\left(-P, 0, -R\tfrac{1}{1-\alpha}, 0\right), \\ &\Theta_0^{22} = \operatorname{diag}\left(0_n, Q, R, S\right). \end{aligned} \tag{4.31}$$

If there exist $P \in \mathbb{S}_+^n$ and $Q, R, S \in \mathbb{R}^+$ such that the following LMI holds:

$$\begin{bmatrix} \mathcal{E}_0 & -\mathcal{A}_0 \end{bmatrix}^{\perp\top} \Theta_0 \begin{bmatrix} \mathcal{E}_0 & -\mathcal{A}_0 \end{bmatrix}^{\perp} \succeq 0 \tag{4.32}$$

for Θ_0, $\mathcal{E}_0$ and $\mathcal{A}_0$ defined in (4.31) and (4.30), then system (4.1) is input/output stable.

Proof : With the proposed structure of Θ_0, for all $s \in \bar{\mathbb{C}}^+ \backslash \{0\}$, the following holds:

$$\Xi_0 = \begin{bmatrix} I \\ \nabla_0(s) \end{bmatrix}^* \Theta_0 \begin{bmatrix} I \\ \nabla_0(s) \end{bmatrix} = \left[\begin{array}{c|c} \Xi_\oplus & 0_{n+2,1} \\ \hline 0_{1,n+2} & S\left(|\delta_0(s)|^2 - \tau^2\right) \end{array}\right]. \tag{4.33}$$

Using Jensen's inequality (Proposition E.3) on the function $u \mapsto e^{us}$ leads to:

$$\begin{aligned} \forall (s,\tau) \in \bar{\mathbb{C}}^+ \backslash \{0\} \times \mathbb{R}^+, \qquad |\delta_0(s)|^2 - \tau^2 &= \left|\frac{1-e^{-\tau s}}{s}\right|^2 - \tau^2 = \left|\int_{-\tau}^0 e^{us} du\right|^2 - \tau^2 \\ &\leq \tau \int_{-\tau}^0 |e^{us}|^2 du - \tau^2 \leq 0. \end{aligned} \tag{4.34}$$

Consequently, the previous result together with Proposition 4.5, we get $\Xi_0 \preceq 0$. According to Theorem 4.2, $\Sigma(\mathcal{E}_0, \mathcal{A}_0, \nabla_0)$ is wellposed if (4.32) holds. Using Theorem 4.3 about extended systems, we can conclude that $\Sigma(\mathcal{E}_\oplus, \mathcal{A}_\oplus, \nabla_\oplus)$ is wellposed. Consequently, using Proposition 4.4, we get that system (4.1) is input/output stable. ♢

Remark 4.10

The disturbance component δ_0 is related to Jensen inequality (see for instance [65] and Proposition E.3), a widely used inequality in the analysis of time-delay systems.

This stability condition is related to traditional results obtained using a Lyapunov approach [59] and Jensen inequality. It is known that it provides a conservative test [141, 142]. In the following section, we study a way to enhance inequality (4.34), which is the main cause of conservatism.

4.3.3 Towards a hierarchy of inequalities

In the previous part, we have given a special structure for Θ which has helped to obtain a feasible test for (4.20). Nevertheless, the less optimal the inequalities assessing (4.20) are, the more conservative the choice of Θ is. Equation (4.34) is a good approximation for small delay τ but becomes a rude approximation as τ increases. In this part, we describe a method to get better inequalities and consequently, a better separator Θ.

There are several solutions to improve (4.34). We can first find an ellipse which gives a better estimate of $|\delta_0|^2$. This solution is not investigated here but can be found in [63]. Instead, we will try to find a transfer function δ_+ such that the inequality

$$\forall s \in \bar{\mathbb{C}}^+\backslash\{0\}, \quad \begin{bmatrix} \delta_0(s)^* & \delta_+(s)^* \end{bmatrix} \begin{bmatrix} \delta_0(s) \\ \delta_+(s) \end{bmatrix} \leq \tau^2 \tag{4.35}$$

is verified. If we find such a δ_+, expending the previous expression leads to $|\delta_0(s)|^2 + |\delta_+(s)|^2 \leq \tau^2$. This new inequality is better than (4.34) in the sense that the gap between the two sides of the equation is thiner. This last transfer function is then employed to derive an extension of $\Sigma_\oplus$. In [142], the authors used Wirtinger inequality to get $\delta_+(s) = \frac{1}{s}\left(1 - \frac{2}{\tau s} + (1 + \frac{2}{\tau s})e^{-\tau s}\right)$. This Wirtinger-based inequality encompasses Jensen inequality since it always provides a better bound. The idea was once again enhanced in [143] using Bessel inequality (Proposition E.4), leading to a hierarchy of inequalities, at a price of a large extended system.

From now on, we choose the unique polynomial basis of $L^2(-\tau, 0)$ with respect to the scalar product $\langle \cdot, \cdot \rangle_{L^2(-\tau,0)}$, called the basis of shifted Legendre polynomials $\{\mathcal{L}_k\}_{k\in\mathbb{N}}$ which is defined in Appendix E, Definition E.1. Applying Proposition E.5 to the complex exponential leads to the following result, called frequency-Bessel inequality.

Lemma 4.1: Frequency-Bessel inequality [14]

Let $\tau > 0$ and $N \in \mathbb{N}$, then the following inequality holds:

$$\forall s \in \bar{\mathbb{C}}^+\backslash\{0\}, \quad \delta_N^*(s)\delta_N(s) \leq \tau^2, \tag{4.36}$$

$$\text{with } \delta_N(s) = \sqrt{\tau}\left[\left\langle e^{\theta s}, \frac{\mathcal{L}_0(\theta)}{\|\mathcal{L}_0\|}\right\rangle_{L^2(-\tau,0)} \quad \cdots \quad \left\langle e^{\theta s}, \frac{\mathcal{L}_N(\theta)}{\|\mathcal{L}_N\|}\right\rangle_{L^2(-\tau,0)}\right]^\top.$$

Proof : Let $s \in \bar{\mathbb{C}}^+\backslash\{0\}$, Bessel inequality (Proposition E.5) applied to function $\theta \mapsto e^{\theta s}$ gives:

$$\delta_N(s)^*\delta_N(s) = \tau \sum_{k=0}^{N} \left| \left\langle e^{\theta s}, \frac{\mathcal{L}_k(\theta)}{\|\mathcal{L}_k\|} \right\rangle_{L^2(-\tau,0)} \right|^2 \leq \tau \|e^{\theta s}\|^2_{L^2(-\tau,0)}.$$

This leads to: $\delta_N^*(s)\delta_N(s) \leq \tau \left| \int_{-\tau}^0 e^{\theta(s+s^*)} d\theta \right|$. As $s \in \bar{\mathbb{C}}^+\backslash\{0\}$, the right-hand side is bounded by τ^2 and that ends the proof. ♢

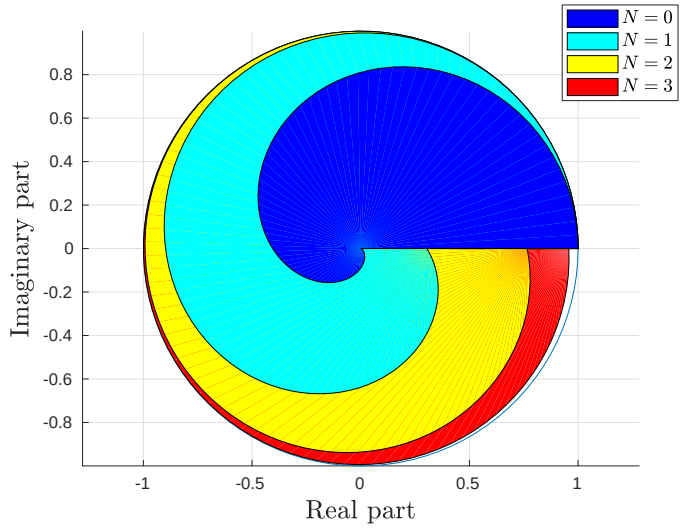

Figure 4.4: Plot of $\theta \mapsto \|\delta_N(i\theta)\|^2 e^{i\theta}$ for $\tau = 1$ and $\theta \in [0, 2\pi]$ and $N \in \{0, 1, 2, 3\}$. The more N increases, the closer the colored area is to the unit disk, meaning that the gap in inequality (4.36) is smaller. We can also note the hierarchy between the inequalities, each area at an order N is included in all smaller order areas.

This new inequality is an enhancement of inequality (4.34) since for $N = 0$, we recover it. Inequality (4.36) is less and less conservative as N increases. This is shown in Figure 4.4. To understand this figure, we first need to grasp what is the signification of each colored area. The deep blue area corresponds to the image of the function $(r, \theta) \in \mathbb{R}^+ \times [0, 2\pi] \mapsto \|\delta_0(i\theta)\|^2 e^{-ri\theta}$. Thanks to (4.36), we know that it is inside the disk of radius $\tau = 1$. The light and deep blue area is the image of the function $(r, \theta) \in \mathbb{R}^+ \times [0, 2\pi] \mapsto \|\delta_1(i\theta)\|^2 e^{-ri\theta}$. And we continue this way till $N = 3$. We see that the colored area is close to the unit disk, that means for $N = 3$, inequality (4.36) is nearly optimal for $s = i\theta$ and $\theta = [0, 2\pi]$. We can note that for small θ, Jensen inequality gives indeed a very good estimate and $|\delta_0|^2 \simeq \tau^2$. This estimate gets worse as θ increases.

4.3.4 Extended stability analysis

Using inequality (4.36), we need to define new signals. To keep consistence with subsection 4.3.2, δ_N is applied to $K\dot{X}$, in its Laplace form, we get:

$$\forall s \in \bar{\mathbb{C}}^+ \backslash \{0\}, \quad s\delta_N(s) K\hat{X}(s) = \mathcal{V}_N(s) = \begin{bmatrix} \nu_0(s) & \cdots & \nu_N(s) \end{bmatrix}^\top,$$

where, according to (E.3), $\nu_k(s) = s\sqrt{2k+1} \left\langle e^{\theta s}, \mathcal{L}_k(\theta) \right\rangle_{L^2(-\tau,0)} K\hat{X}(s)$. We then naturally introduce for $k \in [0, N]$:

$$\chi_k(s) = \left\langle e^{\theta s}, \mathcal{L}_k(\theta) \right\rangle_{L^2(-\tau,0)} K\hat{X}(s) \text{ and } \mathfrak{X}_N(s) = \begin{bmatrix} \chi_0(s) & \cdots & \chi_N(s) \end{bmatrix}^\top.$$

Consequently, defining $\tilde{I}_N = \text{diag}\left(\left\{\frac{1}{\sqrt{2k+1}}\right\}_{k\in[0,N]}\right)$, we get that:

$$\forall s \in \bar{\mathbb{C}}^+\backslash\{0\}, \quad \mathcal{V}_N(s) = s\tilde{I}_N^{-1}\mathfrak{X}_N(s).$$

There is also another definition for $\mathfrak{X}_N$, coming from the following integration by part for $k \in [0, N]$ and using (E.3):

$$\begin{aligned}\forall s \in \bar{\mathbb{C}}^+\backslash\{0\}, \quad \chi_k(s) = \int_{-\tau}^{0} e^{\theta s}\mathcal{L}_k(\theta)d\theta \; K\hat{X}(s) &= \left(\left[\tfrac{e^{\theta s}}{s}\mathcal{L}_k(\theta)\right]_{-\tau}^{0} - \frac{1}{s}\int_{-\tau}^{0} e^{\theta s}\tfrac{d}{d\theta}\mathcal{L}_k(\theta)d\theta\right) \\ &= s^{-1}\left(1-(-1)^k e^{-\tau s}\right)K\hat{X}(s) - \frac{1}{\tau s}\sum_{i=0}^{k-1}\ell_{ik}\chi_i(s).\end{aligned}$$

Gathering all these results leads to the following formulation for the block diagram in Figure 4.1:

$$\forall s \in \bar{\mathbb{C}}^+\backslash\{0\}, \qquad \begin{cases} \hat{\omega}_N(s) - \hat{\bar{\omega}}_N(s) = \nabla_N(s)\hat{z}_N(s), \\ \mathcal{E}_N\left(\hat{z}_N(s) - \hat{\bar{z}}_N(s)\right) = \mathcal{A}_N\hat{\omega}_N(s), \end{cases}$$

where

$$\begin{gathered} z_N(t) = \begin{bmatrix} z_\oplus(t) \\ K\dot{X}(t) \\ \dot{\mathfrak{x}}_{N-1}(t) \end{bmatrix}, \qquad \omega_N(t) = \begin{bmatrix} \omega_\oplus(t) \\ \mathcal{V}_N(t) \\ \mathfrak{x}_{N-1}(t) \end{bmatrix}, \\ \nabla_N(s) = \text{diag}\left(\nabla_\oplus(s),\ \delta_N(s),\ s^{-1}I_N\right), \end{gathered} \tag{4.37}$$

and with

$$\mathcal{E}_N = \left[\begin{array}{ccc|cc} \multicolumn{3}{c|}{\mathcal{E}_\oplus} & \multicolumn{2}{c}{0} \\ \hline -K & 0 & 0 & 1 & 0 \\ 0 & \mathbb{1}_N & -\bar{\mathbb{1}}_N & 0 & 0 \\ 0 & 0 & 0 & 0 & I_N \end{array}\right], \quad \mathcal{A}_N = \left[\begin{array}{c|cc} \mathcal{A}_\oplus & \multicolumn{2}{c}{0} \\ \hline & 0 & 0 \\ 0 & \tilde{I}_N & L_N \\ & \tilde{I}_N(1\!:\!N,:) & 0 \end{array}\right], \tag{4.38}$$

and

$$\begin{aligned} L_N &= \frac{1}{\tau}\left[\ell_{ik}\right]_{i\in[0,N],k\in[0,N-1]}, \\ \mathbb{1}_N &= \begin{bmatrix} 1 & \cdots & 1 \end{bmatrix}^\top \in \mathbb{R}^{N+1}, \qquad \bar{\mathbb{1}}_N = \begin{bmatrix} (-1)^0 & \cdots & (-1)^k & \cdots & (-1)^N \end{bmatrix}^\top \in \mathbb{R}^{N+1}. \end{aligned}$$

The zeros in the previous matrices refer to the null matrices of appropriate dimensions. We obtain the following theorem which gives a sufficient condition for the wellposedness of $\Sigma(\mathcal{E}_N, \mathcal{A}_N, \nabla_N)$.

Theorem 4.6: Extended Quadratic Separation stability test

Let $N \in \mathbb{N}$ and assume $\det(A+BK) \neq 0$ with $\tau, c_0 > 0$ given and fixed. If there exist $P_N = \left[\begin{smallmatrix} P_{11} & P_{12} \\ P_{12}^\top & P_{22} \end{smallmatrix}\right] \in \mathbb{S}_+^{n+N}$ and $Q, R, S \in \mathbb{R}^+$ such that

$$\begin{bmatrix} \mathcal{E}_N & -\mathcal{A}_N \end{bmatrix}^{\perp\top} \Theta_N \begin{bmatrix} \mathcal{E}_N & -\mathcal{A}_N \end{bmatrix}^{\perp} \succeq 0 \tag{4.39}$$

holds for $\Theta_N = \left[\begin{smallmatrix} \Theta_{N,1} & \Theta_{N,2} \\ \Theta_{N,2}^\top & \Theta_{N,3} \end{smallmatrix}\right]$ where

$$\begin{aligned} \Theta_{N,1} =& \operatorname{diag}\left(0_n, -Q, R\tfrac{1}{1-\alpha}, -\tau^2 S, 0_N\right), \\ \Theta_{N,3} =& \operatorname{diag}\left(0_n, Q, R, S \otimes I_{N+1}, 0_N\right), \\ \Theta_{N,2} =& \begin{bmatrix} -P_{11} & 0 & 0 & 0 & -P_{12} \\ 0 & 0 & 0 & 0 & 0 \\ 0 & 0 & -R(1-\alpha) & 0 & 0 \\ 0 & 0 & 0 & 0 & 0 \\ -P_{12}^\top & 0 & 0 & 0 & -P_{22} \end{bmatrix}, \end{aligned} \tag{4.40}$$

then system (4.1) is input/output stable.

Proof : The proof is a consequence of Theorem 4.2. We need then to show that the following inequality holds:

$$\forall s \in \bar{\mathbb{C}}^+ \backslash \{0\}, \quad \Xi_N(s) = \begin{bmatrix} I_{n+N+3} \\ \nabla_N(s) \end{bmatrix}^* \Theta_N \begin{bmatrix} I_{n+N+3} \\ \nabla_N(s) \end{bmatrix} \preceq 0.$$

Define the following variable:

$$\bar{\Xi}_N(s) = \begin{bmatrix} I_n & 0_{n,3} & 0_{n,N} \\ 0_{N,n} & 0_{N,3} & I_N \\ 0_{3,n} & I_3 & 0_{3,N} \end{bmatrix} \Xi_N(s) \begin{bmatrix} I_n & 0_{n,3} & 0_{n,N} \\ 0_{N,n} & 0_{N,3} & I_N \\ 0_{3,n} & I_3 & 0_{3,N} \end{bmatrix}^\top,$$

then $\bar{\Xi}_N(s) \preceq 0$ is equivalent to $\Xi_N(s) \preceq 0$. Expending $\bar{\Xi}_N$ leads to:

$$\bar{\Xi}_N(s) = \operatorname{diag}\left(-2P_N \mathfrak{Re}(s^{-1}),\ Q\left(|e^{-\tau s}|^2 - 1\right),\ R\delta_{-1}(s),\ S\left(|\delta_N(s)|^2 - \tau^2\right)\right).$$

Applying Proposition 4.5 and Lemma 4.1, we then get $\Xi_N(s) \preceq 0$ for $s \in \bar{\mathbb{C}}^+ \backslash \{0\}$. Together with (4.39), we get that $\Sigma(\mathcal{E}_N, \mathcal{A}_N, \nabla_N)$ is wellposed. Since $\mathcal{E}_N$ is non-singular, $\Sigma(\mathcal{E}_N, \mathcal{A}_N, \nabla_N)$ is an extension of $\Sigma(\mathcal{E}_\oplus, \mathcal{A}_\oplus, \nabla_\oplus)$ (as defined in Definition 4.4). Then Theorem 4.3 states that $\Sigma(\mathcal{E}_\oplus, \mathcal{A}_\oplus, \nabla_\oplus)$ is wellposed. Proposition 4.4 yields that system (4.1) is input/output stable. ♢

Remark 4.11

Note that setting $N = 0$ in Theorem 4.6 resumes to Theorem 4.5.

Remark 4.12: On the number of decision variables

The number of decision variables for this extended theorem is $\frac{(n+N)^2+n+N}{2} + 3$. Increasing the order implies a quadratic increase in the number of decision variables. Traditional semi-definite algorithm can handle problems with up to 3000 decision variables in less than 30s on an Intel Core i7 processor. Consequently, for a small system ($n = 20$), the maximum order N is around 50, but for a larger system ($n = 75$), we cannot solve the problem with $N \geq 0$ in less than 30s, meaning that increasing the size of the system is a critical issue.

4.4 Numerical examples & discussion

In this section, we study the stability of three systems with different characteristics. The aim is to show that the techniques developed along this chapter can handle a large variety of problems with a relatively good accuracy. We used the software Yalmip [98] to formulate Semi-Definite Problems (SDP) and the algorithm used for the resolution is SDPT-3 [159].

4.4.1 A and $A + BK$ Hurwitz with $\|\mathcal{H}\|_\infty < 1$

The first case is the same as (4.15). Consequently, the Small-Gain Theorem 4.1 applies and gave the stability chart displayed in Figure 4.2. The Quadratic Separation methodology also applies, leading to Figure 4.5. This figure has been obtained considering a griding and evaluating LMI (4.39) at each point. The color of each area corresponds to the lowest feasible order.

We can clearly see that the detected stability area is larger than the one detected by Theorem 4.1. Indeed, using the Small-Gain Theorem, we get the stability for $\alpha < 0.0244$. This is quite normal since Quadratic Separation can be viewed as an extension of the Small-Gain Theorem. Nevertheless, even at order 3, there is a gap between the estimated stable area and the exact stable area given by CTCR, meaning that some stable areas are not detected. It seems that no matter the order, there will be a difference between the exact stable area and the estimated one using Quadratic Separation. Denoting by $\mathcal{S}_i$ the stable area at an order $i \in \mathbb{N}$, the following holds for this example: $\mathcal{S}_i \subseteq \mathcal{S}_{i+1}$.

4.4.2 A not Hurwtiz but $A + BK$ Hurwitz

This second example is defined as follows:

$$A = \begin{bmatrix} -1 & 0 \\ 0 & 0 \end{bmatrix}, \quad B = \begin{bmatrix} 0 \\ 1 \end{bmatrix}, \text{ and } K = \begin{bmatrix} 0 & -5 \end{bmatrix}. \tag{4.41}$$

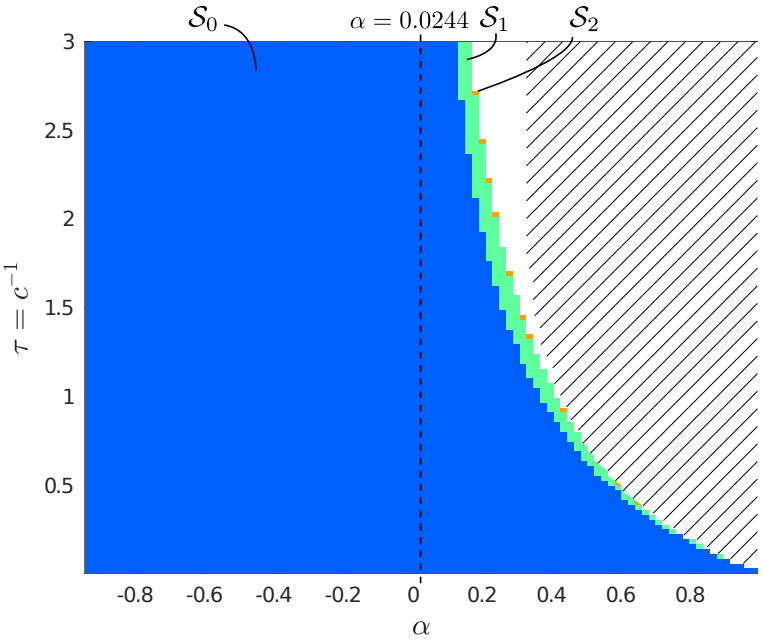

Figure 4.5: Stability chart for (4.15). The hatched area is unstable according to the CTCR algorithm presented in Section 4.1.3, while Theorem 4.6 gives that the colored area is stable. The areas marked as $\mathcal{S}_i$ are stable areas up to an order i.

Note that the open-loop system is not stable but the closed loop is. Consequently, the Small-Gain Theorem cannot apply. The results of Theorem 4.6 obtained for $N = 0$ up to $N = 5$ are drawn in Figure 4.6. We can see that there is no more improvement when increasing the order. Compared to the unstable area detected by CTCR, the estimated stability area is then not very accurate, even at high order. This might be due to the estimation of $\delta(s)$ done in Proposition 4.5 which is not optimal.

4.4.3 A and $A + BK$ are not Hurwitz

This second example is borrowed from [5] where

$$A = \begin{bmatrix} 0 & 1 \\ -2 & 0.1 \end{bmatrix}, \quad B = \begin{bmatrix} 0 \\ 1 \end{bmatrix}, \quad K = \begin{bmatrix} 1 & 0 \end{bmatrix}. \tag{4.42}$$

This system is very special as neither A nor $A+BK$ are Hurwitz, meaning that the open and closed-loop systems are both unstable. This case corresponds to Scenario 2 in the previous chapter. Nevertheless, there does exist a stable area for the interconnected system (3.8). This area is a pocket that cannot be detected by the Small-Gain theorem. However, the Quadratic Separation framework provides an inner-estimation of the stable area for an order $N \geq 1$ as we can see in Figure 4.7. Furthermore, two main observations can be made.
First, the estimation at $\alpha = 0$ is close the exact stable area. That means the behavior of the wave around $\alpha = 0$ is well captured using Quadratic Separation. For this case, we get a time-delay system and, consequently, using techniques coming from the analysis of such systems, should indeed catch the correct behavior when the interconnected

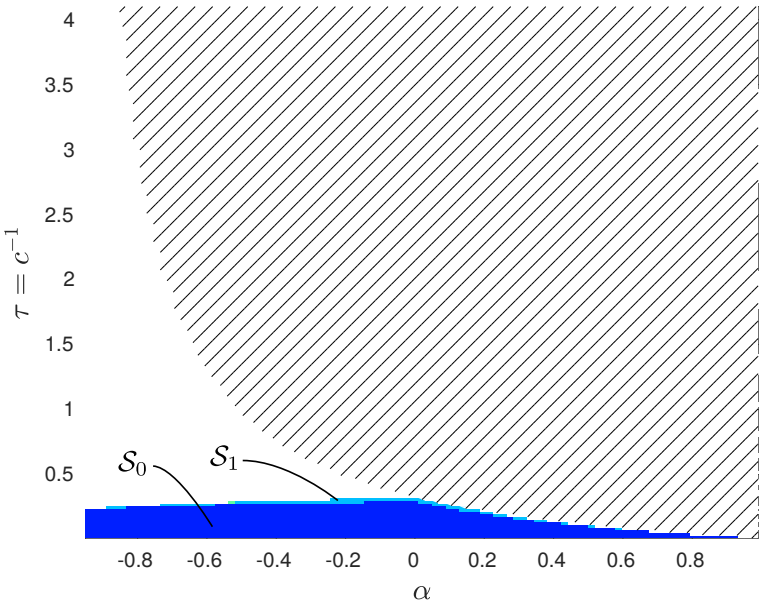

Figure 4.6: Stability chart for (4.41). The hatched area is unstable according to the CTCR algorithm presented in Section 4.1.3, while Theorem 4.6 gives that the colored area is stable. The areas marked as $\mathcal{S}_i$ are stable areas up to an order i.

system (3.8) is close to be a time-delay system.
The other observation is less understood. It seems that for $\alpha > 0.35$, LMI (4.39) is unfeasible. That means there is an upper-bound for α beyond which the Quadratic Separation methodology cannot apply in the way we derived it. This problem is further analyzed in the discussion part.

4.4.4 An example with stability pockets

For this last example, the system is taken from [65, 143][2]. It is known to possess multiple stable intervals (pockets) along the delay axis for $\alpha = 0$. We investigate whether or not QS can detect these pockets. The system matrices are given by:

$$A = \begin{bmatrix} 0 & 0 & 1 & 0 \\ 0 & 0 & 0 & 1 \\ -11 & 10 & 0 & 0 \\ 5 & -15 & 0 & -0.25 \end{bmatrix}, \; B = \begin{bmatrix} 0 \\ 0 \\ 1 \\ 0 \end{bmatrix}, \; K = \begin{bmatrix} 1 \\ 0 \\ 0 \\ 0 \end{bmatrix}^\top. \tag{4.43}$$

This example is a very good benchmark since the stability area is not so simple. Figure 4.8 represents the estimated and exact stable areas up to an order 7. We can clearly see that increasing the order helps reaching higher stable values of c^{-1}. Nevertheless, the further we are from $\alpha = 0$, the worse the estimation is.

[2]In [65], it is said that this state-space representation models a chatter machinery for $\alpha = 0$. More information can be found in the given reference.

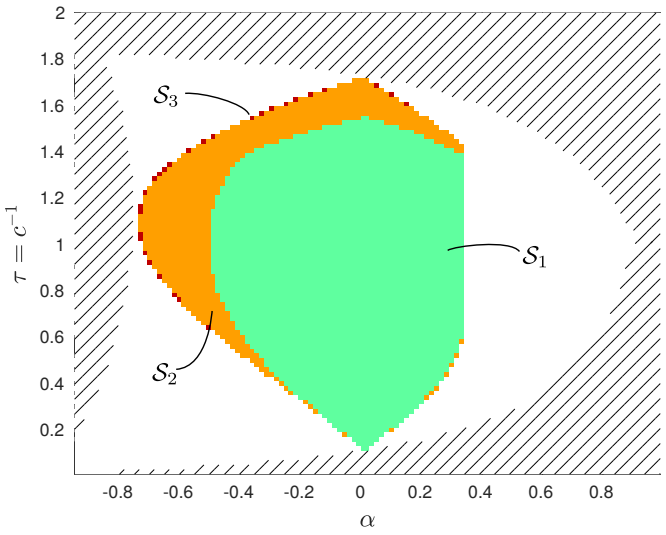

Figure 4.7: Stability chart for (4.42). The hatched area is unstable according to the CTCR algorithm presented in Section 4.1.3, while Theorem 4.6 gives that the colored area is stable. The areas marked as $\mathcal{S}_i$ are stable areas up to an order i.

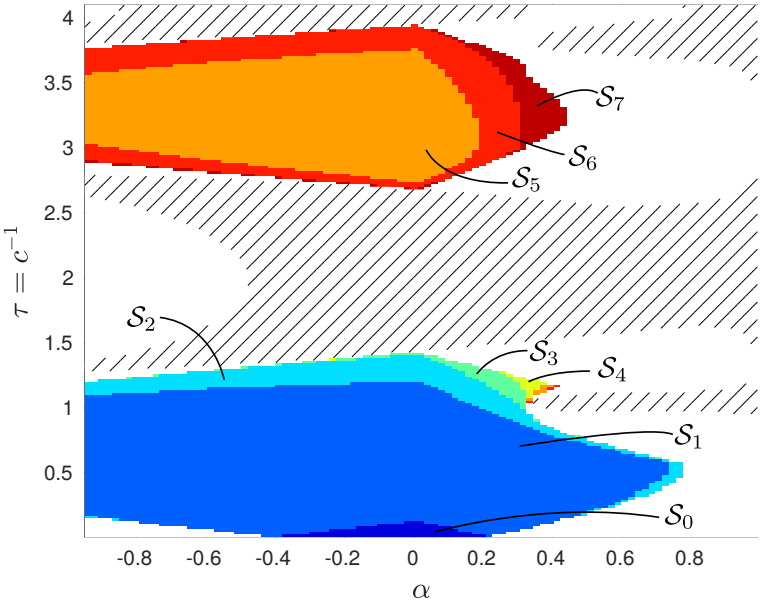

Figure 4.8: Stability chart for (4.43). The hatched area is unstable according to the CTCR algorithm presented in Section 4.1.3, while Theorem 4.6 gives that the colored area is stable. The areas marked as $\mathcal{S}_i$ are stable areas up to an order i.

4.4.5 Discussion

Before closing this chapter, we provide a short discussion about some points raised when analyzing the examples. First of all, we can note that the three approaches are coherent one with the others. We indeed get a more conservative result using the Small-Gain theorem. As the order increases, Quadratic Separation gives better result than the Small-Gain but remains quite conservative and far from the exact stable area. Moreover, it seems that when c^{-1} increases, we need a higher order N to ensure its stability using Quadratic Separation. A higher c^{-1} means a smaller speed c, it is indeed much harder to state the stability of the interconnected system if the wave is slow because it may induce instabilities [114].

One could argue the benefit of using Quadratic Separation for many reasons:

1. CTCR and the Small-Gain theorems provides a simple and fast test for ensuring the stability;
2. The CTCR algorithm gives the exact stable area, and this, much faster;
3. Quadratic Separation seems also quite conservative.

These three arguments are indeed true but we can try to answer each of them. First of all, the fastest test is the Small-Gain theorem. It indeed provides a straightforward expression and enables a global analysis as demonstrated by Proposition 4.2. CTCR is not that fast and requires many symbolic calculations before reaching the conclusion. In this sense, it is also subject to uncertainties when finding roots of polynomials. It is consequently more and more difficult to use this stability test as the order n of the system increases. This is not always the case for Quadratic Separation because it can handle quite large systems for a small order N. Moreover, the CTCR algorithm applies for system (3.8) but if we use other boundary conditions, the algorithm may not be applicable and consequently, this is a problem-dependent solution while Quadratic Separation and the Small-Gain Theorem applies whatever the linear boundary condition used.

Secondly, as noticed previously, the CTCR algorithm does not provide the exact stable areas since it might be subject to rounding errors. Moreover, plotting the chart sometimes requires a sharp griding along α. Indeed, we may miss a pole-crossing if the griding is rude and then the stability chart is wrong. This issue is not encountered using Quadratic Separation since it is evaluated at each point[3]. Moreover, it is possible to extend the stability test obtained with Quadratic Separation to get a robust result and then to prevent the errors encountered when griding.

Finally, it seems that Theorem 4.6 is quite conservative. We were expecting that when N goes to infinity, the exact stability area would be recovered, meaning an asymptotically exact estimation. This is not true but we can make the following claim.

Conjecture 4.1: Another state extension

The state extension used here only takes into account the forward part of the wave equation. Indeed, equation (4.2) shows that the wave is the sum of two

[3]Note that we may miss unstable areas if we use a rude griding.

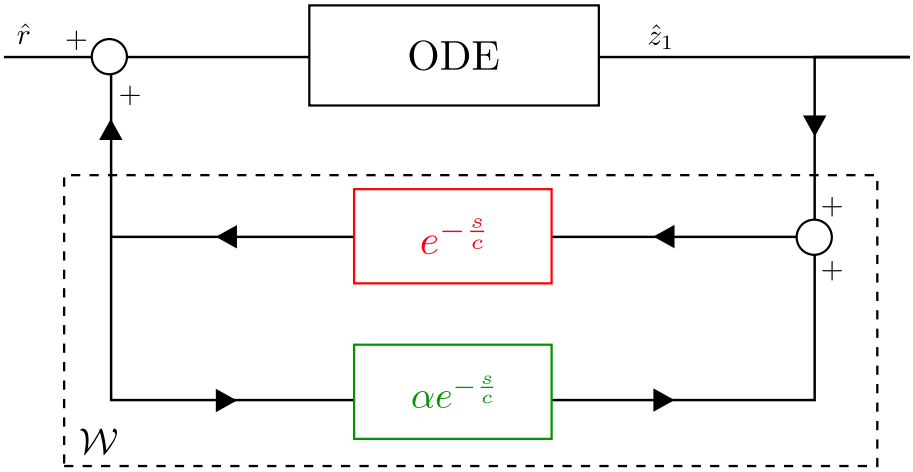

Figure 4.9: Block diagram of system (4.1) expressed with the delay operator only and where $\hat{r}$ is the input and $\hat{y} = K\hat{X}$, the output.

signals, and considering $\mathcal{W}(1, s)$ means that we only consider the incoming wave while the contribution of the second wave is not used and described in $\delta_{-1}(s)$. We claim that using the block diagram of Figure 4.9 with the projections of the two exponential leads to a better stability test, at a price of a higher number of decision variables.

We did not prove the previous assertion, but we have the intuition that it should provide a more accurate stability test. Taking the backward wave into account is not natural in this context but would lead to a better analysis for $\alpha > 0$ and probably solve the problem encountered in the second case for $\alpha > 0.35$.
One last point would be about the hierarchy property. It was not proven that increasing the order N leads to better results. Nevertheless, according to the results obtained for time-delay systems using this methodology [143] and the three examples below, we make this second claim.

Conjecture 4.2: The hierarchy property

Denote by $\mathcal{S}_N$ the stable estimated area for a given system A, B and K using Theorem 4.6 at an order N. We then get:

$$\mathcal{S}_N \subseteq \mathcal{S}_{N+1}.$$

4.5 Conclusion

In this chapter, we have developed tools to assess the input/output stability of system (3.8). Three approaches have been studied: a pole-crossing approach, a Small-Gain theorem and finally, a Quadratic Separation formulation. These three theorems provide numerically tractable stability tests and can handle different problems.
The first technique used relies on the number of unstable poles at each speed c of the

wave. This methodology is very efficient and proposes an exact stability test. Nevertheless, it is hard to extend this approach to other systems and it is not robust to parameter uncertainties.
The second stability test is very easy to compute numerically, provides a robust stability test with many practical consequences. However, it is very conservative and can be applied in very few cases.
The last result is coming from robust analysis and extends the Small-Gain approach in order to reduce the conservatism but keeping its robustness property. This approach leads to an LMI test which requires a semi-definite solver. The use of Bessel inequality helps getting less conservative results. Then, this extension can be seen as an improvement of Jensen inequality.

Nevertheless, it has to be noted that the robust stability tools did not provide asymptotic convergence to the exact stability test. The following chapter uses similar extensions but inside a Lyapunov framework to try to get a better estimate of the stable area.

5

Lyapunov stability analysis of a coupled ODE/boundary-damped string equation

The previous chapter was dedicated to the input/output stability analysis of coupled system (3.8). A complementary approach relies on the Lyapunov theory. This theory takes its fundamentals in the thesis of Aleksandr Mikhailovich Lyapunov [101], and is closely related to the decrease of energy of a system. This methodology applies very well in our context since the semi-group theory (as detailed in Section 3.1.2) requires some inequalities which are also used in the Lyapunov methodology.

The system under study is the same as (3.1) and it is reminded below for clarity:

$$\dot{X}(t) = AX(t) + Bu(1,t), \qquad t \geq 0, \tag{5.1a}$$
$$u_{tt}(x,t) = c^2 u_{xx}(x,t), \qquad x \in [0,1], t \geq 0, \tag{5.1b}$$
$$u(0,t) = KX(t), \qquad t \geq 0, \tag{5.1c}$$
$$u_x(1,t) = -c_0 u_t(1,t), \qquad t \geq 0, \tag{5.1d}$$

where c and c_0 are given and fied, with initial conditions:

$$u(x,0) = u^0(x), \qquad x \in [0,1], \tag{5.2a}$$
$$u_t(x,0) = v^0(x), \qquad x \in [0,1], \tag{5.2b}$$
$$X(0) = X^0, \tag{5.2c}$$

where $u^0(0) = KX^0$, $v^0(0) = K(A+BK)X^0$ and $u_x^0(1) = -c_0 v^0(1)$ such that (u^0, v^0, X^0) belongs to the domain of the operator as defined in Chapter 3.

This chapter firstly introduces the theory of Lyapunov adapted to an infinite-dimensional context. The first section is devoted to a literature review with some basic definitions and useful properties for the sequel. Then, we do a preliminary analysis of system (5.2). The problem is divided into two subproblems for which the Lyapunov theory has already been derived. A simple Lyapunov functional is proposed and some examples are investigated. This approach is then extended in the third part where the projection methodology is explained. That leads to an extended stability theorem and a corollary about robust stability is also proposed. Finally, some numerical examples conclude this chapter and open problems are discussed.

5.1 An introduction to Lyapunov stability theory

One of the theoretical tools to assess stability of a system is related to the application of the Lyapunov theorem. It consists in looking for a kind of energy function that has particular properties. The meaning of this function is examined after providing its definition, adapted to our infinite-dimensional context.

Definition 5.1: Lyapunov functional [136, Definition 8.1]

A function $V : \mathscr{D}(\mathscr{A}) \to \mathbb{R}^+$ is **a Lyapunov functional** for system (5.2) if there exist $\varepsilon_1, \varepsilon_2, \varepsilon_3 > 0$ and $\mu \geq 0$ such that the following holds:

$$\varepsilon_1 \|(X,u,v)\|^2_{\mathscr{D}(\mathscr{A})} \leq V(X,u,v) \leq \varepsilon_2 \|(X,u,v)\|^2_{\mathscr{D}(\mathscr{A})}, \tag{5.3a}$$

$$\left\langle \nabla V(X,u,u_t),\ \mathscr{A}\begin{bmatrix} X \\ u \\ u_t \end{bmatrix} \right\rangle_{\mathbb{R}^n \times \mathbb{X}} + 2\mu V(X,u,u_t) \leq -\varepsilon_3 \|(X,u,u_t)\|^2_{\mathscr{D}(\mathscr{A})}, \tag{5.3b}$$

where $\nabla V(X,u,u_t) = \operatorname{col}\left(\partial_X V(X,u,u_t), \partial_u V(X,u,u_t), \partial_{u_t} V(X,u,u_t)\right)$.

Remark 5.1

Usually, we choose V as an integral-quadratic functional since it verifies easily the first inequality and the second one can be bounded by a quadratic term.

Before stating the main theorems of the chapter, let interpret the two inequalities (5.3). First, (5.3a) means that $\sqrt{V}$ is an equivalent norm to $\|\cdot\|_{\mathbb{R}^n \times \mathbb{X}}$. Since all the norms are not equivalent in infinite dimension, this inequality is required. Note that the existence of $\varepsilon_1 > 0$ implies that V is positive and ε_2 ensures its definitiveness.

The second equation (5.3b) with $\mu = 0$ can be understood as the time derivation of $t \mapsto V(X(t), u(t), v(t))$ to be strictly negative, meaning that this function is strictly decreasing along time. Of course, this second statement is close to the notion of dissipative system explored in Section 3.1.2. If $\mu > 0$, since V is positive (due to (5.3a)), we require V to decrease with a given decay-rate. This will be clarified by the following proposition where the existence of a Lyapunov functional is related to the exponential stability.

Proposition 5.1: [19, Theorem 1]

If there exists a Lyapunov functional for system (5.2), then the origin of $\mathscr{D}(\mathscr{A})$ is exponentially stable in the sense of $\|\cdot\|_{\mathscr{D}(\mathscr{A})}$ with a decay-rate of at least μ.

Proof : Since $\mathscr{D}(\mathscr{A}) \subset \mathbb{R}^n \times \mathbb{X}$, we can use the canonical scalar product on $\mathbb{R}^n \times \mathbb{X}$. If V is a Lyapunov functional for system (5.2), then the following holds for $t \geq 0$:

$$\begin{aligned} \frac{d}{dt}\left(V(X(t),u(t),u_t(t)\right) &= \left\langle \nabla V(X(t),u(t),u_t(t)), \frac{d}{dt}\begin{bmatrix} X(t) \\ u(t) \\ u_t(t) \end{bmatrix} \right\rangle_{\mathbb{R}^n \times \mathbb{X}} \\ &\leq -2\mu V(X(t),u(t),u_t(t)) - \varepsilon_3 \|(X(t),u(t),u_t(t))\|^2_{\mathscr{D}(\mathscr{A})} \\ &\leq -\left(\mu + \frac{\varepsilon_3}{\varepsilon_2}\right) V(X(t),u(t),u_t(t)). \end{aligned}$$

Written differently, we get:

$$\frac{d}{dt}\left(V(X(t),u(t),u_t(t))e^{\left(2\mu+\frac{\varepsilon_3}{\varepsilon_2}\right)t}\right)\leq 0.$$

Integrating the previous expression leads to:

$$\forall t\geq 0,\quad V(X(t),u(t),u_t(t))\leq V(X^0,u^0,v^0)e^{-\left(2\mu+\frac{\varepsilon_3}{\varepsilon_2}\right)t},$$

or, more conveniently,

$$\forall t\geq 0,\quad \|(X(t),u(t),u_t(t))\|_{\mathscr{D}(\mathscr{A})}\leq\sqrt{\frac{\varepsilon_2}{\varepsilon_1}}\|(X^0,u^0,v^0)\|_{\mathscr{D}(\mathscr{A})}\exp\left(-\left(\mu+\frac{\varepsilon_3}{2\varepsilon_2}\right)t\right),$$

which is the definition of exponential stability with decay-rate of at least μ (see Definition 3.7). ♢

Remark 5.2: Asymptotic convergence

The second inequality in Definition 5.1 is the key point for proving exponential stability as shown in the previous proof. To prove asymptotic stability, one can set $\mu=\varepsilon_3=0$ and use LaSalle Invariance Principle [136, Theorem 8.4]. This requires far more care for infinite-dimensional systems.

The previous proposition shows that the existence of a Lyapunov functional implies exponential stability. For linear time-invariant finite-dimensional systems, there is an equivalence between the two statements[1] and the Lyapunov function is quadratic. This special form makes it very easy to solve using semi-definite programming.

For time-delay systems, such an equivalence also exists as shown in [47, 76, 83] and the Lyapunov functional is integral quadratic (see [65, Theorem 5.18] for instance). The interested reader can refer to the works [59, 65, 143] which provides Lyapunov functionals for time-delay systems.

Since time-delay systems are a special class of coupled ODE/transport equation, there is some hope to get the equivalence between the existence of a Lyapunov functional and the exponential stability of (5.2). This has been indeed done by Richard Datko first in [45] and then enriched in [46]. This result has been adapted to our problem in the following theorem.

Theorem 5.1: [46]

System (5.2) is exponentially stable if and only if there exists a Lyapunov functional for this system.

The main consequence of this latter theorem is the versatility of the Lyapunov theory. Indeed, that means there exists a Lyapunov function if the system is exponentially stable. Nevertheless, this functional might not be explicit and therefore, may not be quadratic. The aim of the following parts is to propose a quadratic Lyapunov functional which is close to the "ideal" functional but leading to a numerically tractable stability conditions, in terms of LMIs for instance.

[1] This has been proved in many books, see [82, Theorem 4.6] for instance.

5.2 Preliminary stability analysis

As in the finite-dimensional case, finding a Lyapunov functional for a coupled ODE/PDE system is not easy. Indeed, since the two subsystems are of different nature, it is quite difficult to propose a Lyapunov functional taking into account the specificity of each subsystem. Traditionally, we define a Lyapunov function $\mathcal{V}_{ODE}$ for the ODE part and a functional $\mathcal{V}_{PDE}$ for the infinite-dimensional part as done in [54, 87, 152]. The natural and first idea to build a Lyapunov functional V for the whole system is to sum up of $\mathcal{V}_{ODE}$ and $\mathcal{V}_{PDE}$ as we will do in the following subsection.

Remark 5.3: Global exponential stability

As stated in Proposition 3.3, global exponential stability can be achieved if there is a unique equilibrium point. We therefore assume that $A+BK$ is non singular.

5.2.1 A Lyapunov functional for the wave equation

The PDE considered in system (5.2) is of second order in time. As we want to use some tools already designed for first order hyperbolic systems, we propose to define some new states using modified Riemann coordinates, which satisfy a set of coupled first order hyperbolic PDEs. Let us introduce these coordinates, defined as follows:

$$\chi(x,t) = \begin{bmatrix} u_t(x,t) + cu_x(x,t) \\ u_t(1-x,t) - cu_x(1-x,t) \end{bmatrix} = \begin{bmatrix} \chi^+(x,t) \\ \chi^-(x,t) \end{bmatrix}.$$

The introduction of such variables is not new and the reader can refer to the articles [27, 122] or the books [20, 39] and references therein about Riemann invariants. $\chi^+ \in L^2$ and $\chi^- \in L^2$ are related the eigenfunctions of the wave operator associated to the eigenvalue c. Using this new coordinate system, the wave equation itself rewrites as:

$$\forall t \geq 0, \quad \forall x \in [0,1], \qquad \chi_t(x,t) = c\chi_x(x,t), \tag{5.4}$$

with the adequate boundary conditions.

Remark 5.4

The norm of the modified state χ can be directly related to the norm of the functions u_t and u_x. Indeed simple calculations and a change of variables give:

$$\|\chi\|_{L^2}^2 = 2\left(\|u_t\|_{L^2}^2 + c^2\|u_x\|_{L^2}^2\right). \tag{5.5}$$

If $u(0,t) = 0$, using Proposition E.6 and the previous equality lead to:

$$\frac{1}{2}\left(1 + \frac{2}{c^2}\right)\|\chi\|_{L^2}^2 \geq \|u_t\|_{L^2}^2 + c^2\|u_x\|_{L^2}^2 + \|u\|_{L^2}^2. \tag{5.6}$$

Since the variable χ is the solution of a transport equation, the following Lyapunov functional candidate is proposed:

$$\mathcal{V}_{PDE}(\chi) = \int_0^1 \chi^\top(x)\,(S + xR)\,\chi(x)dx, \tag{5.7}$$

where $S, R \in \mathbb{S}^2_{++}$. This functional is an enhancement of the one proposed in [20, 38, 39] and has been proposed in [130].

Remark 5.5

In [20, 39], the authors did not introduce the exact same Lyapunov functional but the following one:

$$\mathcal{V}_{Bastin}(\chi) = \int_0^1 \chi^\top(x)\chi(x)e^{-\frac{\delta x}{c}}dx$$

for $\delta > 0$. That leads to similar results but it is easier in the sequel to use an affine term. In [131] for instance, the authors use a combination of both terms.

The following proposition is an adaption of [16, Theorem 1 and Corollary 2].

Proposition 5.2

Let $c, c_0 > 0$. Then, the following system

$$\begin{aligned}
u_{tt}(x,t) &= c^2 u_{xx}(x,t), && x \in [0,1], t \geq 0, && \text{(5.8a)}\\
u(0,t) &= 0, && t \geq 0, && \text{(5.8b)}\\
u_x(1,t) &= -c_0 u_t(1,t), && t \geq 0, && \text{(5.8c)}\\
\begin{bmatrix} u(x,0) \\ u_t(x,0) \end{bmatrix} &= \begin{bmatrix} u^0(x) \\ v^0(x) \end{bmatrix}, && x \in [0,1], && \text{(5.8d)}
\end{aligned}$$

where $(u^0, v^0) \in H^2 \times H^1$ such that they verify (5.8c) is exponentially stable.

Proof : The existence of a solution to system (5.8) has been studied in [38, 64] for instance. It has been proved that (u, u_t) belongs to $C^1(0, +\infty, \mathbb{X})$. We are interested here in the stability analysis only.

Since $c_0 > 0$, there exist $S_1, S_2 > 0$ such that the following holds:

$$S_2 < S_1 \qquad \text{and} \qquad S_1(1 - cc_0)^2 < S_2(1 + cc_0)^2. \tag{5.9}$$

Indeed, the previous conditions rewrite as $S_2 < S_1 < \alpha^{-2} S_2$ where $\alpha = \frac{1-cc_0}{1+cc_0}$. The existence of S_1 and S_2 is equivalent to $\alpha < 1$, which is the case if and only if $cc_0 > 0$. Let now $S, R \in \mathbb{S}^2_{++}$ verifying $S \preceq \left[\begin{smallmatrix} S_1 & 0 \\ 0 & S_2 \end{smallmatrix}\right] \preceq S + R$. We want to show that $\mathcal{V}_{PDE}$ is a Lyapunov functional for system (5.8). To this extend, we desire to apply Proposition 5.1 and we are therefore looking for the existence of $\varepsilon_1, \varepsilon_2$ and $\varepsilon_3 > 0$ such that (5.3) holds with $\mu = 0$.

Existence of ε_1 and ε_2: Since $S, R \in \mathbb{S}^2_{++}$, that means there exists ε_1 and ε_2 such that for $x \in [0,1]$:

$$\frac{\varepsilon_1}{2}\left(1+\frac{2}{c^2}\right) I_2 \preceq S \preceq S + xR \preceq S + R \preceq \frac{\varepsilon_2}{2} I_2.$$

Consequently, using (5.6), the following inequality on $\mathcal{V}_{PDE}$ holds:

$$\mathcal{V}_{PDE}(\chi(\cdot,t)) \geq \frac{\varepsilon_1}{2}\left(1+\frac{2}{c^2}\right)\|\chi\|^2_{L^2} \geq \varepsilon_1\left(\|u\|^2_{L^2} + c^2\|u_x\|^2_{L^2} + \|u_t\|^2_{L^2}\right).$$

Similarly, we get:

$$\mathcal{V}_{PDE}(\chi(\cdot,t)) \leq \varepsilon_2\left(\|u_t\|^2_{L^2} + c^2\|u_x\|^2_{L^2}\right) \leq \varepsilon_2\left(\|u\|^2_{L^2} + c^2\|u_x\|^2 + \|u_t\|^2_{L^2}\right).$$

Existence of ε_3: Taking the time-derivative of $\mathcal{V}_{PDE}$ leads to:

$$\begin{aligned}\dot{\mathcal{V}}_{PDE}(\chi(\cdot,t)) &= 2\int_0^1 \chi_t^\top(x,t)(S+xR)\chi(x,t) = 2c\int_0^1 \chi_x^\top(x,t)(S+xR)\chi(x,t)dx \\ &= 2c\left(\left[\chi^\top(x,t)(S+xR)\chi(x,t)\right]_0^1 - \langle\chi(\cdot,t), R\chi(\cdot,t)\rangle_{L^2}\right) \\ &\qquad -\dot{\mathcal{V}}_{PDE}(\chi(\cdot,t)).\end{aligned}$$

In other words, we get:

$$\dot{\mathcal{V}}_{PDE}(\chi(\cdot,t)) = c\left(\|\chi(1,t)\|^2_{S+R} - \|\chi(0,t)\|^2_S - \langle\chi(\cdot,t), R\chi(\cdot,t)\rangle_{L^2}\right). \tag{5.10}$$

Since $R \succ 0$, there exists $\varepsilon_3 > 0$ and small enough such that $R \succeq \frac{\varepsilon_3}{2c}\left(1+\frac{2}{c^2}\right) I_2$. This inequality together with (5.6) lead to:

$$\begin{aligned}\dot{\mathcal{V}}_{PDE}(\chi(\cdot,t)) &\leq c\left(\|\chi(1,t)\|^2_{S+R} - \|\chi(0,t)\|^2_S\right) - \tfrac{\varepsilon_3}{2}\left(1+\tfrac{2}{c^2}\right)\|\chi(\cdot,t)\|^2_{L^2} \\ &\leq c\left(\|\chi(1,t)\|^2_{S+R} - \|\chi(0,t)\|^2_S\right) - \varepsilon_3\left(\|u_t\|^2_{L^2} + \|u\|^2_{L^2} + c^2\|u_x\|^2_{L^2}\right).\end{aligned}$$

Using the previous inequality, but replacing $\chi(1,t)$ and $\chi(0,t)$ by their expression leads to:

$$\begin{aligned}\|\chi(1,t)\|^2_{S+R} &\leq S_1(u_t(1,t) + cu_x(1,t))^2 + S_2(u_t(0,t) - cu_x(0,t))^2 \\ &\leq S_1(1-cc_0)^2 u_t(1,t)^2 + S_2c^2u_x(0,t)^2, \\ \|\chi(0,t)\|^2_S &\geq S_1(u_t(0,t) + cu_x(0,t))^2 + S_2(u_t(1,t) - cu_x(1,t))^2 \\ &\geq S_1c^2u_x(0,t)^2 + S_2(1+cc_0)^2u_t(1,t)^2.\end{aligned}$$

Finally, we get the following:

$$\begin{aligned}\dot{\mathcal{V}}_{PDE}(\chi(\cdot,t)) \leq c^3(S_2-S_1)u_x(0,t)^2 + c\left(S_1(1-cc_0)^2 - S_2(1+cc_0)^2\right)u_t(1,t)^2 \\ -\varepsilon_3\left(\|u_t\|^2_{L^2} + \|u\|^2_{L^2} + c^2\|u_x\|^2_{L^2}\right).\end{aligned}$$

Since (5.9) holds, we get:

$$\dot{\mathcal{V}}_{PDE}(\chi(\cdot,t)) \leq -\varepsilon_3\left(\|u_t\|^2_{L^2} + \|u\|^2_{L^2} + c^2\|u_x\|^2_{L^2}\right).$$

and $\mathcal{V}_{PDE}$ is a Lyapunov functional for system (5.8), meaning that it is exponentially stable. ♢

One could argue about the difficult procedure for proving that system (5.8) is exponentially stable while doing in a similar way as [39] would lead to easier calculations. Actually, we tried here to generate the most general structure a Lyapunov functional candidate can have. Thus, it is possible to adapt the theorem according to the situation, and possibly get better results. This will become clearer in the sequel. We know, from pole location arguments [69], that the condition $c_0 > 0$ is equivalent to the exponential stability of system (5.8). Consequently, we get that system (5.8) is exponentially stable if and only if there exist $S, R \in \mathbb{S}^2_+$ such that $\mathcal{V}_{PDE}$ is a Lyapunov functional for (5.8).

5.2.2 Lyapunov functional of the coupled system

As said previously, in this section, we provide a first Lyapunov functional candidate for coupled system (5.2). To do so, we just add a Lyapunov function for the finite-dimensional part and (5.7). That leads to:

$$V(X,\chi) = \mathcal{V}_{ODE}(X) + \mathcal{V}_{PDE}(\chi) = X^\top P X + \int_0^1 \chi^\top(x)(S + xR)\chi(x)dx. \tag{5.11}$$

This functional candidate is not new and it has been used in [54, 152] or [153] for instance. The following theorem expresses under which condition V is a Lyapunov functional.

Theorem 5.2: Simple Lyapunov functional

Let $c, c_0 > 0$. If there exist $P \in \mathbb{S}^n_{++}$ and $R, S \in \mathbb{S}^2_{++}$ such that

$$\Theta = \mathrm{He}\left(D^\top P F\right) + c\left(H^\top(S+R)H - G^\top S G\right) - c\tilde{R} \prec 0$$

where

$$F = \begin{bmatrix} I_n & 0_{n,4} \end{bmatrix}, \qquad \tilde{B} = \frac{1}{2c}\begin{bmatrix} 1 & -1 \end{bmatrix},$$
$$D = \begin{bmatrix} A + BK & \tilde{B} & 0_{n,2} \end{bmatrix}, \qquad \tilde{R} = \mathrm{diag}\left(0_n, R, 0_2\right),$$
$$g = \begin{bmatrix} 0 & 1 \\ 1 + cc_0 & 0 \end{bmatrix}, \qquad G = \begin{bmatrix} 0_{2,n+2} & g \end{bmatrix} + \begin{bmatrix} K \\ 0_{1,n} \end{bmatrix} D,$$
$$h = \begin{bmatrix} 1 - cc_0 & 0 \\ 0 & -1 \end{bmatrix}, \qquad H = \begin{bmatrix} 0_{2,n+2} & h \end{bmatrix} + \begin{bmatrix} 0_{1,n} \\ K \end{bmatrix} D.$$

then V with the parameters P, S and R is a Lyapunov functional for system (5.2).

Proof : The proof follows the same line as in the proof of Proposition 5.2 and is very similar to the proof of [19, Theorem 1]. We want to apply Proposition 5.1 and we are therefore looking for the existence of $\varepsilon_1, \varepsilon_2$ and $\varepsilon_3 > 0$ such that (5.3) holds with $\mu = 0$.

Existence of ε_1: Since $P, S, R \in \mathbb{S}_+$, there there exists ε_1 such that:

$$P \succeq \varepsilon_1 I_n + 2K^\top K, \quad S + xR \succeq \frac{\varepsilon_1}{2}\left(1 + \frac{2}{c^2}\right) I_2.$$

These inequalities lead to:

$$\begin{aligned} V(X,\chi) &\geq \varepsilon_1 \left(\|X\|_{\mathbb{R}^n}^2 + |KX|^2 + \frac{1}{2}\left(1 + \frac{2}{c^2}\right) \|\chi\|_{L^2}^2 \right) \\ &\geq \varepsilon_1 \|(X,u,u_t)\|_{\mathscr{D}(\mathscr{A})}^2 + \varepsilon_1 \left(2\|u_x\|_{L^2}^2 + 2|u(0)|^2 - \|u\|_{L^2}^2 \right). \end{aligned}$$

where we recall that $u(0) = KX$. Applying Proposition E.6 ensures that the last term is positive and concludes on the existence of ε_1.

Existence of ε_2: This is the same reasoning as in the previous proof with $P \leq \varepsilon_2 I_n$ for $\varepsilon_2 > 0$ and it is therefore omitted.

Existence of ε_3: First of all, note that:

$$\dot{V}(X(t), \chi(\cdot,t)) = \mathrm{He}\left(\dot{X}^\top(t) P X(t) \right) + \dot{\mathcal{V}}_{PDE}(\chi(\cdot,t))$$

We start by rewriting the ODE in a more convenient form, similarly to what has been done in the proof of Theorem 3.1:

$$\begin{aligned} \dot{X}(t) &= AX(t) + Bu(1,t) = (A+BK)X(t) + B\int_0^1 u(x,t)dx \\ &= (A+BK)X(t) + \frac{1}{2c} B \left(\int_0^1 \chi^+(x,t)dx - \int_0^1 \chi^-(x,t)dx \right) \\ &= (A+BK)X(t) + \tilde{B}\mathfrak{X}(t), \end{aligned}$$

where $\mathfrak{X}(t) = \int_0^1 \chi(x,t)dx$. We introduce the following extended state:

$$\xi(t) = \mathrm{col}\left(X(t),\ \mathfrak{X}(t),\ u_t(1,t),\ u_x(0,t) \right).$$

Note then that $X(t) = D\xi(t)$, $\dot{X}(t) = D\xi(t)$, $\chi(0,t) = G\xi(t)$ and $\chi(1,t) = H\xi(t)$, where the matrices are defined in the statement of this theorem. Using equation (5.10), we get:

$$\begin{aligned} \dot{V}(X(t),\chi(\cdot,t)) &= \xi^\top(t) \left\{ \mathrm{He}\left(D^\top P F \right) + c\left(H^\top (S+R) H - c G^\top S G \right) \right\} \xi(t) \\ &\qquad - c\langle \chi(\cdot,t), R\chi(\cdot,t) \rangle_{L^2} \\ &= \xi^\top(t) \Theta\ \xi(t) + c\mathfrak{X}^\top(t) R \mathfrak{X}(t) - \int_0^1 \chi^\top(x,t) R \chi(x,t) dx, \end{aligned}$$

Since $R \succ 0$ and $\Theta \prec 0$, there exists a small enough $\varepsilon_3 > 0$ such that:

$$R \ \succeq\ \frac{\varepsilon_3}{2c}\frac{2+c^2}{c^2} I_2, \qquad \Theta \ \preceq\ -\varepsilon_3 \,\mathrm{diag}\left(I_n + 2K^\top K, \frac{2+c^2}{2c^2} I_2, 0_2 \right).$$

Using Jensen inequality (see Proposition E.3), we get the following bound on the derivative of the functional along the trajectories of (5.2):

$$\begin{aligned}\dot{V}(X(t),\chi(\cdot,t)) \leq -\varepsilon_3 \left(\|X(t)\|^2_{\mathbb{R}^n} + 2|u(0,t)|^2 + \frac{2+c^2}{2c^2}\|\chi(\cdot,t)\|^2_{L^2} \right) \\ +c\mathfrak{X}^\top(t)\left(R - \frac{\varepsilon_3}{2c}\frac{2+c^2}{c^2}I_2\right)\mathfrak{X}(t) \\ -c\int_0^1 \chi^\top(x,t)\left(R - \frac{\varepsilon_3}{2c}\frac{2+c^2}{c^2}I_2\right)\chi(x,t)dx \\ \leq -\varepsilon_3 \left(\|X(t)\|^2_{\mathbb{R}^n} + 2|u(0,t)|^2 + \frac{2+c^2}{2c^2}\|\chi(\cdot,t)\|^2_{L^2} \right).\end{aligned} \tag{5.12}$$

Using now Proposition E.6 in (5.12) and following a similar proof than for Proposition 5.2, one obtains that:

$$\dot{V}(X(t),\chi(\cdot,t)) \leq -\varepsilon_3 \|(X,u,u_t)\|^2_{\mathscr{D}(\mathscr{A})}.$$

Then V is a Lyapunov functional for system (5.2). ♢

Remark 5.6: Necessary for Theorem 5.2

- Assume Theorem 5.2 holds, then $\Theta \prec 0$. Consequently, $F^\top \Theta F$ must be definite positive. That leads to:

$$(A+BK)^\top P + P(A+BK) + c(A+BK)^\top K^\top R K (A+BK) \prec 0,$$

  which imposes $A+BK$ to be Hurwitz.

- In the case of cascaded system ($B = 0$ or $K = 0$), the previous remark implies that A must be Hurwitz.

- Similarly to the previous remark, a necessary condition for $\Theta \prec 0$ is $[0_{2,n+2}\ I_2]\,\Theta\,[0_{2,n+2}\ I_2]^\top \prec 0$. This leads to $h^\top(S+R)h - g^\top S g \prec 0$, and there exist positive definite matrices R and S in $\mathbb{S}^2_{++}$ verifying this latter condition if and only if $c_0 > 0$. In other words, the PDE must be stable.

Remark 5.7: Special case of fast string equation

The Lyapunov functional used here is the same than in [34]. In this paper, the authors proved that for c sufficiently large and $A+BK$ Hurwitz, there exist parameters P, S and R such that V is a Lyapunov functional and the coupled system is then exponentially stable. This is indeed verified in the examples of the following section.

As noted in the second chapter, we introduce here a short discussion about cascaded and coupled systems[2]. The Lyapunov functional derived here is interesting for cascaded systems. Indeed, a cascade means that one subsystem - the wave equation or the ODE

[2]See Figure 3.2 for a reminder of these notions.

- influences the other but the reverse is not true. It means that, in system (5.2), either B or K is set to zero.

The case $K = 0$ implies that the PDE generates a perturbation for the ODE. Since $c_0 > 0$, the wave itself is exponentially stable and the resulted perturbation is going exponentially to 0. The ODE will not be affected by this perturbation as long as it is exponentially stable, which is the case if A is Hurwitz. This is the input to state stability property of the ODE.

The other case $B = 0$ implies that the ODE generates a perturbation which feeds the wave and consequently, we want to know if the PDE is impacted by this perturbation. Since there is no feedback, the ODE must be stable. In other words, we want the wave to be input to state stable[3]. with respect to a perturbation generated by a linear ODE.

The interesting case arises when the system is coupled. Since the wave must be damped for the theorem to hold, if $A + BK$ is Hurwitz, then it might exist a solution. Note that when $c \to \infty$, the wave has a very fast dynamic[4] and can then be approximated by the identity operator. Consequently, assuming $A + BK$ Hurwitz means that for high speed damped waves, the coupled system is stable. Even if A is not Hurwitz, the coupling might enforce stability of the overall system as noted in Remark 5.7. This feature will be illustrated in the following subsection.

5.2.3 Numerical results

This subsection follows the same line as Section 4.4. The stability analysis of three systems is conducted using Theorem 5.2.

A and $A + BK$ Hurwitz with $\|\mathcal{H}\|_\infty < 1$

This example is the same as in the previous chapter:

$$A = \begin{bmatrix} -2 & 1 \\ 0 & -1 \end{bmatrix}, \quad B = \begin{bmatrix} 1 \\ 1 \end{bmatrix}, \text{ and } K = \begin{bmatrix} 0 & -\frac{20}{21} \end{bmatrix}. \tag{5.13}$$

The stability chart obtained using Theorem 5.2 is shown in Figure 5.1a. As a comparison, the Small Gain theorem stated that the system is guaranteed to be stable for $\alpha < 0.0224$. The result here is totally different since the stable area detected by the Small Gain theorem is not part of the new detected stability area. We note that for high speed, we get a relatively accurate estimation of the stability area.

A not Hurwitz but $A + BK$ Hurwitz

We propose here to consider system (5.2) with the following matrices:

$$A = \begin{bmatrix} -1 & 0 \\ 0 & 0 \end{bmatrix}, \quad B = \begin{bmatrix} 0 \\ 1 \end{bmatrix}, \text{ and } K = \begin{bmatrix} 0 & -5 \end{bmatrix}. \tag{5.14}$$

[3] See [150, 151] for more information about input to state stability.

[4] Indeed, $|\alpha| = \left|\frac{1-cc_0}{1+cc_0}\right| \xrightarrow[c\to\infty]{} 1$ and the poles of the wave are going to $-\infty$ as seen in (4.3).

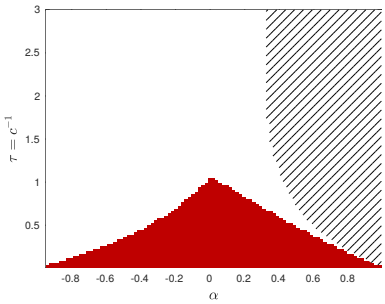

(a) System (5.13)

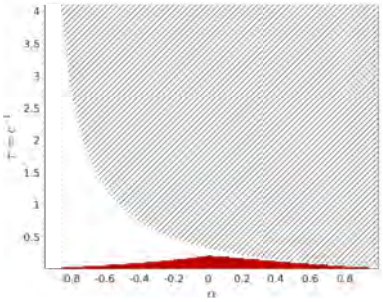

(b) System (5.14)

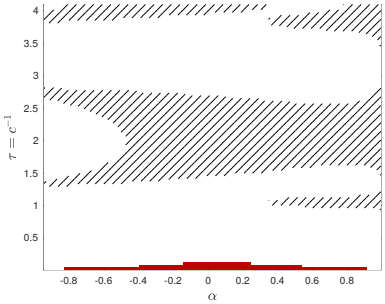

(c) System (5.15)

Figure 5.1: Stability charts of the different systems using Lyapunov functional (5.11). The hatched area is unstable according to the CTCR algorithm presented in Section 4.1.3, while Theorem 5.2 gives that the colored area is stable.

Note that A is not Hurwitz but $A + BK$ is. Theorem 5.2 has been applied to this system and we obtain the stability chart of Figure 5.1b. We can see that when c is large (τ is small), system (5.2) is stable as expected.

An example with stability pockets

Let us come back to the example presented in (4.42) with the following matrices:

$$A = \begin{bmatrix} 0 & 0 & 1 & 0 \\ 0 & 0 & 0 & 1 \\ -11 & 10 & 0 & 0 \\ 5 & -15 & 0 & -0.25 \end{bmatrix}, \; B = \begin{bmatrix} 0 \\ 0 \\ 1 \\ 0 \end{bmatrix}, \; K = \begin{bmatrix} 1 \\ 0 \\ 0 \\ 0 \end{bmatrix}^\top. \tag{5.15}$$

As said in the previous chapter, this example is interesting for performing some benchmarking since its stability chart is not straightforward. We applied Theorem 5.2 on this system and we found the chart in Figure 5.1c. We can see that the stable area according to Theorem 5.2 is very small compared to the real stable area.

Discussion

The proposed approach based on Lyapunov functional (5.11) gives interesting results. Indeed, we saw that the Lyapunov theory can apply to coupled systems. Considering the

sum of Lyapunov functionals for each subsystem indeed leads to a Lyapunov functional for system (5.2). Even if it is powerful for assessing the stability of cascaded systems, it leads to poor results when considering interconnected systems with low speed c. The next section will provide a functional with an improved stability analysis.

5.3 Extended stability analysis

Considering the Lyapunov functional derived in (5.11) for the overall coupled system leads to a poor stability analysis since we do not consider interactions between the subsystems. This interaction can be modeled by cross-terms between the states of the ODE and the PDE. In this section, we provide an extension to the previous analysis answering this problem.

5.3.1 The projection methodology seen as a state extension

The methodology given below is described in the context of the stability analysis of system (5.2). It was originally developed in [143] for time-delay systems but it can be extended to other systems since the concept is quite general. Nevertheless, the interpretation given in this subsection is relatively new. It relies on an estimation of the infinite-dimensional state. First of all, we need to find what we denote by the "state" of the problem. In [120, 121], the state is defined as the minimal quantity of information that determines uniquely the system and its future evolution. In our case, the state would be for $t \geq 0$:

$$X_\infty(t) = \begin{bmatrix} X(t) \\ \chi(\cdot,t) \end{bmatrix} = \begin{bmatrix} X(t) \\ \chi^+(\cdot,t) \\ \chi^-(\cdot,t) \end{bmatrix} \in \mathbb{R}^n \times L^2 \times L^2.$$

Since $X_\infty(t)$ belongs to a functional space, it is of infinite dimension. It is then not possible to apply the techniques developed in the finite-dimensional case. One solution is then to approximate this state on a finite-dimensional space. To this extend, let $(e_k)_{k\in\mathbb{N}}$ be an orthogonal and dense family of L^2 and define the following:

$$\chi_N^+(x,t) = \sum_{k=0}^{N} \Omega_k^+(t) \frac{e_k(x)}{\|e_k\|_{L^2}}, \quad \Omega_k^+(t) = \int_0^1 \chi^+(x,t) \frac{e_k(x)}{\|e_k\|_{L^2}} dx.$$

Ω_k^+ is called the projection coefficient of order k of χ^+. Then, the following holds for $t \geq 0$ and $x \in [0,1]$:

$$\begin{aligned} \min_{y \in \mathrm{Span}(e_k)_{k\leq N}} \|\chi^+(\cdot,t) - y\|_{L^2}^2 &= \|\chi^+(\cdot,t) - \chi_N^+(\cdot,t)\|_{L^2}^2 \\ &= \|\chi^+(\cdot,t)\|_{L^2}^2 - 2\langle \chi^+(\cdot,t), \chi_N^+(\cdot,t)\rangle + \|\chi_N^+(\cdot,t)\|_{L^2}^2 \\ &= \|\chi^+(\cdot,t)\|_{L^2}^2 - \|\chi_N^+(\cdot,t)\|_{L^2}^2. \end{aligned}$$

	System (5.2)	Truncated system (5.2)
State	$X_\infty(t) = \begin{bmatrix} X(t) \\ \chi^+(\cdot,t) \\ \chi^-(\cdot,t) \end{bmatrix}$	$X_N(t) = \begin{bmatrix} X(t) \\ \langle \chi^+(\cdot,t), e_0 \rangle_{L^2} \\ \langle \chi^-(\cdot,t), e_0 \rangle_{L^2} \\ \vdots \\ \langle \chi^+(\cdot,t), e_N \rangle_{L^2} \\ \langle \chi^-(\cdot,t), e_N \rangle_{L^2} \end{bmatrix} = \begin{bmatrix} X(t) \\ \mathfrak{X}_0(t) \\ \vdots \\ \mathfrak{X}_N(t) \end{bmatrix}$
Space	$\mathbb{R}^n \times L^2 \times L^2$	$\mathbb{R}^n \times \mathbb{R}^{2(N+1)}$

Table 5.1: Original and truncated state for system (5.2).

Using Bessel inequality E.4 and Parseval's identity, we get the two following relations:

$$\min_{y \in \mathrm{Span}(e_k)_{k \leq N}} \|\chi^+(\cdot,t) - y\|_{L^2}^2 \geq 0, \qquad \min_{y \in \mathrm{Span}(e_k)_{k \leq N}} \|\chi^+(\cdot,t) - y\|_{L^2}^2 \xrightarrow[N \to \infty]{} 0.$$

The previous calculations show that χ_N^+ is the projection of χ^+ on the subspace spanned by the family $(e_k)_{k \leq N}$ and is consequently the optimal approximation (with respect to the norm $\|\cdot\|_{L^2}$) of u on the former family. By doing the same for $\chi^-(\cdot,t)$, the previous analysis shows that we can build a truncation $X_N(t)$ of $X_\infty(t)$, which belongs to the finite-dimensional space $\mathbb{R}^n \times \mathbb{R}^{2(N+1)}$. Table 5.1 draws a summary of this part.

Note that for $R \succeq 0$, the following inequality is a consequence of Proposition E.4 applied in this context:

$$\int_0^1 \chi^\top(x,t) R \chi(x,t) dx \geq \sum_{k=0}^{N} \frac{1}{\|e_k\|_{L^2}^2} \mathfrak{X}_k^\top(t) R \mathfrak{X}_k(t), \tag{5.16}$$

where

$$\mathfrak{X}_k(t) = \begin{bmatrix} \langle \chi^+(\cdot,t), e_k \rangle \\ \langle \chi^-(\cdot,t), e_k \rangle \end{bmatrix}.$$

This study shows that we can build an augmented finite-dimensional system, whose trajectories will be close in norm to the ones of system (5.2). This augmented system describes the dynamic of the state X and of the projections coefficients. Consequently, that leads to the following Lyapunov functional candidate:

$$V_N(X,\chi) = X_N^\top P_N X_N + \int_0^1 \chi^\top(x) \left(S + xR\right) \chi(x) dx, \tag{5.17}$$

where $P_N \in \mathbb{S}^{n+2(N+1)}$ and $S, R \in \mathbb{S}^2$. This new functional is actually made up of three terms:

- A quadratic term in X introduced by the ODE;
- A functional $\mathcal{V}_{PDE}$ for the stability of the string equation;
- Cross-terms between $\mathfrak{X}_0, \dots, \mathfrak{X}_N$ and X described by the extended state X_N.

Remark 5.8: Projection of a generic Lyapunov functional

It is possible to relate the state extension to the parametrization of the Lyapunov functional. Inspired from the work of [47, 76, 83] on time-delay systems, we can propose the following Lyapunov functional candidate of the very generic form:

$$V_c(X,\chi) = \int_0^1 \int_0^1 \begin{bmatrix} X \\ \chi(x_1) \end{bmatrix}^\top \begin{bmatrix} P & \mathcal{Q}(x_2) \\ \mathcal{Q}^\top(x_1) & \mathcal{T}(x_1,x_2) \end{bmatrix} \begin{bmatrix} X \\ \chi(x_2) \end{bmatrix} dx_1 dx_2 + \mathcal{V}_{PDE}(\chi),$$

where $P \in \mathbb{S}^n$, $\mathcal{Q} \in L^2([0,1],\mathbb{R}^{n\times 2})$ and $\mathcal{T} \in L^2([0,1]^2,\mathbb{S}^2)$. Such a Lyapunov functional has been studied in [129, 130] for coupled ODE/transport equation. Assuming $V_N = V_c$ leads to:

$$\mathcal{Q}(x_1) = \sum_{k=0}^{N} Q_k e_k(x_1), \quad \mathcal{T}(x_1,x_2) = \sum_{k=0}^{N}\sum_{i=0}^{N} T_{k,i} e_k(x_1) e_i(x_2),$$

with $Q_k \in \mathbb{R}^{n\times 2}$ and $T_{k,i} \in \mathbb{R}^{2\times 2}$, $T_{k,i} = T_{i,k}^\top$ and $T_{i,i} \in \mathbb{S}^2$. Consequently, using the functional defined in (5.17), we have:

$$P_N = \begin{bmatrix} P & Q_0 & \cdots & Q_N \\ Q_0^\top & T_{0,0} & \cdots & T_{0,N} \\ \vdots & \vdots & \ddots & \vdots \\ Q_N^\top & T_{N,0} & \cdots & T_{N,N} \end{bmatrix}.$$

We can interpret the state extension as the projection of the operator $\mathcal{Q}$ on the basis $\{e_k\}_{k\leq N}$; and on the basis $\{(x_1,x_2)\mapsto e_k(x_1)e_i(x_2)\}_{k,i\leq N}$ for the other operator $\mathcal{T}$.

We will show in the following subsection that there exist numerically tractable tests ensuring that V_N is a Lyapunov functional.

5.3.2 Extended Lyapunov stability Theorem

In this subsection, we derive a theorem showing that system (5.2) is exponentially stable using the projection methodology. We decide to use the basis of Legendre polynomials, referred to as $\{\mathcal{L}_k\}_{k\in\mathbb{N}}$, as a polynomial basis of L^2. This basis is described in Definition E.1. The choice of this basis will be discussed later on but we can already note

that it is the unique[5] orthogonal polynomial basis of L^2 equipped with its canonical inner-product $\langle \cdot, \cdot \rangle_{L^2}$.

The main theorem of this chapter is written below. This theorem originally comes from [18, Theorem 1] and is an extension of [19, Theorem 2].

Theorem 5.3: Extended stability analysis of (5.2)

Let $N \in \mathbb{N}$ and $c, c_0 > 0$. If there exist $P_N \in \mathbb{S}^{n+2(N+1)}$ and $R, S \in \mathbb{S}^2_{++}$ such that

$$\begin{cases} \Xi_N = P_N + \mathrm{diag}(0_n, S, 3S, \dots, (2N+1)S) \succ 0, \\ \Theta_N = \mathrm{He}\left(D_N^\top P_N F_N\right) + c\left(H_N^\top (S+R) H_N - G_N^\top S G_N - \tilde{R}_N\right) \prec 0, \end{cases} \tag{5.18}$$

where

$$F_N = \begin{bmatrix} 0_{n+2(N+1),2} & I_{n+2(N+1)} \end{bmatrix}, \qquad D_N = \begin{bmatrix} J_N \\ M_N \end{bmatrix},$$

$$J_N = \begin{bmatrix} 0_{n,2} & A + BK & \tilde{B} & 0_{n,2N} \end{bmatrix},$$

$$M_N = c\left(\mathbb{1}_N H_N - \bar{\mathbb{1}}_N G_N - \begin{bmatrix} 0_{2(N+1),2+n} & L_N \end{bmatrix}\right),$$

$$\tilde{B} = \frac{1}{2c}\begin{bmatrix} 1 & -1 \end{bmatrix}, \qquad \tilde{R}_N = \mathrm{diag}\left(0_{n+2}, R, 3R \cdots, (2N+1)R\right),$$

$$G_N = \begin{bmatrix} g & 0_{2,n+2(N+1)} \end{bmatrix} + \begin{bmatrix} K \\ 0_{1,n} \end{bmatrix} J_N, \quad g = \begin{bmatrix} 0 & 1 \\ 1 + cc_0 & 0 \end{bmatrix},$$

$$H_N = \begin{bmatrix} h & 0_{2,n+2(N+1)} \end{bmatrix} + \begin{bmatrix} 0_{1,n} \\ K \end{bmatrix} J_N, \quad h = \begin{bmatrix} 1 - cc_0 & 0 \\ 0 & -1 \end{bmatrix},$$

$$L_N = \left[\ell_{ik} I_2\right]_{i,k \in [0,N]},$$

$$\mathbb{1}_N = \mathrm{col}(I_2, \dots, I_2) \in \mathbb{R}^{2(N+1)\times 2}; \quad \bar{\mathbb{1}}_N = \mathrm{col}((-1)^0 I_2, \dots, (-1)^N I_2) \in \mathbb{R}^{2(N+1)\times 2}.$$

Then V_N is a Lyapunov functional for system (5.2).

Proof : The proof follows the same line as for Theorem 5.2. We want to apply Proposition 5.1 and we there need the existence of $\varepsilon_1, \varepsilon_2$ and $\varepsilon_3 > 0$ such that (5.3) holds with $\mu = 0$. The main difference with Theorem 5.2 lies in the use of Bessel inequality. Based on Proposition E.5, this inequality writes in this context as follows:

$$\sum_{k=0}^{N} (2k+1) \mathfrak{X}_k^\top R \mathfrak{X}_k \leq \int_0^1 \chi^\top(x) R \chi(x) dx, \tag{5.19}$$

where $R \in \mathbb{S}^2_{++}$.

Existence of ε_1: The proof of existence of $\varepsilon_1 > 0$ is modified compared to the previous theorem since we do not require P_N to be definite positive now. This relaxed

[5] up to a normalization coefficient.

condition first appears in [65, 143] and starts by writing the following:

$$V_N(X,\chi) \geq X_N^\top \Xi_N X_N - \sum_{k=0}^{N}(2k+1)\mathfrak{X}_k^\top S \mathfrak{X}_k + \int_0^1 \chi^\top(x) S \chi(x) dx. \tag{5.20}$$

Since $\Xi_N \succ 0$, there exists $\varepsilon_1 > 0$ such that the following holds:

$$\Xi_N \succeq \varepsilon_1 \left(\operatorname{diag}(I_n, 0_{2(N+1)}) + \delta \operatorname{diag}(0_n, I_{2(N+1)}) \right),$$

where $\delta = \frac{1}{2}\left(1 + \frac{2}{c^2}\right)$. Plugged into (5.20), it leads to:

$$V_N(X,\chi) \geq \varepsilon_1 \|X\|_{\mathbb{R}^n}^2 - \sum_{k=0}^{N}(2k+1)\mathfrak{X}_k^\top \left(S - \varepsilon_1 \delta I_2\right) \mathfrak{X}_k \\ + \int_0^1 \chi^\top(x)(S - \varepsilon_1 \delta I_2)\chi(x)dx + \varepsilon_1 \delta \|\chi\|_{L^2}^2.$$

Since $S \succ 0$, for ε_1 sufficiently small, we get $S - \varepsilon_1 \delta I_2 \succ 0$ and then, applying (5.19) leads to:

$$V_N(X,\chi) \geq \varepsilon_1 \left(\|X\|_{\mathbb{R}^n}^2 + \delta \|\chi\|_{L^2}^2 \right).$$

Using (5.5) and Proposition E.6 leads to $V_N(X_N,\chi) \geq \varepsilon_1 \|(X,u,u_t)\|_{\mathscr{Y}(\mathscr{A})}^2$.

Existence of ε_2: This part is the same as previously and is therefore omitted.

Existence of ε_3: First note that the time-derivation of V_N along the trajectories of (5.2) leads to:

$$\frac{d}{dt} V_N(X(t),\chi(\cdot,t)) = \operatorname{He}\left(\dot{X}_N^\top(t) P_N X_N(t) \right) + \dot{\mathcal{V}}_{PDE}(\chi).$$

From equation (5.10), we get:

$$\frac{d}{dt} V_N(X(t),\chi(\cdot,t)) = \operatorname{He}\left(\dot{X}_N^\top(t) P_N X_N(t) \right) + c \Big(\chi(1,t)^\top (S+R)\chi(1,t) \\ - \chi(0,t)^\top S \chi(0,t) - \langle \chi(\cdot,t), R\chi(\cdot,t)\rangle_{L^2} \Big). \tag{5.21}$$

Let us introduce the following extended state variable:

$$\xi_N(t) = \operatorname{col}\left(u_t(1,t), u_x(0,t), X(t), \mathfrak{X}_0(t), \ldots, \mathfrak{X}_N(t)\right), \tag{5.22}$$

Using Lemma C.1, we get that:

$$\frac{d}{dt}\begin{bmatrix} \mathfrak{x}_0 \\ \vdots \\ \mathfrak{x}_N \end{bmatrix} = M_N \xi_N,$$

hence, noting that $\dot{X}(t) = J_N \xi_N(t)$, $\chi(0,t) = H_N \xi_N(t)$ and $\chi(1,t) = G_N \xi_N(t)$, equation (5.21) rewrites as:

$$\dot{V}_N(X(t),\chi(\cdot,t)) = \xi_N^\top(t) \left\{ \operatorname{He}\left(D_N^\top P_N F_N \right) + c\left(H_N^\top (S+R) H_N - c G_N^\top S G_N \right) \right\} \xi_N(t) \\ - c\langle \chi(\cdot,t), R\chi(\cdot,t)\rangle_{L^2} \\ = \xi_N^\top(t) \Theta_N \ \xi_N(t) + c \sum_{k=0}^{N}(2k+1)\mathfrak{X}_k^\top(t) R \mathfrak{X}_k(t) \\ - \int_0^1 \chi^\top(x,t) R \chi(x,t) dx.$$

Remark 5.9

Notice that $\mathfrak{X} = \int_0^1 \chi(x,t)dx$ introduced in the proof of Theorem 5.2 is nothing more than $\mathfrak{X}_0$.

Since $R \succ 0$ and $\Theta_N \prec 0$, there exists $\varepsilon_3 > 0$ such that:

$$\begin{aligned} R &\succeq \frac{\varepsilon_3}{2c}\left(1+\frac{2}{c^2}\right) I_2, \\ \Theta_N &\preceq -\varepsilon_3 \operatorname{diag}\left(0_2, I_n + 2K^\top K, \frac{1}{2}\left(1+\frac{2}{c^2}\right)\tilde{I}_N\right), \\ \tilde{I}_N &= \operatorname{diag}(I_2, 3I_2, \ldots, (2N+1)I_2). \end{aligned}$$

The previous inequality on $\dot{V}_N$ becomes:

$$\begin{aligned} \dot{V}_N(X(t),\chi(\cdot,t)) \leq -\varepsilon_3 \Big(\|X\|^2_{\mathbb{R}^n} + 2|u(0,t)|^2 + \frac{1}{2}\left(1+\frac{2}{c^2}\right)\|\chi\|^2_{L^2}\Big) \\ - c\sum_{k=0}^{N}(2k+1)\mathfrak{X}_k^\top(t)\left(R - \frac{\varepsilon_3}{2c}\left(1+\frac{2}{c^2}\right)I_2\right)\mathfrak{X}_k^\top(t) \\ + c\int_0^1 \chi^\top(x)\left(R - \frac{\varepsilon_3}{2c}\left(1+\frac{2}{c^2}\right)I_2\right)\chi(x)dx. \end{aligned}$$

We conclude by using (5.19) and Proposition E.6, similarly to what was done in the proof of Theorem 5.2. ♢

Remark 5.10: Necessary conditions to apply Theorem 5.3

- $\Theta_N \prec 0$ is feasible if the block $\begin{bmatrix} 0_{n,2} & I_n & 0_{n,2(N+1)} \end{bmatrix}^\top \Theta_N \begin{bmatrix} 0_{n,2} & I_n & 0_{n,2(N+1)} \end{bmatrix}$ is definite negative. That leads to:

  $$(A+BK)^\top P + P(A+BK) + c(A+BK)^\top K^\top RK(A+BK) + Q \prec 0,$$

  where P is a positive definite matrix and $Q \in \mathbb{S}^n$. In other words, $A+BK$ must be not singular but since Q is not necessarily positive if $N > 0$, $A+BK$ can be not Hurwitz. This case is investigated in the example section.

- Similarly to Theorem 5.2, the first 2×2 diagonal block of Θ_N must be definite negative to have $\Theta_N \prec 0$. Simple calculations show that this imply $c_0 > 0$, and the string equation must be damped.

The previous theorem is interesting because there is a hierarchy property on the order N. This is discussed in the following subsection.

5.3.3 Hierarchy of LMI conditions

As said previously, we expect to get a better analysis if we increase the order N in Theorem 5.3. This would be in accordance with Bessel Inequality since the two vectors

X_∞ and X_N get close in norm. The following proposition draws clearly the hierarchy property.

Proposition 5.3: Hierarchy of LMI conditions in Theorem 5.3

If Theorem 5.3 holds for an order N^*, then for all $N \geq N^*$, there exist matrices P_N, S and R such that V_N is a Lyapunov functional for system (5.2).

Proof : This proof is based on induction. Assume the two LMIs (5.18) are verified for an order N. We want to show that Theorem 5.3 for the order $N+1$ also holds. Denote by P_N, S and R a solution of (5.18) for the order N. Because L_N as defined in the previous is strictly lower diagonal, we get the following:

$$
\begin{aligned}
F_{N+1} &= \mathrm{diag}(F_N, I_2), \quad J_{N+1} = \begin{bmatrix} J_N & 0_2 \end{bmatrix}, \quad H_{N+1} = \begin{bmatrix} H_N & 0_2 \end{bmatrix}, \quad G_{N+1} = \begin{bmatrix} G_N & 0_2 \end{bmatrix}, \\
M_{N+1} &= \begin{bmatrix} \mathbb{1}_N H_{N+1} \\ H_{N+1} \end{bmatrix} - \begin{bmatrix} \bar{\mathbb{1}}_N G_{N+1} \\ G_{N+1} \end{bmatrix} - \begin{bmatrix} 0_{2(N+1),2+n} & L_N & 0_{2(N+1),2} \\ 0_{2,2+n} & l_{N+1} & 0_2 \end{bmatrix} \\
&= \begin{bmatrix} M_N & 0_{2(N+1),2} \\ m_{N+1} & 0_2 \end{bmatrix}, \\
D_{N+1} &= \begin{bmatrix} D_N & 0_{2+2(N+1),2} \\ m_{N+1} & 0_2 \end{bmatrix}
\end{aligned}
$$

Assume that for $\varepsilon \in \mathbb{R}$, $P_{N+1} = \mathrm{diag}(P_N, \varepsilon I_2)$, we get:

$$
\Xi_{N+1} = \begin{bmatrix} \Xi_N & 0_{n+2(N+1),2} \\ 0_{2,n+2(N+1)} & \varepsilon I_2 + (2N+3)S \end{bmatrix}, \quad \Theta_{N+1} = \begin{bmatrix} \Theta_N & \varepsilon m_{N+1}^\top \\ \varepsilon m_{N+1} & -c(2N+3)R \end{bmatrix}.
$$

Applying Schur complement on Θ_{N+1} shows that there exists $\varepsilon > 0$ small enough such that $\Xi_{N+1} \succ 0$ and $\Theta_{N+1} \prec 0$. Consequently, V_{N+1} is a Lyapunov functional for system (5.2). ♢

Proposition 5.3 shows that increasing the order can only lead to better or identical results. Nevertheless, there is no evidence that if the system (5.2) is exponentially stable then there exists an order $N \in \mathbb{N}$ such that V_N would be a Lyapunov functional. A more detailed discussion on that point is provided later on.

Remark 5.11

Note that the case $N = 0$ does not correspond to Theorem 5.2. Indeed, the state X_0 has already one extension. It would better correspond to the order $N = -1$. The hierarchy property stated in Proposition 5.3 shows that the Lyapunov functional V_N encompasses the simple Lyapunov functional V defined in (5.11).

5.3.4 Discussion about the basis of projection

As we can see in the proof of Proposition 5.3, the most important point to get a hierarchy is that L_N is strictly lower diagonal. In other words, the derivation of a Legendre polynomial is expressed using strictly lower degree of Legendre polynomials that are already in the basis. If we want the hierarchy property to hold with another basis $\{e_k\}_{k\in\mathbb{N}}$, then we should choose a basis such that the following holds:

$$\forall k \in \mathbb{N}, \quad \frac{d}{dx} e_k \in \text{Span}(e_0, \dots, e_{k-1}). \tag{5.23}$$

For this reason, we assume in the sequel that e_k is a polynomial of degree at most k. Such a sequence indeed verifies (5.23). Since Bessel inequality is the key for deriving Theorem 5.3, we will also require that the sequence $\{e_k\}_{k\in\mathbb{N}}$ is orthogonal for a given scalar product. If we choose $\langle\cdot,\cdot\rangle_{L^2}$ then the unique orthogonal polynomial sequence (up to a normalization coefficient) is the sequence of Legendre polynomials.

For instance, let us consider the Fourier basis $\{\mathcal{F}_k\}_{k\in\mathbb{N}}$ defined as:

$$\mathcal{F}_0 = 1, \qquad \forall k \geq 1, \forall x \in [0,1], \quad \mathcal{F}_k(x) = \text{diag}\left(\cos(2k\pi x), \sin(2k\pi x)\right).$$

This is an orthogonal basis of L^2 and we get for $k \geq 1$ that $\frac{d}{dx}\mathcal{F}_k = \begin{bmatrix} 0 & -2k\pi \\ 2k\pi & 0 \end{bmatrix} \mathcal{F}_k$. Consequently, the derivation matrix is not strictly lower diagonal and the proof of the hierarchy cannot apply.

An interesting research would be to define another scalar product of L^2 and then find another orthogonal basis which respects equation (5.23). This may provide better stability analysis results but there is no evidence that a basis is better than another nor a scalar product to another. This is left to future research.

5.4 Robust stability analysis

The main advantage of using LMIs for stability analysis is to move easily to robust stability analysis. Here, we propose an extension of Theorem 5.3 to deal with uncertainties on the parameters A and B. The main assumption is that A and B are subject to polytopic uncertainties, that means the following holds:

$$[\ A\ B\ ] \in \text{Co}_{i=1,\dots,m} \left\{ [\ A_i\ B_i\ ] \right\}, \tag{5.24}$$

where $m \in \mathbb{N}$, and the matrices A_i and B_i for $i = 1, \dots, m$ are known and constant. The notation "Co" means that the matrix $[\ A\ B\ ]$ belongs to a convex set defined by the vertices $[\ A_i\ B_i\ ]$. In other words, there exist unknown weighting scalar functions λ_i, for $i = 1, \dots, m$ such that $\sum_{i=1}^m \lambda_i = 1$ and

$$[\ A\ B\ ] = \sum_{i=1}^{m} \lambda_i [\ A_i\ B_i\ ]. \tag{5.25}$$

Note that this definition allows a time-varying A and B as long as (5.24) is verified for all $t \geq 0$.

This kind of uncertainties is commonly used because it fits perfectly in the LMI formulation. Indeed, a convexity argument helps getting a larger LMI ensuring the robust stability. The number of edges to define the polytope is directly related to the complexity of the new LMIs and can then dramatically increase the computational burden. Moreover, to transform the original non-convex problem into a convex one, there exist lemmas (see [29, 31] for instance) that multiply the number of decision variables. An example of such a result is given by the following corollary.

Corollary 5.1: Robust stability analysis of (5.2)

Let $N \in \mathbb{N}$, $c > 0, c_0 > 0$ and A, B such that (5.24) holds. If there exist $P_N \in \mathbb{S}^{n+2(N+1)\times n+2(N+1)}, S, R \in \mathbb{S}^2_{++}, Y_N \in \mathbb{R}^{2\times(n+2N+6)}$ and $\kappa > 0$ following LMIs are satisfied:

$$\begin{cases} \Xi_N = P_N + \operatorname{diag}(0_n, S, 3S, \dots, (2N+1)S) \succ 0, \\ \Theta^r_N(A_i, B_i) \prec 0, \text{ for all } i \in [1, m] \end{cases} \tag{5.26}$$

with

$$\begin{aligned}
\Theta^r_N(A,B) &= \begin{bmatrix} \mathcal{M}_N(A,B) + \operatorname{He}(Y_N^\top \mathcal{W}_N(A,B)) & Y_N^\top & \mu \mathcal{W}_N^\top(A,B) \\ \star & -\kappa I_2 - cS & 0_2 \\ \star & \star & -\kappa I_2 \end{bmatrix}, \\
\mathcal{M}_N(A,B) &= \begin{bmatrix} \operatorname{He}\left(Z_N^\top(A,B) P_N F_N\right) - c\tilde{R}_N & H_N^\top(A,B)(S+R) \\ (S+R)H_N(A,B) & -\frac{1}{c}(S+R) \end{bmatrix}, \\
\mathcal{W}_N(A,B) &= \begin{bmatrix} G_N(A,B) & 0_2 \end{bmatrix}, \\
G_N(A,B) &= \begin{bmatrix} g & 0_{2,n+2(N+1)} \end{bmatrix} + \begin{bmatrix} K \\ 0_{1,n} \end{bmatrix} J_N(A,B), \\
H_N(A,B) &= \begin{bmatrix} h & 0_{2,n+2(N+1)} \end{bmatrix} + \begin{bmatrix} 0_{1,n} \\ K \end{bmatrix} J_N(A,B), \\
J_N(A,B) &= \begin{bmatrix} 0_{n,2} & A + BK & \tilde{B} & 0_{n,2N} \end{bmatrix}.
\end{aligned}$$

then, V_N is a Lyapunov functional for system (5.2).

The proof of the previous corollary is rather technical and does not bring notable insights compared to Theorem 5.3. It is provided in [18]. However, it is important to state such an extension to make the conservative approach using Lyapunov functionals relevant regarding the frequency analysis which provides sometimes necessary and sufficient conditions when no uncertainties.

The following section provides some numerical examples to show the effectiveness of this method.

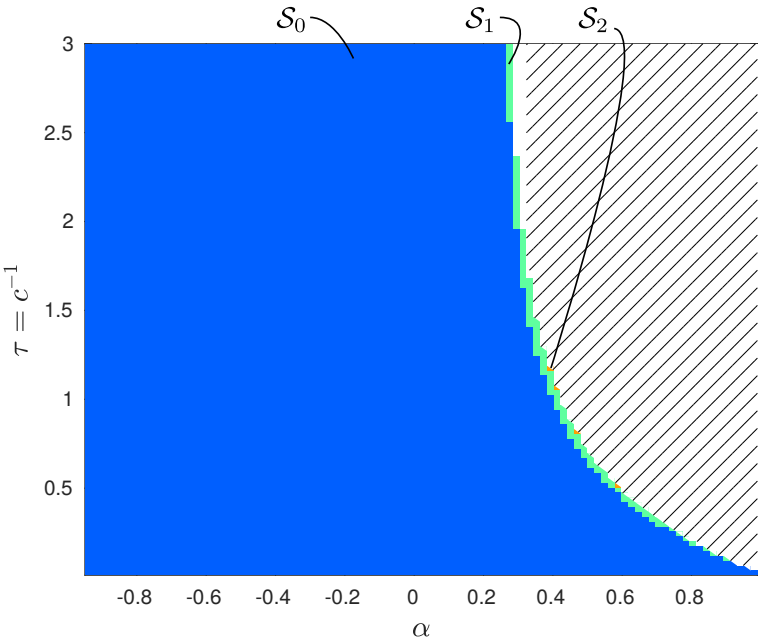

Figure 5.2: Stability chart for (5.27). The hatched area is unstable according to the CTCR algorithm presented in Section 4.1.3, while Theorem 5.3 gives that the colored area is stable. The areas marked as $\mathcal{S}_i$ are stable areas up to an order i.

5.5 Numerical examples and discussion

5.5.1 A and $A + BK$ are Hurwitz with $\|\mathcal{H}\|_\infty < 1$

This example is taken from the previous chapter where the system is defined as follows:

$$A = \begin{bmatrix} -2 & 1 \\ 0 & -1 \end{bmatrix}, \quad B = \begin{bmatrix} 1 \\ 1 \end{bmatrix}, \text{ and } K = \begin{bmatrix} 0 & -\frac{20}{21} \end{bmatrix}. \tag{5.27}$$

We can clearly see in Figure 5.2 that Theorem 5.3 provides an accurate inner-approximation of the stability area. Indeed, even at order 0, the stable area is very large and increasing the order slightly improves the result but not significantly. Compared to Figures 4.2, 4.5 and 5.1a, the detected stability is much larger here. That is due to the projection of the whole function χ while before, only part of it was projected. The price to pay is a huge increase of the number of decision variables.

5.5.2 A is not Hurwitz but $A + BK$ is Hurwitz

This second example is of main interest because the coupling induces the stability to the interconnected system (5.2). The system is defined as follows:

$$A = \begin{bmatrix} -1 & 0 \\ 0 & 0 \end{bmatrix}, \quad B = \begin{bmatrix} 0 \\ 1 \end{bmatrix}, \text{ and } K = \begin{bmatrix} 0 & -5 \end{bmatrix}. \tag{5.28}$$

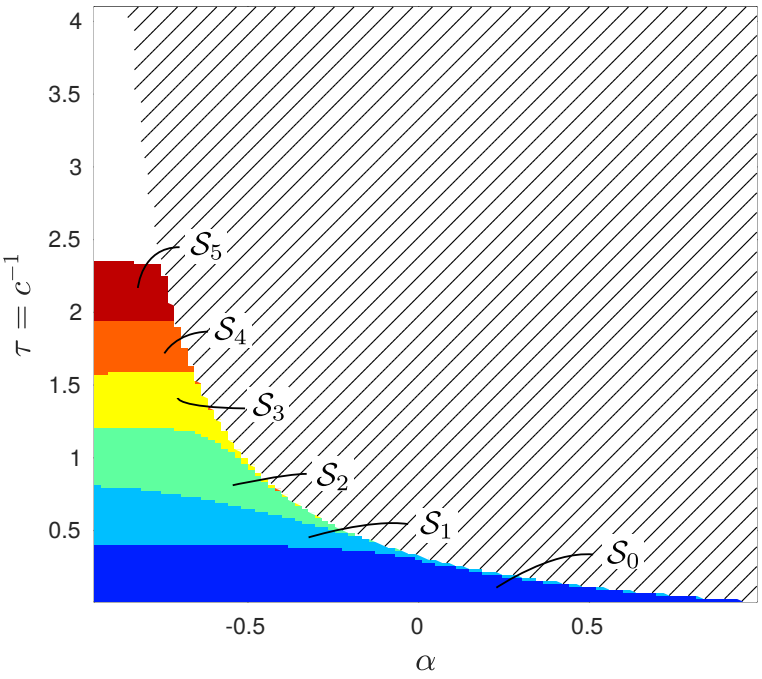

Figure 5.3: Stability chart for (5.28). The hatched area is unstable according to the CTCR algorithm presented in Section 4.1.3, while Theorem 5.3 gives that the colored area is stable. The areas marked as $\mathcal{S}_i$ are stable areas up to an order i.

The result of Theorem 5.3 is shown in Figure 5.3. We can see that the estimated stable area is close to the exact stable area for high speed and low orders N. The stable area $\mathcal{S}_0$ is larger than the stable area detected using Theorem 5.2 (Figure 5.1b). The hierarchy is easier to see than in the previous example and we indeed get $\mathcal{S}_0 \subset \mathcal{S}_1 \subset \mathcal{S}_2$.

5.5.3 A and $A + BK$ are not Hurwitz

This system is the same as in (4.42), and is reminded below:

$$A = \begin{bmatrix} 0 & 1 \\ -2 & 0.1 \end{bmatrix}, B = \begin{bmatrix} 0 \\ 1 \end{bmatrix}, \text{ and } K = \begin{bmatrix} 1 & 0 \end{bmatrix}. \tag{5.29}$$

Neither A nor $A+BK$ are Hurwitz, meaning that it was impossible with the Lyapunov functional (5.11) to assess stability. Without any surprise, for the order $N = 0$, there is no result, but the area grows significantly when increasing the order and at $N = 3$, nearly the whole stability area is correctly estimated. Figure 4.6 in the previous chapter treated the same example but using Quadratic Separation and the two results differs significantly because it was impossible to fill the whole area previously.

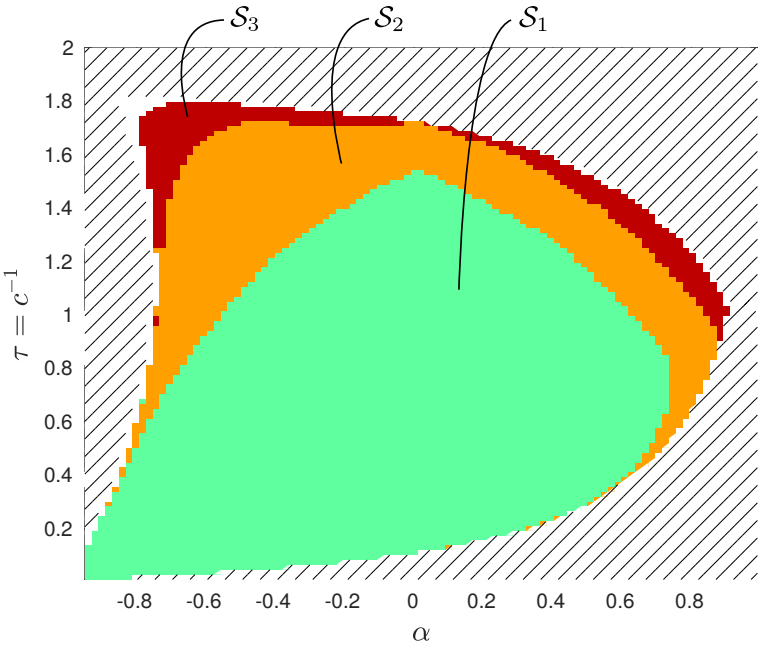

Figure 5.4: Stability chart for (5.29). The hatched area is unstable according to the CTCR algorithm presented in Section 4.1.3, while Theorem 5.3 gives that the colored area is stable. The areas marked as $\mathcal{S}_i$ are stable areas up to an order i.

5.5.4 An example with stability pockets

This last example is an extension to what was proposed in Section 4.4.4. Let system (5.2) with $k \geq 0$ and

$$A(k) = \begin{bmatrix} 0 & 0 & 1 & 0 \\ 0 & 0 & 0 & 1 \\ -10-k & 10 & 0 & 0 \\ 5 & -15 & 0 & -0.25 \end{bmatrix}, \; B(k) = \begin{bmatrix} 0 \\ 0 \\ k \\ 0 \end{bmatrix}, \; K = \begin{bmatrix} 1 \\ 0 \\ 0 \\ 0 \end{bmatrix}^\top. \tag{5.30}$$

For $k = 1$, we get back to (4.43) in the previous chapter or (5.15) in the previous section. Theorem 5.3 has been applied on this system for $k = 1$ and we get Figure 5.5. Compared to Figures 4.8 and 5.1c, we see that the estimated stability area is much larger. The hierarchy property is clearly visible. $\mathcal{S}_4 \backslash \mathcal{S}_3$ and $\mathcal{S}_5 \backslash \mathcal{S}_4$ are surprisingly large sets. Increasing the order sometimes brings a large contribution.

At this stage, we would like to study the robustness of the previous system using Corollary 5.1 in two cases: when $k \in (0.1, 1.5)$ and $k \in (1, 2)$. Denote by $\mathcal{C}_k$ the unstable area for a given gain k determined using the CTCR algorithm. It is possible to get an inner estimation of the unstable area for the two cases by constructing the two following sets:

$$\mathcal{C}_{k\in(0.1,1.5)} = \bigcup_{k\in\{0.1,0.5,0.8,1\}} \mathcal{C}_k \text{ and } \mathcal{C}_{k\in(1,2)} = \bigcup_{k\in\{1,1.2,1.5,2\}} \mathcal{C}_k.$$

We then get Figure 5.6 for $N = 7$ (see a similar study done in [18]). We can conclude that Corollary 5.1 is apparently conservative because there is a huge gap between the

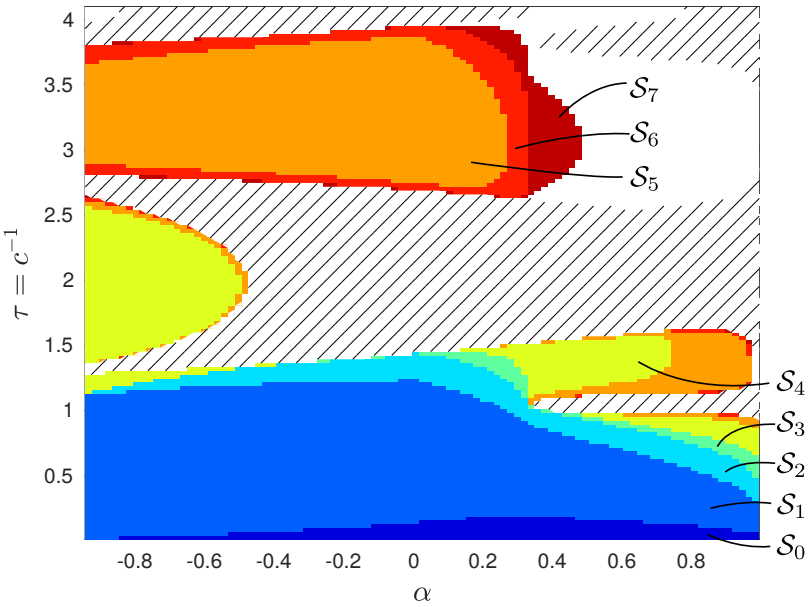

Figure 5.5: Stability chart for (5.30). The hatched area is unstable according to the CTCR algorithm presented in Section 4.1.3, while Theorem 5.3 gives that the colored area is stable. The areas marked as $\mathcal{S}_i$ are stable areas up to an order i.

estimated unstable area and the estimated stable area. Nevertheless, the estimated unstable area $\mathcal{C}$ might be quite far from the real unstable area since it is calculated for some fixed values of A and B while they may vary in the polytopic set in the sense that they are uncertain.

5.5.5 Discussion

First of all, the previous subsection shows the effectiveness of the proposed methodology. We get a very accurate estimation of the stability area, even at low orders. The order increases, we detect a stable area for larger τ so smaller c. This is quite expected since the influence of the string is higher when its speed is small. Since the results are very accurate for a high N, we make the following conjecture.

Conjecture 5.1: Necessary and sufficient condition for stability

System (5.2) is exponentially stable if and only if there exists $N \in \mathbb{N}$ such that LMIs (5.18) hold.

There are different ways to try to prove this assertion. Trying to find an expression of the complete Lyapunov functional[6] and to see that V_N is getting as close as we want to V when N increases. Another approach would consider the equivalence already proven using DJ-scaling [117]. This is apparently not an easy task.

For the order $N = 0$, we obtain a more precise stability analysis test than using the Lyapunov functional (5.11). This is due to two contributions. First, the positivity

[6]A complete Lyapunov functional V is such that V_N is a Lyapunov functional if and only if the system is exponentially stable.

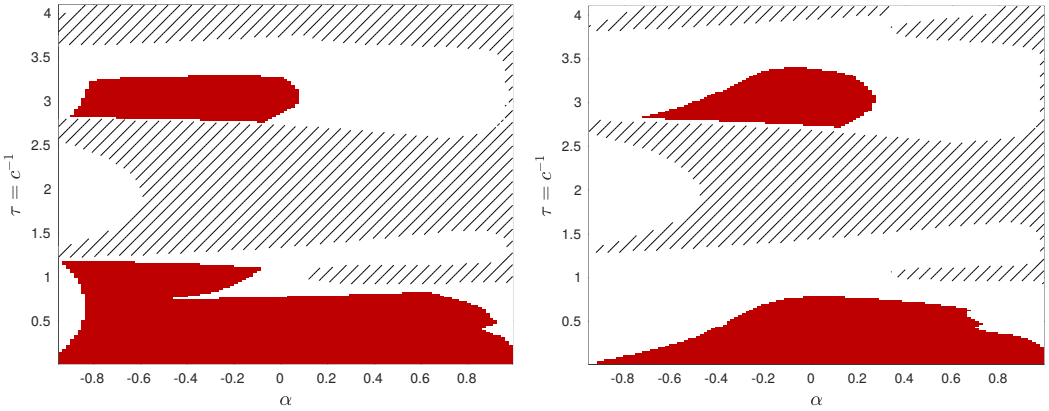

(a) $k \in (0.1, 1.5)$ (b) $k \in (1, 2)$

Figure 5.6: Robust stability analysis of system (5.2) in two cases and using Corollary 5.1 for $N = 7$. The unstable area is an inner-estimation using $\mathcal{C}_{k\in(0.1,1.5)}$ in case (a), and $\mathcal{C}_{k\in(1,2)}$ in case (b).

Order	Theorem 4.6	Theorem 5.3
$N \in \mathbb{N}$	$\frac{n^2+n+N^2+N}{2} + Nn + 3$	$\frac{n^2+n}{2} + 2(N^2+n) + 5N + Nn + 9$
$N = 0$	13	27
$N = 2$	24	61
$N = 5$	48	142

Table 5.2: Number of decision variables for Theorem 4.6 and Theorem 5.3 for different orders and $n = 4$.

condition $P \succ 0$ has been relaxed to a less constrained one. The other modification is in the estimated state, where the projection on $\mathcal{L}_0$ has been added in V_N while it was not the case in V. These two modifications relaxed the LMIs and cannot lead to worse results. It appears than in Figures 5.2 and 5.3 the estimated stable area is much larger, this contributions are then of main importance.

Compared to Theorem 4.6 of the previous chapter, we get better results here. This is not so easy to understand why but looking at the complexity between the two algorithms provides one answer. Indeed, Table 5.2 enlightens the difference in the number of decision variables between the two theorems. We indeed get a better result using Theorem 5.3 but at a price of many more decision variables, making the computational time much longer. We can say that, for α close to 0, it is better to use Theorem 4.6, which is as efficient as the Lyapunov-based theorem and less greedy. But when $|\alpha|$ is close to 1, it is better to use Theorem 5.3. Appendix C proposes another way to reduce the computational burden of the Lyapunov-based theorem with a moderate increase of the conservatism.

This last aspect is of main importance since the robust analysis of Corollary 5.1 requires additional decision variables. Indeed, to make the LMI affine in A and B, the numerical complexity increases dramatically. It is then of main importance to

maintain a low complexity for classical theorems such that it is possible to move to robust stability analysis. We cannot evaluate the conservatism introduced by the robust stability corollary 5.1 because we only get an inner estimation of the stable area. It seems very difficult to provide an exact computation of the stability area since the CTCR methodology does not adapt to a polytopic uncertainty. The easy extension to robust stability is one of the advantages of considering a Lyapunov-based stability test.

5.6 Conclusions

This chapter focuses on the Lyapunov stability analysis of system (5.2). A simple Lyapunov functional for this system is made up of two terms: one for the stability of the ODE and another one for the stability of the string equation. We show that this functional leads to good results in some cases but they are limited. That is why we proposed to use the projection methodology, originally developed for time-delay systems.

This approach relies on an estimation of the infinite-dimensional state. We consider a truncation of this state such that it becomes finite-dimensional. Such a methodology leads to a hierarchy of Lyapunov functionals which encompass the simple functional proposed as a first step.

This methodology presents many advantages. First of all, the simulation results show a very good accuracy when the order increases. Secondly, it is quite easy to extend the result to polytopic uncertainties on matrices A and B, which is an interesting robust extension. Finally, the Lyapunov approach is very adaptable and for the same PDE but under different boundary conditions, a similar reasoning should lead to a robust stability analysis. This is explored for instance in the following chapter. Nevertheless, we must choose a trade-off between numerical complexity and accuracy because this approach can be quite demanding.

The previous chapter was using Bessel inequality to encompass Jensen's inequality, while in this chapter, it is used to parametrize the operators of the Lyapunov functional, or equivalently, to extend the state. Then, we get three complementary visions of the same methodology. Depending on which context they are applied, they provide different results but they rely on the same basis. The following chapter uses the ideas developed in this chapter to give an answer to the original problems for the drilling pipe mechanism.

6

Stability analysis of a drilling mechanism

Many phenomena can occur while drilling as bit bouncing, stick-slip or whirling [35]. The challenge is then to design a controller for removing, or at least weakening, these undesirable effects. Many control techniques were applied on the finite dimensional system from the simple PI controller investigated in [32, 36], to more advance controllers as sliding mode control [111] or H_∞ design [140].

We focus here on the treatment of stick-slip with a PI controller. Hence, on a first step, applying the describing function methodology on the finite dimensional model presented in (2.1) leads to Figure 6.1 (see Appendix D for more details). Note first that this result is an estimation and there is no guarantee that it is true. It appears that even with a controller, the stick-slip effect is still there. The amplitude of the oscillations is the desired angular speed Ω_0, when this latter one is small. If Ω_0 is large, the oscillations disappears. Comparing with Figure 2.2, the amplitude of the oscillations are not well-estimated.

It has already been shown in [158, 157] that a PI controller stabilizes the linear infinite-dimensional system. Here, we propose to revisit the stability analysis of a PI controlled infinite-dimensional model of a drilling pipe using the methodology presented in the previous chapter. Then, we aim at providing a bound on the oscillations and we investigate the influence of the controller coefficients on the oscillations.

This chapter is organized as follows. The first section is the problem statement. The second section is dedicated to the study of the linear torsion system. This is a first step before dealing with the nonlinear system, which is the purpose of next section. Section 4 focuses on the stability analysis of the axial dynamic. Each section is illustrated with some simulations and a discussion on the results.

6.1 PI controller for the torsional dynamic

The control of vibrations in a drillstring is a problem that was investigated many times because the vibrations may damage the equipment [133], lead to a slower drilling [44] and even interfere with the measurement tools [94]. All these undesirable effects lead to an increase of the cost to maintain the efficiency of the system.

To counteract this phenomenon, many controllers were proposed. We do not aim here at comparing them but we can list some of them[1]:

[1] A more complete list of available controls can be found in [133, Part III].

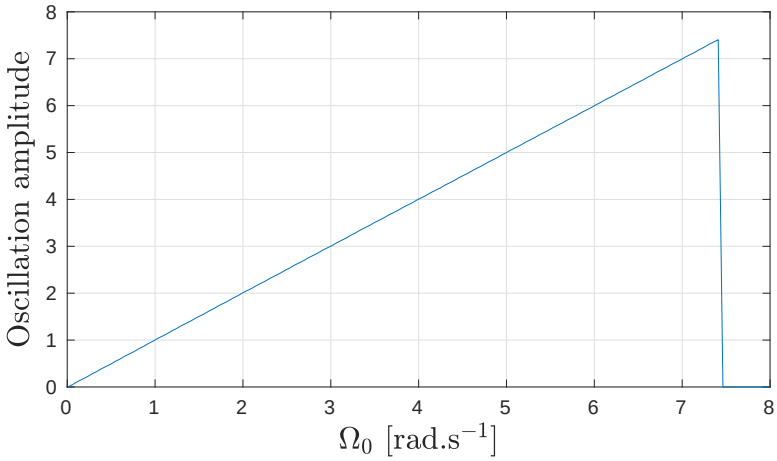

Figure 6.1: Describing function analysis of (2.1) with a PI controller. The proportional gain is 10^{-3} and the integrator gain is 1. The oscillations amplitudes refer to B_c and Ω_0 is the reference speed, in rad.s^{-1}.

Low order controllers These controllers are used on real drillstring platforms. They just ensure that the rotation speed of the rotary table is constant without any care for the control of vibrations. They are classically a PI controller as in [32, 157, 158, 160] or an H_∞ controller [140].

Sliding-mode controllers The obtained control law is then discontinuous and aims at effectively reducing the stick-slip effect. The sliding surface as defined in [74, 96] is related to the error between the angular velocity at the bottom and the desired angular speed. The two cited article uses a high-order sliding mode control.

Flatness-based controllers Such controllers are explored in [132, 133] for instance. This is done in two stages, the first one is an open-loop control computing the trajectory by taking the flatness property the system. Once the trajectory is defined, a feedback control is designed to ensure that the errors between the proposed trajectory and the real trajectory is indeed going to zero exponentially.

Backstepping controllers This kind of control is probably one of the most recent. It can be split into three categories. The general backstepping problem on the linear system is for example described in [127]. The target system is a boundary and internally damped wave equation similarly to the toy-example system described in this manuscript. The second class of backstepping controllers is using adaptive control as in [26] for instance. The aim is to stabilize the drilling pipe without an explicit knowledge of the damping terms. Finally, an observer based-technique (as developed in [21]) aims at building an observer which estimates the rotational speed at the bottom of the pipe with only surface measurements. Then, the classical backstepping design technique can apply with the estimated signals.

The aim of this chapter is not to design a control law ensuring the stability of the mechanism but to analyze the effect of the most basic controller: a proportional-integral.

We then introduce the following control laws:

$$\begin{aligned} \tilde{u}_1(t) &= -k_p^\phi \left(\phi_t(0,t) - \Omega_0\right) - k_i^\phi z_2(t), \\ \dot{z}_2(t) &= \phi_t(0,t) - \Omega_0, \end{aligned} \tag{6.1}$$

for the torsional dynamic. Here, k_p^ϕ is the two proportional gain and k_i^ϕ is the integral gain. Note that this controller has already been studied in many other articles [32, 36, 157] in a different setting. There are two main advantages with such a structure. First of all, it is a very simple controller which is already implemented in the drilling machines [10]. And secondly, it requires few measurements, indeed the only assumed knowledge is the rotational speed of the rotary table $\phi_t(0,\cdot)$ which is of course measurable. Implementing this control law in (2.7) leads to:

$$\begin{cases} \phi_{tt}(x,t) = \tilde{c}_t^2 \phi_{xx}(x,t) - \gamma_t \phi_t(x,t), \\ \phi_x(0,t) = (\tilde{g} + k_p^\phi)\phi_t(0,t) - k_p^\phi \Omega_0 + k_i C_2 Z(t), \\ \phi_t(1,t) = C_1 Z(t), \\ \dot{Z}(t) = A_\phi Z(t) + B_\phi \begin{bmatrix} \phi_t(0,t) \\ \phi_x(1,t) \end{bmatrix} + F_\phi \begin{bmatrix} \Omega_0 \\ T_{nl}(z_1(t)) \end{bmatrix}, \end{cases} \tag{6.2}$$

for the torsional dynamic where

$$A_\phi = \begin{bmatrix} -\frac{c_b}{I_B} & 0 \\ 0 & 0 \end{bmatrix}, \quad B_\phi = \begin{bmatrix} 0 & -\alpha_1 \\ 1 & 0 \end{bmatrix}, \quad F_\phi = \begin{bmatrix} 0 & -\alpha_2 \\ -1 & 0 \end{bmatrix}, \quad Z = \begin{bmatrix} z_1 \\ z_2 \end{bmatrix},$$
$$C_1 = \begin{bmatrix} 1 & 0 \end{bmatrix}, \qquad C_2 = \begin{bmatrix} 0 & 1 \end{bmatrix}.$$

As noted in [157], this kind of controller is very efficient in the case of large desired angular speed Ω_0 and on a linearized system. The following part is focusing on the analysis of a linear approximation of the torsional system (6.2) with a PI controller.

6.2 Stability of the linear torsional dynamic

System (6.2) is a nonlinear system because of the friction term T_{nl} introduced in (2.2). Nevertheless, for a high desired angular speed Ω_0, T_{nl} can be assumed constant as seen in Figure 2.3. Moreover, studying this linear system can be seen as a first step before studying the nonlinear system, which relies mostly on the stability theorem derived in this section.
The proposed linear model of T around $\Omega_0 \gg 1$ is

$$T(\theta) = c_b\theta + T_{nl}(\Omega_0) = c_b\theta + T_0. \tag{6.3}$$

For high values of Ω_0, $T_0 = T_{nl}(\Omega_0)$ is close to $T_{smooth}(\Omega_0)$ and at the limit when Ω_0 tends to infinity, they are equal. Hence the nonlinear friction term for relatively large

angle does not influence much the system. We therefore propose the following linear approximation:

$$\begin{cases} \phi_{tt}(x,t) = \tilde{c}_t^2 \phi_{xx}(x,t) - \gamma_t \phi_t(x,t), \\ \phi_x(0,t) = (\tilde{g} + k_p^\phi)\phi_t(0,t) - k_p^\phi \Omega_0 + k_i C_2 Z(t), \\ \phi_t(1,t) = C_1 Z(t), \\ \dot{Z}(t) = A_\phi Z(t) + B_\phi \begin{bmatrix} \phi_t(0,t) \\ \phi_x(1,t) \end{bmatrix} + F_\phi \begin{bmatrix} \Omega_0 \\ T_0 \end{bmatrix}, \end{cases} \tag{6.4}$$

Remark 6.1

Note that we use the notation ϕ to refer both to a solution to linear system (6.4) and to nonlinear system (6.2). In this section, it refers only to the solution to the linear system.

Remark 6.2: On the linear system

System (6.4) is not the linearization of (6.2) around $\Omega_0 > 0$ since we did not linearized T_{nl} but we considered a static approximation of the latter.

For simplicity in the sequel, we denote by

$$X_\phi = (\phi_x, \phi_t, z_1, z_2) \in C^1([0,\infty), \mathcal{H})$$

with $\mathcal{H} = L^2 \times L^2 \times \mathbb{R}^2$ the infinite dimensional state of system (6.4). The control objective in the linear case is to achieve the exponential stabilization of any equilibrium point of (6.4) in angular speed, i.e. $\phi_t(1)$ is going exponentially to a given constant reference value Ω_0.

Since the problem does not rephrase as in Chapter 3, we propose the following definitions of norm on $\mathcal{H}$, equilibrium points and exponential stability.

Definition 6.1: Norm on $\mathcal{H}$

For $X_\phi \in \mathcal{H}$, we define the following norm on $\mathcal{H}$:

$$\|X_\phi\|_{\mathcal{H}}^2 = z_1^2 + z_2^2 + \tilde{c}_t^2 \|\phi_x\|_{L^2}^2 + \|\phi_t\|_{L^2}^2.$$

The definition of an equilibrium point of (6.4) is given as follows.

Definition 6.2: Equilibrium point of (6.4)

$X_\phi^\infty \in \mathcal{H}$ is an **equilibrium point** of (6.4) if for the trajectory $X_\phi \in C^1([0,\infty), \mathcal{H})$ of (6.4) with initial condition X_ϕ^∞, the following holds:

$$\forall t > 0, \quad \|\dot{X}_\phi(t)\|_{\mathcal{H}} = 0.$$

The notion of exponential stability is then adapted in the following definition.

Definition 6.3: Exponential stability of X_ϕ^∞

Let X_ϕ^∞ be an equilibrium point of (6.4). X_ϕ^∞ is said to be **μ-exponentially stable** if the following holds for $\gamma \geq 1$, $\mu > 0$ and for any initial conditions $X_\phi^0 \in \mathcal{H}$ satisfying the boundary conditions:

$$\forall t > 0, \quad \|X_\phi(t) - X_\phi^\infty\|_\mathcal{H} \leq \gamma \, \|X_\phi^0 - X_\phi^\infty\|_\mathcal{H} \, e^{-\mu t},$$

where X_ϕ is the trajectory of (6.4) whose initial condition is X_ϕ^0. X_ϕ^∞ is said to be **exponentially stable** if μ is unknown.

Similarly to what was done in the first part, a lemma about the equilibrium points of (6.4) is proposed.

Lemma 6.1: Equilibrium points of (6.4)

Assume $k_i^\phi \neq 0$, then there exists a unique equilibrium point

$$X_\phi^\infty = (\phi_x^\infty, \phi_t^\infty, z_1^\infty, z_2^\infty) \in \mathcal{H}$$

of (6.4) and it satisfies $\phi_t^\infty = \Omega_0$.

Proof : An equilibrium point X_ϕ^∞ of (6.4) is such that:

$$\left\|\dot{X}_\phi^\infty\right\|_\mathcal{H} = \|(\phi_{xt}^\infty, \ \phi_{tt}^\infty, \ \dot{z}_1^\infty, \ \dot{z}_2^\infty)\|_\mathcal{H} = 0.$$

From $\frac{d}{dt} z_2^\infty = \phi_t^\infty(0,t) - \Omega_0 = 0$, we get that $\phi_t^\infty(0,t) = \Omega_0$. Moreover $\partial_x \phi_t^\infty = 0$ and $\partial_t \phi_t^\infty = 0$, that leads to $\phi_t^\infty = \Omega_0$ and in particular $z_2^\infty = \Omega_0$.

We also get from $\phi_{xx}^\infty = 0$ and $\partial_t \phi_x^\infty = 0$ that ϕ_x^∞ is a first order polynomial in x. Together with the boundary conditions, the system of equations has a unique solution if $k_i \neq 0$ such as:

$$X_\infty = \left(\phi_x^\infty, \Omega_0, \Omega_0, \frac{\phi_x^\infty(0) - \tilde{g}\Omega_0}{k_i^\phi}\right),$$

where for $x \in [0,1]$:

$$\phi_x^\infty(x) = \frac{\gamma_t \Omega_0}{\tilde{c}_t^2}(x-1) - \frac{c_b}{\alpha_1 I_B}\Omega_0 - \frac{\alpha_2}{\alpha_1} T_0.$$

♢

Remark 6.3: Equilibrium points for the nonlinear system

Note that the previous proof holds also for the nonlinear system since for $\Omega_0 > 0$ T_{nl} is bijective.

The aim of the following subsection is then to show that this unique equilibrium point of (6.4) is globally exponentially stable.

6.2.1 Exponential stability of the linear system

To prove the exponential stability, we will use the Lyapunov methodology described in the previous chapter. It results in the following theorem.

Theorem 6.1: Exponential stability of the linearized system [13]

Let $N \in \mathbb{N}$ and $\tilde{c}_t,\ \gamma_t > 0$ known and constant. Assume there exist $P_N \in \mathbb{S}^{2+2(N+1)}$, $R = \text{diag}(R_1, R_2) \succeq 0, S = \text{diag}(S_1, S_2) \succ 0$, $Q \in \mathbb{S}^2_+$ such that the following LMIs hold:

$$\begin{aligned} &\Theta_N = \tilde{c}_t\, \Theta_{1,N} + \Theta_{2,N} - Q_N \prec 0, \\ &P_N + S_N \succ 0, \end{aligned} \tag{6.5}$$

$$\text{and} \qquad \tilde{c}_t R + \frac{\gamma_t}{2} U_0 \succeq Q, \qquad \tilde{c}_t R + \frac{\gamma_t}{2} U_1 \succeq Q, \tag{6.6}$$

where

$$\begin{aligned}
\Theta_{1,N} &= H_N^\top \begin{bmatrix} (S_1+R_1) & 0 \\ 0 & -S_2 \end{bmatrix} H_N - G_N^\top \begin{bmatrix} S_1 & 0 \\ 0 & -S_2-R_2 \end{bmatrix} G_N, \quad \Theta_{2,N} = \text{He}\left(D_N^\top P_N F_N\right), \\
F_N &= \begin{bmatrix} I_{2+2(N+1)} & 0_{2+2(N+1),2} \end{bmatrix}, \ D_N = \text{col}(J_N, M_N), \ J_N = \begin{bmatrix} A_\phi & 0_{2,2(N+1)} & B_\phi \end{bmatrix}, \\
M_N &= \Lambda_N H_N - \bar{\Lambda}_N G_N - \begin{bmatrix} 0_{2(N+1),2} & L_N & 0_{2(N+1),2} \end{bmatrix}, \\
U_0 &= \begin{bmatrix} 2S_1 & S_1+S_2+R_2 \\ \star & 2(S_2+R_2) \end{bmatrix}, \qquad U_1 = \begin{bmatrix} 2(S_1+R_1) & S_1+S_2+R_1 \\ \star & 2S_2 \end{bmatrix}, \\
G_N &= \begin{bmatrix} \tilde{c}_t k_i^\phi C_2 & & \\ & 0_{2,2(N+1)} & G \\ -\tilde{c}_t k_i^\phi C_2 & & \end{bmatrix}, \quad G = \begin{bmatrix} 1+\tilde{c}_t(\tilde{g}+k_p^\phi) & 0 \\ 1-\tilde{c}_t(\tilde{g}+k_p^\phi) & 0 \end{bmatrix}, \\
H_N &= \begin{bmatrix} C_1 & & \\ & 0_{2,2(N+1)} & H \\ C_1 & & \end{bmatrix}, \qquad H = \begin{bmatrix} 0 & \tilde{c}_t \\ 0 & -\tilde{c}_t \end{bmatrix}, \\
Q_N &= \text{diag}(0_2, Q, \cdots, (2N+1)Q, 0_2), \quad S_N = \text{diag}\left(0_2, S, \cdots, (2N+1)S\right), \\
L_N &= \left[\ell_{j,k}\Lambda\right]_{j,k\in[0,N]} - \frac{\gamma_t}{2}\,\text{diag}\left(\left[\begin{smallmatrix} 1 & 1 \\ 1 & 1 \end{smallmatrix}\right], \ldots, \left[\begin{smallmatrix} 1 & 1 \\ 1 & 1 \end{smallmatrix}\right]\right), \\
\Lambda_N &= \begin{bmatrix} \Lambda \\ \vdots \\ \Lambda \end{bmatrix}, \quad \bar{\Lambda}_N = \begin{bmatrix} \Lambda \\ \vdots \\ (-1)^N \Lambda \end{bmatrix}, \quad \Lambda = \begin{bmatrix} \tilde{c}_t & 0 \\ 0 & -\tilde{c}_t \end{bmatrix},
\end{aligned} \tag{6.7}$$

then the equilibrium point of system (6.4) is exponentially stable.

Proof : As we aim at showing that X_ϕ^∞ is an exponentially stable equilibrium point of system (6.4) in the sense of Definition 6.2, the following variable is consequently defined for $t \geq 0$:

$$\tilde{X}_\phi(t) = X_\phi(t) - X_\phi^\infty = \left(\tilde{\phi}_x(\cdot,t), \tilde{\phi}_t(\cdot,t), \tilde{z}_1(t), \tilde{z}_2(t)\right),$$

where X_ϕ is a trajectory of system (6.4). We then want to show that there exists a Lyapunov functional as defined in Definition 5.1 for the previous system. As shown in Proposition 5.1, X_ϕ^∞ will then be exponentially stable.

This proof is then divided into three parts. The first one is dedicated to the formulation of a functional candidate. The second part aims at showing that this functional verifies that the functional is positive, i.e. the positivity inequality (5.3a) holds. The last part is about proving that if (6.5) holds, then the gradient of the Lyapunov functional candidate is negative along the trajectories of (6.4), in other words, equation (5.3b) is verified.

Choice of a Lyapunov functional candidate

The following notations are used in this section for $k \in \mathbb{N}$:

$$\tilde{\chi}(x) = \begin{bmatrix} \tilde{\phi}_t(x) + \tilde{c}_t \tilde{\phi}_x(x) \\ \tilde{\phi}_t(x) - \tilde{c}_t \tilde{\phi}_x(x) \end{bmatrix}, \quad \tilde{\mathfrak{X}}_k(t) = \int_0^1 \tilde{\chi}(x,t)\mathcal{L}_k(x)dx, \tag{6.8}$$

where $\{\mathcal{L}_k\}_{k\in\mathbb{N}}$ is the orthogonal family of Legendre Polynomials on $[0,1]$ as defined in Definition E.1.

$\tilde{\mathfrak{X}}_k$ is then the projection coefficient of $\tilde{\chi}$ along the Legendre polynomial of degree k. $\tilde{\chi}$ refers to the Riemann coordinates similarly to what was done in the previous chapter.

We decide to use a hierarchical Lyapunov functional candidate. Let $N \in \mathbb{N}$, following the same structure than previously, we propose the following:

$$V_N(\tilde{X}_\phi) = \tilde{Z}_N^\top P_N \tilde{Z}_N + \mathcal{V}_{PDE}(\tilde{\chi}) \tag{6.9}$$

where $\tilde{Z}_N = \begin{bmatrix} \tilde{z}_1 & \tilde{z}_2 & \tilde{\mathfrak{X}}_0^\top & \cdots & \tilde{\mathfrak{X}}_N^\top \end{bmatrix}^\top$ and

$$\mathcal{V}_{PDE}(\tilde{\chi}) = \int_0^1 \tilde{\chi}^\top(x) \begin{bmatrix} S_1 + xR_1 & 0 \\ 0 & S_2 + (1-x)R_2 \end{bmatrix} \tilde{\chi}(x)dx.$$

V_N is equivalent to $\|\cdot\|_{\mathcal{H}}^2$

We need to prove that there exist $\varepsilon_1, \varepsilon_2 > 0$ such that the following holds:

$$\varepsilon_1 \|\tilde{X}_\phi\|_{\mathcal{H}}^2 \leq V_N(\tilde{X}_\phi) \leq \varepsilon_2 \|\tilde{X}_\phi\|_{\mathcal{H}}^2.$$

Existence of ε_1: The inequalities $P_N + S_N \succ 0, S \succ 0$ and $R \succeq 0$ imply the existence of $\varepsilon_1 > 0$ such that:

$$\begin{aligned} P_N + S_N &\succeq \varepsilon_1 \begin{bmatrix} I_2 & 0_{2,2(N+1)} \\ 0_{2(N+1),2} & \frac{1}{2}\tilde{I}_N \end{bmatrix}, \\ S &\succeq \tfrac{\varepsilon_1}{2} I_2, \end{aligned} \tag{6.10}$$

with $\tilde{I}_N = \operatorname{diag}\{(2k+1)I_2\}_{k\in[0,N]}$. This statement implies the following on V_N:

$$\begin{aligned} V_N(\tilde{X}_\phi) &\geq \tilde{Z}_N^\top \left(P_N + \begin{bmatrix} 0_2 & 0_{2,2(N+1)} \\ 0_{2(N+1),2} & S_N \end{bmatrix} \right) \tilde{Z}_N - \sum_{k=0}^{N} (2k+1)\tilde{\mathfrak{X}}_k^\top S \tilde{\mathfrak{X}}_k + \frac{\varepsilon_1}{2}\|\tilde{\chi}\|_{L^2}^2 \\ &\qquad + \int_0^1 \tilde{\chi}(x)^\top \left(S - \frac{\varepsilon_1}{2} I_2 \right) \tilde{\chi}(x)dx \\ &\geq \varepsilon_1 \left(\tilde{z}_1^2 + \tilde{z}_2^2 + \frac{1}{2}\|\tilde{\chi}\|_{L^2}^2 \right) - \sum_{k=0}^{N} (2k+1)\tilde{\mathfrak{X}}_k^\top \tilde{S} \tilde{\mathfrak{X}}_k + \int_0^1 \tilde{\chi}^\top(x)\tilde{S}\tilde{\chi}(x)dx \\ &\geq \varepsilon_1 \|\tilde{X}_\phi\|_{\mathcal{H}}^2, \end{aligned}$$

where $\tilde{S} = S - \frac{\varepsilon_1}{2} I_2 \succ 0$. To get the last inequality, we applied Bessel inequality. That ends the proof of existence of ε_1.

Existence of ε_2: Following the same line as previously, the following holds for a sufficiently large $\varepsilon_2 > 0$:

$$\begin{aligned} P_N &\preceq \varepsilon_2 \begin{bmatrix} I_2 & 0_{2,2(N+1)} \\ 0_{2(N+1),2} & \frac{1}{4}\tilde{I}_N \end{bmatrix}, \\ S + R &\preceq \tfrac{\varepsilon_2}{4} I_2. \end{aligned}$$

Using these inequalities in (6.9) leads to:

$$\begin{aligned} V_N(\tilde{X}) &\leq \varepsilon_2 \left(\tilde{z}_1^2 + \tilde{z}_2^2 + \sum_{k=0}^{N} \frac{2k+1}{4} \tilde{\mathfrak{x}}_k^\top \tilde{\mathfrak{x}}_k + \frac{1}{4} \|\tilde{\chi}\|_{L^2}^2 \right) \leq \varepsilon_2 \left(\tilde{z}_1^2 + \tilde{z}_2^2 + \frac{1}{2} \|\tilde{\chi}\|_{L^2}^2 \right) \\ &\leq \varepsilon_2 \|\tilde{X}\|_{\mathcal{H}}^2. \end{aligned}$$

The last inequality is a direct application of Proposition E.5.

V_N has a negative gradient along the trajectories

This part deals with the existence of $\varepsilon_3 > 0$ such that:

$$\dot{V}_N(\tilde{X}) \leq -\varepsilon_3 \|\tilde{X}_\phi\|_{\mathcal{H}}^2.$$

Before dealing with the existence of ε_3, the following lemma, useful for the time derivation, is derived.

Lemma 6.2: State derivation [13]

For any function $\tilde{\chi} \in L^2$ satisfying (6.8), the following expression holds for any N in $\mathbb{N}$:

$$\frac{d}{dt} \begin{bmatrix} \tilde{\mathfrak{x}}_0 \\ \vdots \\ \tilde{\mathfrak{x}}_N \end{bmatrix} = \Lambda_N \tilde{\chi}(1) - \bar{\Lambda}_N \tilde{\chi}(0) - L_N \begin{bmatrix} \tilde{\mathfrak{x}}_0 \\ \vdots \\ \tilde{\mathfrak{x}}_N \end{bmatrix}. \tag{6.11}$$

Proof : This proof is highly inspired from [19]. Since $\tilde{\chi} \in L^2$ satisfies (6.8), equation (6.13) can be derived and the following holds:

$$\frac{d}{dt} \tilde{\mathfrak{x}}_k = \int_0^1 \tilde{\chi}_t(x) \mathcal{L}_k(x) dx. \tag{6.12}$$

Note that the time-derivation of $\tilde{\chi}$ leads to:

$$\tilde{\chi}_t(x) = \Lambda \tilde{\chi}_x(x) - \gamma_t \begin{bmatrix} 1 \\ 1 \end{bmatrix} \tilde{\phi}_t(x).$$

Since $\tilde{\phi}_t(x) = \frac{1}{2} \begin{bmatrix} 1 & 1 \end{bmatrix} \tilde{\chi}(x)$, we get:

$$\tilde{\chi}_t(x) = \Lambda \tilde{\chi}_x(x) - \frac{\gamma_t}{2} \begin{bmatrix} 1 & 1 \\ 1 & 1 \end{bmatrix} \tilde{\chi}(x). \tag{6.13}$$

Consequently, (6.12) rewrites as:

$$\frac{d}{dt}\tilde{\mathfrak{X}}_k = \Lambda\left[\tilde{\chi}(x)\mathcal{L}_k(x)\right]_0^1 - \Lambda\int_0^1 \tilde{\chi}(x)\mathcal{L}'(x)dx - \frac{\gamma_t}{2}\begin{bmatrix}1 & 1\\ 1 & 1\end{bmatrix}\tilde{\mathfrak{X}}_k.$$

Using the derivation rule and the boundary values of Legendre polynomials as defined in Definition E.1 lead to the proposed result in equation (6.11). ♢

The proof of existence of ε_3 is detailed since it is not a straightforward adaption of the previous chapter.

Existence of ε_3: The time-derivative of $\mathcal{V}_{PDE}$ along the trajectories of (3.1) leads to:

$$\dot{\mathcal{V}}_{PDE}(\tilde{\chi}) = 2\tilde{c}_t\mathcal{V}_1(\tilde{\chi}) - \frac{\gamma_t}{2}\mathcal{V}_2(\tilde{\chi}),$$

where

$$\mathcal{V}_1(\tilde{\chi}) = \int_0^1 \tilde{\chi}_x^\top(x)\begin{bmatrix}S_1+xR_1 & 0\\ 0 & -S_2-(1-x)R_2\end{bmatrix}\tilde{\chi}(x)dx, \quad \mathcal{V}_2(\tilde{\chi}) = \int_0^1 \tilde{\chi}^\top(x)U(x)\tilde{\chi}(x)dx,$$

with

$$U(x) = \begin{bmatrix}2(S_1+xR_1) & S_1+S_2+xR_1+(1-x)R_2\\ S_1+S_2+xR_1+(1-x)R_2 & 2(S_2+(1-x)R_2)\end{bmatrix}.$$

An integration by part on $\mathcal{V}_1$ shows that:

$$2\mathcal{V}_1(\tilde{\chi}) = \tilde{\chi}^\top(1)\begin{bmatrix}S_1+R_1 & 0\\ 0 & -S_2\end{bmatrix}\tilde{\chi}(1) - \tilde{\chi}^\top(0)\begin{bmatrix}S_1 & 0\\ 0 & -S_2-R_2\end{bmatrix}\tilde{\chi}(0) - \int_0^1 \tilde{\chi}^\top(x)\begin{bmatrix}R_1 & 0\\ 0 & R_2\end{bmatrix}\tilde{\chi}(x)dx.$$

The previous calculations lead to the following derivative:

$$\dot{\mathcal{V}}_{PDE}(\tilde{\chi}) = \tilde{c}_t\left(\tilde{\chi}^\top(1)\begin{bmatrix}S_1+R_1 & 0\\ 0 & -S_2\end{bmatrix}\tilde{\chi}(1) - \tilde{\chi}^\top(0)\begin{bmatrix}S_1 & 0\\ 0 & -S_2-R_2\end{bmatrix}\tilde{\chi}(0)\right) - \int_0^1 \tilde{\chi}^\top(x)\left(\tilde{c}_tR + \frac{\gamma_t}{2}U(x)\right)\tilde{\chi}(x)dx. \quad (6.14)$$

We create the following extended state variable:

$$\tilde{\xi}_N = \mathrm{col}\left(\tilde{Z}_N, \tilde{\phi}_t(0), \tilde{\phi}_x(1)\right), \quad (6.15)$$

Noting that $U_0 = U(0)$ and $U_1 = U(1)$, a convexity argument implies that if (6.6) is verified then $\tilde{c}_tR+U(x) \succeq Q \succ 0$ holds for $x \in [0,1]$. Since $\tilde{\chi}(0) = G_N\tilde{\xi}_N$, $\tilde{\chi}(1) = H_N\tilde{\xi}_N$, we then get:

$$\dot{\mathcal{V}}_{PDE}(\tilde{\chi}) \leq \tilde{c}_t\tilde{\xi}_N^\top\Theta_{1,N}\tilde{\xi}_N - \int_0^1 \tilde{\chi}^\top(x)Q\tilde{\chi}(x)dx. \quad (6.16)$$

Consequently, we get the following:

$$\begin{aligned}\dot{V}_N(\tilde{X}_\phi) &= \mathrm{He}\left(\dot{\tilde{Z}}_N^\top P_N\tilde{Z}_N\right) + \dot{\mathcal{V}}_{PDE}(\tilde{\chi})\\ &\leq \tilde{\xi}_N^\top\Theta_N\tilde{\xi}_N + \sum_{k=0}^{N}(2k+1)\tilde{\mathfrak{X}}_k^\top Q\tilde{\mathfrak{X}}_k - \int_0^1 \tilde{\chi}^\top(x)Q\tilde{\chi}(x)dx,\end{aligned} \quad (6.17)$$

where Θ_N is defined in (6.5). To obtain the previous equation, one should note that using Lemma 6.2, we get $\dot{\tilde{Z}}_N = D_N\tilde{\xi}_N$ and $\tilde{Z}_N = F_N\tilde{\xi}_N$. Since $\Theta_N \prec 0$ and $Q \succ 0$, we get:

$$\begin{aligned} \Theta_N &\preceq -\varepsilon_3 \operatorname{diag}\left(I_2, \tfrac{1}{2}I_2, \tfrac{3}{2}I_2, \ldots, \tfrac{2N+1}{2}I_2, 0_2\right), \\ Q &\succeq \tfrac{\varepsilon_3}{2}I_2. \end{aligned}$$

Then, $\dot{V}_N$ is upper bounded by:

$$\begin{aligned} \dot{V}_N(\tilde{X}_\phi) &\leq -\varepsilon_3\left(\tilde{z}_1^2 + \tilde{z}_2^2 + \frac{1}{2}\|\tilde{\chi}\|_{L^2}^2\right) + \sum_{k=0}^{N}(2k+1)\tilde{\mathfrak{X}}_k^\top\left(Q - \frac{\varepsilon_3}{2}I_2\right)\tilde{\mathfrak{X}}_k \\ &\qquad - \int_0^1 \tilde{\chi}^\top(x)\left(Q - \frac{\varepsilon_3}{2}I_2\right)\tilde{\chi}(x)dx \\ &\leq -\varepsilon_3\|\tilde{X}_\phi\|_{\mathcal{H}}^2. \end{aligned}$$

The last inequality comes from a direct application of Bessel's inequality E.5.

Conclusion

Using Proposition 5.1 and the results of the previous subparts, the assumptions of Theorem 6.1 indeed leads to the exponential convergence of all trajectories of (6.4) to the desired equilibrium point. ♢

The previous theorem is useful to know that the system is exponentially stable but it does not give any estimate on the convergence rate. The following subpart characterizes the decay-rate of the solutions of (6.4).

6.2.2 Exponential stability of the linearized system with a guaranteed decay-rate

It is possible to estimate the decay-rate μ of the exponential convergence with a slight modification of the LMIs as it is proposed in the following corollary.

Corollary 6.1: Exponential stability with a guaranteed decay-rate

Let $N \in \mathbb{N}$, $\mu > 0$ and $\gamma_t \geq 0$. If there exist $P_N \in \mathbb{S}^{2+2(N+1)}$, $R = \operatorname{diag}(R_1, R_2) \succeq 0, S = \operatorname{diag}(S_1, S_2) \succ 0, Q \in \mathbb{S}_+^2$ such that (6.6) and the following LMIs hold:

$$\begin{aligned} &\Theta_{N,\mu} = \Theta_N + 2\mu F_N^\top\left(P_N + S_N\right)F_N \prec 0, \\ &P_N + S_N \succ 0, \end{aligned} \tag{6.18}$$

where the parameters are defined as in Theorem 6.1, then the equilibrium point of system (6.4) is μ-exponentially stable.

Proof : To prove the exponential stability with a decay-rate of at least $\mu > 0$, we use Proposition 5.1. Similarly to the previous proof, we have the existence of $\varepsilon_1, \varepsilon_2 > 0$.

The existence of ε_3 is slightly different. First, note that for the Lyapunov functional candidate (6.9), we get:

$$V_N(\tilde{X}_\phi) \geq \tilde{Z}_N^\top P_N \tilde{Z}_N + \int_0^1 \tilde{\chi}^\top(x) S \tilde{\chi}(x) dx \geq \tilde{Z}_N^\top P_N \tilde{Z}_N + \sum_{k=0}^{N} (2k+1) \tilde{\mathfrak{X}}_k^\top S \tilde{\mathfrak{X}}_k.$$

This inequality was obtained using Proposition E.5. Using the notations of the previous theorem and (6.15) yields:

$$V_N(\tilde{X}_\phi) \geq \tilde{\xi}_N^\top F_N^\top \left(P_N + S_N\right) F_N \tilde{\xi}_N. \tag{6.19}$$

Coming back to (6.17), the following holds:

$$\dot{V}_N(\tilde{X}_\phi) \leq \tilde{\xi}_N^\top \Theta_N \tilde{\xi}_N + \sum_{k=0}^{N} (2k+1) \tilde{\mathfrak{X}}_k^\top Q \tilde{\mathfrak{X}}_k - \int_0^1 \tilde{\chi}^\top(x) Q \tilde{\chi}(x) dx,$$

Using (6.18), the previous expression becomes:

$$\dot{V}_N(\tilde{X}_\phi) \leq \tilde{\xi}_N^\top \Theta_{N,\mu} \tilde{\xi}_N - 2\mu \tilde{\xi}_N^\top \left(F_N^\top P_N F_N + S_N\right) \tilde{\xi}_N + \sum_{k=0}^{N} (2k+1) \tilde{\mathfrak{X}}_k^\top Q \tilde{\mathfrak{X}}_k - \int_0^1 \tilde{\chi}^\top(x) Q \tilde{\chi}(x) dx.$$

Injecting inequality (6.19) into the previous inequality leads to:

$$\dot{V}_N(\tilde{X}_\phi) \leq \tilde{\xi}_N^\top \Theta_{N,\mu} \tilde{\xi}_N - 2\mu V_N(\tilde{X}_\phi) + \sum_{k=0}^{N} (2k+1) \tilde{\mathfrak{X}}_k^\top Q \tilde{\mathfrak{X}}_k - \int_0^1 \tilde{\chi}^\top(x) Q \tilde{\chi}(x) dx.$$

Using the same techniques than for the previous proof leads to the existence of $\varepsilon_3 > 0$ such that:

$$\dot{V}_N(\tilde{X}_\phi) + 2\mu V_N(\tilde{X}_\phi) \leq -\varepsilon_3 \|\tilde{X}_\phi\|_{\mathcal{H}}^2.$$

Proposition 5.1 concludes then on the exponential stability with a guaranteed decay-rate of at least μ. ♢

Remark 6.4: Maximum allowable decay-rate

As seen earlier, wave equations can sometimes be modeled as neutral time-delay systems. Ensuring the small τ-stabilizability brings some necessary stability conditions as noted in [14, 20]. In the book [20] for instance, the following criterion is derived:

$$\mu \leq \frac{\tilde{c}_t}{2} \log \left| \frac{1 + \tilde{c}_t(\tilde{g} + k_p^\phi)}{1 - \tilde{c}_t(\tilde{g} + k_p^\phi)} \right| = \mu_{max}. \tag{6.20}$$

This result implies that there exists a maximum decay-rate and if this maximum is negative, then the system is unstable. The LMI condition $\Theta_{N,\mu} \prec 0$ contains the same necessary condition, meaning that the neutral aspect of the system is well-captured.

6.2.3 Strong stability against small delays in the loop

A practical consequence of the neutral aspect of system (6.4) is that it is very sensitive to delay in the control and in the measure [69]. To study the robustness of our system to a delay, we fictionally introduce a delay $\tau \geq 0$ in the control. To this extend, the Laplace transform of the system (6.4) with this additional delay is presented below:

$$\begin{cases} s^2\tilde{\phi}(x,s) = \tilde{c}_t^2\phi_{xx} - s\gamma_t\tilde{\phi}(x,s), \\ \tilde{\phi}_x(0,s) = s\left(\tilde{g} + k_p^\phi e^{-\tau s}\right)\tilde{\phi}(0,s) + k_i^\phi z_2(s)e^{-\tau s}, \\ s\tilde{\phi}(1,s) = z_1(s), \\ sz_1(s) = -\dfrac{c_b}{I_B}z_1(s) - \alpha_1\phi_x(1,s), \\ sz_2(s) = su(0,s), \end{cases} \tag{6.21}$$

where $s \in \mathbb{C}$ and $\tau \geq 0$. To ease the computation, we assume in the sequel that $\gamma_t = 0$, it does not change the conclusion one may draw after this subsection. The previous system has then the following solution:

$$\tilde{\phi}(x,s) = A(s)e^{sx/\tilde{c}_t} + B(s)e^{-sx/\tilde{c}_t},$$

where A and B are two transfer functions verifying

$$\begin{cases} s\left(s + \dfrac{c_b}{I_B}\right)\left(A(s)e^{s/\tilde{c}_t} + B(s)e^{-s/\tilde{c}_t}\right) = -\alpha_1\dfrac{s}{\tilde{c}_t}\left(A(s)e^{s/\tilde{c}_t} - B(s)e^{-s/\tilde{c}_t}\right), \\ A(s) - B(s) = \tilde{c}_t\left(A(s) + B(s)\right)\left(\tilde{g} + k_p^\phi e^{-\tau s} + k_i^\phi\dfrac{e^{-\tau s}}{s}\right). \end{cases}$$

The previous system has a unique solution, the common denominator of A and B is the characteristic equation of (6.21), which is:

$$c_{eq}(s) = c\left(a_2\left(e^{-s}\right)s^2 + a_1\left(e^{-s}\right)s + a_0\left(e^{-s}\right)\right)$$

where a_2, a_1 and a_0 are polynomials. The expression of a_2 is given by:

$$\begin{aligned} a_2(\theta) &= 1 + \tilde{c}_t\tilde{g} + (1 - \tilde{c}_t\tilde{g})\theta^{2/\tilde{c}_t} + \tilde{c}_t k_p^\phi\left(\theta^\tau - \theta^{\tau+2/\tilde{c}_t}\right) \\ &= a_{2,0} + a_{2,2/\tilde{c}_t}\theta^{2/\tilde{c}_t} + a_{2,\tau}\theta^\tau + a_{2,\tau+2/\tilde{c}_t}\theta^{\tau+2/\tilde{c}_t}, \end{aligned}$$

where

$$\begin{aligned} a_{2,0} &= 1 + \tilde{c}_t\tilde{g}, & a_{2,2/\tilde{c}_t} &= 1 - \tilde{c}_t\tilde{g}, \\ a_{2,\tau} &= \tilde{c}_t k_p^\phi, & a_{2,\tau+2/\tilde{c}_t} &= \tilde{c}_t k_p^\phi. \end{aligned}$$

Definition 4.1 and [69, Corollary 3.3] implies that (6.21) is small-τ stabilizable if the following condition is respected:

$$\frac{|a_{2,2/\tilde{c}_t}| + |a_{2,\tau}| + |a_{2,\tau+2/\tilde{c}_t}|}{|a_{2,0}|} < 1.$$

Theorem \ Order	$N=0$	$N=1$	$N=2$	$N=3$	$N=4$	μ_{max}
[13, Corollary 1] ($\times 10^{-3}$)	4.21	6.39	6.39	6.39	6.39	7.73
Corollary 6.1 ($\times 10^{-3}$)	0.096	4.25	7.19	7.65	7.73	7.73

Table 6.1: Estimated decay-rate μ as a function of the order N used. μ_{max} is calculated using (6.20) for $k_p = 10^{-3}$, $k_i = 10$.

In our case, we get[2]:

$$\left|\frac{1-\tilde{c}_t\tilde{g}}{1+\tilde{c}_t\tilde{g}}\right| + 2\left|\frac{\tilde{c}_t k_p^{\phi}}{1+\tilde{c}_t\tilde{g}}\right| < 1$$

Hence, to be robust to delay in the loop, one then needs to ensure the following:

$$0 \leq k_p^{\phi} \leq \frac{1}{2\tilde{c}_t}\left(|1+\tilde{c}_t\tilde{g}| - |1-\tilde{c}_t\tilde{g}|\right) = \tilde{g} = 2.1 \cdot 10^{-3}.$$

This inequality on k_p comes when considering the infinite-dimensional problem and does not arise when dealing with any finite-dimensional model. That point enlightens that it is more realistic to consider the infinite-dimensional problem because it can explain several phenomena arising in the reality [10].

6.2.4 Numerical simulations

Using Yalmip with SDPT-3 [98, 159], it appears that the LMIs of Theorem 6.1 are feasible for the parameters in Table 2.2, that means system (6.4) is exponentially stable. Table 6.1 contains the estimation of the decay-rate of the solution depending on the order used in Corollary 6.1. It also compares with the corollary derived in [13, Corollary 1]. Note that even if at low order Corollary 6.1 gives a very bad bound, it tends to the maximal value μ_{max} while [13, Corollary 1] gives a better estimation at low order but presents a bias. In short, using the projection methodology helps getting better results and we will see in the following section that estimating the decay-rate of system (6.4) is critical to assess the practical stability.

We can use a discretization algorithm using a Euler forward scheme to approximate the angular velocity ϕ in the pipe in (6.2) and (6.4). Figure 6.2 highlights that for high desired angular speed Ω_0 and an initial condition close to the equilibrium point, linear system (6.4) and nonlinear system (6.2) behave similarly. The downhole velocity differs more significantly than the surface one, which is normal because the nonlinearity acts on the bit only.

Figure 6.3 displays the result for a zero initial condition on the linear and nonlinear systems. It appears that the nonlinear system has generally less overshoot than the linear one. For high desired angular speed Ω_0, the two systems behave similarly (Figures 6.3a and 6.3b) and they are asymptotically stable. As noted previously, this is not

[2]Note that in the case $k_p^{\phi} = 0$, we recover the condition $\mu > 0$ in (6.20) from the following equation.

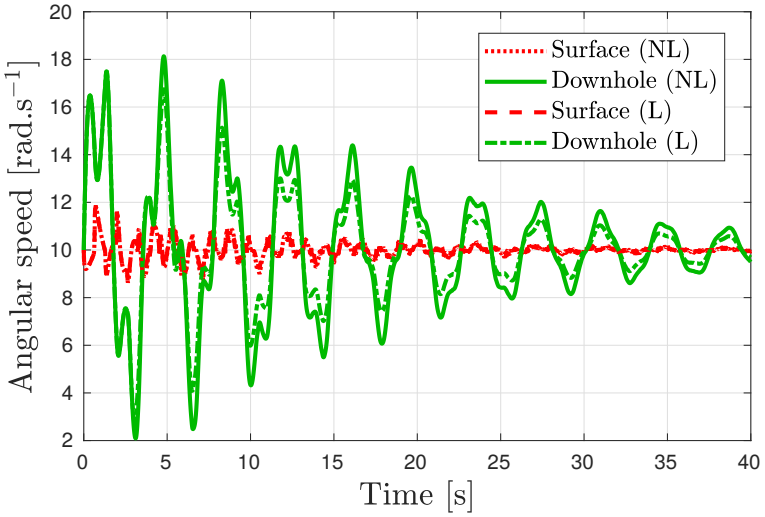

Figure 6.2: Numerical simulations for system (6.4) with $k_p = 10^{-3}$, $k_i = 10$ and $\Omega_0 = 10$. The parameters are $\phi^0(x) = (1 + 0.32\sin(x)) \int_0^x \phi_x^\infty(s)ds$, $\phi^1 = \Omega_0$ and $Z(0) = (z_1^\infty \; z_2^\infty)^\top$. (L) refers to the solution of the linear approximation and (NL) to the solution of system (6.2).

the case for a small Ω_0 where the linear system is still asymptotically stable while the nonlinear system is just stable. We can clearly see on 6.3d the stick-slip effect occurring.

In this section, we derived an LMI condition to ensure that the linear system (with a static approximation for T_0) is exponentially stable. In the next section, we will prove its practical stability using similar tools.

6.3 Stability analysis of system (6.2)

The experiments conducted previously show that there exists a neighborhood $\mathcal{N}_{X_\phi^\infty}$ of X_ϕ^∞ such that for any initial condition $X_\phi^0 \in \mathcal{N}_{X_\phi^\infty}$, the trajectory of the nonlinear system (6.2) goes exponentially to X_ϕ^∞. In other words, the previous result is a local stability test for the nonlinear system and does not extend straightforward to a global analysis.

6.3.1 Practical stability of (6.2)

We propose in this part a solution to Problems 1 and 2. We want then to show that system (6.2) is practically stable, meaning that there exists z_{bound} such that the following holds:

$$\forall \eta > 0, \quad \exists T > 0, \quad \forall t \geq T, \qquad |z_1(t) - \Omega_0| \leq z_{bound} + \eta. \tag{6.22}$$

We also want to get an estimation of this z_{bound}.

Practical stability relies mostly on the bounding of T_{nl}, that is why the following lemma presents three sector conditions related to the non linear friction term.

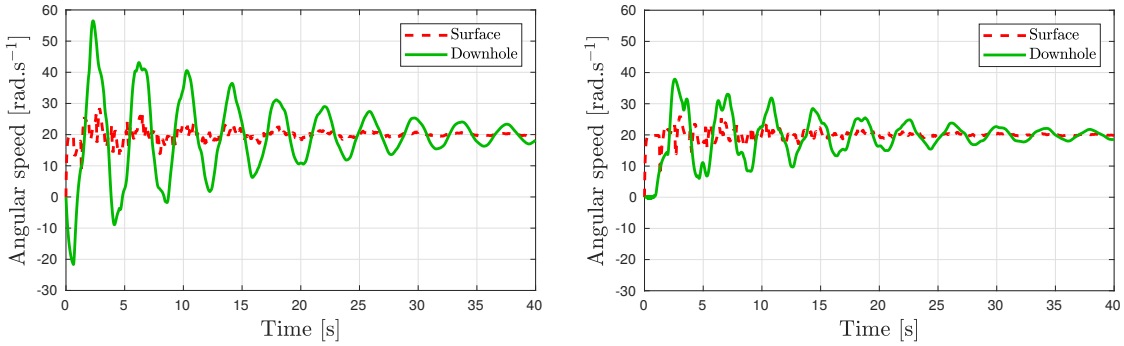

(a) Linear system with $\Omega_0 = 20$

(b) Nonlinear system with $\Omega_0 = 20$

(c) Linear system with $\Omega_0 = 5$

(d) Nonlinear system with $\Omega_0 = 5$

Figure 6.3: Numerical simulations for system (6.4) and (6.2) for two desired angular velocities and with a $0_{\mathcal{H}}$ initial condition.

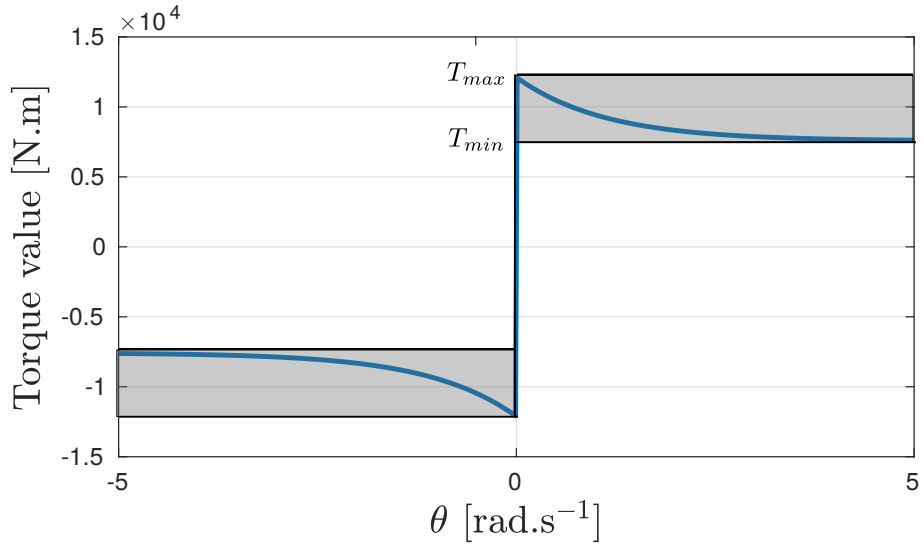

Figure 6.4: The sector conditions defined in (6.23) encapsulate the nonlineary T_{nl} inside the gray box.

Lemma 6.3: Sector conditions on T_{nl} [13]

For almost all $\tilde{z}_1 \in \mathbb{R}$, the following holds:

$$T_{nl}(\tilde{z}_1 + \Omega_0)^2 \leq T_{sb}^2 \mu_{sb}^2 = T_{max}^2, \tag{6.23a}$$
$$T_{nl}(\tilde{z}_1 + \Omega_0)^2 \geq T_{sb}^2 \mu_{cb}^2 = T_{min}^2, \tag{6.23b}$$
$$-2\,(\tilde{z}_1 + \Omega_0)\,T_{nl}(\tilde{z}_1 + \Omega_0) \leq 0. \tag{6.23c}$$

Proof : These inequalities can be easily verified using Figure 6.4 or the following expression of T_{nl}:

$$T_{nl}(\theta) = T_{sb}\left(\mu_{cb} + (\mu_{sb} - \mu_{cb})\, e^{-\gamma_b|\theta|}\right) \operatorname{sign}(\theta), \tag{6.24}$$

where the parameters are defined in Table 2.1. Indeed, equation (6.23c) is obtained noting that T_{nl} is an odd function. Since it is strictly decreasing for $\theta > 0$, we get equations (6.23a) and almost everywhere, we get (6.23b). ♢

Theorem 6.2: Practical stability of the drilling pipe [13]

Let $N \in \mathbb{N}$ and $V_{max} > 0$. If there exist $P_N \in \mathbb{S}^{2+2(N+1)}$, $R = \operatorname{diag}(R_1, R_2) \succeq 0, S = \operatorname{diag}(S_1, S_2) \succ 0, Q \in \mathbb{S}_+^2, \tau_0, \tau_1, \tau_2, \tau_3 \geq 0$ such that (6.6) holds together with:

$$\begin{aligned} &\Xi_N = \bar{\Theta}_N - \tau_0\Pi_0 - \tau_1\Pi_1 - \tau_2\Pi_2 - \tau_3\Pi_3 \prec 0, \\ &P_N + S_N \succ 0, \end{aligned} \tag{6.25}$$

where

$$\begin{aligned}
\bar{\Theta}_N &= \operatorname{diag}(\Theta_N, 0_2) - \alpha_2 \operatorname{He}\left((F_{m1} - T_0 F_{m2})^\top e_1^\top P_N \tilde{F}_N\right), \\
\tilde{F}_N &= \left[F_N\ 0_{2(N+1)+2,2}\right], & e_1 &= \left[1\ 0_{1,2(N+1)+1}\right]^\top, \\
F_{m1} &= \left[0_{1,2(N+1)+4}\ 1\ 0\right], & F_{m2} &= \left[0_{1,2(N+1)+4}\ 0\ 1\right], \\
\Pi_0 &= V_{max} F_{m2}^\top F_{m2} - \tilde{F}_N^\top (P_N + S_N)\, \tilde{F}_N, \\
\Pi_1 &= \pi_2^\top \pi_2 - T_{max}^2 \pi_3^\top \pi_3, & \Pi_2 &= T_{min}^2 \pi_3^\top \pi_3 - \pi_2^\top \pi_2, \\
\Pi_3 &= -\operatorname{He}((\pi_1 + \Omega_0 \pi_3)^\top \pi_2), \\
\pi_1 &= \left[1, 0_{1,2(N+1)+3}, 0, 0\right], \quad \pi_2 = \left[0_{1,2(N+1)+4}, 1, 0\right], \quad \pi_3 = \left[0_{1,2(N+1)+4}, 0, 1\right],
\end{aligned}$$

and all the parameters defined as in Theorem 6.1, then the equilibrium point X_ϕ^∞ of system (6.2) is practically stable. More precisely, equation (6.22) holds and

$$z_{bound} = \sqrt{\frac{V_{max}}{\varepsilon_1}},$$

where ε_1 verifies $S \succeq \frac{\varepsilon_1}{2} I_2$ and is the smallest eigenvalue of $\tilde{P}_N$ defined by:

$$\tilde{P}_N = (P_N + S_N) \begin{bmatrix} I_2 & 0 \\ 0 & \tilde{I}_N^{-1} \end{bmatrix}.$$

Some practical consequences of Theorem 6.2 are given after the proof.

Proof : First, let do the same change of variable as before:

$$\tilde{X}_\phi = X_\phi - X_\phi^\infty.$$

We use the same Lyapunov functional as in (6.9). The positivity is ensured in the exact same way.

Bounding of $\dot{V}_N(\tilde{X}_\phi)$ Since the nonlinearity affects only the ODE part of system (6.2), the difference with the previous part lies in the dynamic of $\tilde{Z}$:

$$\begin{aligned}\dot{\tilde{Z}}(t) &= \frac{d}{dt}\left(Z(t) - \begin{bmatrix} z_1^\infty \\ z_2^\infty \end{bmatrix}\right) \\ &= A_\phi \tilde{Z}(t) + B_\phi \begin{bmatrix} \tilde{\phi}_t(0,t) \\ \tilde{\phi}_x(1,t) \end{bmatrix} + F_\phi \begin{bmatrix} 0 \\ T_{nl}(\tilde{z}_1(t) + \Omega_0) - T_0 \end{bmatrix}.\end{aligned}$$

For the bound on the time derivative, following the same strategy as before, we easily get:

$$\begin{aligned}\dot{V}_N(\tilde{X}_\phi) \leq \tilde{\xi}_N^\top \Theta_N \tilde{\xi}_N - 2\alpha_2 (T_{nl}(\tilde{z}_1 + \Omega_0) - T_0) e_1^\top P_N \tilde{Z}_N \\ + \sum_{k=0}^{N} (2k+1) \tilde{\mathfrak{X}}_k^\top Q \tilde{\mathfrak{X}}_k - \int_0^1 \tilde{\chi}^\top(x) Q \tilde{\chi}(x) dx.\end{aligned} \tag{6.26}$$

We introduce a new extended state variable $\bar{\xi}_N = \begin{bmatrix} \tilde{\xi}_N^\top & T_{nl}(\tilde{z}_1 + \Omega_0) & 1 \end{bmatrix}^\top$. Using the notation of Theorem 6.2, equation (6.26) rewrites as:

$$\dot{V}_N(\tilde{X}_\phi) \;\leq\; \bar{\xi}_N^\top \bar{\Theta}_N \bar{\xi}_N^\top + \sum_{k=0}^{N} (2k+1) \tilde{\mathfrak{X}}_k^\top Q \tilde{\mathfrak{X}}_k - \int_0^1 \tilde{\chi}^\top(x) Q \tilde{\chi}(x) dx. \tag{6.27}$$

The negativity of the bound would be ensured if $\bar{\Theta}_N \prec 0$. Since its last 2 by 2 diagonal block is 0_2, it is impossible to get such an inequality. We then use the definition of practical stability.

Definition of practical stability of (6.2) If we rewrite (6.22) in terms of V_N, the system is practically stable if there exists $V_{max} > 0$ such that following holds:

$$\forall \eta > 0, \quad \exists T > 0, \quad \forall t > T, \qquad V_N\left(\tilde{X}_\phi(t)\right) \leq V_{max} + \eta.$$

In other words, the ball $\mathcal{S} = \left\{\tilde{X}_\phi \in \mathcal{H} \mid V_N\left(\tilde{X}_\phi\right) \leq V_{max}\right\}$ is attractive and invariant. This implies that V_N is strictly decreasing when outside $\mathcal{S}$, and that leads to Figure 6.5, which illustrates this concept in a two-dimension plane. Hence, we want the existence of $\varepsilon_3 > 0$ such that the following holds:

$$\forall \tilde{X}_\phi \in \mathcal{H}, \quad \text{such that} \quad V_N(\tilde{X}_\phi) - V_{max} \geq 0 \quad \Rightarrow \quad \dot{V}_N(\tilde{X}_\phi) \leq -\varepsilon_3 \|\tilde{X}_\phi\|_{\mathcal{H}}. \tag{6.28}$$

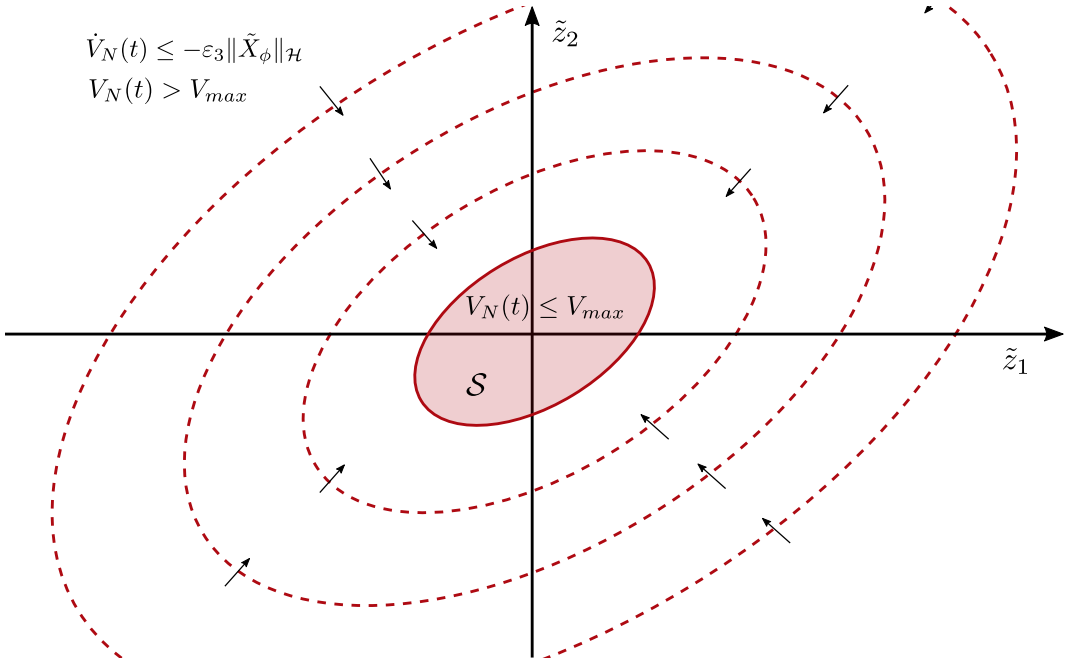

Figure 6.5: Illustration of the practical stability of (6.2). This is a projection of $\tilde{X}_\phi$ on $(\tilde{z}_1, \tilde{z}_2)$. The dotted lines are isolines of V_N. The ball $\mathcal{S}$ refers to $V_N \leq V_{max}$.

A sufficient condition to get $V_N(\tilde{X}_\phi) - V_{max} \geq 0$ is:

$$\begin{aligned} V_N(\tilde{X}_\phi) - V_{max} &\geq \tilde{Z}_N^\top P_N \tilde{Z}_N + \int_0^1 \tilde{\chi}^\top(x) S \tilde{\chi}(x) dx - V_{max} \\ &\geq -\bar{\xi}_N^\top \Pi_0 \bar{\xi}_N \geq 0. \end{aligned}$$

The previous inequality is obtained using Bessel inequality (Proposition E.5) on $\int_0^1 \tilde{\chi}^\top(x) S \tilde{\chi}(x) dx$. Hence, a sufficient condition for $\mathcal{S}$ to be invariant and attractive is:

$$\forall \tilde{X}_\phi \in \mathcal{H}, \quad \text{such that} \quad \bar{\xi}_N^\top \Pi_0 \bar{\xi}_N \leq 0 \quad \Rightarrow \quad \dot{V}_N(\tilde{X}_\phi) \leq -\varepsilon_3 \|\tilde{X}_\phi\|_{\mathcal{H}}.$$

Noting that $\tilde{z}_1 = \pi_1 \bar{\xi}_N, T_{nl}(\tilde{z}_1 + \Omega_0) = \pi_2 \bar{\xi}_N$ and $1 = \pi_3 \bar{\xi}_N$, Lemma 6.3 rewrites as:

$$\forall i \in \{1, 2, 3\}, \quad \bar{\xi}_N \, \Pi_i \, \bar{\xi}_N \leq 0.$$

Using the estimate calculated in (6.27) and in a similar way as for Theorem 6.1, a sufficient condition to be practically stable is:

$$\forall \bar{\xi}_N \neq 0 \text{ s. t. } \forall i \in [0, 4], \quad \bar{\xi}_N^\top \Pi_i \bar{\xi}_N \leq 0, \qquad \bar{\xi}_N^\top \bar{\Theta}_N \bar{\xi}_N < 0. \tag{6.29}$$

The technique called *S-variable*, explained in [53] for instance, translates the previous inequalities into an LMI condition. Indeed, Theorem 1.1 from [53] shows that condition (6.29) is verified if

$$\exists \tau_0, \tau_1, \tau_2, \tau_3 \geq 0, \qquad \bar{\Theta}_N - \tau_0 \Pi_0 - \tau_1 \Pi_1 - \tau_2 \Pi_2 - \tau_3 \Pi_3 < 0.$$

Practical stability in the sense of $\|\cdot\|_{\mathcal{H}}$ Consequently, condition (6.25) implies that $\mathcal{S}$ is an invariant and attractive set for system (6.2). Using (6.10), we then get the following:

$$\left\{\tilde{X}_\phi \in \mathcal{H} \mid \|\tilde{X}_\phi\|_{\mathcal{H}} \leq X_{bound} = V_{max}^{1/2}\varepsilon_1^{-1/2}\right\} \supseteq \mathcal{S},$$

Then, the equilibrium point X_ϕ^∞ of system (6.2) verifies:

$$\forall \eta > 0, \quad \exists T > 0, \quad \forall t \geq T, \quad \|X_\phi - X_\phi^\infty\|_{\mathcal{H}} \leq X_{bound} + \eta. \tag{6.30}$$

Since, by definition of $\|\cdot\|_{\mathcal{H}}$, $|z_1 - \Omega_0| \leq \|\tilde{X}_\phi\|_{\mathcal{H}}$, we get that for $X_{bound} = z_{bound}$ the desired objective (6.22) indeed holds. ♢

6.3.2 On the optimization of z_{bound}

The condition (6.25) is a Bilinear Matrix Inequality (BMI) since P_N, τ_0 and V_{max} are decision variables and it is therefore difficult to get its global optimum. Nevertheless, the following lemma gives a sufficient condition for the existence of a solution to this problem.

Corollary 6.2: Equivalent condition for practical stability [13]

There exist $\tau_0 > 0$ and V_{max} such that Theorem 6.2 holds if and only if there exists $N > 0$ such that LMIs (6.6) and (6.5) are satisfied.
In other words, the equilibrium point of system (6.2) is practically stable if and only if the linear system (6.4) is exponentially stable.

Proof : Note first that expending (6.25) with $\tau_3 = 0$ leads to:

$$\Xi_N = \left[\begin{array}{c|cc} \Theta_{N,\tau_0/2} & \multicolumn{2}{c}{\kappa_{P_N}} \\ \hline & \tau_2 - \tau_1 & 0 \\ \kappa_{P_N}^\top & \multirow{2}{*}{0} & \multirow{2}{*}{$\begin{array}{c}\tau_1 T_{max}^2 - \tau_2 T_{min}^2 \\ -\tau_0 V_{max}\end{array}$} \\ & & \end{array}\right], \tag{6.31}$$

where $\kappa_{P_N} \in \mathbb{R}^{(4+2(N+1))\times 2}$ depends only on P_N.

Proof of sufficiency: Assume there exists $N > 0$ such that LMIs (6.6) and (6.5) are satisfied. Considering $\tau_2 = 0$ and using Schur complement on Ξ_N, we get:

$$\Xi_N \prec 0 \Leftrightarrow \Theta_N + \tau_0(F_N^\top P_N F_N + S_N) - \kappa_{P_N}\begin{bmatrix} -\frac{1}{\tau_1} & 0 \\ 0 & \frac{1}{\tau_1 T_{max}^2 - \tau_0 V_{max}} \end{bmatrix}\kappa_{P_N}^\top \prec 0,$$

with $\tau_0 V_{max} > \tau_1 T_{max}^2$. Since $\Theta_N \prec 0$, considering τ_0 small enough, τ_1 large and $V_{max} > \tau_1\tau_0^{-1}T_{max}^2$ the previous condition is always satisfied and Theorem 6.2 applies.

Proof of necessity: Assume $\Xi_N \prec 0$ and (6.6) holds. Then its first diagonal block must be definite negative. Consequently $\Theta_{N,\tau_0/2} \prec 0$ and, according to Corollary 6.1,

system (6.4) is exponentially stable with a decay-rate of at least $\tau_0/2$. ♢

Remark 6.5: On the optimization of V_{max}

Equation (6.31) shows that the larger τ_0 is, the smaller V_{max} can be. In other words, having the largest τ_0 improves the bound on the functional V_N. We then want τ_0 as large as possible.
The upper-left block of Ξ_N in (6.31) is nothing more than $\Theta_{N,\tau_0/2}$. Then τ_0 is related to the decay-rate of the linear system and using (6.20), we get the following necessary condition:

$$\tau_0 \leq 2\mu_{max}.$$

As seen in the previous section, the projection methodology helps giving a better estimate of the decay-rate and consequently a higher τ_0 and a smaller V_{max}. Thus, the projection methodology helps having a better optimization.

Thanks to Corollary 6.2, the following algorithm should help solving the BMI if Theorem 6.1 is verified.

Algorithm 6.1: Finding the smallest z_{bound}

Assume that equations (6.5) and (6.6) are verified for a given $N \in \mathbb{N}$.

1. Fix $\tau_0 = 2\mu_{max}$ as defined in (6.20).
2. Check that equations (6.5), (6.6) and (6.25) are satisfied for V_{max} a strictly positive decision variable. If this is not the case, then decrease τ_0 and do this step again.
3. Thanks to Corollary 6.2, there exists a τ_0 small enough for which equations (6.5), (6.6) and (6.25) hold. Once τ_0 is found, freeze this value.
4. Since the problem is unbounded, it is possible to fix a variable without loss of generality, let $V_{max} = 10^4$ for instance and solve the following optimization problem:

$$\begin{aligned} \min_{P_N,S,R,Q,\tau_1,\tau_2,\tau_3,\varepsilon_P} \quad & -\varepsilon_P \\ & (6.5), (6.6) \text{ and } (6.25), \\ \text{subject to} \quad & P_N + S_N - \operatorname{diag}(\varepsilon_P, 0_{2N+3}) \succ 0, \\ & R \succeq 0, S \succ 0, Q \succ 0. \end{aligned}$$

5. Then compute $z_{bound} = \sqrt{V_{max}\varepsilon_1^{-1}}$ where ε_1 is defined in (6.10).

This algorithm does converge because of Corollary 6.2. Nevertheless, it is not proven to converge to the minimal value of z_{bound}.

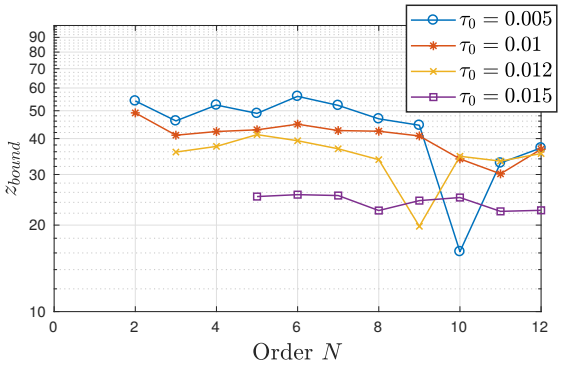

(a) $k_p^\phi = 10^{-3}$, $k_i^\phi = 10$ and $\Omega_0 = 5$ and some values of τ_0. The limit is $z_{bound} = 25$.

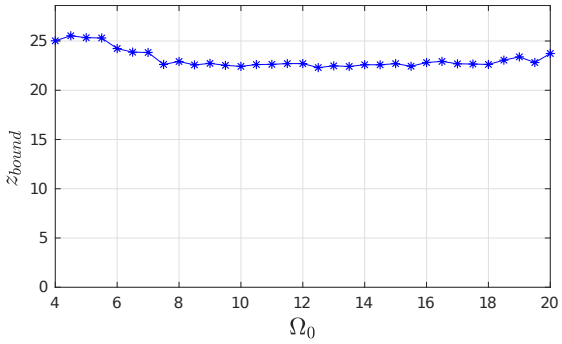

(b) $k_p^\phi = 10^{-3}$, $k_i^\phi = 10$ and $N \in [5, 7]$.

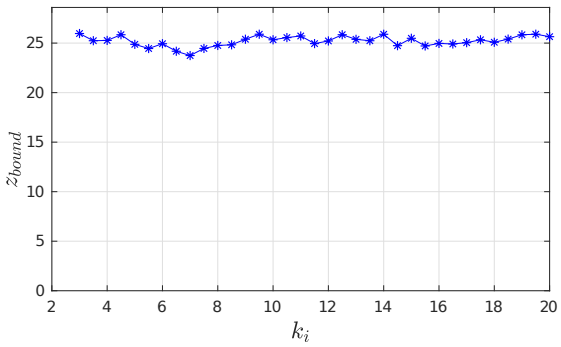

(c) $k_p^\phi = 10^{-3}$, $\Omega_0 = 5$ and $N \in [5, 7]$.

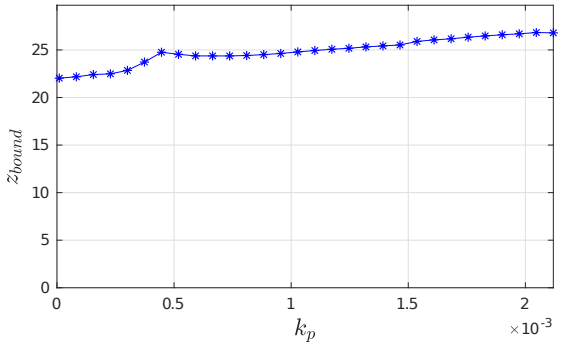

(d) $k_i^\phi = 10$, $\Omega_0 = 5$ and $N \in [5, 7]$.

Figure 6.6: Solution z_{bound} of BMI (6.25) with algorithm 6.1.

Remark 6.6: Objective of the optimization problem

In step 4, we maximize ε_P. This variable is highly related to ε_1. Actually, using (6.19), we have:

$$V_N(\tilde{X}_\phi) \geq \varepsilon_P (z_1 - \Omega_0)^2,$$

and $\varepsilon_1 \leq \varepsilon_P$. For numerical issues, it is better to optimize on ε_P than on ε_1.

6.3.3 Numerical Simulations & discussion

First of all, since Theorem 6.1 applies, then Corollary 6.2 holds and system (6.2) is practically stable. We apply the numerical procedure described in Algorithm 6.1 to find the minimal z_{bound}. Figure 6.6 illustrates the results obtained.

In Figure 6.6a, we study the effect of τ_0 on the optimization process. First note the optimization errors when N gets higher than 8. This is quite common when we use Yalmip with an objective function. Nevertheless, it appears that when τ_0 increases, we indeed get a smaller z_{bound}, which is in accordance with Remark 6.5. We also see that when we increase τ_0, we then need to increase the order N to get feasible LMIs (as noted in Table 6.1).

Figure 6.6b describes the variation of the bound z_{bound} when Ω_0 varies. There is a slight decrease of the bound until $\Omega_0 = 7\text{rad.s}^{-1}$. For the integral gain, we can see that

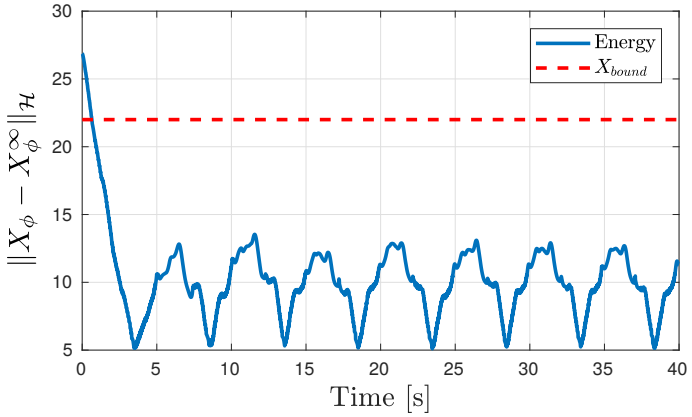

Figure 6.7: Energy of X_ϕ for $k_p^\phi = 10^{-3}$, $k_i^\phi = 10$ and $\Omega_0 = 5$. The initial condition is $\phi^0(x) = (1 + 1.2\sin(2x)) \int_0^x \phi_x^\infty(s)ds$, $\phi^1 = \Omega_0$ and $Z(0) = [z_1^\infty \ z_2^\infty]^\top$.

there is no sensible variations on $z_{bound} \in [24, 26]$ when k_i^ϕ varies between 3 and 20. A similar observation can be made for the dependence on k_p^ϕ. That does mean there is apparently not much influence of the parameters of the PI controller on the oscillations due to the stick-slip. To stay robustly stable against small delays in the loop, as noted in Section 6.2.3, we should consider $0 \leq k_p^\phi \leq 2.1 \cdot 10^{-3}$ which does not offer a large set of choices. It appears that the minimum of z_{bound} is obtained for k_p^ϕ close to 0. Consequently, increasing the gain k_p^ϕ seems not to reduce the stick-slip effect.

As a conclusion, if a PI controller does not weaken the stick-slip effect, the equilibrium point of the controlled system is practically stable. Moreover, it does enable an oscillation around the desired equilibrium point and a local convergence to that point. Figure 6.7 illustrates the previous statement and shows that the obtained bound is not very far from the real bound for this example.

Remark 6.7: Using T_{smooth} instead of T_{nl}

If we use another model for the nonlinearity, we will get different results. For example, using T_{smooth} as defined in (2.3), inequality (6.23b) is not valid anymore, and we must choose $\tau_2 = 0$. The two other sector conditions of (6.23) are still valid. Since there is less decision variable, the new optimization problem cannot lead to a lower z_{bound}. We conducted similar tests with $\tau_2 = 0, k_p^\phi = 10^{-1}, k_i = 10, \Omega_0 = 5$ and $N = 7$. We get $z_{bound} = 328$, which is far more than previously.

This observation makes us think on the importance of the chosen model before analysis. It is clear that T_{nl} is not smooth, and consequently, the solution is less regular than considering T_{smooth}. However, the analysis is better with the discontinuous T_{nl}. There is a compromise to do.

The torsional dynamic has been studied in the two last sections of this chapter. We now move to the axial stability analysis, using slightly different tools.

6.4 Conclusion

This chapter was about the stability analysis of a drilling pipe, controlled by a PI controller. We saw that the projection methodology applied in this specific context helps characterizing the exponential stability of the linear model. Indeed, we can get a precise estimate of the decay-rate. This estimation plays an important role when it comes to evaluate the amplitude of the oscillations due to the stick-slip effect. We saw that the projection methodology gives a bound on the oscillations. This bound is very close to the obtained bound in simulations. Finally, we saw that a PI controller apparently does not weaken the torsional vibrations, but it ensures the stability of the drilling pipe. This brings an answer to Problems 1 and 2.

Applying the projection methodology on a drilling pipe is still at its beginning. This chapter shows that it seems very promising and should help designing controllers. The perspectives and conjectures which arose during this short study are reported in the Perspective section of the following chapter.

7

Conclusion & Perspectives

7.1 General conclusion

This thesis has considered the stability analysis of a coupled ODE/string equation with application to a drilling mechanism. The modern technique of projecting the infinite-dimensional state on the orthonormal basis of Legendre polynomials has been applied to this specific system, leading to very accurate stability tests. This work was organized in five chapters and the following contributions were obtained.

- The first two chapters dealt with a presentation of the model used for a drilling machine and illustrated the coupled ODE/string equation. Moreover, a proof of existence and uniqueness of a solution was provided for the linear case.

- The third chapter focused on applying the input/output stability analysis tools on a toy-example system. It enlightened the fundamental properties of a wave equation and gave some necessary stability conditions. This chapter also proposed to study the system using the quadratic separation framework. The projection methodology has then been adapted in this context, and it appeared that it can be seen as an inequality improvement. Some theoretical contributions on the study of infinite-dimensional systems using quadratic separation were provided. However, the obtained stability test seems not to converge to exact results.

- Chapter 5 aimed at increasing the accuracy of the previous test considering a Lyapunov-based stability analysis. This chapter introduced the projection methodology as an estimation of the infinite-dimensional state in a finite- dimensional basis. The obtained Lyapunov functional candidate was then interpreted as the projection of the complete one on the same basis. The obtained stability tests are therefore more accurate than the previous ones but are more computationally demanding.

- The last chapter made use of the tools developed in Chapter 5 to analyze the behavior of a PI-controlled drillstring. It was shown that the projection methodology helped estimating the decay-rate of the solution to the linear drilling pipe model. The stability analysis of the nonlinear system was conducted using the notion of practical stability. Its accuracy highly depends on the estimated decay-rate of the linear system. Consequently, increasing the number of projections helps having a better bound on the solution of the nonlinear system.

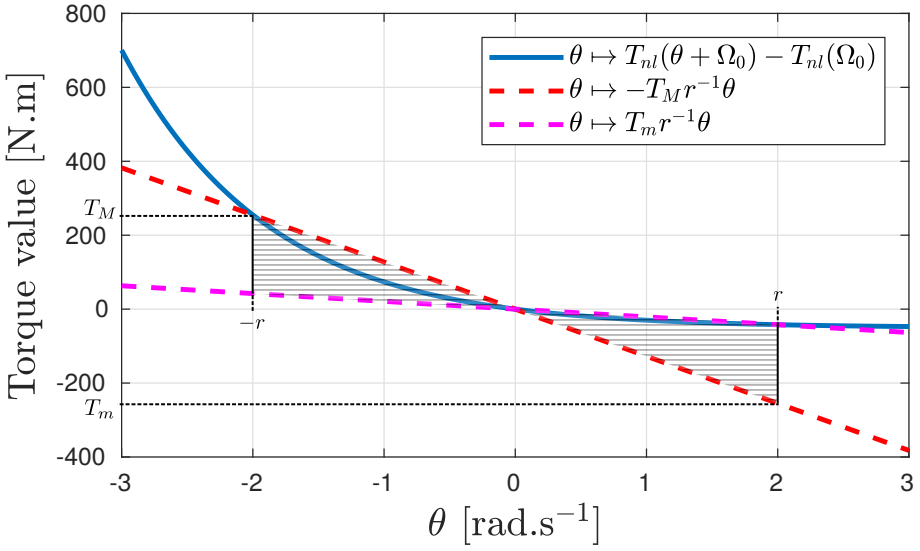

Figure 7.1: Cone-bounded and local sector conditions for $\theta \mapsto T_{nl}(\theta+\Omega_0)-T_{nl}(\Omega_0)$. For that example, we considered $\Omega_0 = 5$ and $r = 2$.

As a conclusion, we can say that the projection methodology is a theoretical tool that helps capturing in an efficient manner the infinite-dimensional properties of coupled systems. We saw that this methodology can be interpreted as an improvement on an inequality, a state extension of a projection of a complete Lyapunov functional.

7.2 Perspectives

The results obtained in the previous chapters show that the projection methodology is a promising tool for the stability analysis of heterogeneous systems. Nevertheless, this is a preliminary work and there are still open questions and new challenges left for future research in this domain. The following subsections give a flavor of what can be investigated at short and long term.

7.2.1 Local and global asymptotic stability of the nonlinear torsional dynamic of a drilling pipe

In Chapter 6, we conducted a global stability analysis. The idea is now to complete this study by doing a local stability analysis. At the core of this idea there is the embedding of the nonlinear term $\theta \in [-r, r] \mapsto T_{nl}(\theta+\Omega_0)-T_{nl}(\Omega_0)$ into a region delimited by linear functions as done in [42, 155] for the saturation. Figure 7.1 shows an example of such a bounding. Then pursuing the same idea than previously with the S-variable approach, we should get a local exponential stability test.

The projection methodology should help having an estimate of the basin of attraction, as done in [144] for a transport equation. When increasing the order, the estimated basin of attraction may converge to the exact one. For a given Ω_0, the aim is then to

get an estimation of the parameter $X_{basin}(\Omega_0) \in \mathbb{R}^+$ such that the following holds:

$$\forall X_\phi^0 \in \mathcal{H} \quad \text{s. t.} \quad \|X_\phi^0 - X_\phi^\infty\|_\mathcal{H} \leq X_{basin}(\Omega_0) \quad \Rightarrow \quad \lim_{t\to\infty} \|X_\phi(t) - X_\phi^\infty\|_\mathcal{H} = 0,$$

where X_ϕ is the solution of system (6.2) with initial condition X_ϕ^0. Of course, the value X_{basin} highly depends on the desired angular speed Ω_0. For a given T_m and T_M as defined in Figure 7.1, a quick analysis of the torque function T_{nl} (as defined in (2.2)) shows that $\lim_{\Omega_0\to\infty} r(\Omega_0) = \infty$, in other words, the region where the encapsulation is true increases with Ω_0. Consequently, we make the following conjecture.

Conjecture 7.1

The volume of the basin of attraction X_{basin} has the following properties:

$$\begin{cases} \forall \Omega_0 > 0, \quad \dfrac{d}{d\Omega_0} X_{basin}(\Omega_0) > 0, \\ \lim\limits_{\Omega_0\to\infty} X_{basin}(\Omega_0) = \infty. \end{cases}$$

If the previous conjecture is verified, that means there exists an Ω_{min} such that for all desired angular speed Ω_0 higher than Ω_{min}, $X_{basin}(\Omega_0)$ is strictly less than $X_{bound}(\Omega_0)$ defined in (6.30) as

$$\forall \eta > 0 \quad \exists T > 0, \quad \forall t \geq T, \qquad \|X_\phi(t) - X_\phi^\infty\|_\mathcal{H} \leq X_{bound}(\Omega_0) + \eta.$$

The attractive and invariant ball $\mathcal{S}_{\Omega_0} = \left\{ X_\phi \in \mathcal{H} \mid \|X_\phi - X_\phi^\infty\|_\mathcal{H} \leq X_{bound} \right\}$ determined using the notion of practical stability in Chapter 6 appears to be slightly decreasing with Ω_0, we get then $X_{bound}(\Omega_0) \leq X_{bound}(0^+) \simeq 25$. Then, there exists Ω_{min} such that for $\Omega_0 > \Omega_{min}$, the ball $\mathcal{S}_{\Omega_0}$ is included in the basin of attraction of (6.2) (see Figure 7.2), and the system is globally asymptotically stable. This would be in accordance with the result obtained using the describing function analysis conducted in Appendix D (see Figure D.6).

Conjecture 7.1 leads to the possible use a controller which makes the solution moves from a basin of attraction to another, ensuring the global asymptotic stability, as done for linear parameter varying systems in [30, 137] for instance. That would bring a rigorous proof of what is done in practice as noted in [133, Chap. 8] or [10].

7.2.2 On a more general coupled ODE/PDE system

Along this thesis, we used the quadratic separation framework or Lyapunov-based arguments to conclude on the stability of a coupled ODE/string equation system. There is another famous framework used to prove input/output stability which was not used here. This other framework is highly related to quadratic separation and uses Integral Quadratic Constraints (IQCs) to encapsulate the uncertain operator [103, 163]. During my stay in Stuttgart with Professor Carsten Scherer, we considered the case where the uncertainty is an infinite-dimensional dynamic, defined in the sequel.

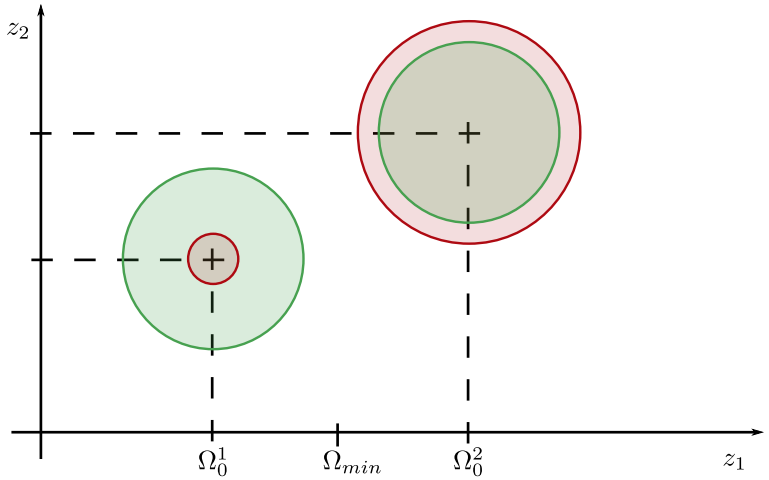

Figure 7.2: This schematic represents the attractive and invariant ball (in green) and the basin of attraction (in red) of system (6.2) for two values of desired angular speed $\Omega_0^1 < \Omega_{min} < \Omega_0^2$. This is a projection on the plane (z_1, z_2).

We are interested now in the more general coupled ODE/PDE system described in Figure 7.3 and where the uncertainty follows these equations:

$$\begin{cases} \mathscr{A} z(x,t) = \sum_{k=0}^{m} F_k \partial_x^{(k)} z(x,t), & t > 0, \quad x \in (0,1), \\ w(t) = L\mathscr{B}_m(z)(t), & t > 0, \\ z(x,0) = 0_{l,1}, & x \in [0,1], \end{cases} \tag{7.1}$$

where $z(x,t) \in \mathbb{R}^l$ and $L \in \mathbb{R}^{r \times 2ml}$. The domain of the operator $\mathscr{A}$ is:

$$\mathscr{D}(\mathscr{A}) = \{ z \in H^m(0,1) \mid K_{\mathscr{B}} \mathscr{B}_m(z) = K_y y \}, \tag{7.2}$$

where $K_{\mathscr{B}} \in \mathbb{R}^{ml \times 2ml}$ has full-rank, $K_y \in \mathbb{R}^{ml \times p}$ and

$$\mathscr{B}_m(z)(t) = \operatorname{col}\left(z(0,t),\ z(1,t), \ldots, \partial_x^{(m)} z(0,t),\ \partial_x^{(m)} z(1,t) \right),$$

with $m \in \mathbb{N}$, $m > 0$ and $F_m \neq 0$. The operator $\mathscr{B}_m$ is similar to the trace operator as defined in [28], for instance, whose output is the values of the signal and its derivatives at the two boundary points. The condition expressed by $K_{\mathscr{B}} \mathscr{B}_m(z) = K_y y$ reflects the boundary conditions. A similar but even more general description of this kind of uncertainty appears in [3].

Let the new system described in Figure 7.4 and assume that $\| \cdot \|_{\mathscr{D}(\mathscr{A})}$ is a semi-norm on $\mathscr{D}(\mathscr{A})$. The definition of an IQC with terminal cost Z introduced in [138] for finite-dimensional systems can be extended for an infinite-dimensional state z as:

$$\forall T > 0, \qquad \int_0^T \psi_z(t)^\top M \psi_z(t) dt + \xi^\top(T) Z \xi(T) \geq \varepsilon \| z(T, \cdot) \|^2_{\mathscr{D}(\mathscr{A})}. \tag{7.3}$$

where $\varepsilon > 0$, M and Z are not signed matrices of appropriate dimensions. ξ is the state of filter Ψ_z and ψ_z is its output. An IQC relates then the energy spent in the system

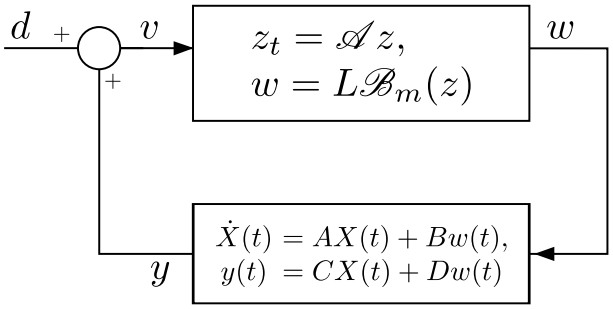

Figure 7.3: General coupled ODE/PDE system.

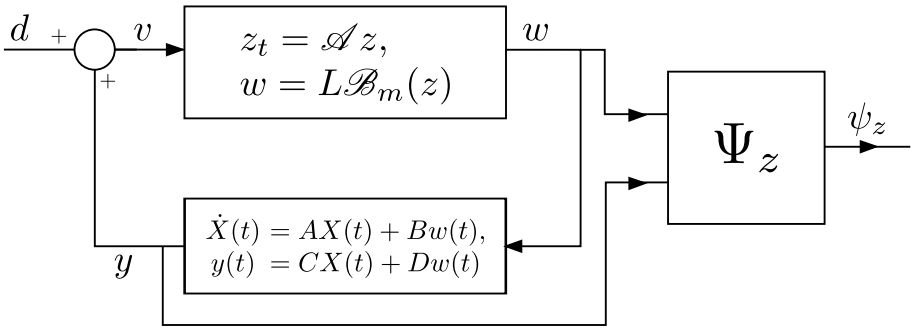

Figure 7.4: General coupled ODE/PDE system within the IQC framework.

between 0 and T and the remaining energy at time T. This is then a kind of dissipation inequality.

This framework is well adapted to our study since it proposes a new interpretation of the projection methodology. Indeed, the filter Ψ_z can be seen as the generator of the projection coefficients of z and then ψ_z is the collection of the projection coefficients. Then inequality (7.3) can be seen as a time integration of Bessel inequality (Proposition E.5).

The main advantage of this framework lies in its elegant formulation which enables a very simple expression of the stability in terms of LMIs. The current work aims at expending the result obtained in Theorem 3 from [138] to infinite-dimensional systems. Nevertheless, the stability analysis of a very general class of systems such as (7.1) seems idyllic and it appears rapidly that each class of equations[1] must be explored independently. This is on going work.

7.2.3 Other perspectives

The two previous points were deeply developed during my PhD but there are other perspectives, which are of main interest as well and would be relevant for future work. About the general coupled ODE/PDE system, the following axes are proposed.

On the wellposedness: the notion of wellposedness developed in Definition 4.3 is highly related to the notion of wellposedness in Hadamar sense [41, p. 15] which

[1] A class of equation is defined by its degree m.

requires existence, uniqueness and continuous dependency on the initial state. We can investigate under which condition a general coupled ODE/PDE system as in Figure 7.3 can be translated into (4.16).

Move from stability analysis to controller design: we derived in this manuscript LMIs, which assess stability of a given coupled ODE/string equation system. The idea would be to design controllers using the same methodology. Nevertheless, transforming analysis LMIs to control design LMIs usually leads to conservative conditions. In [12, 15], I have developed algorithms that perform well for time-delay systems. We can then hope that it is possible to extend them to PDEs.

Observer of the projection coefficients: following the same vein than previously, it would be interesting to develop more advanced controllers, which make use of the projection coefficients. Since these coefficients are time-varying, the idea would be to use an observer as in [139]. This can be considered as a finite-dimensional observer of an infinite-dimensional system. Such a tool would help building finite-dimensional controllers for coupled system by discretizing a backstepping control law.

For the specific problem of drilling, the following avenues are given:

Input to state stability and position tracking for the axial dynamic: in Chapter 6, the derived controllers ensure a convergence in speed of the torsional system, but to prevent any axial compression, a similar controller can be used, leading to an input to state stability of the axial dynamic with respect to a perturbation generated by the torque at the bottom. This does work well since the axial system is in cascade with the torsional one. Nevertheless, a position tracking would also be necessary. This requires a control on $\psi(0, \cdot)$ as investigated in [134] for instance.

Using a DOSKIL controller: in [32], a more advance controller using an observer is used to suppress the stick-slip phenomenon on a finite-dimensional model. The idea would be to use this model as an observer to estimate the oscillations at the bottom of the pipe and then use a modified PI controller to reduce the vibrations.

Stability analysis of other controllers: as noted in Chapter 6, there already exist many controllers for a drilling system. Nevertheless, it is difficult to compare them. It would be interesting to use the methodology derived in this manuscript to draw a comparison of the efficiency of each controller.

Coupling with backstepping: many controllers for a drilling pipe are issued from the so-called backstepping [21, 27, 87, 132]. This manuscript did not propose any comparisons nor simulations with a backstepping controlled drillstring since we focused on stability analysis. The aim is not to replace backstepping but one can imagine merging these two methodologies to synthesize controllers with the desired performances. Indeed, the main idea behind backstepping is to find a map between the original system and a stable target system. So far, the target system is chosen quite simple to be sure that it is stable with some robustness margin. Using the projection methodology would help considering more complex target systems with more desirable properties.

A

Appendix to Chapter 3

This appendix is devoted to the proof of Theorem 3.1, which is a direct consequence of Proposition 3.2. The first part of this proof aims at deriving equation (3.6) and the second part is about proving (3.7).

Quasi-dissipativity of system (3.4)

According to Proposition 3.2, we first need to show that inequality (3.6) holds for $w \in \mathbb{R}$. What follows is an adaptation of [20, Theorem A.1] and [56].

First, we introduce the following scalar product[1] on $\mathscr{D}(\mathscr{A})$ for $\varepsilon \in (0,1)$:

$$\left\langle \begin{bmatrix} X \\ u \\ v \end{bmatrix}, \begin{bmatrix} \bar{X} \\ \bar{u} \\ \bar{v} \end{bmatrix} \right\rangle_{\mathscr{D}(\mathscr{A})} = X^\top \bar{X} + \langle u, \bar{u} \rangle_{L^2} + \langle \zeta_+, \bar{\zeta}_+ \rangle_{L^2} + (1-\varepsilon)\langle \zeta_-, \bar{\zeta}_- \rangle_{L^2},$$

where, as in [39], $\zeta_+, \zeta_-, \bar{\zeta}_+$ and $\bar{\zeta}_-$ are the so-called Riemann invariants:

$$\begin{aligned} \zeta_+ &= v + cu_x, & \bar{\zeta}_+ &= \bar{v} + c\bar{u}_x, \\ \zeta_- &= v - cu_x, & \bar{\zeta}_- &= \bar{v} - c\bar{u}_x. \end{aligned}$$

Note that the norm derived from this inner product is as follows:

$$\|(X,u,v)\|^2_{\mathscr{D}(\mathscr{A})} = X^\top X + \|u\|^2_{L^2} + (2-\varepsilon)\left(c^2\|u_x\|^2_{L^2} + \|v\|^2_{L^2}\right) - 2\varepsilon\langle v, cu_x\rangle_{L^2}.$$

To prove quasi-dissipativity, we use the following notation:

$$\begin{bmatrix} \bar{X} \\ \bar{u} \\ \bar{v} \end{bmatrix} = \mathscr{A} \begin{bmatrix} X \\ u \\ v \end{bmatrix} = \begin{bmatrix} AX + Bu(1) \\ v \\ c^2 u_{xx} \end{bmatrix}.$$

Consequently, $\bar{\zeta}_+ = c\partial_x \zeta_+$ and $\bar{\zeta}_- = -c\partial_x \zeta_-$. Note now that for $(X,u,v) \in \mathscr{D}(\mathscr{A})$, we get $u(1) = \chi + KX$ because $u(0) = KX$ with the notation $\chi = \int_0^1 u_x(x)dx$. Consequently, the following holds:

$$\begin{aligned} \left\langle \mathscr{A} \begin{bmatrix} X \\ u \\ v \end{bmatrix}, \begin{bmatrix} X \\ u \\ v \end{bmatrix} \right\rangle_{\mathscr{D}(\mathscr{A})} &= X^\top (A+BK)^\top X + \chi^\top B^\top X + \langle u, v \rangle_{L^2} \\ &\quad + c\int_0^1 \left(\partial_x \zeta_+^\top(x)\zeta_+(x) - (1-\varepsilon)\partial_x \zeta_-^\top(x)\zeta_-(x)\right) dx. \end{aligned}$$

[1] Since it is related to the canonical scalar product on $\mathbb{R}^n \times \mathbb{X}$, we indeed get that $\langle \cdot, \cdot \rangle_{\mathscr{D}(\mathscr{A})}$ is a symmetric positive definite bilinear form on $\mathscr{D}(\mathscr{A})$ for $\varepsilon < 1$.

A direct integration leads to:

$$\left\langle \mathscr{A}\left[\begin{smallmatrix} X \\ u \\ v \end{smallmatrix}\right], \left[\begin{smallmatrix} X \\ u \\ v \end{smallmatrix}\right] \right\rangle_{\mathscr{D}(\mathscr{A})} = \frac{1}{2} X^\top \operatorname{He}(A+BK)X + \frac{1}{2}\operatorname{He}\left(\chi^\top B^\top X\right) + \langle u, v\rangle_{L^2} + \frac{c}{2}\left[\zeta_+^\top(x)\zeta_+(x) - (1-\varepsilon)\zeta_-^\top(x)\zeta_-(x)\right]_0^1.$$

Introduce the variable $\xi(x) = \operatorname{col}(X, \chi, u(x), v(x), cu_x(0), v(1))$ for $x \in [0,1]$, the boundary conditions writes as:

$$\begin{aligned}
\zeta_+(0) &= K(A+BK)X + KB\chi + cu_x(0) = H_+\xi(x), \quad \zeta_+(1) = (1-cc_0)v(1) = G_+\xi(x),\\
\zeta_-(0) &= K(A+BK)X + KB\chi - cu_x(0) = H_-\xi(x), \quad \zeta_-(1) = (1+cc_0)v(1) = G_-\xi(x),
\end{aligned}$$

where

$$\begin{aligned}
H_+ &= \begin{bmatrix} K(A+BK) & KB & 0 & 0 & 1 & 0 \end{bmatrix}, \quad G_+ = \begin{bmatrix} 0 & 0 & 0 & 0 & 0 & (1-cc_0) \end{bmatrix},\\
H_- &= \begin{bmatrix} K(A+BK) & KB & 0 & 0 & -1 & 0 \end{bmatrix}, \quad G_- = \begin{bmatrix} 0 & 0 & 0 & 0 & 0 & (1+cc_0) \end{bmatrix}.
\end{aligned}$$

Finally, we get:

$$\begin{aligned}
\left\langle \mathscr{A}\left[\begin{smallmatrix} X \\ u \\ v \end{smallmatrix}\right], \left[\begin{smallmatrix} X \\ u \\ v \end{smallmatrix}\right] \right\rangle_{\mathscr{D}(\mathscr{A})} &= \frac{1}{2}\int_0^1 \begin{bmatrix} X \\ \chi \\ u(x) \\ v(x) \end{bmatrix}^\top \begin{bmatrix} \operatorname{He}(A+BK) & B & 0 & 0 \\ B^\top & 0 & 0 & 0 \\ 0 & 0 & 0 & I \\ 0 & 0 & I & 0 \end{bmatrix} \begin{bmatrix} X \\ \chi \\ u(x) \\ v(x) \end{bmatrix} \\
&\qquad + c\,\xi^\top(x)\left(G_+^\top G_+ - H_+^\top H_+\right)\xi^\top(x) \\
&\qquad - (1-\varepsilon)c\,\xi^\top(x)\left(G_-^\top G_- - H_-^\top H_-\right)\xi(x)dx. \\
&= \int_0^1 \xi^\top(x)\Pi\xi(x)dx,
\end{aligned} \tag{A.1}$$

where $\Pi = \left[\begin{smallmatrix} \Pi_{11} & \Pi_{12} \\ \Pi_{12}^\top & \Pi_{22} \end{smallmatrix}\right]$, with Π_{11} and Π_{12} are symmetric matrices which are not needed in the sequel but Π_{22} has the following form:

$$\Pi_{22} = \frac{c}{2}\begin{bmatrix} -\varepsilon & 0 \\ 0 & \varepsilon(1+cc_0)^2 - 4cc_0 \end{bmatrix}.$$

Picking a small enough ε ensures that Π_{22} is negative definite. Consequently, using Schur complement (Proposition E.1), we get:

$$\begin{bmatrix} \Pi_{11} - \Gamma(w) & \Pi_{12} \\ \Pi_{12}^\top & \Pi_{22} \end{bmatrix} \prec 0 \Leftrightarrow \Pi_{11} - \Gamma(w) - \Pi_{12}\Pi_{22}^{-1}\Pi_{12}^\top \prec 0, \tag{A.2}$$

where

$$\Gamma(w) = w\operatorname{diag}\begin{bmatrix} I_n & 0 & 0 & 0 \\ 0 & 2(1-\varepsilon)c^2 & 0 & 0 \\ 0 & 0 & 1 & 0 \\ 0 & 0 & 0 & 2(1-\varepsilon) \end{bmatrix}.$$

Assuming again that ε is sufficiently small so that, for $w > 0$, we get $\Gamma \succ 0$, then there always exists w large enough such that (A.2) holds. In other words, for w large enough, $\Pi \prec \operatorname{diag}(\Gamma(w), 0_2)$ and (A.1) becomes:

$$\left\langle \mathscr{A} \begin{bmatrix} X \\ u \\ v \end{bmatrix}, \begin{bmatrix} X \\ u \\ v \end{bmatrix} \right\rangle_{\mathscr{D}(\mathscr{A})} = \int_0^1 \xi^\top(x)\Pi\xi(x)dx \leq \int_0^1 \xi^\top(x)\Gamma(w)\xi(x)dx.$$

Consequently, there exists $w > 0$ such that the following holds:

$$\left\langle \mathscr{A} \begin{bmatrix} X \\ u \\ v \end{bmatrix}, \begin{bmatrix} X \\ u \\ v \end{bmatrix} \right\rangle_{\mathscr{D}(\mathscr{A})} \leq w \left\{ X^\top X + \|u\|_{L^2}^2 + 2(1-\varepsilon)\left(\|v\|_{L^2}^2 + c^2\chi^\top\chi\right)\right\}.$$

Using Jensen inequality E.3 implies that $\chi^\top\chi \leq \|u_x\|_{L^2}^2$, that leads to:

$$\begin{aligned}\left\langle \mathscr{A} \begin{bmatrix} X \\ u \\ v \end{bmatrix}, \begin{bmatrix} X \\ u \\ v \end{bmatrix} \right\rangle_{\mathscr{D}(\mathscr{A})} &\leq w \left\{ X^\top X + \|u\|_{L^2}^2 + (2-\varepsilon)\left(\|v\|_{L^2}^2 + c^2\|u_x\|_{L^2}^2\right)\right\} \\ &\qquad -w\varepsilon\left(\|v\|_{L^2}^2 + c^2\|u_x\|_{L^2}^2\right) \\ &\leq w\|(X,u,v)\|_{\mathscr{D}(\mathscr{A})}^2 - w\varepsilon\left(\|v\|_{L^2}^2 + c^2\|u_x\|_{L^2}^2 - 2|\langle v, cu_x\rangle_{L^2}|\right).\end{aligned}$$

Noting that $\|v - cu_x\|_{L^2}^2 = \|v\|_{L^2}^2 - 2\langle v, cu_x\rangle_{L^2} + c^2\|u_x\|_{L^2}^2 \geq 0$, the previous inequality implies the following:

$$\exists w \in \mathbb{R}, \quad \left\langle \mathscr{A} \begin{bmatrix} X \\ u \\ v \end{bmatrix}, \begin{bmatrix} X \\ u \\ v \end{bmatrix} \right\rangle_{\mathscr{D}(\mathscr{A})} \leq w\|(X,u,v)\|_{\mathscr{D}(\mathscr{A})}^2,$$

and the system is quasi-dissipative.

The range condition for system (3.4)

We want to show that the following holds:

$$\exists s_0 > 0, \forall s > s_0, \quad \left\{(sI - \mathscr{A}) \begin{bmatrix} X \\ u \\ v \end{bmatrix} \mid \begin{bmatrix} X \\ u \\ v \end{bmatrix} \in \mathscr{D}(\mathscr{A})\right\} = \mathbb{R}^n \times \mathbb{X}. \tag{A.3}$$

We will proceed by double inclusion.

1. Since $\mathscr{D}(\mathscr{A}) \subset \mathbb{R}^n \times \mathbb{X}$, we get the following:

$$\forall s > 0, \quad \left\{(sI - \mathscr{A}) \begin{bmatrix} X \\ u \\ v \end{bmatrix} \mid \begin{bmatrix} X \\ u \\ v \end{bmatrix} \in \mathscr{D}(\mathscr{A})\right\} \subseteq \mathbb{R}^n \times \mathbb{X}. \tag{A.4}$$

2. We want now to prove that

$$\exists s_0 > 0, \forall s > s_0, \quad \left\{(sI - \mathscr{A}) \begin{bmatrix} X \\ u \\ v \end{bmatrix} \mid \begin{bmatrix} X \\ u \\ v \end{bmatrix} \in \mathscr{D}(\mathscr{A})\right\} \supseteq \mathbb{R}^n \times \mathbb{X}. \tag{A.5}$$

We follow the same lines as in [19, 107].
Let $(r, g, h) \in \mathbb{R}^n \times \mathbb{X}$, we assume that there exists $(s, X, u, v) \in \mathbb{R}^+ \times \mathscr{D}(\mathscr{A})$ for which the following set of equations is verified:

$$sX - AX - Bu(1) = r, \tag{A.6a}$$
$$su(x) - v(x) = g(x), \tag{A.6b}$$
$$sv(x) - c^2u_{xx}(x) = h(x), \tag{A.6c}$$

for all $x \in [0,1]$. Equations (A.6b), (A.6c) give:

$$\forall x \in (0,1), \quad u(x) = k_1 \exp(sc^{-1}x) + k_2 \exp(-sc^{-1}x) + G(x)$$

where $G(x) = \int_0^x \frac{sg(\nu)+h(\nu)}{sc} \sinh\left(\frac{s}{c}(\nu - x)\right) d\nu \in H^2$ and $k_1, k_2 \in \mathbb{R}$ are constants to be determined. Using the boundary conditions $u(0) = KX$, we get the following equivalent system for all $x \in [0,1]$:

$$sX - AX - Bu(1) = r, \tag{A.7a}$$
$$u(x) = 2k_1 \sinh(sc^{-1}x) + KXe^{-sc^{-1}x} + G(x), \tag{A.7b}$$
$$su(x) - v(x) = g(x). \tag{A.7c}$$

Taking its derivative with respect to x at the boundary $x = 1$, we get:

$$u_x(1) = 2sc^{-1}k_1 \cosh(sc^{-1}) - sc^{-1}KXe^{-sc^{-1}} + G_x(1),$$

We also have $u_x(1) + c_0 v(1) = 0$, leading to a uniquely defined $k_1 \in \mathbb{R}$. Then, we get:

$$u(1) = G_2 + KXf(sc^{-1})$$

with $G_2 \in \mathbb{R}$ and $f(y) = \left(1 - \frac{(cc_0-1)\sinh(y)}{2(\cosh(y)+cc_0\sinh(y))}\right) e^{-y}$. Then using (A.6a), we get:

$$\left(sI_n - (A + BKf(sc^{-1}))\right) X = r + BG_2.$$

Since f is continuous, $f(0) = 1$ and $\lim_{y\to\infty} f(y) = 0$ then f is bounded over $\mathbb{R}^+$ and there exist $(f_{min}, f_{max}) \in \mathbb{R}^2$ such that $f(y) \in [f_{min}, f_{max}]$ for $y \in \mathbb{R}^+$. Let

$$s_0 = \max_{f_m \in [f_{min}, f_{max}]} \lambda_{max}(A + f_m BK),$$

where $\lambda_{max}(M)$ for $M \in \mathbb{R}^{n\times n}$ is the maximum eigenvalue of M in terms of modulus. s_0 is consequently the modulus of the highest eigenvalue of $A + BKf(sc^{-1})$ for $s > 0$. We then get:

$$\forall s > s_0, \quad \det\left(sI_n - (A + BKf(sc^{-1}))\right) \neq 0.$$

Consequently, for all $s > s_0$, $sI_n - (A + BKf(sc^{-1}))$ is invertible and we get:

$$X = \left(sI_n - (A + BKf(sc^{-1}))\right)^{-1} (r + BG_2), \tag{A.8a}$$
$$u(x) = 2k_1 \sinh(sc^{-1}x) + KXe^{-sc^{-1}x} + G(x), \tag{A.8b}$$
$$v(x) = su(x) - g(x), \tag{A.8c}$$

and $(X, u, v) \in \mathscr{D}(\mathscr{A})$. The assertion is then proved and (A.3) holds.

B

Appendix to Chapter 4

B.1 Proof of Theorem 4.3

First of all, since $\mathcal{E}_\circ$ and $\mathcal{E}_e$ are full column rank, then there exist $\mathcal{E}_\circ^+$, $\mathcal{E}_e^+$ and $\mathcal{E}_2^+$ which are left pseudo-inverses of $\mathcal{E}_\circ$, $\mathcal{E}_e$ and $\mathcal{E}_2$, respectively. We then get that there exists $\mathcal{E}_1^+$ such that the following holds:

$$\mathcal{E}_e^+ = \begin{bmatrix} \mathcal{E}_\circ^+ & 0 \\ \mathcal{E}_1^+ & \mathcal{E}_2^+ \end{bmatrix}.$$

Using Proposition 4.3, the wellposedness of Σ_e is equivalent to

$$\forall s \in \bar{\mathbb{C}}^+ \backslash \{0\}, \quad \det\left(\begin{bmatrix} I & -\mathcal{E}_e^+\mathcal{A}_e \\ -\nabla_e(s) & I \end{bmatrix}\right) \neq 0.$$

The above inequality is equivalent to

$$\forall s \in \bar{\mathbb{C}}^+ \backslash \{0\}, \quad \det\left(\left[\begin{array}{cc|c|c} \multicolumn{2}{c|}{\multirow{2}{*}{I}} & -\mathcal{E}_\circ^+\mathcal{A}_\circ & 0 \\ \cline{3-4} \multicolumn{2}{c|}{} & -\mathcal{E}_1^+\mathcal{A}_\circ^+ - \mathcal{E}_2^+\mathcal{A}_1 & -\mathcal{E}_2^+\mathcal{A}_2 \\ \hline -\nabla_\circ & 0 & \multicolumn{2}{c}{\multirow{2}{*}{I}} \\ \cline{1-2} -\nabla_1 & -\nabla_2 & \multicolumn{2}{c}{} \end{array}\right]\right) \neq 0.$$

Inverting columns 2 and 3 and lines 2 and 3 leads to:

$$\forall s \in \bar{\mathbb{C}}^+ \backslash \{0\}, \quad \det\left(\left[\begin{array}{cc|cc} I & -\mathcal{E}_\circ^+\mathcal{A}_\circ & \multicolumn{2}{c}{\multirow{2}{*}{0}} \\ -\nabla_\circ & I & \multicolumn{2}{c}{} \\ \hline 0 & -\mathcal{E}_1^+\mathcal{A}_\circ^+ - \mathcal{E}_2^+\mathcal{A}_1 & I & -\mathcal{E}_2^+\mathcal{A}_2 \\ -\nabla_1 & 0 & -\nabla_2 & I \end{array}\right]\right) \neq 0.$$

Using the block-determinant formula, we get that:

$$\forall s \in \bar{\mathbb{C}}^+ \backslash \{0\}, \quad \begin{cases} \det\left(\begin{bmatrix} I & -\mathcal{E}_\circ^+\mathcal{A}_\circ \\ -\nabla_\circ & I \end{bmatrix}\right) \neq 0, \\ \det\left(\begin{bmatrix} I & -\mathcal{E}_2^+\mathcal{A}_2 \\ -\nabla_2 & I \end{bmatrix}\right) \neq 0. \end{cases}$$

Using Proposition 4.3, we get that $\Sigma(\mathcal{E}_\circ, \mathcal{A}_\circ, \nabla_\circ)$ is wellposed.

B.2 Proof of Proposition 4.4

Let us first recall the transfer function $\mathcal{F}$ (defined in (4.5)) can be written as follows:

$$\mathcal{F}(s) = \frac{KB}{sI - A - BK\delta(s)e^{-\tau s}}.$$

Assume that the system is wellposed. In light of Proposition 4.3, we get:

$$\forall s \in \bar{\mathbb{C}}^+\backslash\{0\}, \qquad \det\left(\begin{bmatrix} I_{n+2} & -\mathcal{A}_\oplus \\ -\nabla_\oplus(s) & I_{n+2} \end{bmatrix}\right) \neq 0.$$

Proposition E.2 translates the previous expression into its equivalent:

$$\forall s \in \bar{\mathbb{C}}^+\backslash\{0\}, \qquad \det\left(I_{n+2} - \nabla_\oplus(s)\mathcal{A}_\oplus\right) \neq 0. \tag{B.1}$$

Expanding (B.1) leads to the following:

$$\forall s \in \bar{\mathbb{C}}^+\backslash\{0\}, \qquad \det\left(\begin{bmatrix} I_n - s^{-1}A & 0_{n,1} & -s^{-1}B \\ -Ke^{-\tau s} & 1 & 0 \\ 0_{1,n} & -\delta(s) & 1 \end{bmatrix}\right) \neq 0.$$

Define the following matrices $T_{left}(s) = \begin{bmatrix} sI_n & 0_{n,2} \\ 0_{2,n} & I_2 \end{bmatrix}$ and $T_{right}(s) = \begin{bmatrix} I_n & 0_{n,1} & 0 \\ 0_{1,n} & 1 & 0 \\ 0_{1,n} & \delta(s) & 1 \end{bmatrix}$. Since T_{left} and T_{right} are invertible for all $s \in \bar{\mathbb{C}}^+\backslash\{0\}$, we get that (B.1) is equivalent to:

$$\forall s \in \bar{\mathbb{C}}^+\backslash\{0\}, \qquad \det\left(T_{left}(s)\begin{bmatrix} sI_n - A & 0_{n,1} & -B \\ -Ke^{-\tau s} & 1 & 0 \\ 0_{1,n} & -\delta(s) & 1 \end{bmatrix} T_{right}(s)\right) \neq 0.$$

Expending the previous expression and using the block-determinant formula lead to:

$$\forall s \in \bar{\mathbb{C}}^+\backslash\{0\}, \qquad \det\left(\begin{bmatrix} sI_n - A & -B\delta(s) \\ -Ke^{-\tau s} & 1 \end{bmatrix}\right) \neq 0.$$

Again, Proposition E.2 allows us to write the equivalent formulation that is:

$$\forall s \in \bar{\mathbb{C}}^+\backslash\{0\}, \qquad \det\left(sI_n - A - BK\delta(s)e^{-\tau s}\right) \neq 0.$$

Since c_0 is assumed to be strictly positive, in order to fulfill the assumptions of Corollary 4.1, it remains to ensure that the determinant is also not zero at $s = 0$, which is done by assumption.

C

Appendix to Chapter 5

C.1 Differentiation of the extended state

The differentiation of the vector $\mathrm{col}(\mathfrak{X}_0, \dots, \mathfrak{X}_N)$ is not straightforward. The following lemma, taken from [19] deals with this issue.

Lemma C.1

For any function $\chi \in L^2$, the following expression holds for any N in $\mathbb{N}$:

$$\frac{d}{dt}\begin{bmatrix}\mathfrak{x}_0(t)\\ \vdots \\ \mathfrak{x}_N(t)\end{bmatrix} = c\left(\mathbb{1}_N\chi(1,t) - \bar{\mathbb{1}}_N\chi(0,t) - L_N\begin{bmatrix}\mathfrak{x}_0(t)\\ \vdots \\ \mathfrak{x}_N(t)\end{bmatrix}\right).$$

Proof : For a given integer k in $\mathbb{N}$, differentiating $\mathfrak{X}_k$ along the trajectories of (5.2) yields $\dot{\mathfrak{X}}_k(t) = c\int_0^1 \chi_x(x,t)\mathcal{L}_k(x)dx$. Then, integrating by parts, we get:

$$\dot{\mathfrak{X}}_k(t) = c\left([\chi(x)\mathcal{L}_k(x)]_0^1 - \int_0^1 \chi(x)\mathcal{L}_k'(x)dx\right).$$

Use the properties of the Legendre polynomials given in Definition E.1 yields:

$$\dot{\mathfrak{X}}_k(t) = c\Big(\chi(1,t) - (-1)^k\chi(0,t)\Big) - c\sum_{j=0}^{N}\ell_{k,j}\mathfrak{X}_j(t),$$

where the coefficient $\ell_{k,j}$ are defined in equation (E.3). The end of the proof consists in gathering the previous expression from $k=0$ to $k=N$. ♢

C.2 Towards a lower complexity of Theorem 5.3

This section is dedicated to a slightly different formulation of Theorem 5.3 which helps getting similar results with a more flexible complexity. The theorem is as follows.

Theorem C.1: Extended stability analysis of (5.2)

Let $N_1, N_2 \in \mathbb{N}$. If there exist $P_{N_1,N_2} \in \mathbb{S}^{n+N_1+N_2+2}$ and $S, R \in \mathbb{S}^2_{++}$ and $\tilde{s}, \bar{s} \in \mathbb{R}^+$ such that

$$\begin{cases}\Xi_{N_1,N_2} = P_{N_1,N_2} + \tilde{S}_{N_1} + \bar{S}_{N_2} \succ 0,\\ S - \tilde{S} - \bar{S} \succeq 0,\\ \Theta_{N_1,N_2} = \mathrm{He}\left(D_{N_1,N_2}^\top P_{N_1,N_2} F_{N_1,N_2}\right) + c\left(H_N^\top(S+R)H_N - G_N^\top S G_N - \tilde{R}_N\right) \prec 0,\end{cases}$$

with the notations of Theorem 5.3 and

$$
\begin{aligned}
F_{N_1,N_2} &= \begin{bmatrix} 0_{n,2} & I_n & 0_{n,2(N+2)} \\ 0_{N_1+1,2} & 0_{N_1+1,n} & \tilde{I}_{N_1,N} \\ 0_{N_2+1,2} & 0_{N_2+1,n} & \tilde{I}_{N_2,N} \end{bmatrix}, \qquad D_{N_1,N_2} = \begin{bmatrix} J_N \\ \tilde{I}_{N_1,N} M_N \\ \tilde{I}_{N_2,N} M_N \end{bmatrix}, \\
\tilde{I}_{N^*,N} &= \begin{bmatrix} I_{N^*+1} & 0_{N^*+1,N-N^*} \end{bmatrix}, \\
\tilde{S}_{N_1} &= \tilde{s}\,\mathrm{diag}(0_n, 1, 3, \ldots, 2N_1+1, 0_{N_2+1}), \qquad \tilde{S} = \tilde{s} \begin{bmatrix} 1 & -1 \\ -1 & 1 \end{bmatrix}, \\
\bar{S}_{N_2} &= \bar{s}\,\mathrm{diag}(0_{n+N_1+1}, 1, 3, \ldots, 2N_2+1), \qquad \bar{S} = \bar{s} \begin{bmatrix} 1 & 1 \\ 1 & 1 \end{bmatrix},
\end{aligned}
\tag{C.1}
$$

then system (5.2) is exponentially stable.

Proof : The idea is very simple and lies in a different estimation of X_∞ as presented in Table 5.1. Expressed in the original variables u, the coefficients related to the projections of u_t and cu_x are defined as follows for $k \in \mathbb{N}$:

$$
\mathfrak{U}_{x,k} = \begin{bmatrix} 1 & -1 \end{bmatrix} \mathfrak{X}_k, \qquad \mathfrak{U}_{t,k} = \begin{bmatrix} 1 & 1 \end{bmatrix} \mathfrak{X}_k.
$$

Consequently, we consider the following state extension for $N_1, N_2 \in \mathbb{N}$:

$$
X_{N_1,N_2} = \mathrm{col}\left(X, \mathfrak{U}_{x,0}, \ldots, \mathfrak{U}_{x,N_1}, \mathfrak{U}_{t,0}, \ldots, \mathfrak{U}_{t,N_2}\right).
$$

It appears then that for $N = \max(N_1, N_2)$, $X_{N_1,N_2} \in \mathrm{Span}(X_N)$ and for $N_1 = N_2 = N$ and $\mathrm{Span}(X_{N,N}) = \mathrm{Span}(X_N)$, meaning that $X_{N,N}$ is just a re-arrangement of X_N but they represent the same vector. This naturally introduces the following Lyapunov functional:

$$
V_{N_1,N_2} = X_{N_1,N_2}^\top P_{N_1,N_2} X_{N_1,N_2} + \int_0^1 \chi^\top(x)(S + xR)\chi(x)dx,
$$

where $P_{N_1,N_2} \in \mathbb{S}^{n+N_1+N_2+2}$ and $S, R \in \mathbb{S}^2$. Of course, for $N_1 = N_2 = N$, this is the same Lyapunov functional as in (5.17). Now, we want to apply Proposition 5.1.

Existence of ε_1: Similarly to the proof of Theorem 5.3, a lower bound of V_{N_1,N_2} can be easily obtained:

$$
\begin{aligned}
V_{N_1,N_2}(X,\chi) \geq X_{N_1,N_2}^\top \Xi_{N_1,N_2} X_{N_1,N_2} - \tilde{s} \sum_{k=0}^{N_1} (2k+1) \mathfrak{U}_{x,k}^\top \mathfrak{U}_{x,k} - \bar{s} \sum_{k=0}^{N_2} (2k+1) \mathfrak{U}_{t,k}^\top \mathfrak{U}_{t,k} \\
+ \int_0^1 \chi^\top(x) S \chi(x) dx.
\end{aligned}
$$

Let $N = \max(N_1, N_2)$, since $\tilde{s}, \bar{s} \in \mathbb{R}^+$, the previous expression becomes:

$$
V_{N_1,N_2}(X,\chi) \geq X_{N_1,N_2}^\top \Xi_{N_1,N_2} X_{N_1,N_2} - \sum_{k=0}^{N} (2k+1) \mathfrak{X}_k^\top \left(\tilde{S} + \bar{S}\right) \mathfrak{X}_k + \int_0^1 \chi^\top(x) S \chi(x) dx.
$$

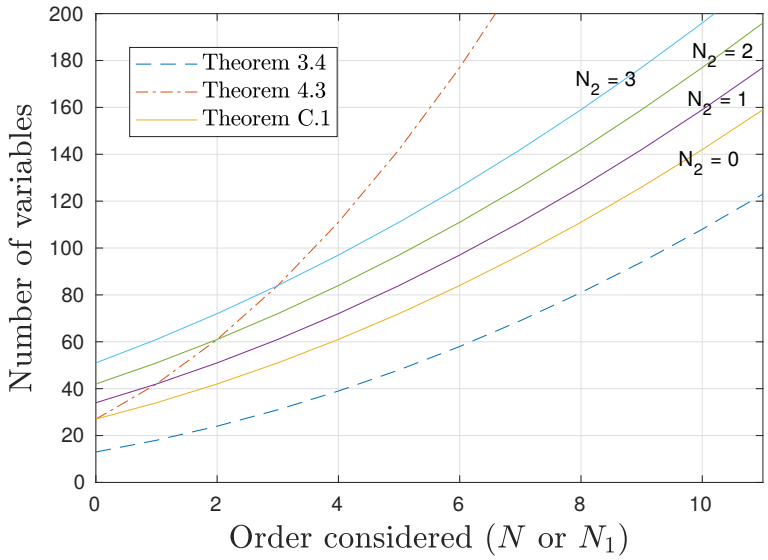

Figure C.1: Number of decision variables for Theorem 4.6 and Theorem 5.3 for different orders.

Using the fact that $S \succeq \tilde{S} + \bar{S}$ leads to:

$$V_{N_1,N_2}(X,\chi) \geq X_{N_1,N_2}^\top \Xi_{N_1,N_2} X_{N_1,N_2} - \sum_{k=0}^{N}(2k+1)\mathfrak{X}_k^\top S \mathfrak{X}_k + \int_0^1 \chi^\top(x) S \chi(x) dx.$$

The end is the same as in the proof of Theorem 5.3.

Existence of ε_2: This part is very similar to the one in the proof of Theorem 5.3.

Existence of ε_3: Let $N = \max(N_1, N_2)$. Using equation (5.22), we get that $X_{N_1,N_2} = F_{N_1,N_2}\xi_N$ and $\dot{X}_{N_1,N_2} = D_{N_1,N_2}\xi_N$. The existence of ε_3 now follows the same line as in the proof of Theorem 5.3. ♢

The previous theorem is interesting because when it is possible to increase N_1 independently of N_2. This is of main importance since they might play different roles, as we can see in the simulations proposed in Figure C.2. First of all, note that Figure C.2f is the same than using Theorem 5.3 with $N = 5$, and for approximately the same number of variables. One can see that for values around $\alpha = 0$, it is not needed to increase both N_1 and N_2. Indeed, they play a similar role in this area and we get a very good estimation of the stability area for $N_1 = 0$ and increasing the other variable. When α is far from 0, then we may need to increase both N_1 and N_2 to get a better result.

As a conclusion, we can say that assessing the stability when $\alpha \neq 0$ is more challenging and requires more decision variables. Moreover, it seems that increasing the order of N_1 or N_2 helps getting stability results for low speed waves. Quantifying the importance of a projection with respect to another seems a real challenge and, so far, one gets only observations. This would help reducing the computational burden of the methodology.

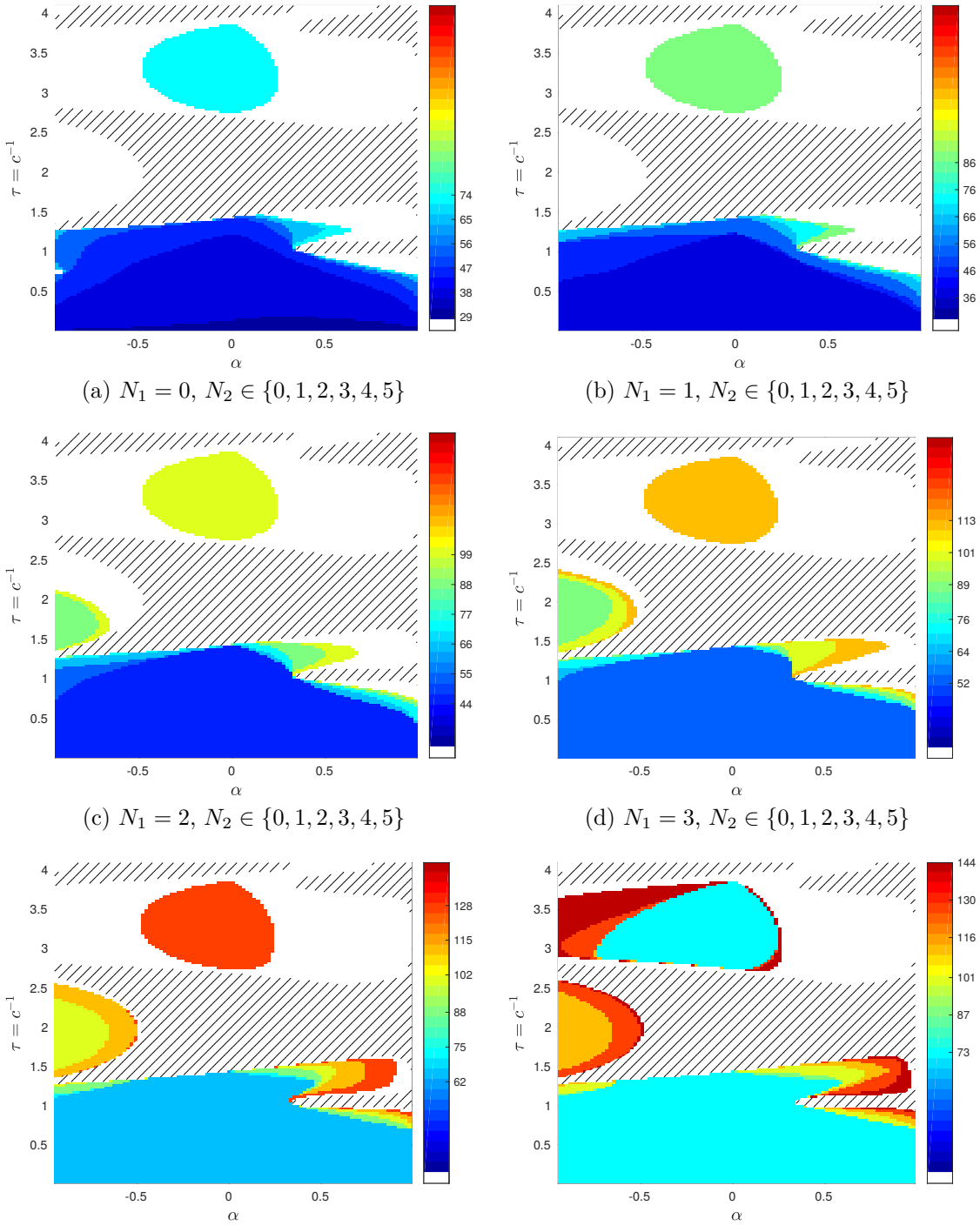

(a) $N_1 = 0$, $N_2 \in \{0, 1, 2, 3, 4, 5\}$

(b) $N_1 = 1$, $N_2 \in \{0, 1, 2, 3, 4, 5\}$

(c) $N_1 = 2$, $N_2 \in \{0, 1, 2, 3, 4, 5\}$

(d) $N_1 = 3$, $N_2 \in \{0, 1, 2, 3, 4, 5\}$

(e) $N_1 = 4$, $N_2 \in \{0, 1, 2, 3, 4, 5\}$

(f) $N_1 = 5$, $N_2 \in \{0, 1, 2, 3, 4, 5\}$

Figure C.2: Stability chart for (5.28). The hatched area is unstable according to the CTCR algorithm presented in Section 4.1.3, while Theorem C.1 gives that the colored area is stable. The number of decision variables needed to get the stability is reported in the color bar.

D

Appendix to Chapter 6

This appendix is devoted to the use of describing functions for the analysis of the stick-slip phenomenon. The describing function analysis [8] is a nonlinear tool to approximate the behavior of a system and characterize its output. It is particularly efficient when the output is periodic and its Fourier decomposition shows a dominant fundamental and first harmonic. As seen in Figure D.1, the stick-slip phenomenon has a fundamental which corresponds to a non-zero mean value in the time representation and a first harmonic around 0.18 Hz. This observation was first noticed in [32]. We derive here a very similar study than in [32] but with the nonlinear friction term (2.2).

We want to derive an estimation of the stick-slip behavior, we will use the LPM system derived in (2.1) instead of the DPM system (2.7). This system is reminded below:

$$\begin{cases} I_r\ddot{\Phi}_r + \lambda_r(\dot{\Phi}_r - \dot{\Phi}_b) + k(\Phi_r - \Phi_b) + d_r\dot{\Phi}_r = u_1, \\ I_b\ddot{\Phi}_b + \lambda_b(\dot{\Phi}_b - \dot{\Phi}_r) + k(\Phi_b - \Phi_r) + (d_b + c_b)\dot{\Phi}_b = -u_2, \\ u_2 = T_{nl}(\Phi_b). \end{cases} \tag{D.1}$$

We denote by $G = \begin{bmatrix} G_{11} & G_{12} \\ G_{21} & G_{22} \end{bmatrix}$ the transfer function from (u_1, u_2) to $(\dot{\Phi}_r, \dot{\Phi}_b)$. Using a PI controller on the surface velocity leads to the block diagram of Figure D.2.

Simplifying the block diagram leads to the one of Figure D.3 with the following

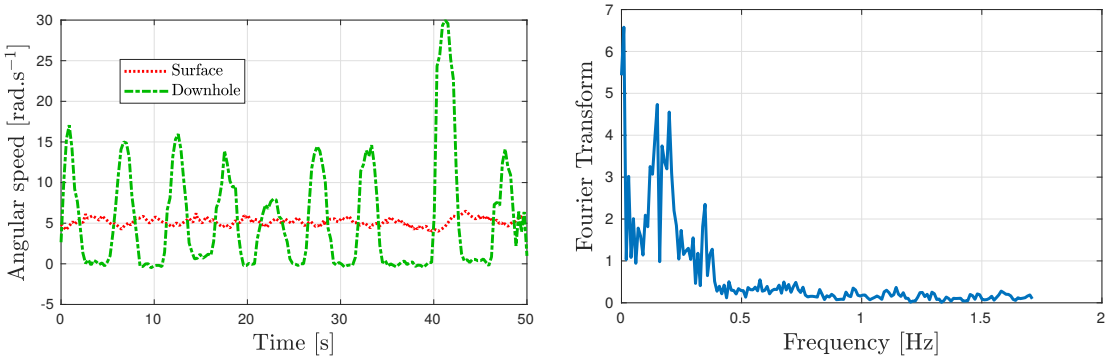

(a) On-field measurements [140]

(b) Fourier transform of the downhole velocity

Figure D.1: Downhole and surface velocity angle for a drilling machine. a) is the temporal signal and b) represents the Fourier transform of the downhole velocity.

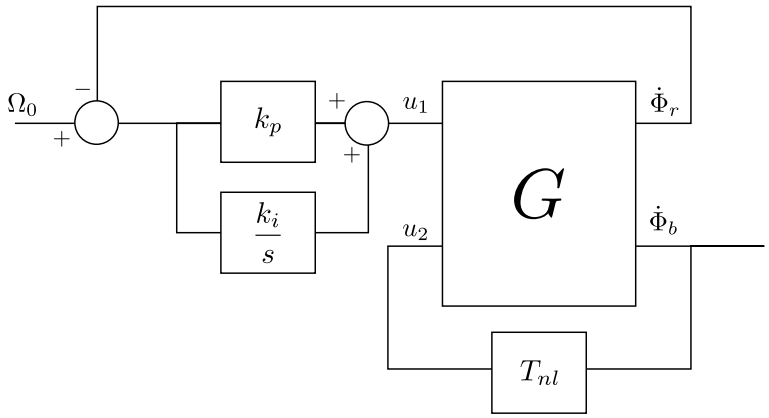

Figure D.2: Block diagram of (D.1).

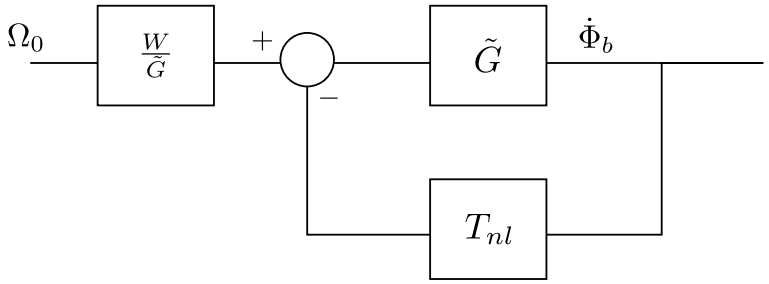

Figure D.3: Modified block diagram of (D.1).

definition:

$$\tilde{G}(s) = \frac{R(s)G_{12}(s)G_{21}(s)}{1+G_{11}(s)R(s)} - G_{22}(s), \quad W(s) = \frac{G_{21}(s)R(s)}{1+G_{11}(s)R(s)}, \quad R(s) = k_p + \frac{k_i}{s}. \tag{D.2}$$

With this second diagram, it is relevant to use the describing function approach if $\tilde{G}$ is a low-pass filter. This can be verified on the Bode plot of $\tilde{G}$ in Figure D.4. We then need to find the linear approximation of T_{nl}. Let consider the following:

$$\begin{cases} e(A,B,t) = A + B\sin(t), \\ T_{nl}(e(A,B,t)) \simeq s(A,B,t) = a_0(A,B) + a_1(A,B)\cos(t) + b_1(A,B)\sin(t), \end{cases}$$

where $a_0(A,B) = \frac{1}{2\pi}\int_{-\pi}^{\pi} T_{nl}(e(A,B,t))dt$, $a_1(A,B) = \frac{1}{\pi}\int_{-\pi}^{\pi} T_{nl}(e(A,B,t))\cos(t)dt$ and $b_1(A,B) = \frac{1}{\pi}\int_{-\pi}^{\pi} T_{nl}(e(A,B,t))\sin(t)dt$. s is then the first harmonic approximation of $T_{nl}(e)$. We create the two following pseudo-transfer functions:

$$\begin{cases} N_0(A,B) = \dfrac{a_0(A,B)}{A}, \\ N_1(A,B) = \dfrac{a_1(A,B)j + b_1(A,B)}{B}, \end{cases}$$

where j is the imaginary number. Performing numerical integration leads to the approximations of N_0 and N_1 presented in Figure D.5. Note that N_0 and N_1 are both real because T_{nl} is odd and consequently $a_1 = 0$. We remark that N_1 has a peak just after

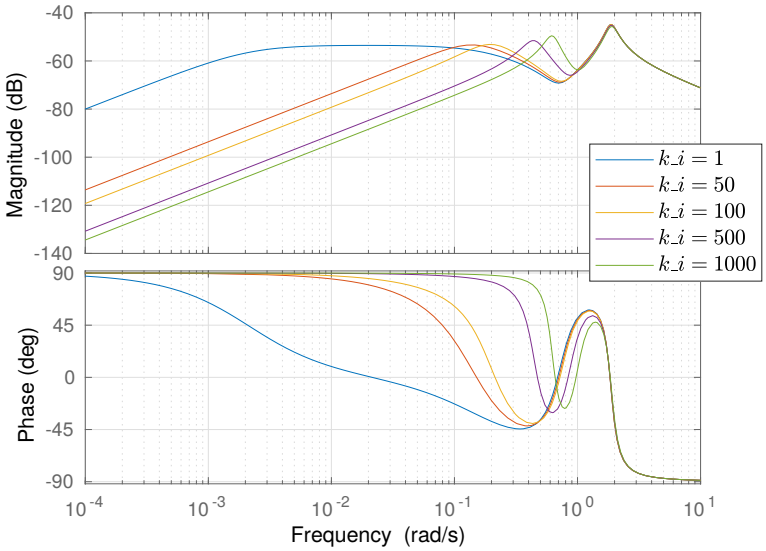

Figure D.4: Bode plot of $\tilde{G}$.

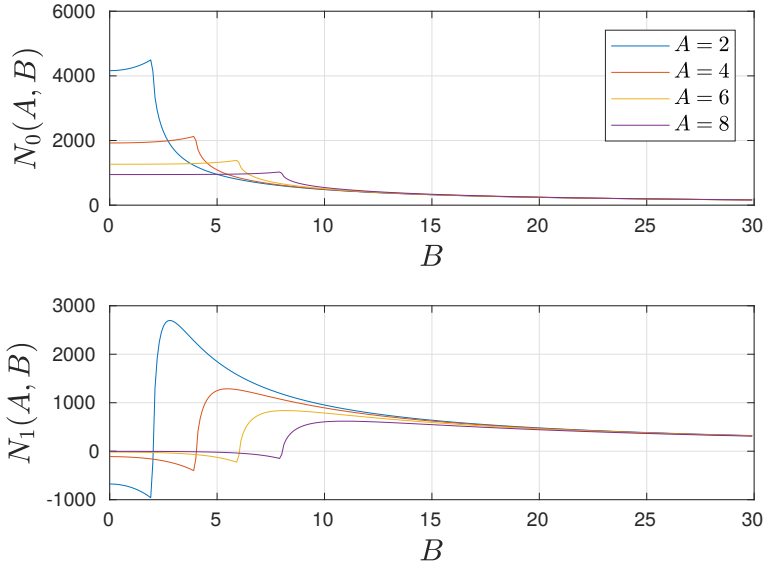

Figure D.5: Numerical computation of N_0 and N_1 for different values of bias A.

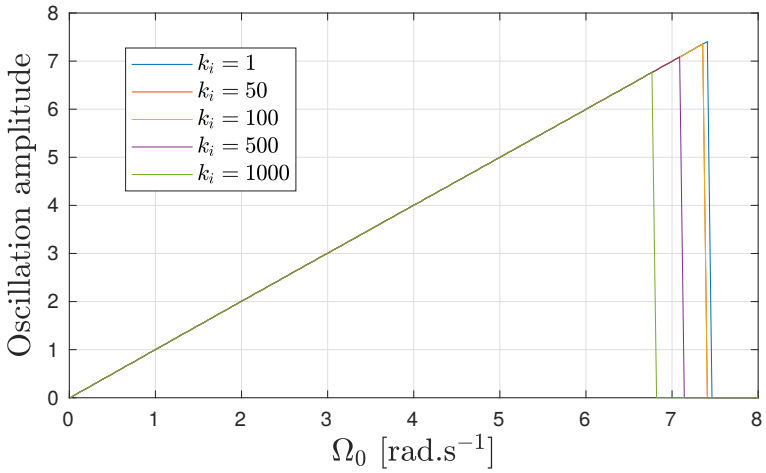

Figure D.6: Plot of solutions to (D.3). The oscillations amplitudes refers to B_c and Ω_0 is the reference speed, in rad.s^{-1}.

A and switches sign from negative to positive. As A increases, the negative damping tends to go to 0. These remarks are of main importance in the sequel.

Applying harmonic balance, necessary conditions for the existence of oscillations with pulsation w_0, amplitude B_c and bias A_c are:

$$\tilde{G}(j\omega_0) = \frac{-1}{N_1(A_c, B_c)}, \qquad A_c(1 + \tilde{G}(0)N_0(A_c, B_c)) = W(0)\Omega_0. \tag{D.3}$$

Since there $k_i \neq 0$, there is an integrator in the loop and consequently $\tilde{G}(0) = 0$, leading to $A_c = \Omega_0$. We note that $\tilde{G}(j\omega_0)$ is real for $\omega_0 = 1.836$ rad.s^{-1}. The value of $\tilde{G}(j\omega_0)$ at this frequency changes with k_i and a dichotomy algorithm can solve (D.3) leading to Figure D.6. We note that there are auto-oscillations for $\Omega_0 \in [0, \Omega_{0max}(k_i)]$. Ω_{0max} is a decreasing function of k_i but for small k_i (meaning less than 100), there is no real change in Ω_{0max}. Moreover, the oscillations are of amplitude Ω_0 because of the switch of sign in N_1 around $B = A$. Compared to Figure D.1, the amplitude estimation is not correct but the frequency of the oscillations is close.

E

Useful inequalities

This appendix aims at gathering inequalities used in the thesis.

E.1 Matrix inequalities

This first inequality provides an equivalent formulation for the positivity of a matrix.

Proposition E.1: Schur Complement [24]

The following statements are equivalent:

1. $M = \begin{bmatrix} M_{11} & M_{12} \\ M_{12}^\top & M_{22} \end{bmatrix} \prec 0,$
2. $M_{22} \prec 0$ and $M_{11} - M_{12}^\top M_{22}^{-1} M_{12} \prec 0.$

This formula stays the same if $\prec$ becomes $\succ$. It has many uses and it can help "linearizing" a matrix inequality for instance.

When dealing with wellposedness, it is quite often required to assure that the determinant of a matrix is non-null. The following proposition is of great help with that.

Proposition E.2

Let $M_{11} \in \mathbb{C}^{n\times n}, M_{12} \in \mathbb{C}^{n\times p}$ and $M_{21} \in \mathbb{C}^{p\times n}$. The following statements are equivalent:

1. $\det(M) \neq 0$ where $M = \begin{bmatrix} M_{11} & M_{12} \\ M_{21} & I_p \end{bmatrix}$.
2. $\det(M_{11} - M_{12}M_{21}) \neq 0.$

Proof : Note first the following equality:

$$M \begin{bmatrix} I_n & 0_{n,p} \\ -M_{21} & I_p \end{bmatrix} = \begin{bmatrix} M_{11} - M_{12}M_{21} & M_{12} \\ 0_{p,n} & I_p \end{bmatrix}.$$

Taking the determinant of the previous expression leads to:

$$\det(M)\det\left(\begin{bmatrix} I_n & 0_{n,p} \\ -M_{21} & I_p \end{bmatrix}\right) = \det(M_{11} - M_{12}M_{21})\det(I_p).$$

The previous equality directly leads to the equivalence proposed in Proposition E.2. $\diamondsuit$

E.2 Inequalities on signals

E.2.1 Jensen and Bessel Inequalities

Many inequalities are used on signals during this thesis. The most useful ones are derived thereafter.

Proposition E.3: Jensen's inequality [65, Proposition B.8]

For $a, b \in \mathbb{R}$ such that $a < b$ and $f \in L^2(a,b)$, the following holds:

$$\left|\int_a^b f(x)dx\right|^2 \leq (b-a)\int_a^b |f(x)|^2 dx. \tag{E.1}$$

Jensen's inequality is originally a result on convexity of a function [78] and the previous proposition is a direct application with the square function. This leads to the classical Cauchy-Schwartz inequality with the canonical scalar product of $L^2(a,b)$. It can be seen, in this context, as a first order Bessel inequality (on the constant vector 1).

Proposition E.4: Bessel Inequality [40]

Let $a < b$ and $f \in L^2(a,b)$. For any orthogonal sequence e_k of $L^2(a,b)$ with respect to the inner product $\langle \cdot, \cdot \rangle_{L^2(a,b)}$, the following inequality holds for all $N \in \mathbb{N}$:

$$\sum_{k=0}^{N} \left| \left\langle f, \frac{e_k}{\|e_k\|} \right\rangle_{L^2(a,b)} \right|^2 \leq \|f\|^2_{L^2(a,b)}. \tag{E.2}$$

Moreover, Parseval identity ensures that this inequality tends to an equality when N tends to infinity.

Proof : The proof is quite simple. Let $N \in \mathbb{N}$ and

$$\forall x \in [a,b], \quad f_N(x) = \sum_{k=0}^{N} \left\langle f, \frac{e_k}{\|e_k\|_{L^2(a,b)}} \right\rangle_{L^2(a,b)} \frac{e_k(x)}{\|e_k\|_{L^2(a,b)}}.$$

The orthogonal property allows us to write the following:

$$\|f - f_N\|^2_{L^2(a,b)} = \|f\|^2_{L^2(a,b)} - 2\langle f, f_N \rangle_{L^2(a,b)} + \|f_N\|^2_{L^2(a,b)} = \|f\|^2_{L^2(a,b)} - \|f_N\|^2_{L^2(a,b)} \geq 0.$$

♢

In this thesis, we are using a polynomial base, defined in the following.

Definition E.1: Orthogonal basis of Legendre polynomials

The only polynomial orthogonal basis of $L^2(a,b)$ for $a < b$ is called the basis of Legendre polynomials and it is defined as follows:

$$\forall x \in [a,b], \qquad \mathcal{L}_k(x) = (-1)^k \sum_{l=0}^{k} (-1)^l \binom{k}{l} \binom{k+l}{l} \left(\frac{x+b-a}{b-a}\right)^l.$$

These polynomials have the following properties:

$$\mathcal{L}_k(a) = (-1)^k, \qquad \mathcal{L}_k(b) = 1, \qquad \|\mathcal{L}_k\|^2 = \frac{b-a}{2k+1},$$
$$\frac{d}{dx}\mathcal{L}_k(x) = \frac{1}{b-a}\sum_{j=0}^{k} \ell_{kj}\mathcal{L}_j(x), \quad \ell_{ik} = \begin{cases} 0, & \text{if } k \geq i, \\ (2k+1)\left(1-(-1)^{k+i}\right), & \text{otherwise.} \end{cases} \tag{E.3}$$

No detailed proof of these properties is given here but they can be found in [40] for the original Legendre polynomials and in [143] for the shifted ones. A special case of Bessel inequality on $L^2(a,b)$ with Legendre polynomials is reported below.

Proposition E.5: Bessel's inequality with Legendre polynomials

For any $f \in L^2(a,b)$ and $N \in \mathbb{N}$, the following holds:

$$\sum_{k=0}^{N} (2k+1)\langle f, \mathcal{L}_k\rangle^2_{L^2(-\tau,0)} \leq (b-a)\|f\|^2_{L^2(-\tau,0)}. \tag{E.4}$$

Proof : This statement is an immediate consequence of Proposition E.4 with the basis of Legendre polynomials defined in the previous definition. ♢

Remark E.1

Taking $N = 0$, (E.2) rewrites as

$$\langle f, 1\rangle^2_{L^2(a,b)} \leq (b-a)\|f\|^2_{L^2(a,b)},$$

which is inequality (E.1). The first order of (E.2) leads to the celebrated Wirtinger-based inequality of [142].

E.2.2 1-D Poincaré-Wirtinger inequality

When dealing with Sobolev spaces, one of the most famous inequality is the so-called Poincaré inequality [28, Proposition 8.13] which helps for norm inequalities. In the case of a 1-D signal, it can be obtained quite easily by the following proposition.

Proposition E.6: [19, Lemma 1]

For $u \in H^1$, the following inequality holds:

$$\|u\|_{L^2}^2 \leq 2\|u_x\|_{L^2}^2 + 2|u(0)|^2.$$

Proof : Since $u_x \in H^1$, we get for $x \in [0,1]$:

$$u(x)^2 = \left(\int_0^x u_s(s)ds + u(0)\right)^2 = \left(\int_0^x u_s(s)ds\right)^2 + 2u(0)\int_0^x u_s(s)ds + |u(0)|^2.$$

Using Young and Jensen inequalities leads to:

$$u(x)^2 - 2|u(0)|^2 \leq 2\left(\int_0^x u_s(s)ds\right)^2 \leq 2\int_0^x u_s^2(s)ds \leq 2\int_0^1 u_s^2(s)ds.$$

Integrating between 0 and 1 leads to the result. ♢

Remark E.2

The previous inequality can be reversed without any difference in the proof, leading to:

$$\forall u \in H^1, \qquad \|u\|_{L^2}^2 \leq 2\|u_x\|_{L^2}^2 + 2|u(1)|^2.$$

Note that these two inequalities can be found with a totally different proof in [87, Lemma A.1].

F

Stabilization of an unstable wave equation using an infinite-dimensional dynamic controller

In recent years, we have seen a renewed interest in the control of infinite-dimensional systems for both practical and theoretical considerations. Indeed, many complex systems may be easily modeled by Partial Differential Equations (PDE). These include delay systems [130], string/payload [72], MEMS [57] or drilling pipes [27, 133], among many others [20]. From a theoretical point of view, one has witnessed many contributions to these problems: backstepping method [91], saturated control [122] or event-based control [54].

Concerning the case of hyperbolic PDE and especially the string equation in a finite domain, even if the model is quite simple, there exist various control laws which can be distributed or only at the boundary for example. Firstly, notice that many different kinds of instabilities can affect the system as for instance internal anti-damping [58, 71] or an unstable Robin boundary condition [88]. These two instabilities generally lead to a finite number of unstable poles. Another possible boundary condition which induces infinitely many unstable poles are reported in [92]. As noted in [92, 93], this instability arises from the unstable difference operator which appears if the wave equation is modeled as a neutral time-delay system. The control of this anti-stable wave is therefore much more challenging. Furthermore, in general, if a standard feedback control law is designed, it is known to be not robust to input/output-delays [48, 49].

This paper deals with the stabilization of an antistable wave equation of the latter kind with Dirichlet actuation. Several methodologies have been proposed to stabilize this model as [66, 93]. Among them, a very popular approach refers to the backstepping methodology for infinite-dimensional systems introduced in [87, 91]. The idea is to determine a feedback law such that the closed-loop system behaves as an asymptotically or exponentially stable system with the desired properties, for instance a one side boundary damped wave equation. This leads to the design of an infinite-dimensional control law which requires a distributed measure all over the domain [86, 149]. Notice that if these measurements are not available, an observer can be designed to estimate this whole state, measuring the state and its derivative at one boundary [88]. The proposed methodology follows the same starting point. We aim at finding a control law in order to get, in closed-loop, a two sided boundary damped wave equation but contrary to the backstepping approach the target system is extended in the space domain (see

for instance [70]). This new idea simplifies the design of the control law. Firstly, it results in a very simple dynamic control law of infinite dimension. Secondly, the control law requires the measurement of only the state at one boundary. Furthermore, this methodology allows to obtain performances similar to approaches such as backstepping. An interesting feature relies also on the robustness of the approach since the parameters of the original system could be uncertain.

The paper is organized as follows. In Section 2, the model for the wave equation as well as the control objectives are detailed. In Section 3, a new controller design is proposed. The existence and uniqueness of a solution to the closed-loop system is then studied. Therefore, an exponential stability result is derived and some extensions are provided. As the main result is formulated in terms of a Linear Matrix Inequality (LMI), the exponential stability result is extended in Section 4 to a robust stability analysis. Section 5 provides a numerical application of the proposed controller on two examples together with a comparison with the backstepping methodology.

Notations: Throughout this paper, the notation u_t stands for $\frac{\partial u}{\partial t}$. The common spaces of square integrable functions on $[0,1]$ is denoted $L^2 = L^2([0,1];\mathbb{R})$ and $H^n = \left\{z \in L^2; \forall m \leq n, \frac{\partial^m z}{\partial x^m} \in L^2\right\}$ for the Sobolov spaces. L^2 is equipped with the norm $\|z\|^2 = \int_0^1 |z(x)|^2 dx = \langle z, z\rangle$. For any square matrices A and B, diag is defined as $\text{diag}(A,B) = \left[\begin{smallmatrix} A & 0 \\ 0 & B \end{smallmatrix}\right]$. A matrix $P \in \mathbb{R}^{n\times n}$ is positive definite if it belongs to the set $\S_+^n$ or more simply $P \succ 0$. I_n is the identity matrix of dimension $n \times n$ and $0_{n,m}$ is the null matrix of size $n \times m$.

F.1 Problem Statement

The wave equation studied in this paper is described by the following model:

$$\begin{cases} u_{tt}(x,t) = c_1^2 u_{xx}(x,t), & x \in (0,1), \\ u_x(0,t) = g u_t(0,t), & \\ u(1,t) = w(t), & \\ y(t) = u_x(1,t), & \\ u(x,0) = u^0(x),\ u_t(x,0) = u_t^0(x), & x \in (0,1), \end{cases} \tag{F.1}$$

It represents the evolution of a wave equation of amplitude u of speed c_1. At $x = 0$, there is a well-known boundary damping condition [92]. At $x = 1$, there is a Dirichlet actuation and w is the control law. The only measurement is y, which is the space derivative of u at $x = 1$.

g is closely related to the reflection coefficient at the boundary $x = 0$. It is well-known from [92] that for $g < 0$, this wave is unstable. Actually, this issue has also been discussed in [69] where it is compared to a neutral time-delay system. Indeed, for $g < 0$, the neutral time-delay system has a non-stable difference operator, making its stabilization possible only if $u_t(1,\cdot)$ is exactly and perfectly measured. This measurement is, in general, difficult to get since it relies on specific sensors which cannot provide the derivative at time t but at a sightly delayed time. As enlighten in [48, 49], a proportional feedback control on $u_t(1,\cdot)$ is not robust to time-delay. That is the reason why

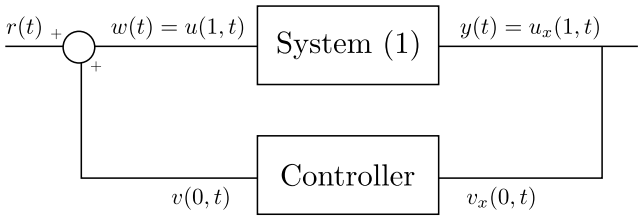

Figure F.1: Block diagram of closed-loop system (F.1)-(F.2).

we need to consider that the measure of $u_t(1,\cdot)$ is not available, making the synthesis of a control law a real challenge. Notice that the famous methodology of backstepping, described in [87] explains for instance how to build such a control law but it relies on the full distributed measurements of the state u which are practically difficult to get.

Here, considering $g < 0$, we aim at showing that there exists an infinite-dimensional controller ensuring which is not issued from a backstepping methodology ensuring the L_2-stability of the closed-loop system without an explicit measurement of $u_t(1,\cdot)$.

F.2 Controller Design

The proposed controller is as follows where $h > 0$ and q are the control design parameters:

$$\begin{cases} v_{tt}(x,t) = c_2^2 v_{xx}(x,t), & x \in (0,1), \\ v_x(0,t) = y(t), & \\ v_x(1,t) = -hv_t(1,t) - qv(1,t), & \\ w(t) = v(0,t) + r(t), & \\ v(x,0) = v^0(x),\ v_t(x,0) = v_t^0(x), & x \in (0,1). \end{cases} \tag{F.2}$$

The reference is r and we assume, without loss of generality, that $r \equiv 0$. This control is of infinite dimension and describes a wave equation. Even if an explicit control formulation of w depending on the initial conditions and y can be derived (using [99] for example), this controller is seen as an infinite-dimensional dynamic controller depicted in Fig. F.1. Note that, if $c_1 = c_2 = c$, controller (F.2) is an extension of system (F.1). Indeed, the closed-loop system is then an extended wave over a domain of length 2 and speed c with two damping or anti-damping boundary conditions. The stability of this interconnected system seems then quite simple and a stability test is provided in Section 3. The most interesting part comes when deriving a robust stability criterion to uncertainties on c_1 and g, as discussed in Section 4.

Remark F.1

The same methodology applies (and similar results are obtained) considering other boundary conditions: $u_x(1,t) = w(t)$ and $y(t) = u(1,t)$ for system (F.1) while for the controller we use: $v(0,t) = y(t)$. The closed-loop is still an extension of the wave on the larger interval $(0,2)$.

F.2.1 Existence and uniqueness

As the string equation is a second order in time and space, the state u must be regular enough such that the derivations have a sense. Then, as done in [87, 162], the following space is defined:

$$\mathcal{H} = \left\{(u, u_t, v, v_t) \in H^1 \times L^2 \times H^1 \times L^2,\ u(1) = v(0)\right\}.$$

In some practical cases like in drilling systems [27], a convergence in speed is required with no care on the position. Then, similarly to [87, 149], a seminorm on $\mathcal{H}$ is defined:

$$\|(u, u_t, v, v_t)\|_{\mathcal{H}}^2 = c_1^2\|u_x\|^2 + \|u_t\|^2 + c_2^2\|v_x\|^2 + \|v_t\|^2. \tag{F.3}$$

Together with space $\mathcal{H}$, this is a semi-norm because a convergence in the sense of $\|\cdot\|_{\mathcal{H}}$ means u_t, u_x, v_t and v_x are converging to 0 but there is no constraint on u and v.

If a convergence in position is needed, the previous subspace is equipped with the following norm:

$$\|(u, u_t, v, v_t)\|_{\mathcal{H}_0}^2 = \|(u, u_t, v, v_t)\|_{\mathcal{H}}^2 + v(1)^2. \tag{F.4}$$

This norm implies the convergence of u_x, u_t, v_x, v_t and $v(1)$ meaning u and v are converging to 0 in L_2 norm. With these previous definitions, $(\mathcal{H}, \|\cdot\|_{\mathcal{H}})$ and $(\mathcal{H}, \|\cdot\|_{\mathcal{H}_0})$ are Hilbert spaces.

Definition F.1: Dissipative system

System (F.1)-(F.2) is said to be **dissipative** in $(\mathcal{H}, \|\cdot\|_{\mathcal{H}})$ (resp. $(\mathcal{H}_0, \|\cdot\|_{\mathcal{H}_0})$) if there is a seminorm $\|\cdot\|$ equivalent to $\|\cdot\|_{\mathcal{H}}$ (resp. $\|\cdot\|_{\mathcal{H}_0}$) for which $\frac{d}{dt}\|(u, u_t, v, v_t)\| < 0$.

The following proposition states the existence and uniqueness of solutions to (F.1)-(F.2).

Proposition F.1: Existence and regularity of a solution

For any initial condition $(u^0, u_t^0, v^0, v_t^0) \in \mathcal{H}$, there exists a unique solution to the latter system if system (F.1)-(F.2) is dissipative in $(\mathcal{H}, \|\cdot\|_{\mathcal{H}})$.

The proof is very similar to the one given in [162, Ch. 3.9] on the wave equation with boundary damping. Assuming the dissipativity of the abstract operator T related to system (F.1)-(F.2), it is enough to show that T is invertible to apply Lumer-Phillips Theorem (see for instance Theorem 3.8.4 in [162]). Once the solution is defined, the study of its equilibrium points can be pursued.

Proposition F.2: Equilibrium point

An equilibrium point (u^e, v^e) of system (F.1)-(F.2) verifies: $u^e = v^e \in \mathbb{R}$ and $qu^e = 0$. If $q \neq 0$, then the only equilibrium point is $0_{\mathcal{H}}$.

Proof : Assume (u^e, v^e) is an equilibrium point. Then for $x \in (0, 1)$, u^e and v^e are two first order polynomials. The boundary condition on v^e at $x = 1$ gives $v^e(0) = 0$ if

$q \neq 0$. Since $u_x^e(0) = 0$, we get $u^e \in \mathbb{R}$. Then, since we have $u^e(1) = v^e(0)$, that gives $u^e = 0$ and, consequently, $u^e = 0$. If $q = 0$, we only get $u^e = v^e \in \mathbb{R}$. ♢

The desired property throughout this paper is the exponential stability of system (F.1)-(F.2) defined as follows.

Definition F.2: $\mathcal{H}$-exponentially stable

A solution of system (F.1)-(F.2) with initial condition $(u^0, u_t^0, v^0, v_t^0) \in \mathcal{H}$ is said to be **$\mathcal{H}$-exponentially stable** if there exist $\gamma > 1, \alpha > 0$ such that the following inequality holds for $t \geq 0$:

$$\|(u(t), u_t(t), v(t), v_t(t))\|_{\mathcal{H}} \leq \gamma \|(u^0, u_t^0, v^0, v_t^0)\|_{\mathcal{H}} e^{-\alpha t}. \tag{F.5}$$

Definition F.3: $\mathcal{H}_0$-exponentially stable

A solution of system (F.1)-(F.2) with initial condition $(u^0, u_t^0, v^0, v_t^0) \in \mathcal{H}$ is said to be **$\mathcal{H}_0$-exponentially stable** if there exist $\gamma > 1, \alpha > 0$ such that the following inequality holds for $t \geq 0$:

$$\|(u(t), u_t(t), v(t), v_t(t))\|_{\mathcal{H}_0} \leq \gamma \|(u^0, u_t^0, v^0, v_t^0)\|_{\mathcal{H}_0} e^{-\alpha t}. \tag{F.6}$$

After these very general results, the proof of dissipativity is given thanks to the construction of a Lyapunov functional, which has a strictly negative derivative along the trajectories of system (F.1)-(F.2).

F.2.2 Main theorem

As a first step, we consider the case $q \neq 0$, and the following theorem is derived for a convergence in speed and position.

Theorem F.1: $\mathcal{H}_0$-exponential stability theorem

The unique solution of system (F.1)-(F.2) with initial condition $(u^0, u_t^0, v^0, v_t^0) \in \mathcal{H}$ is $\mathcal{H}_0$-exponentially stable and converges to $0_{\mathcal{H}}$ if there exists real numbers $S_1, S_2, S_3, S_4, S_5 > 0$ such that the following LMI holds with $q \neq 0$:

$$\Psi_{c_1,c_1g}(0) \prec 0, \tag{F.7}$$

with

$$\begin{aligned}
\Psi_{c_1,c_1g}(\alpha) &= H_{c_1,c_1g}^\top E_\alpha(1) S H_{c_1,c_1g} - G_{c_1,g}^\top S G_{c_1,c_1g} + Q_\alpha, \\
H_{c_1,c_1g} &= \begin{bmatrix} 0 & c_1 & 1 & 0 & 0 \\ 1-c_1g & 0 & 0 & 0 & 0 \\ 0 & 0 & 0 & 1-c_2h & -c_2q \\ 0 & -c_2 & 1 & 0 & 0 \end{bmatrix}, \quad G_{c_1,c_1g} = \begin{bmatrix} 1+c_1g & 0 & 0 & 0 & 0 \\ 0 & -c_1 & 1 & 0 & 0 \\ 0 & c_2 & 1 & 0 & 0 \\ 0 & 0 & 0 & 1+c_2h & c_2q \end{bmatrix}, \\
Q_\alpha &= \operatorname{diag}\left(0_{3,3}, \begin{bmatrix} 0 & S_5 \\ S_5 & 2\alpha S_5 \end{bmatrix}\right), \qquad S = \operatorname{diag}(S_1, S_2, S_3, S_4), \\
E_\alpha(x) &= \operatorname{diag}(e^{2\alpha x c_1^{-1}} I_2, e^{2\alpha x c_2^{-1}} I_2).
\end{aligned}$$

Proof : Let us introduce the following variable:

$$\chi(x,t) = \begin{bmatrix} u_t(x,t) + c_1 u_x(x,t) \\ u_t(1-x,t) - c_1 u_x(1-x,t) \\ v_t(x,t) + c_2 v_x(x,t) \\ v_t(1-x,t) - c_2 v_x(1-x,t) \end{bmatrix},$$

for $t \geq 0, x \in (0,1)$. This variable is based on modified Riemann invariant [19, 20], which has the following property: $\chi_t = \Lambda \chi_x$ with $\Lambda = \text{diag}(c_1, c_1, c_2, c_2)$. Following [19, 39, 107], we introduce a Lyapunov functional:

$$\mathcal{V}_\alpha(\chi, v(1)) = \int_0^1 \chi^\top(x) E_\alpha(x) \Lambda^{-1} S \chi(x) dx + S_5 v^2(1), \tag{F.8}$$

where the time variable has been omitted for the sake of simplicity. Note that $\mathcal{V}_\alpha$ is equivalent to $\|\cdot\|_{\mathcal{H}_0}$ and its derivative along the trajectories of system (F.1)-(F.2) gives:

$$\begin{aligned} \dot{\mathcal{V}}_\alpha(\chi, v(1)) &= 2\int_0^1 \chi_x^\top(x) E_\alpha(x) S \chi(x) dx + 2S_5 v(1) v_t(1) \\ &= \left[\chi^\top(x) E_\alpha(x) S \chi(x)\right]_0^1 - 2\alpha \int_0^1 \chi^\top(x) E_\alpha(x) \Lambda^{-1} S \chi(x) dx \\ &\qquad + 2S_5 v(1) v_t(1) \\ &= -2\alpha \mathcal{V}_\alpha(\chi, v(1)) + \chi^\top(1) E_\alpha(1) S \chi(1) \\ &\qquad - \chi^\top(0) S \chi(0) + 2\alpha S_5 v^2(1) + 2S_5 v(1) v_t(1). \end{aligned} \tag{F.9}$$

Introducing $\xi = [u_t(0) \;\; u_x(1) \;\; v_t(0) \;\; v_t(1) \;\; v(1)]^\top$, the two states $\chi(0)$ and $\chi(1)$ can be rewritten as $\chi(0) = G_{c_1,c_1 g}\xi$, $\chi(1) = H_{c_1,c_1 g}\xi$ so that we get:

$$\dot{\mathcal{V}}_\alpha(\chi, v(1)) + 2\alpha \mathcal{V}_\alpha(\chi, v(1)) = \xi^\top \Psi_{c_1,c_1 g}(\alpha) \xi \leq 0.$$

As it is continuous with respect to α, if $\Psi_{c_1,c_1 g}(0) \prec 0$, it is also the case for a sufficiently small α. Then, the solutions converge exponentially with respect to $\|\cdot\|_{\mathcal{H}_0}$. ♢

It is possible to prove that the previous theorem does not hold if $h < -1$ but the exponential convergence in semi-norm (F.3) still holds, meaning that the solutions do not converge to $0_{\mathcal{H}}$ but the wave speeds u_x and u_t are indeed going exponentially to 0. This weaker stability condition is expressed in the following corollary, dealing with the case where $q = 0$.

Corollary F.1: $\mathcal{H}$-exponential stability condition

The unique solution of system (F.1)-(F.2) with $q = 0$ and initial condition $(u^0, u_t^0, v^0, v_t^0) \in \mathcal{H}$ is $\mathcal{H}$-exponentially stable if there exists $S_1, S_2, S_3, S_4 > 0$ such that the following LMI holds:

$$\tilde{\Psi}_{c_1,c_1 g} = \begin{bmatrix} I_4 & 0_{4,1} \end{bmatrix} \Psi_{c_1,c_1 g}(0) \begin{bmatrix} I_4 & 0_{4,1} \end{bmatrix}^\top \prec 0, \tag{F.10}$$

Proof : Similarly to the previous proof, we consider another Lyapunov functional:

$$\mathcal{V}_\alpha(\chi) = \int_0^1 \chi^\top(x) E_\alpha(x) \Lambda^{-1} S \chi(x) dx,$$

and the extended state: $\xi = [u_t(0) \;\; u_x(1) \;\; v_t(0) \;\; v_t(1)]^\top$. $\mathcal{V}_\alpha$ is then equivalent to $\|\cdot\|_{\mathcal{H}}$ and it is exponentially stable in the sense of $\|\cdot\|_{\mathcal{H}}$. ♢

The previous results are presented in terms of LMIs but for a stable wave and controller with $q = 0$, these inequalities are always verified as stated in the following corollary.

Corollary F.2: $\mathcal{H}$-exponential stability of a stable wave equation

If $h > 0, g > 0$ with $q = 0$, the unique solution of system (F.1)-(F.2) with initial condition $(u^0, u_t^0, v^0, v_t^0) \in \mathcal{H}$ is $\mathcal{H}$-exponentially stable.

Proof : First of all, note that $h > 0$ and $g > 0$ ensure that $\left|\frac{1-c_1 g}{1+c_1 g}\right| < 1$ and $\left|\frac{1-c_2 h}{1+c_2 h}\right| < 1$. Moreover by selecting $S_1 = S_2 = 0.5$ and $S_4 = S_3 - \varepsilon$, we can rewrite $\tilde{\Psi} = \tilde{\Psi}_{c_1, c_1 g}$ in equation (F.10) as:

$$\tilde{\Psi} = \begin{bmatrix} -2c_1 g & 0 & 0 & 0 \\ 0 & -c_2^2 \varepsilon & c_1 - 2c_2 S_3 + c_2 \varepsilon & 0 \\ 0 & c_1 - 2c_2 S_3 + c_2 \varepsilon & -\varepsilon & 0 \\ 0 & 0 & 0 & S_3(c_2 h - 1)^2 - (S_3 - \varepsilon)(c_2 h + 1)^2 \end{bmatrix}.$$

For $\varepsilon < \frac{c_1}{c_2}$ and $S_3 = \frac{c_1}{2c_2} + \frac{\varepsilon}{2}$ then $\tilde{\Psi}_{c_1, c_1 g} \prec 0$ if and only if $S_3(c_2 h - 1)^2 - (S_3 - \varepsilon)(c_2 h + 1)^2 < 0$. This is ensured by taking ϵ small enough. Consequently system (F.1)-(F.2) is exponentially stable. ♢

Remark F.2

Noting that for $c_1 = c_2 = c$ and $q = 0$, system (F.1)-(F.2) is a wave equation of speed c and length 2. The dynamic controller acts then similarly than the one derived in [66]. The stability of this double boundary damped system is indeed $|\frac{1-cg}{1+cg}\frac{1-ch}{1+ch}| < 1$ as noted in [20, ch. 3.3.1]. The stability chart with respect to cg and ch is depicted in Figure F.2. Its decay-rate is given by the following formula:

$$\alpha_{dyn} = -\frac{c}{4} \log \left| \frac{1 - cg}{1 + cg} \frac{1 - ch}{1 + ch} \right|. \tag{F.11}$$

The previous result can be seen as a robust stability criterion. Indeed, considering system (F.1) with uncertain parameters $c_1 > 0$ and $g > 0$, the coupled system is stable no matter $c_2 > 0$ and $h > 0$.

However, in the case where g is negative, the previous corollary does not apply. This is indeed more difficult because system (F.1) is unstable and controller (F.2) must be

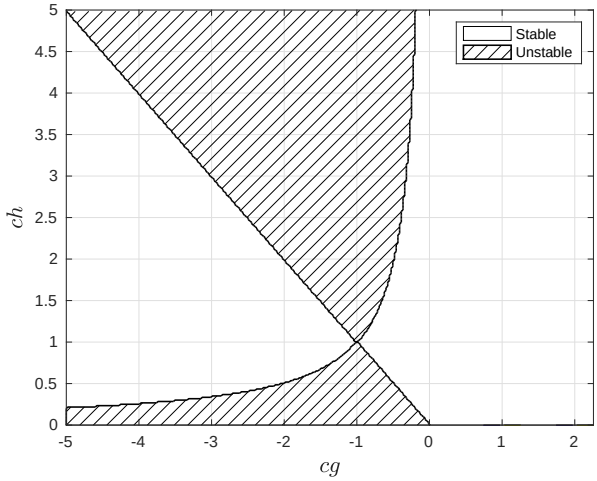

Figure F.2: Stability areas for system (F.1)-(F.2) depending on $c_1 = c_2 = c$, h and g. The hatched area is unstable.

designed to make the interconnection stable. The next step is to derive a stability result for uncertain systems expressed in terms of LMIs and this is the aim of the following part.

F.3 Robustness Analysis / Controller Synthesis

Let us consider that system (F.1) is now an uncertain system, that is the speed c_1 and the damping g are uncertain. Only a nominal system (F.1) with nominal parameters $c = c_n$ and $g = g_n$ is known. We assume that the real speed c_1 is constant and that both c_1 and c_n belong to the interval $[c_{min}, c_{max}] \subset \mathbb{R}^+$. The last parameter g is assumed to be in the set $[g_{min}, g_{max}] \subset \mathbb{R}$ and so does g_n. Then, the uncertain system can be viewed as a deviation from the nominal plan.
If nominal plant (F.1) with a speed c_n and a damping coefficient g_n is potentially unstable, then, a controller of the form of (F.2) can be designed. Indeed, we set $c_2 = c_n$ and choose h such that $(c_n g_n, c_n h)$ is in the stability area presented in Figure F.2. Then the nominal plant is exponentially stable with $q = 0$. The condition derived thereafter states the stability of the uncertain system made up of (F.1) and the previously designed controller.

Theorem F.2: Robust stability theorem

Let us define the following:

$$\delta_{max} = \max_{z\in\mathcal{D}} \left|\tfrac{1-z}{1+z}\right|, z_{max} = \text{Argmax}_{z\in\mathcal{D}} \left|\tfrac{1-z}{1+z}\right|,$$
$$\mathcal{D} = \{z = c_1 g, c_1 \in [c_{min}, c_{max}], g \in [g_{min}, g_{max}]\}.$$

There exists a unique solution of system (F.1)-(F.2) with initial condition $(u^0, u_t^0, v^0, v_t^0) \in \mathcal{H}$ and it is $\mathcal{H}$-exponentially stable if the following holds for

$S_1, S_2, S_3, S_4 > 0$:

$$1 \leq \delta_{max} < \infty \quad \text{and} \quad \begin{cases} \Psi_{c_{min}, z_{max}} \prec 0, \\ \Psi_{c_{max}, z_{max}} \prec 0. \end{cases}$$

Remark F.3

Notice that coefficient $\delta(cg) = \frac{1-cg}{1+cg}$ is a physical parameter for the wave equation and corresponds to the reflexion coefficient (see [14, 99]). Taking $\delta_{max} = \max_{cg \in \mathcal{D}} |\delta(cg)|$ means we are studying the "most" unstable system in the uncertainty set. For $\delta_{max} < 1$, Corollary F.2.2 states that the uncertain system is stable. If $\delta_{max} = +\infty$, there does not exist a controller of the form (F.2) making the system stable. These considerations bring that $\mathcal{D} \subset (-1, +\infty)$ or $\mathcal{D} \subset (-\infty, -1)$.

Proof : The robustness analysis is based on the derivation of a common Lyapunov functional for all the systems inside the uncertainty set. This Lyapunov functional must have a strictly negative derivative along the trajectories. In other words, $\Psi_{c_1,z} \prec 0$ for all $c_1 \in [c_{min}, c_{max}]$ and $z \in \mathcal{D}$.

Noticing that $\Psi_{c_1,z}$ is a block-diagonal matrix, one can write $\Psi_{c_1,z} = \text{diag}(\Phi_z, \Theta_{c_1}, \Xi)$ with

$$\begin{aligned} \Phi_z &= S_2(z-1)^2 - S_1(z+1)^2, \\ \Theta_{c_1} &= \begin{bmatrix} (S_1 - S_2)c_1^2 - (S_3 - S_4)c_2^2 & (S_1 + S_2)c_1 - (S_3 + S_4)c_2 \\ (S_1 + S_2)c_1 - (S_3 + S_4)c_2 & S_1 - S_2 - S_3 + S_4 \end{bmatrix}, \\ \Xi &= \begin{bmatrix} S_3(1 - c_2h)^2 - S_4(1 + c_2h)^2 & -c_2q(S_3(1 - c_2h) + S_4(1 + c_2h)) \\ -c_2q(S_3(1 - c_2h) + S_4(1 + c_2h)) & -S_4(c_2q)^2 \end{bmatrix}. \end{aligned}$$

The aim is now to show that $\Phi_z < 0$, $\Theta_{c_1} \prec 0$ and $\Xi \prec 0$ for all uncertain systems. As $\delta_{max} < \infty$, then, $z \neq -1$ and $\Phi_z(z+1)^{-2} < \Phi_{z_{max}}(z_{max}+1)^{-2} < 0$.

The last part of this proof deals with the negativity of Θ_{c_1}. To derive such a result, one can prove that Θ_{c_1} is convex in c_1. Then if it is negative at its boundary, it is always negative. Using Schur complement, $\Theta_{c_1} \prec 0$ is equivalent to:

$$\begin{cases} p(c_1) = k_2 c_1^2 + k_1 c_1 + k_0 < 0, \\ S_1 - S_2 - S_3 + S_4 < 0, \end{cases} \tag{F.12}$$

with $k_2 = S_1 - S_2 - \frac{(S_1+S_2)^2}{S_1-S_2-S_3+S_4}$ and $k_1, k_0 \in \mathbb{R}$. Considering $\delta_{max} > 1$, we get:

$$S_2 \leq S_2 \delta_{max}^2 < S_1,$$

since $\Phi_{z_{max}} < 0$. Then, $k_2 > 0$ and consequently p in (F.12) is convex with respect to c_1. Thus, if $\Theta_{c_{min}}$ and $\Theta_{c_{max}}$ are negative definite, the inequality $\Theta_{c_1} \prec 0$ straightforwardly

holds for any c_1 in the interval $[c_{min},\ c_{max}]$. In other words, the following implication holds for all $c_1 \in [c_{min}, c_{max}]$ and $z \in \mathcal{D}$:

$$\begin{cases} \Psi_{c_{min},z_{max}} \prec 0, \\ \Psi_{c_{max},z_{max}} \prec 0 \end{cases} \Rightarrow \Psi_{c_1,z} \prec 0,$$

which concludes the proof. ♢

Remark F.4

This proof shows that the result is still true even if g is time-varying, but the restriction $g \in [g_{min}, g_{max}]$ holds. However, a time-varying c_1 is not allowed because it changes the calculations of the derivative along the trajectories of $\mathcal{V}$. If one adds the constraint $q = 0$, the previous robustness result is still valid for $\tilde{\Psi}$ instead of Ψ.

Remark F.5

The proposed controller is not robust to delay in the measure so do the backstepping controllers in [87].

F.4 Examples

Two examples are studied in this part. The first one considers an open-loop stable wave equation and the second one an unstable system (F.1).

F.4.1 Stable wave equation

The first example is an open-loop stable wave equation with a dynamic controller whose parameters are given below:

$$c_1 = c_2 = 1, \quad g = 3, \quad h = 0.9, \quad q = 5.$$

The closed-loop system is stable according to Theorem F.2.2. Thanks to equation (F.11), the dynamic controller aims at making the system faster and converging to $0_{\mathcal{H}}$. The decay-rate of the solution can be obtained considering the maximum α in Theorem F.2.2 for which it is still feasible. The resulting solution has then a decay-rate of 0.157. Notice that, since $q \neq 0$, the closed-loop system converges asymptotically to the only equilibrium point 0, as shown in Figure F.3.

F.4.2 Anti-damped wave equation

This second example aims at comparing two controllers, the dynamic controller developed in this paper and the one coming from backstepping approach [87, 149], which is given by:

$$w(t) = \frac{g - c_1 k}{c_1 - gk} \left(\frac{g}{c_1} u(0,t) + \int_0^1 u_t(x,t) dx \right). \tag{F.13}$$

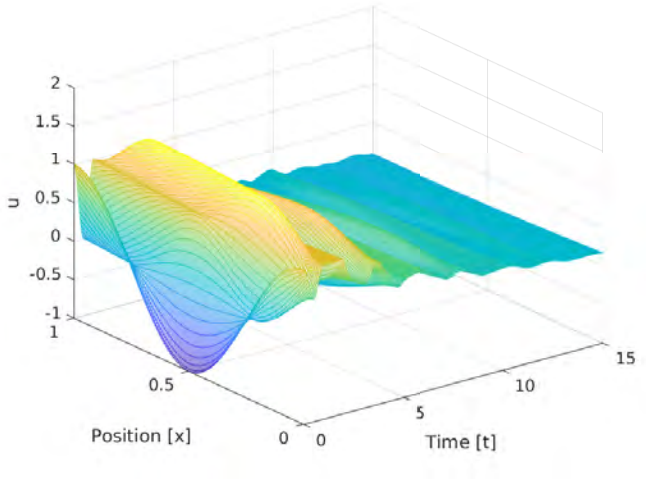

Figure F.3: Time response of system (F.1) with a dynamic control and initial condition: $u^0(x) = \cos(2\pi x)$, $v^0(x) = 1$ and $u_t^0(x) = v_t^0(x) = 0$.

Applying this control law, system (F.1) in closed loop is transformed into the following target system:

$$\begin{cases} z_{tt}(x,t) = c_1^2 z_{xx}(x,t), \quad x \in (0,1), \\ z_x(0,t) = k z_t(0,t), \\ z(1,t) = 0, \end{cases}$$

where the initial conditions are not expressed, since it is the target system. Its decay-rate is then given by $\alpha_b = -\frac{c_1}{2}\log\left|\frac{1-c_1k}{1+c_1k}\right|$. Comparing this expression to the decay rate of the proposed closed-loop target system (F.11), to get a similar decay-rate (i.e. $\alpha_{dyn} = \alpha_b$) and then a fair comparison between the two controls, one must choose:

$$k = c_1^{-1}\frac{1-\sqrt{|\delta_1\delta_2|}}{1+\sqrt{|\delta_1\delta_2|}}, \quad \text{or} \quad k = c_1^{-1}\frac{1+\sqrt{|\delta_1\delta_2|}}{1-\sqrt{|\delta_1\delta_2|}}.$$

The parameters chosen for the simulation are then:

$$c_1 = c_2 = 1, \quad g = -0.27, \quad h = 0.6, \quad q = 0, \quad k = 0.205, \tag{F.14}$$

leading to a decay-rate of 0.208. Figure F.4 shows the simulation results for system (F.1) for both controllers. The comparison between the two control signals is given in Figure F.4c. The poles of each closed-loop system are displayed in Figure F.4d. One can see that controller (F.2) produces more poles than the backstepping control. This is an argument showing that the two controls are indeed of different kind. The backstepping controller seems faster in Figure F.4c but Figure F.4d clearly shows that the poles are indeed with the same real part, and consequently, with the same decay-rate. The backstepping controller seems faster in Figure F.4c but the controllers have been designed to have the same decay-rate.

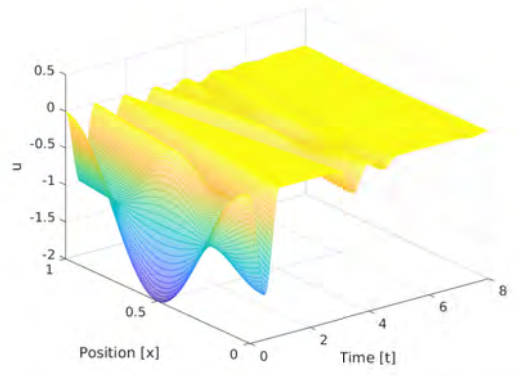

(a) System (F.1) with controller (F.2)

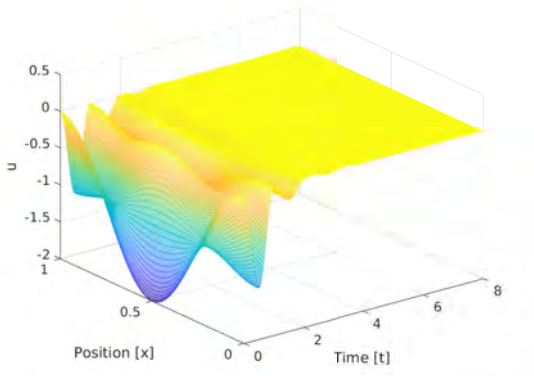

(b) System (F.1) with controller (F.13)

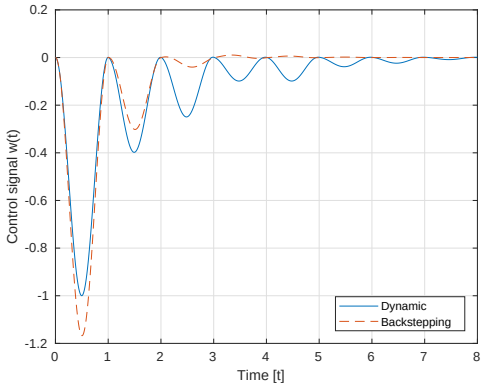

(c) Control signals w based on the dynamic controller (F.2) (blue) and backstepping controller (F.13) (dashed red).

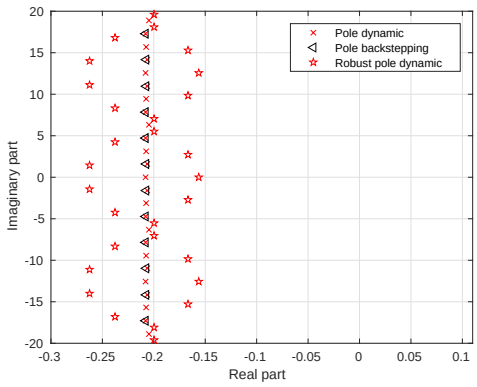

(d) Root locus of the closed-loop systems composed by (F.1) with dynamic controller (F.2) (red) and backstepping controller (F.13) (black)

Figure F.4: System behavior depending on the controller. Figures (a) and (b) are simulations with initial conditions: $u^0(x) = \cos(2\pi x) - 1$, $u_t^0(x) = v^0(x) = v_t^0 = 0$ for $x \in (0, 1)$. Figure (c) is a comparison between the two control laws. Figure (d) is a root locus comparison between the poles in three situations: backstepping (F.13) with parameters (F.14); dynamic controller (F.2) with parameters (F.14) and robust controller (F.2) with parameters (F.14) but a speed mismatch ($c_1 = 0.8$).

One drawback of this methodology is that the dynamic controller does not provide an explicit control law while the backstepping, in this case, gives a relatively simple expression for w. Even if the backstepping methodology formulates w in terms of u, it is also an infinite dimension control law since it uses the integral over space.

The main difference between the two controllers are the needed measurements. While the dynamic controller only requires the measure of $u_x(1,\cdot)$, the backstepping control asks for $u(0,\cdot)$ and $u_t(x,\cdot)$ for $x \in (0,1)$. If these measurements are not available, an infinite-dimension observer has been developed in [149] to estimate the states u_t at each point of the string but requiring the measurement of $u_x(1,\cdot)$ and $u_{xt}(1,\cdot)$. Then, the main advantage of having an explicit control law disappears. In comparison, our methodology provides a simpler control law with only one boundary measurement and a very simple robustness criterion. This is mainly due to the LMI formulation which provides an efficient framework for this kind of study. Moreover, the parameter γ in Definition F.2 and equation (F.5) can be estimated using eigenvalues of S in (F.8).

A robustness analysis has also been conducted in this case using Theorem F.3. We get the exponential stability for the interconnected system with $c_2 = 1, h = 0.6$ and the following uncertainties:

1. $c_1 \in [0.74, 1.45]$ with $g \in [-0.27, +\infty)$;
2. $c_1 \in [0.8, 1.4]$ with $g \in [-0.29, +\infty)$.

There is no upper bound on g as δ_{max} is always obtained for a negative g. According to the previous study, a mismatch between the two speeds ($c_1 = 0.8$ and $c_2 = 1$) leads to a stable interconnected system. In this case with $g = -0.27$, simulations confirm that point.

F.5 Conclusion

An infinite-dimensional controller is derived to stabilize a anti-stable string equation with Dirichlet actuation. It is quite simple and the calculations are easily extended to robust stability. This enables the comparison with backstepping and one can notice similar performances for a much more simple implementation. This study brought the idea of extending systems in order to transform them to a more suitable form for control. This idea can be enlarged to other PDEs and maybe also to cascaded PDEs.

Bibliography

[1] U. J. F. Aarsnes and O. M. Aamo. Linear stability analysis of self-excited vibrations in drilling using an infinite dimensional model. *Journal of Sound and Vibration*, 360:239 – 259, 2016.

[2] U.J.F. Aarsnes and J.S. Roman. Torsional vibrations with bit off bottom: Modeling, characterization and field data validation. *Journal of Petroleum Science and Engineering*, 163:712 – 721, 2018.

[3] M. Ahmadi, G. Valmorbida, and A. Papachristodoulou. Dissipation inequalities for the analysis of a class of PDEs. *Automatica*, 66:163 – 171, 2016.

[4] Y. Ariba, F. Gouaisbaut, and D. Peaucelle. Stability analysis of time-varying delay systems in quadratic separation framework. In *ICNPAA-2008: Mathematical Problems in Engineering, Aerospace and Sciences*, 2008.

[5] Y. Ariba, F. Gouaisbaut, A. Seuret, and D. Peaucelle. Stability analysis of time-delay systems via Bessel inequality: A quadratic separation approach. *International Journal of Robust and Nonlinear Control*, 28(5):pp 1507–1527, March 2018.

[6] B. Armstrong-Helouvry. Stick-slip arising from stribeck friction. In *Proceedings., IEEE International Conference on Robotics and Automation*, pages 1377–1382. IEEE, 1990.

[7] B. Armstrong-Hélouvry, P. Dupont, and C. Canudas De Wit. A survey of models, analysis tools and compensation methods for the control of machines with friction. *Automatica*, 30(7):1083–1138, 1994.

[8] D. P. Atherton and D. R. Towill. Nonlinear control engineering-describing function analysis and design. *IEEE Transactions on Systems, Man, and Cybernetics*, 7(9):678–678, 1977.

[9] J. Auriol. *Robust design of backstepping controllers for systems of linear-hyperbolic PDEs*. Theses, PSL Research University, July 2018.

[10] J. J. Azar and G. R. Samuel. *Drilling engineering*. PennWell books, 2007.

[11] M. Barreau. Stabilité et stabilisation de systèmes linéaires à l'aide d'inégalités matricielles linéaires. *Quadrature*, July 2019.

[12] M. Barreau, F. Gouaisbaut, and A. Seuret. Static state and output feedback synthesis for time-delay systems. In *2018 European Control Conference (ECC)*, pages 1195–1200, 2018.

[13] M. Barreau, F. Gouaisbaut, and A. Seuret. Pratical stability of a drilling pipe under friction with a pi-controller. *IEEE Transaction on Control Systems Technologies*, 2019. Decision pending.

[14] M. Barreau, F. Gouaisbaut, A. Seuret, and R. Sipahi. Input/output stability of a damped string equation coupled with ordinary differential system. *International Journal of Robust and Nonlinear Control*, 28(18):6053–6069, 2018.

[15] M. Barreau, A. Seuret, and F. Gouaisbaut. Wirtinger-based exponential stability for time-delay systems. In *IFAC World Congress, Toulouse*, volume 50, pages 11984–11989. Elsevier, 2017.

[16] M. Barreau, A. Seuret, and F. Gouaisbaut. Exponential Lyapunov stability analysis of a drilling mechanism. In *57th Annual Conference on Decision and Control (CDC), Miami*, pages 2952–2957, 2018.

[17] M. Barreau, A. Seuret, and F. Gouaisbaut. Stabilization of an unstable wave equation using an infinite dimensional dynamic controller. In *57th Annual Conference on Decision and Control (CDC), Miami*, pages 2952–2957, 2018.

[18] M. Barreau, A. Seuret, and F. Gouaisbaut. Lyapunov stability of a coupled ordinary differential system and a string equation with polytopic uncertainties. In *Advances on Delays and Dynamics*. Springer, 2019.

[19] M. Barreau, A. Seuret, F. Gouaisbaut, and L. Baudouin. Lyapunov stability analysis of a string equation coupled with an ordinary differential system. *IEEE Transactions on Automatic Control*, 63(11):3850–3857, 2018.

[20] G. Bastin and J.-M. Coron. *Stability and boundary stabilization of 1-d hyperbolic systems*, volume 88. Springer, 2016.

[21] H.I. Basturk. Observer-based boundary control design for the suppression of stick–slip oscillations in drilling systems with only surface measurements. *Journal of Dynamic Systems, Measurement, and Control*, 139(10):104501, 2017.

[22] R. E. Bellman and K. L. Cooke. *Differential-difference equations*. Academic Press, 1963.

[23] E. Beretta and Y. Kuang. Geometric stability switch criteria in delay differential systems with delay dependent parameters. *SIAM Journal on Mathematical Analysis*, 33(5):1144–1165, 2002.

[24] S. Boyd, L. El Ghaoui, E. Feron, and V. Balakrishnan. *Linear Matrix Inequalities in System and Control Theory*. Studies in Applied Mathematics. SIAM, 1994.

[25] D. Breda, S. Maset, and R. Vermiglio. Pseudospectral differencing methods for characteristic roots of delay differential equations. *SIAM Journal on Scientific Computing*, 27(2):482–495, 2005.

[26] D. Bresch-Pietri and M. Krstic. Adaptive output feedback for oil drilling stick-slip instability modeled by wave PDE with anti-damped dynamic boundary. In *ACC*, pages 386–391, 2014.

[27] D. Bresch-Pietri and M. Krstic. Output-feedback adaptive control of a wave PDE with boundary anti-damping. *Automatica*, 50(5):1407–1415, 2014.

[28] H. Brezis. *Functional analysis, Sobolev spaces and partial differential equations*. Springer Science & Business Media, 2010.

[29] C. Briat. Convergence and equivalence results for the Jensen's inequality - application to time-delay and sampled-data systems. *IEEE Transactions on Automatic Control*, 56(7):1660–1665, 2011.

[30] C. Briat. Linear parameter-varying and time-delay systems. *Analysis, observation, filtering & control*, 3, 2014.

[31] C. Briat and A. Seuret. Robust stability of impulsive systems: A functional-based approach. In *4th IFAC conference on Analysis and Design of Hybrid Systems (ADHS'2012)*, page 6, 2012.

[32] C. Canudas de Wit, F. Rubio, and M. Corchero. DOSKIL: A New Mechanism for Controlling Stick-Slip Oscillations in Oil Well Drillstrings. *IEEE Transactions on Control Systems Technology*, 16(6):1177–1191, November 2008.

[33] F. Castillo, E. Witrant, C. Prieur, and L. Dugard. Dynamic Boundary Stabilization of Linear and Quasi-Linear Hyperbolic Systems. In *51st Annual Conference on Decision and Control (CDC)*, pages 2952–2957, 2012.

[34] E. Cerpa and C. Prieur. Effect of time scales on stability of coupled systems involving the wave equation. In *2017 IEEE 56th Annual Conference on Decision and Control (CDC)*, pages 1236–1241. IEEE, 2017.

[35] N. Challamel. Rock destruction effect on the stability of a drilling structure. *Journal of Sound and Vibration*, 233(2):235–254, 2000.

[36] A. P. Christoforou and A. S. Yigit. Fully coupled vibrations of actively controlled drillstrings. *Journal of sound and vibration*, 267(5):1029–1045, 2003.

[37] R. M. Colombo, G. Guerra, M. Herty, and V. Schleper. Optimal control in networks of pipes and canals. *SIAM Journal on Control and Optimization*, 48(3):2032–2050, 2009.

[38] J. M. Coron. *Control and nonlinearity*. Number 136 in Mathematical Surveys and Monographs. American Mathematical Soc., 2007.

[39] J.M. Coron, B. d'Andrea Novel, and G. Bastin. A strict Lyapunov function for boundary control of hyperbolic systems of conservation laws. *IEEE Trans. on Automatic Control*, 52(1):2–11, Jan 2007.

[40] R. Courant and D. Hilbert. *Methods of mathematical physics*. John Wiley & Sons, Inc., 1989.

[41] R. F. Curtain and H. J. Zwart. *An introduction to infinite-dimensional linear systems theory*, volume 21 of *Texts in Applied Mathematics*. Springer-Verlag, New York, 1995.

[42] J. M. G. Da Silva and S. Tarbouriech. Antiwindup design with guaranteed regions of stability: an LMI-based approach. *IEEE Transactions on Automatic Control*, 50(1):106–111, 2005.

[43] B. d'Andréa Novel, F. Boustany, F. Conrad, and B. P. Rao. Feedback stabilization of a hybrid PDE–ODE system: Application to an overhead crane. *Mathematics of Control, Signals and Systems*, 7(1):1–22, 1994.

[44] D. Dareing, J. Tlusty, and C. Zamudio. Self-excited vibrations induced by drag bits. *Journal of Energy Resources Technology*, 112(1):54–61, 1990.

[45] R. Datko. An extension of a theorem of A. M. Lyapunov to semi-groups of operators. *Journal of Mathematical Analysis and Applications*, 24(2):290–295, 1968.

[46] R. Datko. Extending a theorem of A. M. Lyapunov to Hilbert space. *Journal of Mathematical analysis and applications*, 32(3):610–616, 1970.

[47] R. Datko. An algorithm for computing Lyapunov functionals for some differential-difference equations. In *Ordinary differential equations*, pages 387–398. Elsevier, 1972.

[48] R. Datko. Not all feedback stabilized hyperbolic systems are robust with respect to small time delays in their feedbacks. *SIAM Journal on Control and Optimization*, 26(3):697–713, 1988.

[49] R. Datko, J. Lagnese, and M.P. Polis. An example on the effect of time delays in boundary feedback stabilization of wave equations. *SIAM Journal on Control and Optimization*, 24(1):152–156, 1986.

[50] C. A. Desoer and M. Vidyasagar. *Feedback systems: input-output properties*, volume 55. Siam, 1975.

[51] F. Di Meglio and U.J.F. Aarsnes. A distributed parameter systems view of control problems in drilling. *IFAC-PapersOnLine*, 48(6):272 – 278, 2015. 2nd IFAC Workshop on Automatic Control in Offshore Oil and Gas Production OOGP 2015.

[52] G. Doetsch. *Introduction to the theory and application of the Laplace transformation*. Springer, 2012.

[53] Y. Ebihara, D. Peaucelle, and D. Arzelier. *S-Variable Approach to LMI-Based Robust Control*, volume 17 of *Communications and Control Engineering*. Springer, 2015.

[54] N. Espitia, A. Girard, N. Marchand, and C. Prieur. Event-based control of linear hyperbolic systems of conservation laws. *Automatica*, 70:275–287, 2016.

[55] L. C. Evans. *Partial Differential Equations*. Graduate studies in mathematics. American Mathematical Society, 2010.

[56] F. Ferrante and A. Cristofaro. Boundary Observer Design for Coupled ODEs-Hyperbolic PDEs Systems. *ECC 2019, Italy*, 2019.

[57] G. Flores. Dynamics of a damped wave equation arising from MEMS. *SIAM Journal on Applied Mathematics*, 74(4):1025–1035, 2014.

[58] P. Freitas and E. Zuazua. Stability Results for the Wave Equation with Indefinite Damping. *Journal of Differential Equations*, 132(2):338 – 352, 1996.

[59] E. Fridman. *Introduction to Time-Delay Systems*. Analysis and Control. Birkhäuser, 2014.

[60] E. Fridman, S. Mondié, and B. Saldivar. Bounds on the response of a drilling pipe model. *IMA Journal of Mathematical Control and Information*, 27(4):513–526, 2010.

[61] T. Glad and L. Ljung. *Control Theory*. Control Engineering. Taylor & Francis, 2000.

[62] F. Gouaisbaut and D. Peaucelle. A note on stability of time delay systems. *IFAC Proceedings Volumes*, 39(9):555–560, 2006.

[63] F. Gouaisbaut and D. Peaucelle. Stability of time-delay systems with non-small delay. In *Proceedings of the 45th IEEE Conference on Decision and Control*, pages 840–845, Dec 2006.

[64] J. M. Greenberg and L. T. Tsien. The effect of boundary damping for the quasi-linear wave equation. *Journal of Differential Equations*, 52(1):66–75, 1984.

[65] K. Gu, J. Chen, and V. L. Kharitonov. *Stability of time-delay systems*. Springer, 2003.

[66] M. Gugat. Exponential stabilization of the wave equation by Dirichlet integral feedback. *SIAM Journal on Control and Optimization*, 53(1):526–546, 2015.

[67] J. K. Hale. *Theory of functional differential equations*. Number vol 3 in Applied Mathematical Sciences Series . Springer Verlag, 1977.

[68] J. K. Hale and S. M. V. Lunel. *Introduction to functional differential equations*. Applied mathematical sciences . Springer-Verlag, New York, Berlin, Heidelberg, 1977.

[69] J. K. Hale and S. M. V. Lunel. Effects of small delays on stability and control. In *Operator theory and analysis*, pages 275–301. Springer, 2001.

[70] S. Hansen and E. Zuazua. Exact controllability and stabilization of a vibrating string with an interior point mass. *SIAM journal on control and optimization*, 33(5):1357–1391, 1995.

[71] F. Hassine. Rapid Exponential Stabilization of a 1-D Transmission Wave Equation with In-domain Anti-damping. *Asian Journal of Control*, 19(6):2017–2027, 2017.

[72] W. He, S. Zhang, and S. S. Ge. Adaptive control of a flexible crane system with the boundary output constraint. *IEEE Transactions on Industrial Electronics*, 61(8):4126–4133, 2014.

[73] A. Helmicki, C. A. Jacobson, and C. N. Nett. Ill-posed distributed parameter systems: A control viewpoint. *IEEE Trans. on Automatic Control*, 36(9):1053–1057, 1991.

[74] R. Hernandez-Suarez, H. Puebla, R. Aguilar-Lopez, and E. Hernandez-Martinez. An integral high-order sliding mode control approach for stick-slip suppression in oil drillstrings. *Petroleum Science and Technology*, 27(8):788–800, 2009.

[75] D. Hertz, E. I Jury, and E. Zeheb. Simplified analytic stability test for systems with commensurate time delays. In *IEEE Proceedings D-Control Theory and Applications*, volume 131, pages 52–56. IET, 1984.

[76] E. F. Infante and W. B. Castelan. A Lyapunov functional for a matrix difference-differential equation. *Journal of Differential Equations*, 29(3):439–451, 1978.

[77] T. Iwasaki and S. Hara. Well-posedness of feedback systems: insights into exact robustness analysis and approximate computations. *IEEE Transactions on Automatic Control*, 43(5):619–630, May 1998.

[78] J. L. W. V. Jensen. Sur les fonctions convexes et les inégalités entre les valeurs moyennes. *Acta mathematica*, 30:175–193, 1906.

[79] C. Jin, K. Gu, S. I. Niculescu, and I. Boussaada. Stability analysis of systems with delay-dependent coefficients. *Phd Thesis, IEEE Access*, 2018.

[80] E. W. Kamen. On the relationship between zero criteria for two-variable polynomials and asymptotic stability of delay differential equations. *IEEE Transactions on Automatic Control*, 25(5):983–984, 1980.

[81] D. Karnopp. Computer simulation of stick-slip friction in mechanical dynamic systems. *Journal of dynamic systems, measurement, and control*, 107(1):100–103, 1985.

[82] H.K. Khalil. *Nonlinear Systems*. Pearson Education. Prentice Hall, 1996.

[83] V. Kharitonov and A. Zhabko. Lyapunov–Krasovskii approach to the robust stability analysis of time-delay systems. *Automatica*, 39(1):15–20, 2003.

[84] V. Kolmanovskii and A. Myshkis. *Introduction to the theory and applications of functional differential equations*, volume 463. Springer, 2013.

[85] V. B. Kolmanovskii and V. R. Nosov. *Stability of functional differential equations*, volume 180. Elsevier, 1986.

[86] M. Krstic. Adaptive control of an anti-stable wave PDE. In *American Control Conference, 2009. ACC'09.*, pages 1505–1510. IEEE, 2009.

[87] M. Krstic. *Delay compensation for nonlinear, adaptive, and PDE systems*. Springer, 2009.

[88] M. Krstic, B.-Z. Guo, A. Balogh, and A. Smyshlyaev. Output-feedback stabilization of an unstable wave equation. *Automatica*, 44(1):63 – 74, 2008.

[89] M. Krstic, I. Kanellakopoulos, and P. V. Kokotovic. *Nonlinear and adaptive control design*. Wiley, 1995.

[90] M. Krstic, J. W. Modestino, H. Deng, A. Fettweis, J. L. Massey, M. Thoma, E. D. Sontag, and B. W. Dickinson. *Stabilization of nonlinear uncertain systems*. Springer-Verlag New York, Inc., 1998.

[91] M. Krstic and A. Smyshlyaev. *Boundary control of PDEs: A course on backstepping designs*, volume 16. Siam, 2008.

[92] J. Lagnese. Decay of solutions of wave equations in a bounded region with boundary dissipation. *Journal of Differential equations*, 50(2):163–182, 1983.

[93] I. Lasiecka and R. Triggiani. Uniform stabilization of the wave equation with Dirichlet or Neumann feedback control without geometrical conditions. *Applied Mathematics and Optimization*, 25(2):189–224, 1992.

[94] W. E. Lear and D. W. Dareing. Effect of drillstring vibrations on MWD pressure pulse signals. *Journal of Energy Resources Technology*, 112(2):84–89, 1990.

[95] N. Levinson. Transformation theory of non-linear differential equations of the second order. *Annals of Mathematics*, pages 723–737, 1944.

[96] L. Li, Q. Zhang, and N. Rasol. Time-varying sliding mode adaptive control for rotary drilling system. *JCP*, 6(3):564–570, 2011.

[97] X. Liu, N. Vlajic, X. Long, G. Meng, and B. Balachandran. Coupled axial-torsional dynamics in rotary drilling with state-dependent delay: stability and control. *Nonlinear Dynamics*, 78(3):1891–1906, Nov 2014.

[98] J. Löfberg. YALMIP: A toolbox for modeling and optimization in MATLAB. In *IEEE International Symposium on Computer Aided Control Systems Design*, pages 284–289, 2005.

[99] T. Louw, S. Whitney, A. Subramanian, and H. Viljoen. Forced wave motion with internal and boundary damping. *Journal of applied physics*, 111:14702–147028, 01 2012.

[100] Z.-H. Luo, B.-Z. Guo, and Ö. Morgül. *Stability and stabilization of infinite dimensional systems with applications*. Springer, 2012.

[101] A. M. Lyapunov. The general problem of the stability of motion. *International journal of control*, 55(3):531–534, 1992.

[102] S. Marx, E. Cerpa, C. Prieur, and V. Andrieu. Global stabilization of a korteweg–de vries equation with saturating distributed control. *SIAM Journal on Control and Optimization*, 55(3):1452–1480, 2017.

[103] A. Megretski and A. Rantzer. System analysis via integral quadratic constraints. *IEEE Transactions on Automatic Control*, 42(6):819–830, 1997.

[104] T. Meurer. *Control of Higher–Dimensional PDEs: Flatness and Backstepping Designs*. Springer Science & Business Media, 2012.

[105] T. Meurer and A. Kugi. Tracking control for boundary controlled parabolic PDEs with varying parameters: Combining backstepping and differential flatness. *Automatica*, 45(5):1182–1194, 2009.

[106] I. Miyadera. *Nonlinear semigroups*, volume 109. American Mathematical Soc., 1992.

[107] Ö. Morgül. A dynamic control law for the wave equation. *Automatica*, 30(11):1785–1792, 1994.

[108] Ö. Morgül. On the stabilization and stability robustness against small delays of some damped wave equations. *IEEE Trans. on Automatic Control*, 40(9):1626–1630, 1995.

[109] Ö. Morgül. An exponential stability result for the wave equation. *Automatica*, 38(4):731–735, 2002.

[110] A. D. Myshkis. *Lineare differentialgleichungen mit nacheilendem argument*, volume 17. VEB Deutscher Verlag der Wissenschaften, 1955.

[111] E. Navarro-López. An alternative characterization of bit-sticking phenomena in a multi-degree-of-freedom controlled drillstring. *Nonlinear Analysis: Real World Applications*, 10:3162–3174, 2009.

[112] E. Navarro-López and D. Cortes. Sliding-mode control of a multi-DOF oilwell drillstring with stick-slip oscillations. In *Proceedings of the American Control Conference*, pages 3837 – 3842, 2007.

[113] E. Navarro-López and R. Suarez. Practical approach to modeling and controlling stick-slip oscillations in oil-well drill-strings. In *Proceedings of the 2004 IEEE International Conference on Control Applications, 2004.*, volume 2, pages 1454–1460 Vol.2, 2004.

[114] S. I. Niculescu. *Delay effects on stability: a robust control approach*, volume 269. Springer, 2001.

[115] N. Olgac and R. Sipahi. An exact method for the stability analysis of time-delayed linear time-invariant (LTI) systems. *IEEE Transactions on Automatic Control*, 47(5):793–797, 2002.

[116] N. Olgac and R. Sipahi. A practical method for analyzing the stability of neutral type LTI-time delayed systems. *Automatica*, 40(5):847–853, 2004.

[117] A. Packard and J. Doyle. The complex structured singular value. *Automatica*, 29(1):71–109, 1993.

[118] A. Pazy. *Semigroups of linear operators and applications to partial differential equations*, volume 44. Springer, 1983.

[119] D. Peaucelle, D. Arzelier, D. Henrion, and F. Gouaisbaut. Quadratic separation for feedback connection of an uncertain matrix and an implicit linear transformation. *Automatica*, 43(5):795–804, 2007.

[120] M. M. Peet. A new state-space representation for coupled PDEs and scalable Lyapunov stability analysis in the SOS framework. In *57th Annual Conference on Decision and Control (CDC), Miami*, pages 545–550, 2018.

[121] M. M. Peet. Discussion paper: A new mathematical framework for representation and analysis of coupled PDEs. 2019. Under publication.

[122] C. Prieur, S. Tarbouriech, and J. M. G. da Silva. Wave equation with cone-bounded control laws. *IEEE Trans. on Automatic Control*, 61(11):3452–3463, 2016.

[123] B. S. Razumikhin. *Application of Liapunov's method to problems in the stability of systems with a delay*, volume 21. Automat. i Telemeh., 1960.

[124] Z. V. Rekasius. A stability test for systems with delays. *Proceedings of the joint automatic control conference*, TP9-A, 1980.

[125] T. Richard, C. Germay, and E. Detournay. A simplified model to explore the root cause of stick-slip vibrations in drilling systems with drag bits. *Journal of Sound and Vibration*, 305(3):432–456, 8 2007.

[126] C. Roman. *Boundary control of a wave equation with in-domain damping*. Theses, Université Grenoble Alpes, August 2018.

[127] C. Roman, D. Bresch-Pietri, E. Cerpa, C. Prieur, and O. Sename. Backstepping observer based-control for an anti-damped boundary wave PDE in presence of in-domain viscous damping. In *55th IEEE Conference on Decision and Control (CDC)*, 2016.

[128] M. Safi. *Lyapunov stability of coupled systems involving a transport equation*. Theses, Institut supérieur de l'aéronautique et de l'espace, October 2018.

[129] M. Safi. *Stabilité de Lyapunov de systèmes couplés impliquant une équation de transport*. Université Fédérale Toulouse Midi-Pyrénées, 2018.

[130] M. Safi, L. Baudouin, and A. Seuret. Tractable sufficient stability conditions for a system coupling linear transport and differential equations. *Systems & Control Letters*, 110:1 – 8, 2017.

[131] M. Safi, A. Seuret, and L. Baudouin. Lyapunov stability analysis of a system coupled to a hyperbolic PDE with potential. In *European Control Conference (ECC 2018)*, Limassol, Cyprus, June 2018.

[132] C. Sagert, F. Di Meglio, M. Krstic, and P. Rouchon. Backstepping and flatness approaches for stabilization of the stick-slip phenomenon for drilling. *IFAC Proceedings Volumes*, 46(2):779–784, 2013.

[133] B. Saldivar, I. Boussaada, H. Mounier, and S.-I. Niculescu. *Analysis and Control of Oilwell Drilling Vibrations: A Time-Delay Systems Approach*. Springer, 2015.

[134] B. Saldivar, S. Mondié, and J. C. Ávila Vilchis. The control of drilling vibrations: A coupled PDE–ODE modeling approach. *International Journal of Applied Mathematics and Computer Science*, 2016.

[135] B. Saldivar, S. Mondie, S.-I. Niculescu, H. Mounier, and I. Boussaada. A control oriented guided tour in oilwell drilling vibration modeling. *Annual Reviews in Control*, 42:100–113, September 2016.

[136] S. Saperstone. *Semidynamical Systems in Infinite Dimensional Spaces*. Applied mathematical sciences. Springer-Verlag, New York, 1981.

[137] C. W. Scherer. LPV control and full block multipliers. *Automatica*, 37(3):361–375, 2001.

[138] C. W. Scherer and J. Veenman. Stability analysis by dynamic dissipation inequalities: On merging frequency-domain techniques with time-domain conditions. *Systems and Control Letters*, 2018.

[139] M. Serieye. Construction of observers for hyperbolic systems. Master's thesis, Université Paul Sabatier, 2018. Toulouse.

[140] A. Serrarens, M.J.G. Molengraft, J.J. Kok, and L. van den Steen. H_∞ control for suppressing stick-slip in oil well drillstrings. *IEEE Control Systems*, 18:19 – 30, 05 1998.

[141] A. Seuret and F. Gouaisbaut. Jensen's and Wirtinger's inequalities for time-delay systems. *IFAC Proceedings Volumes*, 46(3):343–348, 2013.

[142] A. Seuret and F. Gouaisbaut. Wirtinger-based integral inequality: application to time-delay systems. *Automatica*, 49(9):2860–2866, 2013.

[143] A. Seuret and F. Gouaisbaut. Hierarchy of LMI conditions for the stability analysis of time-delay systems. *Systems & Control Letters*, 81:1–7, 2015.

[144] A. Seuret, S. Marx, and S. Tarbouriech. Hierarchical estimation of the region of attraction for systems subject to a state delay and a saturated input. In *2017 IEEE European Control Conference (CDC)*. IEEE, 2019.

[145] R. Sipahi, S. I. Niculescu, C. T. Abdallah, W. Michiels, and K. Gu. Stability and stabilization of systems with time delay. *IEEE Control Systems*, 31(1):38–65, 2011.

[146] R. Sipahi and N. Olgac. Degenerate cases in using the direct method. *ASME 2003 International Design Engineering Technical Conferences and Computers and Information in Engineering Conference*, pages 2201–2210, 2003.

[147] O. J. M. Smith. A controller to overcome dead time. *ISA J.*, 6:28–33, 1959.

[148] A. Smyshlyaev and M. Krstic. Closed-form boundary state feedbacks for a class of 1-D partial integro-differential equations. *IEEE Transactions on Automatic Control*, 49(12):2185–2202, 2004.

[149] A. Smyshlyaev and M. Krstic. Boundary control of an anti-stable wave equation with anti-damping on the uncontrolled boundary. *Systems & Control Letters*, 58(8):617–623, 2009.

[150] E. D. Sontag. The ISS philosophy as a unifying framework for stability-like behavior. In *Nonlinear control in the year 2000 volume 2*, pages 443–467. Springer, 2001.

[151] E. D. Sontag. Input to state stability: Basic concepts and results. In *Nonlinear and optimal control theory*, pages 163–220. Springer, 2008.

[152] S. Tang and C. Xie. State and output feedback boundary control for a coupled PDE–ODE system. *Systems & Control Letters*, 60(8):540–545, 2011.

[153] Y. Tang and G. Mazanti. Stability analysis of coupled linear ODE-hyperbolic PDE systems with two time scales. *Automatica*, 85:386 – 396, 2017.

[154] Y. Tang, C. Prieur, and A. Girard. Stability analysis of a singularly perturbed coupled ODE–PDE system. In *2015 54th IEEE Conference on Decision and Control (CDC)*, pages 4591–4596, Dec 2015.

[155] S. Tarbouriech, G. Garcia, J. M. G. da Silva Jr, and I. Queinnec. *Stability and stabilization of linear systems with saturating actuators*. Springer Science & Business Media, 2011.

[156] A. Terrand-Jeanne. *Régulation des systèmes à paramètres distribués : application au forage*. PhD thesis, 2018. Thèse de doctorat dirigée par Valérie Dos Santos Martins, Mélaz Tayakout et Vincent Andrieu.

[157] A. Terrand-Jeanne, V. Andrieu, M. Tayakout-Fayolle, and V. Dos Santos Martins. Regulation of inhomogeneous drilling model with a P-I controller. *IEEE Transactions on Automatic Control*, 2019.

[158] A. Terrand-Jeanne, V. Dos Santo Martins, and V. Andrieu. Regulation of the downside angular velocity of a drilling string with a P-I controller. *ECC 2018, Cyprus*, pages 2647–2652, 2018.

[159] K.-C. Toh, M. J. Todd, and R. H. Tütüncü. SDPT3 - a MATLAB software package for semidefinite programming, version 1.3. *Optimization methods and software*, 11(1-4):545–581, 1999.

[160] W. R. Tucker and C. Wang. On the effective control of torsional vibrations in drilling systems. *Journal of Sound and Vibration*, 224(1):101–122, 1999.

[161] M. Tucsnak. Wellposedness, controllability and stabilizability of systems governed by partial differential equations. *Cours de DEA, Université de Nancy*, 2004.

[162] M. Tucsnak and G. Weiss. *Observation and control for operator semigroups*. Springer, 2009.

[163] J. Veenman, C. W. Scherer, and H. Köroğlu. Robust stability and performance analysis based on integral quadratic constraints. *European Journal of Control*, 31:1–32, 2016.

[164] T. Vyhlídal and P. Zítek. Quasipolynomial mapping based rootfinder for analysis of time delay systems. *IFAC Proceedings Volumes*, 36(19):227–232, 2003.

[165] W. Jr. Weaver, S. P. Timoshenko, and D. H. Young. *Vibration problems in engineering*. John Wiley & Sons, 1990.

[166] H.-N. Wu and J.-W. Wang. Static output feedback control via PDE boundary and ODE measurements in linear cascaded ODE-beam systems. *Automatica*, 50(11):2787–2798, 2014.

[167] G. Zames. On the input-output stability of time-varying nonlinear feedback systems part one: Conditions derived using concepts of loop gain, conicity, and positivity. *IEEE Transactions on Automatic Control*, 11(2):228–238, 1966.

[168] Q.-Z. Zhang, Y.-Y. He, L. Li, and R. Nurzat. Sliding mode control of rotary drilling system with stick slip oscillation. In *2nd International Workshop on Intelligent Systems and Applications*, pages 1–4. IEEE, 2010.

[169] D. Zwillinger. *Handbook of differential equations*, volume 1. Gulf Professional Publishing, 1998.